frontiers | Research Topics

Wastewater-based epidemiological surveillance of respiratory pathogens

Edited by
David Champredon, Peter Vanrolleghem, Charlene Ranadheera and Doug Manuel

Published in
Frontiers in Public Health
Frontiers in Medicine

ISSN 1664-8714
ISBN 978-2-8325-4038-1
DOI 10.3389/978-2-8325-4038-1

About Frontiers

Frontiers is more than just an open access publisher of scholarly articles: it is a pioneering approach to the world of academia, radically improving the way scholarly research is managed. The grand vision of Frontiers is a world where all people have an equal opportunity to seek, share and generate knowledge. Frontiers provides immediate and permanent online open access to all its publications, but this alone is not enough to realize our grand goals.

Frontiers journal series

The Frontiers journal series is a multi-tier and interdisciplinary set of open-access, online journals, promising a paradigm shift from the current review, selection and dissemination processes in academic publishing. All Frontiers journals are driven by researchers for researchers; therefore, they constitute a service to the scholarly community. At the same time, the *Frontiers journal series* operates on a revolutionary invention, the tiered publishing system, initially addressing specific communities of scholars, and gradually climbing up to broader public understanding, thus serving the interests of the lay society, too.

Dedication to quality

Each Frontiers article is a landmark of the highest quality, thanks to genuinely collaborative interactions between authors and review editors, who include some of the world's best academicians. Research must be certified by peers before entering a stream of knowledge that may eventually reach the public - and shape society; therefore, Frontiers only applies the most rigorous and unbiased reviews. Frontiers revolutionizes research publishing by freely delivering the most outstanding research, evaluated with no bias from both the academic and social point of view. By applying the most advanced information technologies, Frontiers is catapulting scholarly publishing into a new generation.

What are Frontiers Research Topics?

Frontiers Research Topics are very popular trademarks of the *Frontiers journals series*: they are collections of at least ten articles, all centered on a particular subject. With their unique mix of varied contributions from Original Research to Review Articles, Frontiers Research Topics unify the most influential researchers, the latest key findings and historical advances in a hot research area.

Find out more on how to host your own Frontiers Research Topic or contribute to one as an author by contacting the Frontiers editorial office: frontiersin.org/about/contact

Wastewater-based epidemiological surveillance of respiratory pathogens

Topic editors

David Champredon — Public Health Agency of Canada (PHAC), Canada
Peter Vanrolleghem — Laval University, Canada
Charlene Ranadheera — National Microbiology Laboratory, Public Health Agency of Canada (PHAC), Canada
Doug Manuel — The Ottawa Hospital, Canada

Citation

Champredon, D., Vanrolleghem, P., Ranadheera, C., Manuel, D., eds. (2023). *Wastewater-based epidemiological surveillance of respiratory pathogens*. Lausanne: Frontiers Media SA. doi: 10.3389/978-2-8325-4038-1

Table of contents

frontiers | Frontiers in Public Health

TYPE Editorial
PUBLISHED 16 November 2023
DOI 10.3389/fpubh.2023.1328452

OPEN ACCESS

EDITED AND REVIEWED BY
Marc Jean Struelens,
Université Libre de Bruxelles, Belgium

*CORRESPONDENCE
David Champredon
✉ david.champredon@canada.ca

RECEIVED 26 October 2023
ACCEPTED 31 October 2023
PUBLISHED 16 November 2023

CITATION
Champredon D and Vanrolleghem PA (2023) Editorial: Wastewater-based epidemiological surveillance of respiratory pathogens. *Front. Public Health* 11:1328452. doi: 10.3389/fpubh.2023.1328452

Editorial: Wastewater-based epidemiological surveillance of respiratory pathogens

David Champredon[1]* and Peter A. Vanrolleghem[2]

[1]Public Health Agency of Canada, Guelph, ON, Canada, [2]Department of Civil Engineering and Water Engineering, modelEAU – Université Laval, Québec, QC, Canada

KEYWORDS

wastewater, data quality, sampling methods, normalization, kinetics, epidemiology, respiratory infections

Editorial on the Research Topic
Wastewater-based epidemiological surveillance of respiratory pathogens

Monitoring the concentration of human pathogens in wastewater for public health has existed for over 80 years (1) but has rarely been performed for respiratory viruses until recently. Indeed, before the COVID-19 pandemic, there were few attempts by public health organizations to integrate the detection of respiratory pathogens in wastewater into their surveillance programs to monitor the prevalence of these infections in the population. This absence of enthusiasm may be explained by the unawareness that fecal (and urinary) shedding of respiratory viruses has a similar profile as the much-better-known respiratory shedding, making wastewater surveillance a potentially valuable indicator to monitor the dynamics of a respiratory epidemic. The COVID-19 pandemic has demonstrated the utility of wastewater-based epidemiology (WBE) during a major epidemiological event involving a respiratory pathogen and its potential value if integrated into existing epidemic surveillance programs.

This Research Topic showcases studies that highlight the emergence of the surveillance of respiratory pathogens from wastewater samples and also the potential challenges ahead.

Wastewater-based surveillance brings many potential benefits to public health activities, notably to complement (but not replace) other data sources as de Melo et al. show with student absenteeism data. One of the main goals of wastewater surveillance is to link the pathogen concentration in wastewater with hospitalizations associated with the pathogen. But, as Kadonsky et al. hint, the pathogen concentration in wastewater may be affected by factors unrelated to its epidemiology and perturb the wastewater concentration/hospitalization relationship. Normalization techniques (such as the one proposed by Dhiyebi et al.) are still being explored to account for exogenous effects to correct non-epidemiological effects on the wastewater signal.

Fecal shedding kinetics for an infected individual, a cornerstone of WBE, is poorly known for most pathogens. Even for the well-studied SARS-CoV-2, we don't know how (or even if) fecal shedding changed as the population got exposed to successive variants and different vaccines. In that spirit, Rioux et al. propose a clinical-data-driven method to correct initial assumptions about fecal kinetics.

Laboratory methods that accurately quantify viral concentration in wastewater are still in their early stages. We are probably several years away from a gold-standard laboratory method, assuming that "gold standard" even makes sense, given the diversity of the wastewater matrix across different sampling situations. In this Research Topic, the studies

by Lucansky et al., Shinde et al., Nagelkerke et al., and Zhao et al. are moving research in that direction.

As an emerging field, WBE must find its place beside more established public health surveillance programs. There is probably no one-size-fits-all solution, but the study by Clark et al. can be helpful as they share a comprehensive framework that has been implemented in a large North American jurisdiction.

The COVID-19 pandemic showed the unexpected utility of WBE for respiratory pathogens. Leveraging this success, many jurisdictions are expanding their WBE to other respiratory pathogens, notably seasonal influenza (de Melo et al.) and RSV, historically the most burdensome respiratory diseases. Prioritizing and right-sizing WBE to new pathogens will be key to improving public health but may also be challenging given the specificities of each jurisdiction. To support such efforts, Gentry et al. propose a ranking system that was applied in a large North American urban center.

The choice regarding the geographical location of sampling sites can provide different spatial levels for epidemiological analyses. Sampling wastewater at wastewater treatment plants is a popular and practical choice to monitor the prevalence of a given infection at the (sub)municipal level. However, more focused sampling can bring unprecedented insights into fine-grained transmission patterns at key "hot spots". For example, the study by Corchis-Scott et al. in this Research Topic samples university residences.

Clearly, WBE for respiratory pathogens is still in its infancy, and many knowledge gaps need to be filled. This Research Topic is a step in that direction. Given the recent expansion of WBE in many different jurisdictions worldwide, it is exciting to see research in this new field that promises to improve public health.

Author contributions

DC: Writing—original draft, Writing—review & editing. PV: Writing—review & editing.

Funding

The author(s) declare that no financial support was received for the research, authorship, and/or publication of this article.

Conflict of interest

The authors declare that the research was conducted in the absence of any commercial or financial relationships that could be construed as a potential conflict of interest.

Publisher's note

References

1. Paul JR, Trask JD, Gard S. Poliomyelitic virus in urban sewage. *J Exp Med.* (1940) 71:765–77. doi: 10.1084/jem.71.6.765

frontiers | Frontiers in Public Health

TYPE Original Research
PUBLISHED 07 March 2023
DOI 10.3389/fpubh.2023.1116636

OPEN ACCESS

EDITED BY
David Champredon,
Public Health Agency of Canada (PHAC), Canada

REVIEWED BY
Robert Delatolla,
University of Ottawa, Canada
Maria Gori,
University of Milan, Italy

*CORRESPONDENCE
Vincent Lucansky
✉ vincent.lucansky@uniba.sk
Marek Samec
✉ marek.samec@uniba.sk

†These authors have contributed equally to this work

SPECIALTY SECTION
This article was submitted to Infectious Diseases: Epidemiology and Prevention, a section of the journal Frontiers in Public Health

RECEIVED 05 December 2022
ACCEPTED 17 February 2023
PUBLISHED 07 March 2023

CITATION
Lucansky V, Samec M, Burjanivova T, Lukacova E, Kolkova Z, Holubekova V, Turyova E, Hornakova A, Zaborsky T, Podlesniy P, Reizigova L, Dankova Z, Novakova E, Pecova R, Calkovska A and Halasova E (2023) Comparison of the methods for isolation and detection of SARS-CoV-2 RNA in municipal wastewater.
Front. Public Health 11:1116636.
doi: 10.3389/fpubh.2023.1116636

Comparison of the methods for isolation and detection of SARS-CoV-2 RNA in municipal wastewater

Vincent Lucansky[1*†], Marek Samec[2*†], Tatiana Burjanivova[3], Eva Lukacova[3], Zuzana Kolkova[1], Veronika Holubekova[1], Eva Turyova[3], Andrea Hornakova[1], Tibor Zaborsky[4], Petar Podlesniy[5], Lenka Reizigova[6], Zuzana Dankova[7], Elena Novakova[8], Renata Pecova[2], Andrea Calkovska[9] and Erika Halasova[1]

[1]Biomedical Centre Martin, Jessenius Faculty of Medicine in Martin (JFMED CU), Comenius University in Bratislava, Martin, Slovakia, [2]Department of Pathophysiology, Jessenius Faculty of Medicine in Martin, Comenius University in Bratislava, Martin, Slovakia, [3]Department of Molecular Biology and Genomics, Jessenius Faculty of Medicine in Martin, Comenius University in Bratislava, Martin, Slovakia, [4]RÚVZ (Regional Office of Public Health), Martin, Slovakia, [5]Centro Investigacion Biomedica en Red Enfermedades Neurodegenerativas (CiberNed), Madrid, Spain, [6]Center for Microbiology and Infection Prevention, Department of Laboratory Medicine, Faculty of Health Care and Social Work, Trnava University, Trnava, Slovakia, [7]Biobank for Cancer and Rare Diseases, Jessenius Faculty of Medicine in Martin (JFMED CU), Comenius University in Bratislava, Martin, Slovakia, [8]Department of Microbiology and Immunology, Jessenius Faculty of Medicine in Martin, Comenius University in Bratislava, Martin, Slovakia, [9]Department of Physiology, Jessenius Faculty of Medicine in Martin, Comenius University in Bratislava, Martin, Slovakia

Introduction: Coronavirus SARS-CoV-2 is a causative agent responsible for the current global pandemic situation known as COVID-19. Clinical manifestations of COVID-19 include a wide range of symptoms from mild (i.e., cough, fever, dyspnea) to severe pneumonia-like respiratory symptoms. SARS-CoV-2 has been demonstrated to be detectable in the stool of COVID-19 patients. Waste-based epidemiology (WBE) has been shown as a promising approach for early detection and monitoring of SARS-CoV-2 in the local population performed *via* collection, isolation, and detection of viral pathogens from environmental sources.

Methods: In order to select the optimal protocol for monitoring the COVID-19 epidemiological situation in region Turiec, Slovakia, we (1) compared methods for SARS-CoV-2 separation and isolation, including virus precipitation by polyethylene glycol (PEG), virus purification *via* ultrafiltration (Vivaspin®) and subsequent isolation by NucleoSpin RNA Virus kit (Macherey-Nagel), and direct isolation from wastewater (Zymo Environ Water RNA Kit); (2) evaluated the impact of water freezing on SARS- CoV-2 separation, isolation, and detection; (3) evaluated the role of wastewater filtration on virus stability; and (4) determined appropriate methods including reverse transcription-droplet digital PCR (RT-ddPCR) and real-time quantitative polymerase chain reaction (RT-qPCR) (targeting the same genes, i.e., *RdRp* and gene *E*) for quantitative detection of SARS-CoV-2 in wastewater samples.

Results: (1) Usage of Zymo Environ Water RNA Kit provided superior quality of isolated RNA in comparison with both ultracentrifugation and PEG precipitation. (2) Freezing of wastewater samples significantly reduces the RNA yield. (3) Filtering is counterproductive when Zymo Environ Water RNA Kit is used. (4) According to the specificity and sensitivity, the RT-ddPCR outperforms RT-qPCR.

Discussion: The results of our study suggest that WBE is a valuable early warning alert and represents a non-invasive approach to monitor viral pathogens, thus protects public health on a regional and national level. In addition, we have shown that the sensitivity of testing the samples with a nearer detection limit can be improved by selecting the appropriate combination of enrichment, isolation, and detection methods.

KEYWORDS

SARS-CoV-2, wastewater, WBE, droplet digital PCR (ddPCR), real-time quantitative polymerase chain reaction (RT-qPCR), COVID-19

1. Introduction

SARS-CoV-2 is a novel member of the coronavirus genus identified in late 2019. It is a causative agent of the infectious disease COVID-19 that can lead to a wide range of manifestations from mild respiratory symptoms or even an asymptomatic course to severe viral pneumonia resulting in death (1). Due to high infectivity and death toll, COVID-19 has become a disease with a significant impact on the health status of the world population as well as on the world economy and politics. On January 30, 2020, the World Health Organization (WHO) Emergency Committee designated COVID-19 as a global health emergency (2). Approximately 648,131,832 cases and 6,640,702 deaths have been attributed to COVID-19 worldwide so far (December 1st, 2022) (3).

Testing soon became an essential part of the COVID-19 pandemic management. However, the strategical selection of appropriate diagnostic approach and its settings is crucial for the quality and usefulness of the COVID-19 testing. An attempt to perform nationwide screening (4) turned out to be cost-ineffective, unpopular, logistically challenging, and potentially risky due to the huge spatiotemporal accumulation of tested individuals. Moreover, the nationwide screening did not provided any long-term improvement of the epidemiological situation or gave any reliable information about the actual dynamics of the pandemic. As we showed in our previous work (5), the usage of rapid antigen testing is not reliable due to a high number of misdiagnosed false-negative virus carriers. The individual real-time quantitative polymerase chain reaction (RT-qPCR) testing is also biased due to the fact that many tested subjects undergo diagnostic procedures not randomly but their participation is motivated by symptom occurrence either on themselves or on the person sharing their work or living environment, thus driven by suspicion. Vice versa, many individuals with in apparent infection are not tested and are not included in case reports.

On the contrary, environmental monitoring of wastewater is independent of the testing of individuals and can therefore become a critical tool for monitoring the epidemiological situation of COVID-19 (6, 7). The presence of SARS-CoV-2 in wastewater has been reported in several studies (6–10). Based on clinically confirmed cases, the observed viral titers were significantly higher than expected viral titers (11). The correlation between SARS-CoV-2 RNA concentration in sewer and the occurrence of new cases has showed to be stronger than that of active cases and cumulative cases obtained by individual testing (12).

Hence, we decided to test several protocols enabling COVID-19 surveillance in sewer water. In particular, we established three concentration protocols for the enrichment of viral RNA from wastewater and its subsequent isolation, followed by two different detection methods. We are aware that the spectrum of techniques is much broader. However, our selection was influenced by a combination of our previous hands-on experience, workplace availability as well as an effort to cover principally different approaches. For the enrichment of viral particles in wastewater, polyethylene glycol (PEG) precipitation and centrifugal membrane concentrator protocols were used. Both methods were followed by an utilization of virus RNA isolation kit. The third approach was applied using the kit combining viral enrichment with RNA isolation in a single protocol. Subsequent detection was performed with the utilization of either quantitative RT-PCR (RT-qPCR), the commonly used diagnostic method for SARS-CoV-2 during the COVID-19 pandemic (13), or reverse transcription-droplet digital PCR (RT-ddPCR) that is considered to provide higher sensitivity and specificity rate compared to RT-qPCR RT-ddPCR thus avoid more false-negative results of samples with low viral load (14). Both PCR assays detected matching genes, namely *RdRp* and *E,* which facilitated the comparison of obtained data.

2. Materials and methods

2.1. Enrichment and SARS-CoV-2 RNA isolation

The wastewater samples were obtained at the sewage treatment plant in Vrútky, which collects wastewater from Martin city and parts of the Turiec region. Sewage water samples for our experiment were collected from April to July 2022. At that time, the epidemiological situation in the Slovak republic was relatively stabilized, characterized by a decline of newly diagnosed cases; thus, SARS-CoV-2 presence in sewage was expected to be at very low levels (see Supplementary Table A in Supplementary material). Samples were transported to the laboratory on ice and then kept at 4°C until further processing on the same day. The first step was debris removal by centrifugation at 4,000 g for 30 min at 4°C. Next, half of the supernatant was filtered using 0.45 μm syringe filters. Samples of both filtered and unfiltered wastewater were either frozen at −20°C or processed further immediately.

For PEG precipitation, the supernatant was incubated with 8% PEG-8000 (Merck), and 0.3 M NaCl (Sigma-Aldrich) overnight

(app. for 16 h) at 4°C. Centrifugation was performed at 10,000 g for 120 min, at 4°C, then the supernatant was removed and the pellet was diluted in 500 μl Opti-MEM™ (Gibco).

When using the Vivaspin centrifugal filter device/molecular weight cut-off 50 kDa (Sartorius), the supernatant was concentrated by centrifuging at 4,000 g for 30 min at 4°C. This centrifugal step was repeated to pass through the entire 50 ml supernatant volume until the final volume of the concentrated sample reached 500 μl. Then the enriched sample was collected and further processed.

Further, after both PEG precipitation and centrifugal filter enrichment protocols, total RNA isolation was carried out using the NucleoSpin™ RNA Virus column (Macherey Nagel). Then, RNA was eluted with 30 μl of RNase-free water according to the manufacturer's protocol. All RNA isolations were performed in triplets.

Zymo Environ Water RNA Extraction kit (Zymo) covers viral enrichment, sample homogenization, and RNA purification in one workflow protocol. We used 5 ml of wastewater that was aliquoted into five separated tubes (1 ml/each). Subsequently, we added 70 μl of Water Concentrating Buffer into each tube. Further steps were processed according to the manufacturers' recommendations.

2.2. SARS-CoV-2 RNA detection

Detection of SARS-CoV-2 viral RNA in the sample of wastewater was performed by a one-step RT-qPCR method using IVD-certificated kit gb SARS-CoV-2 Multiplex (GENERI BIOTECH s.r.o., Hradec Králové, Czech Republic). This kit allows the detection of viral *E* and *RdRP* genes within one reaction with a limit of detection of 2.13 copies of viral RNA per reaction (95 % CI). To avoid false negative results, the PCR process was verified by external positive control (EPC) added to the reaction. Reactions were prepared according to the manufacturer's instructions. Briefly, the PCR reaction with a volume of 20 μl contained 10 μl of Master Mix OneStep Multi, 5 μl of multiplexed Assay CoV-2 *E-RdRP*, 0.25 μl of EPC Template RNA, and 5 μl of extracted RNA. Positive control as well as NTC with distilled water was included in each run. PCR conditions were as follows: reverse transcription at 42°C for 30 min, initial denaturation at 95°C for 3 min, 50 cycles consisting of two steps (denaturation at 95°C for 10 s and annealing plus elongation at 60°C for the 30 s). The fluorescence signal was measured in the FAM channel for viral gene *E*, in the HEX channel for viral *RdRP* gene, and in the Cy5 channel for EPC. Reactions were evaluated as invalid if the signal in the Cy5 channel was not detected.

Reverse transcription-droplet digital PCR (RT-ddPCR) was performed in 20 μl reaction volume, consisting of 17 μl of master mix and 3 μl of the sample. Mastermix contained 5 μl of supermix, 2 μl of reverse transcriptase (RT), and 1 μl of 300 mM dithiothreitol (DTT) solution, all included in One-Step RT-ddPCR Advanced Kit for Probes (Bio-Rad Laboratories, Hercules, California, USA), primers and probes (Generi Biotech, Hradec Králové, Czech Republic) at a final concentration of 500 and 250 nM, respectively. Primer and probe sequences were as follows: RdRp (F): GTGAAATGGTCATGTGTGGCG, RdRp (R): AATGTTAAAAACACTATTAGCATAAGCA, RdRp: CAGGTGGAACCTCATCAGGAGATGC/HEX-IBFQ; E (F): ACAGGTACGTTAATAGTTAATAGCGT, E (R): ATATTGC AGCAGTACGCACA, E: ACACTAGCCATCCTTACTGCGC TTCG/FAM-IBFQ; GAPDH (F): AGTCAGCCGCATCTTCT TTT, GAPDH (R): CCCAATACGACCAAATCCGT, GAPDH: GCGTCGCCAGCCGAGCCACA/HEX-IBFQ. Commercially available SARS-CoV-2 Standard (Exact Diagnostics, Bio-Rad Laboratories, Fort Worth, Texas, USA) manufactured with synthetic RNA transcripts containing five gene targets (*E*, *N*, *ORF1ab*, *RdRP*, and *S* of SARS-CoV-2) was used as a ddPCR quantitative positive control. All samples were analyzed in duplicates for *GAPDH* and single wells for each viral gene, *RdRp* + *GAPDH* and *E* + *GAPDH*. Droplets were generated by an automated droplet generator (Bio-Rad Laboratories, Hercules, California, USA) according to the manufacturer's instructions. PCR was performed using a T100 thermal cycler (Bio-Rad Laboratories, Hercules, California, USA) with the following cycling conditions: reverse transcription at 50°C for 60 min, denaturation at 95°C for 10 min, followed by 40 cycles of denaturation at 94°C for 30 s, followed by annealing/extension at 54°C for 1 min, and droplet stabilization at 98°C for 10 min. Samples were then analyzed using QX200 Droplet Reader (Bio-Rad Laboratories, Hercules, California, USA). Thresholding was carried out by using QuantaSoft Software manually at the lowest amplitude that captures true negative clusters based on the signals of the negative control and positive control samples. The results were reported as positive when at least five copies of each viral gene (*RdRp*, *E*) occurred (15). Data are interpreted as copies per reaction according to previous works evaluating the presence of SARS-CoV-2 in samples by RT-ddPCR (16).

For the schematic visualization of the complete workflow, see Figure 1.

3. Results

3.1. Comparison of two detection methods for the detection of SARS-CoV-2 RNA/sensitivity

To perform the most precise detection of SARS-CoV-2 in wastewater, we compared two quantitative analysis methods, namely RT-qPCR (qTOWER—Analytic Jena) and ddPCR (QX200 Droplet digital PCR system—Biorad). All samples were analyzed in triplicates for higher statistical power of the experiment. The samples were collected three times from April to May 2022. Using filtered wastewater, RT-ddPCR identified 21 positive samples compared to 12 positive results analyzed by RT-qPCR. Furthermore, significant differences were detected in unfiltered wastewater in which RT-ddPCR identified 19 positive samples compared to 12 positive results detected by RT-qPCR (Table 1) Additional information is summarized in the Supplementary material (see Supplementary Table B in Supplementary material).

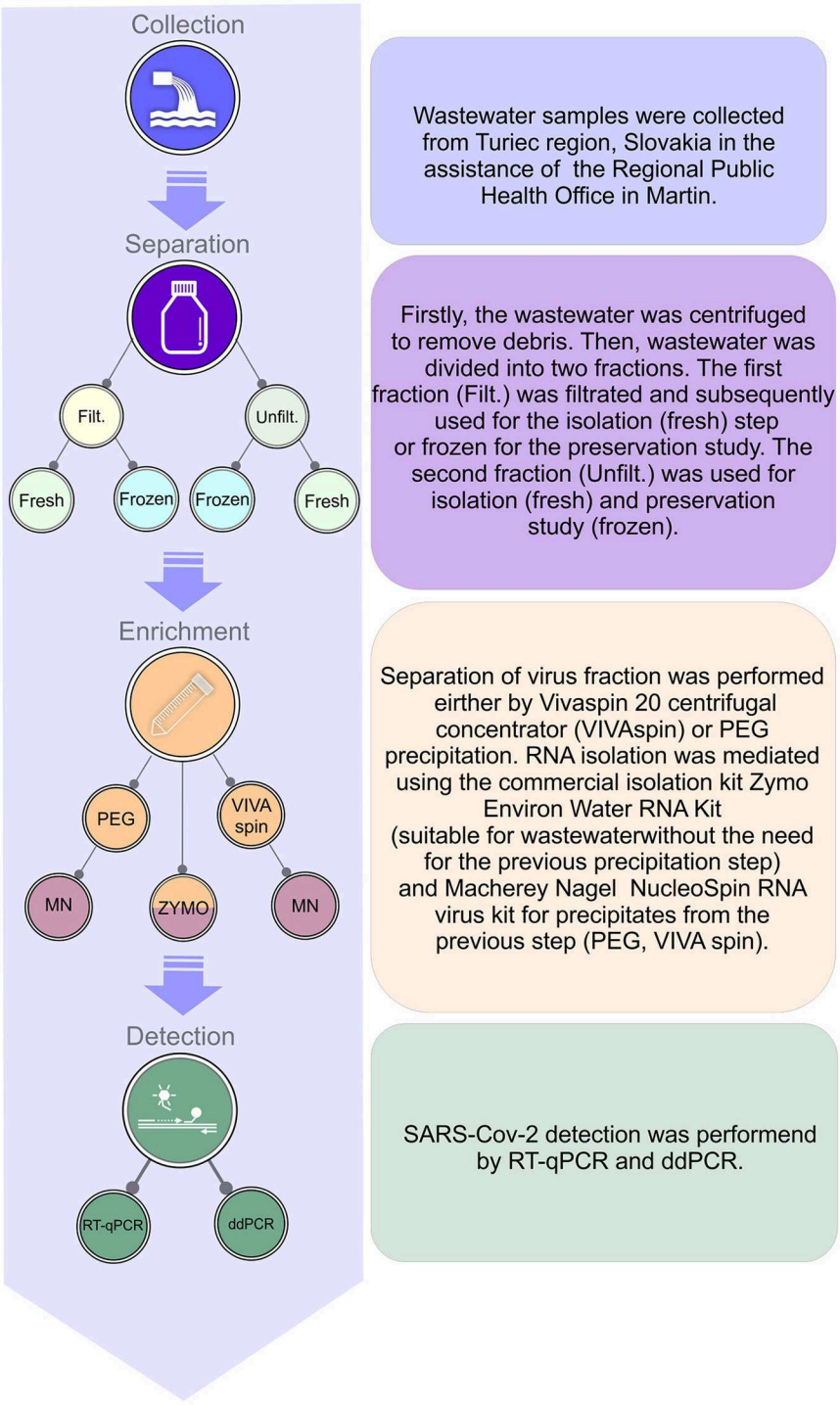

FIGURE 1
Schematic visualization of complete workflow for processing raw sewer sample, enrichment, isolation of RNA, and detection of SARS-CoV-2 in wastewater.

3.2. Comparison of three methods for the concentration and isolation of SARS-CoV-2 RNA

In our study, we compared three different methods for virus concentration and purification (Vivaspin and PEG) and RNA isolation, including NucleoSpin RNA Virus, Mini kit for viral RNA (Macherey-Nagel), and Zymo Environ Water RNA Kit (Zymo) to select the appropriate protocol for subsequent downstream analyses. Using PEG-8000 and NucleoSpin RNA Virus Mini kit, we identified eight positive results in filtered wastewater and nine positive results in unfiltered wastewater using RT-ddPCR. RT-qPCR detected three positive samples (in filtered wastewater), while only one sample was positive for SARS-CoV-2 in unfiltered wastewater. Virus separation using Vivaspin columns and subsequent isolation by NucleoSpin RNA Virus

10.3389/fpubh.2023.1116636

TABLE 1 Comparison of detection methods for viral RNA and workflows suitable for purification, concentration, and isolation of SARS-CoV-2 in wastewater.

Filt./Unfilt. wastewater	Separation and isolation method	Sample (replicates)	Detection method (RT-ddPCR/RT-qPCR)	Wastewater collection		
				1.	2.	3.
Filt.	PEG-8000	1	RT-ddPCR	+	+	+
		2		+	+	+
		3		+	+	?
		1	RT-qPCR	*	+	+
		2		*	*	*
		3		*	+	?
	Vivaspin	1	RT-ddPCR	+	+	?
		2		+	+	?
		3		?	?	–
		1	RT-qPCR	?	–	*
		2		?	–	–
		3		?	–	–
	Zymo	1	RT-ddPCR	+	+	+
		2		+	+	+
		3		+	+	+
		1	RT-qPCR	+	+	+
		2		+	+	+
		3		+	+	+
Unfil.	PEG-8000	1	RT-ddPCR	+	+	?
		2		+	+	+
		3		+	+	+
		1	RT-qPCR	?	*	?
		2		*	–	?
		3		–	+	?
	Vivaspin	1	RT-ddPCR	?	?	?
		2		+	*	–
		3		+	?	?
		1	RT-qPCR	?	*	*
		2		?	+	–
		3		?	+	–
	Zymo	1	RT-ddPCR	+	+	+
		2		+	+	+
		3		+	+	+
		1	RT-qPCR	+	+	+
		2		+	+	+
		3		+	+	+

RT-ddPCR, reverse transcription-droplet digital PCR; RT-qPCR, realtime-quantitative PCR; PEG-8000, polyethylene glycol-8000; Filt., filtered; Unfil., unfiltered.
+, positive; –, negative; *, different coronavirus; ?, invalid result.

Mini kit detected SARS-CoV-2 positivity in four cases (filtered wastewater) compared to two positive outputs after RT-ddPCR analysis identified in unfiltered wastewater. The same workflow applied for RT-qPCR detected the absence of positivity in filtered wastewater; only two positive samples were confirmed in unfiltered wastewater. The protocol for virus purification and RNA isolation

(Zymo Environ Water RNA Kit) identified positivity in all samples after RT-ddPCR as well as RT-qPCR analysis in both filtered and unfiltered wastewater (Table 1).

3.3. Analysis of the usage of unfiltered wastewater vs. wastewater filtered with 0.22 μm strainer using RT-ddPCR

In accordance with our experiment workflow, the collected wastewater included: (1) filtrated with a 0.22 mm strainer or (2) used for further analysis without requiring a filtration step. In the next step, both wastewater samples (filtered/unfiltered) were processed by the aforementioned separation and isolation protocols (Table 1). Data were assessed as copies of viral RNA per reaction using RT-ddPCR. We observed a significantly lower number of copies of viral *RdRp* between samples processed by PEG and samples processed by Vivaspin columns and Zymo kit ($p < 0.05$) using filtered wastewater in the first analysis. Moreover, the level of *GAPDH* copies was significantly lower in samples isolated by Zymo kit compared to samples processed by PEG ($p < 0.05$). In unfiltered wastewater, the number of *GAPDH* copies was significantly lower ($p < 0.01$) in samples purified and isolated by Zymo kit than in samples after PEG precipitation and subsequent RNA isolation by the NucleoSpin RNA Virus kit. The second analysis of wastewater showed a significant decrease in the number of gene *E* ($p < 0.05$), *RdRp* ($p < 0.05$), and *GAPDH* ($p < 0.05$) copies in the samples concentrated by Vivaspin columns compared to samples after PEG precipitation and RNA isolation. Statistical significance was also observed in the number of *gene E* ($p < 0.05$), *RdRp* ($p < 0.01$), and *GAPDH* ($p < 0.01$) copies in samples processed by Zymo kit compared to samples after PEG-mediated virus precipitation and RNA isolation in unfiltered wastewater in the second round of analysis. In addition, a comparison between a number of gene copies in samples processed using Vivaspin and Zymo kit showed significant differences in *RdRp* ($p < 0.05$) and GAPDH ($p < 0.01$) (in filtered water) and *RdRp* ($p < 0.001$), *E* ($p < 0.01$), and *GAPDH* ($p < 0.001$) in unfiltered wastewater. The third analysis showed similar results between samples processed *via* Vivaspin and Zymo kit. The number of *RdRp* ($p < 0.05$) and *GAPDH* ($p < 0.01$) copies was significantly higher in filtered wastewater after the Zymo purification and isolation step. Also, there was statistical significance between *RdRp* ($p < 0.05$), *E* ($p < 0.01$), and *GAPDH* ($p < 0.05$) in unfiltered wastewater processed by Vivaspin and Zymo workflow. Finally, a significantly increased number of *RdRp* copies ($p < 0.05$) was observed in samples after Zymo processing than those after PEG separation in the third analysis. All data are summarized in Figure 2.

3.4. Analysis of the usage of unfiltered wastewater vs. wastewater filtered with 0.22 μm strainer using Zymo Environ Water RNA Kit analyzed by RT-ddPCR

According to previous results, we compared unfiltered and filtered wastewater processed by Zymo Environ Water RNA kit. In the first analysis, there was no statistical significance between filtered and unfiltered wastewater in the number of viral gene copies (*E*, *RdRp*) as well as in housekeeping gene *GAPDH*. The second analysis evaluated by RT-ddPCR revealed differences between the amount of *GAPDH* copies ($p < 0.05$) in unfiltered wastewater compared to filtered wastewater. In the third analysis, we observed a significantly increased level of viral *gene E* ($p < 0.05$) in unfiltered wastewater (Figure 3).

3.5. Determination of suitability of the usage of frozen wastewater vs. fresh

To determine the impact of thaw/freeze on the stability of viral RNA in wastewater samples, we analyzed frozen filtered and unfiltered wastewater (frozen aliquots from the first three collections). In the filtered fraction of wastewater, we observed a significantly decreased number of *GAPDH* copies in samples processed by Vivaspin protocol compared to PEG processing ($p < 0.05$) and an increased number of *GAPDH* in wastewater processed by Zymo kit compared to Vivaspin ($p < 0.05$) in the second analysis. On the other hand, unfiltered fractions manifested more diverse results. In the first analysis, the level of *GAPDH* was decreased in samples processed by both Vivaspin ($p < 0.05$) and Zymo kit ($p < 0.01$) protocols compared to PEG workflow. Moreover, the level of *RdRp* was lower ($p < 0.01$) in samples concentrated by Vivaspin columns than in those processed by PEG precipitation. The second analysis revealed a decrease in *GAPDH* ($p < 0.01$) in samples after Vivaspin centrifugation and Zymo kit processing compared to samples after PEG-mediated precipitation. Furthermore, significance was confirmed between a number of *RdRp* ($p < 0.05$) and *GAPDH* ($p < 0.05$) copies after purification and RNA isolation mediated by Zymo kit and samples selected for Vivaspin centrifugation. The last analysis of unfiltered frozen wastewater showed a significantly decreased level of *GAPDH* in samples after processing by Vivaspin ($p < 0.01$) and Zymo kit ($p < 0.001$) workflow than in samples processed by PEG precipitation (Figure 4).

3.6. Example of the usage of the selected protocol in practical settings

We received total 10 samples (analyzed as triplicates) of wastewater collected over the 2-month period between May 2022 and July 2022. Except for one replicate, all 10 samples were positive for SARS-CoV-2, analyzed by RT-ddPCR. On the other hand, results from RT-qPCR showed inconsistency characterized by negative and invalid results or the presence of different coronavirus (Table 2).

Long-term monitoring revealed an increased amount of SARS-CoV-2 viral gene copies in wastewater samples compared to expectations based on national data acquired by individual testing using RT-qPCR (17). This trend was consistent throughout the last 5 weeks of the analysis (Figure 5).

10.3389/fpubh.2023.1116636

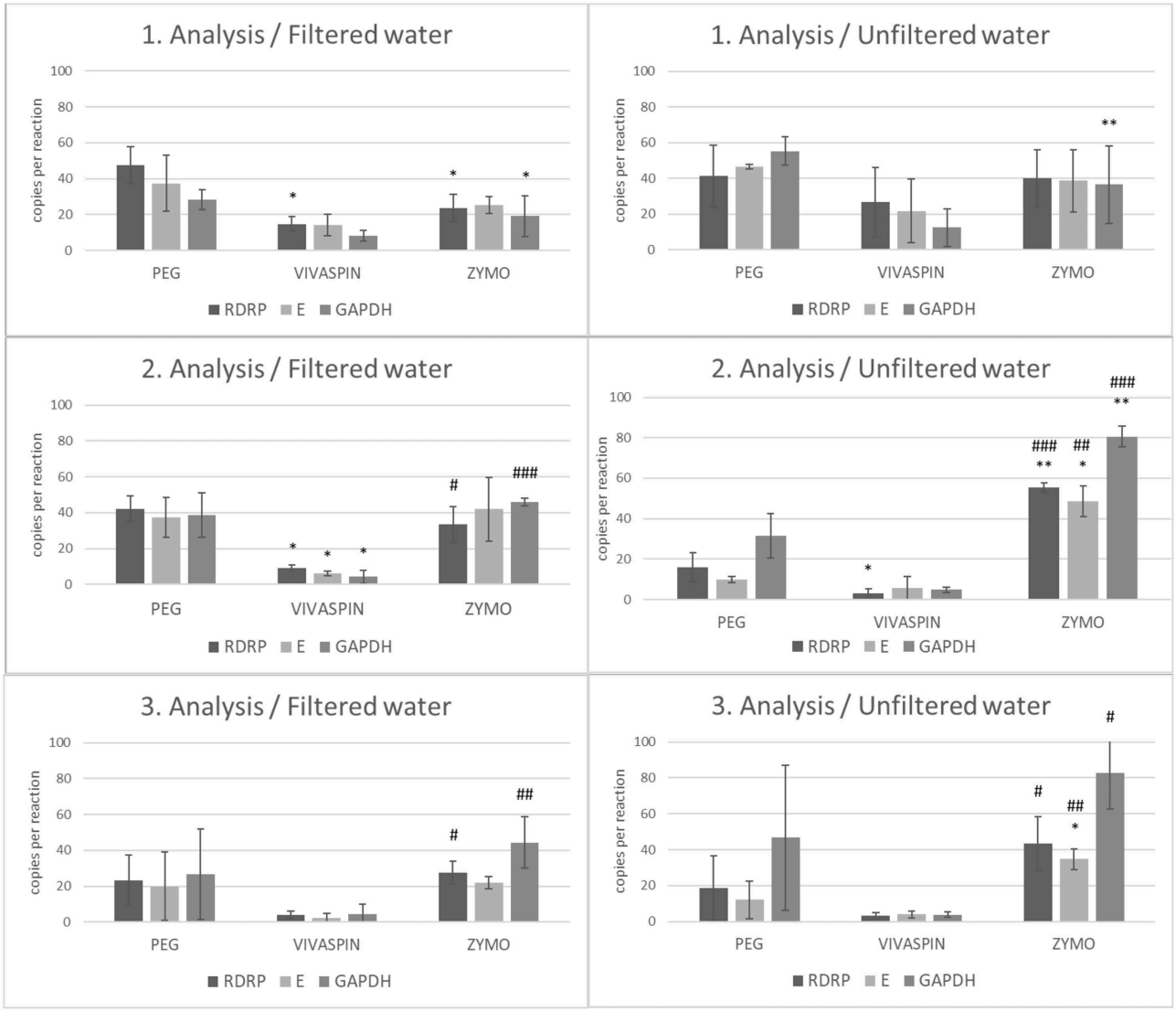

FIGURE 2
The number of copies of SARS-CoV-2 genes (*RdRp*, *E*) and *GAPDH* between filtrated and unfiltered wastewater processed by different separation and isolation protocols measured by RT-ddPCR. Acquired data are expressed as mean ± SEM. Significant difference, $^{*}p < 0.05$, $^{**}p < 0.01$ vs. PEG, $^{\#}p < 0.05$, $^{\#\#}$textitp < 0.01, $^{\#\#\#}p < 0.001$ vs. VIVASPIN.

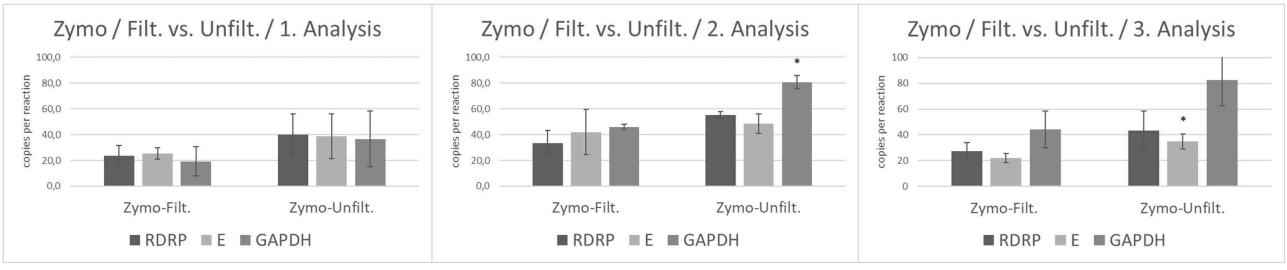

FIGURE 3
The number of copies of SARS-CoV-2 genes (*RdRp*, *E*) and *GAPDH* between filtrated and unfiltered wastewater processed by Zymo Environ Water RNA Kit analyzed by RT-ddPCR. Acquired data are expressed as mean ± SEM. Significant difference, $^{*}p < 0.05$ vs. PEG.

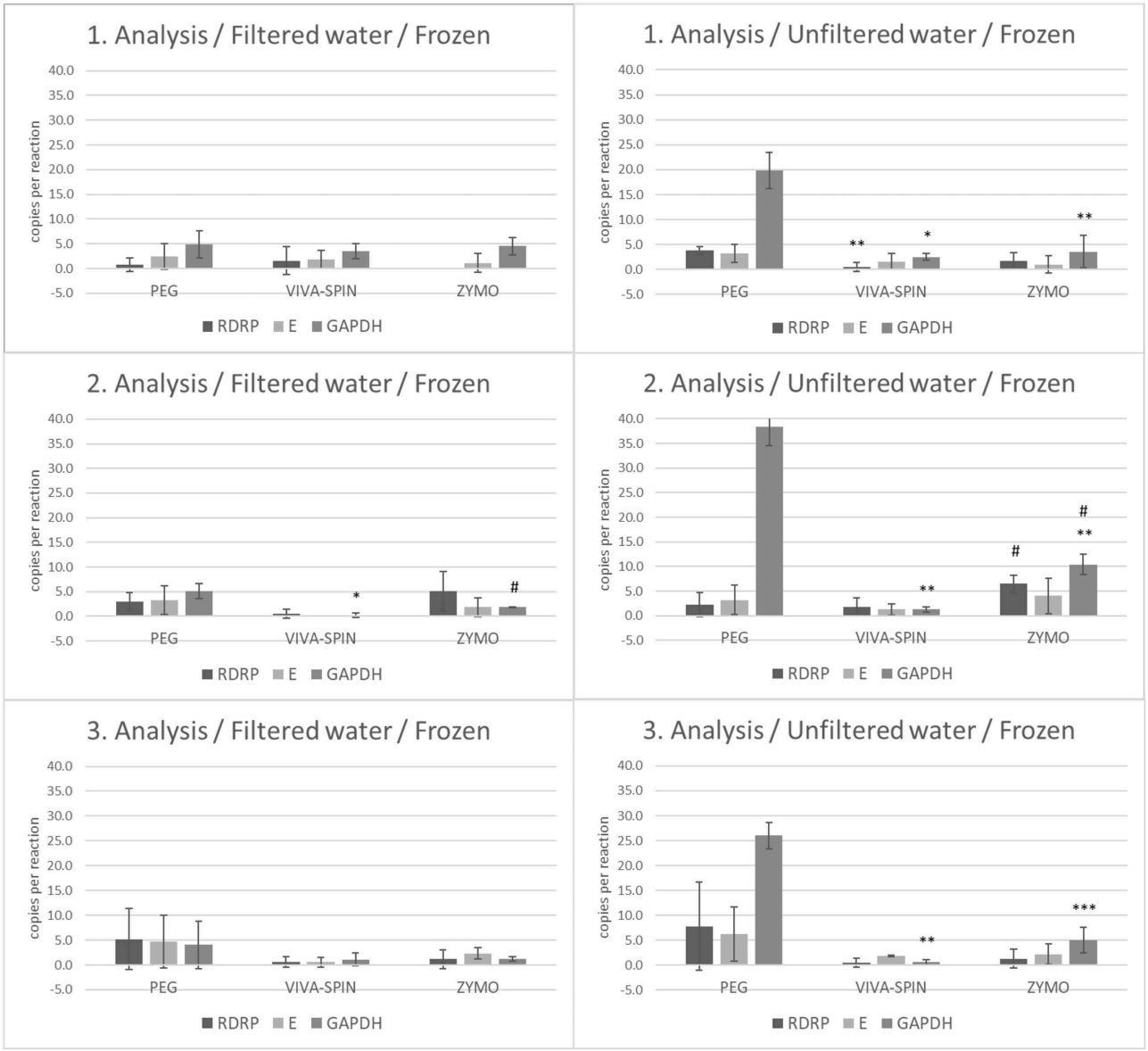

FIGURE 4
The number of copies of SARS-CoV-2 genes (*RdRp*, *E*) and *GAPDH* between frozen filtrated and unfiltered wastewater processed by different separation and isolation protocols measured by RT-ddPCR. Acquired data are expressed as mean ± SEM. Significant difference, $^{*}p < 0.05$, $^{**}p < 0.01$, ***vs. PEG, $^{\#}p < 0.05$ vs. VIVASPIN.

TABLE 2 Comparison of detection methods for viral RNA in weekly analyses of SARS-CoV-2 in wastewater.

Detection method	Replicate	2.5. 2022	9.5. 2022	16.5. 2022	23.5. 2022	30.5. 2022	6.6. 2022	13.6. 2022	20.6. 2022	27.6. 2022	4.7. 2022
RT-ddPCR	1	+	+	+	+	+	+	+	+	+	+
	2	+	+	+	+	+	+	+	+	+	+
	3	+	+	+	+	+	–	+	+	+	+
RT-qPCR	1	+	+	–	+	*	?	–	*	+	+
	2	+	+	+	–	–	?	–	+	–	*
	3	+	+	–	+	–	–	+	+	+	*

RT-ddPCR, reverse transcription-droplet digital PCR; RT-qPCR, realtime-quantitative PCR.
+, positive; –, negative; *, different coronavirus; ?, invalid result.

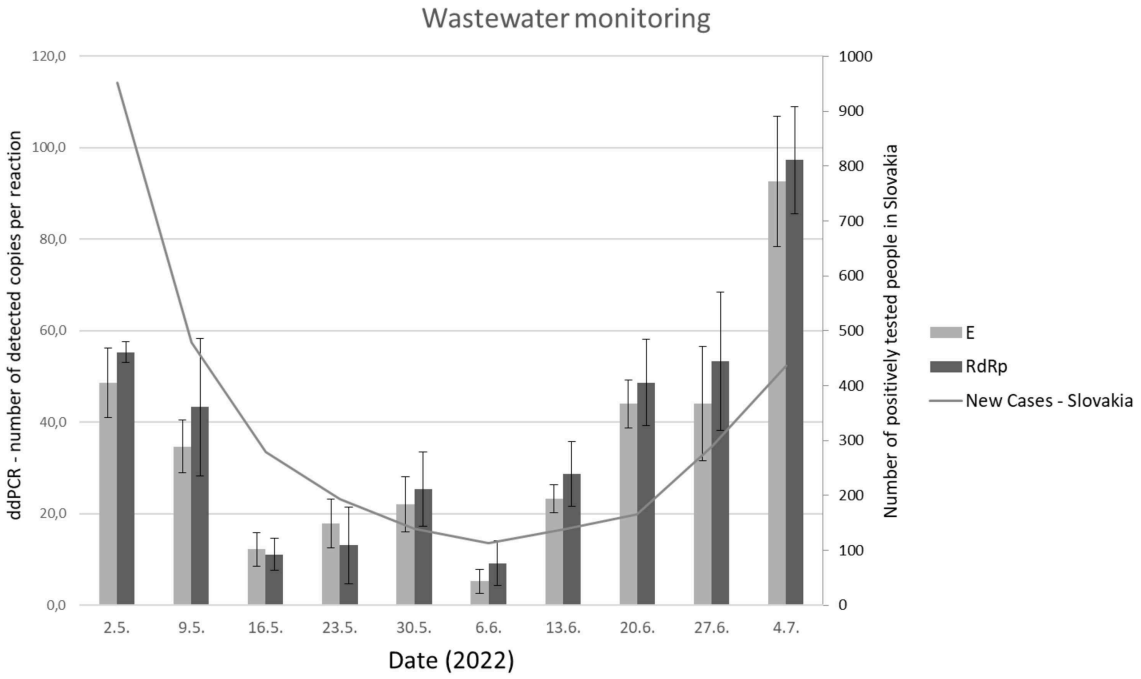

FIGURE 5
The number of copies of viral genes (*RdRp* and *E*) evaluated by RT-ddPCR periodically, from May 2022 to July 2022 in comparison with the epidemiology situation (new cases) in the Slovak republic.

4. Discussion

Waste-based epidemiology (WBE) of SARS-CoV-2 provides a powerful tool for epidemiological monitoring. Specifically, WBE analyses the signals of viral load in wastewater samples pooled by the whole population, regardless of symptoms occurrence, willingness to undergo the testing procedure, or to report the results to the authorities. Hence, WBE offers the possibility of an early warning system for the COVID-19 in the population. Therefore, WBE has rightfully became one of the most potent means for health authorities worldwide to monitor COVID-19 (18). In fact, the predictions of viral transmission dynamics based on such data are resistant to changes in the behavior of the public (e.g., testing practices, healthcare-seeking behavior, etc.) (19). On the other hand, certain limitations like environmental conditions (e.g., actual water temperature, dilution of wastewater due to the increased rainfall, the intermittent presence of chemical compounds that can act as PCR inhibitors, and sampling design) can potentially affect the results of WBE (12). Also, the access of particular demographic groups with specific, often risky, patterns of behavior to the sewage system can be limited. Despite these facts, which indeed need to be taken into consideration, WBE provides the most representative data source for epidemiological surveillance.

The importance of early SARS-CoV-2 detection in wastewater was documented in a recent study by Medema et al. The authors had observed the presence of SARS-CoV-2 RNA in sewage 6 days before the first cases reported in Amersfoort, Netherlands (20). Moreover, Randazzo et al. detected SARS-CoV-2 RNA in wastewater before the first COVID-19 cases confirmed by local authorities in the region of Murcia, Spain (10). Thus, the early identification of SARS-CoV-2 from sewage can play a crucial role in the surveillance of SARS-CoV-2 variants to support public health decision-making concerning measures to limit SARS-CoV-2 spread or allocation of testing or SARS-CoV-2 vaccination (21). Therefore, there is an imminent need to choose the most sensitive and cost-effective workflow for daily routine diagnosis of SARS-CoV-2 from wastewater as a tool to track COVID-19 incidence dynamics through time, even if the positivity rates tested by individual RT-qPCR or rapid antigen tests are low.

In addition to untreated wastewater, primary sludge can also be used as a primary source of viral RNA in the monitoring of the initial, exponential, and re-emergence phase at the epidemic level (22–24). Recent evidence proposed that using a wastewater sludge can be source of SARS-CoV-2 (enveloped virus in wastewater absorbed onto organic matter, resulting in a higher concentration of viral RNA in sludge) (25). Still, wastewater testing remains the most used approach for tracking COVID epidemiology that is appropriate for long-term monitoring of SARS-CoV-2 spreading on the regional level due to inexpensive and easy set-up for laboratory staff (26). However, using the sludge fraction is incompatible with our downstream protocol steps.

The majority of protocols for SARS-CoV-2 RNA isolation from wastewater use initial centrifugation for the removal of debris prior to processing (7, 27, 28). This step is important for reducing the turbidity of wastewater *via* removing larger particles and finer particles, which could inhibit PCR reaction as well as improve virus recovery (mainly for samples nearer the limit of detection) (7, 29–31).

In our study, we compared three different isolation and two detection methods. Centrifugal concentration through the Vivaspin column failed in our experimental settings, although such protocols were successfully performed by other groups (6, 29, 32). We can speculate whether it was caused by the specific physicochemical properties of local wastewater or by the presence of inhibitors that were not removed by filtering procedure, among others. However, due to limited capacity, we did not further investigate the failure of Vivaspin column, just concluded this method as not suitable for our conditions.

We are aware of the existence of multiple variants of PEG precipitation protocols including different combinations of usage of PEG-6000 (33, 34) or PEG-8000 (35, 36), different PEG concentrations ranging from 8%, 10% up to 50% (29, 34), different NaCl concentrations (37–39), and different times of incubation varying from 15 min to overnight (18 h) (11, 40). Not having the capacity to test all of them, we decided to use the protocol utilizing 10% PEG-8000 with 0.3 M NaCl overnight incubation. Despite hands-on experience with this particular procedure, which we performed successfully multiple times, we do not dare to claim it as an optimal technique. Our data are in agreement with Flood et al. and Câmara et al. who concluded that utilization of PEG method provide better virus recovery than the ultrafiltration-based methods (39, 41).

Nevertheless, we demonstrated that the best results were obtained with the Zymo Environ Water RNA Extraction Kit, which is dedicated for the isolation of the RNA from the water medium. Moreover, the Zymo Environ Water RNA kit was the most effective and efficient kit of the four commercial kits tested by O'Brien (42).

RT-qPCR is a commonly used mean of SARS-CoV-2 genome detection for both individual testing (13) and WBE. Only a minority of research groups have carried out molecular assays using RT-ddPCR (43). In contrast, RT-ddPCR demonstrated better results in detecting SARS-CoV-2 gene targets when compared with RT-qPCR in tested wastewater samples (39). According to our experience, RT-ddPCR could identify positive samples more reliably compared to RT-qPCR. For example, sampling from June 6, 2022 provided wastewater with contaminant causing darkish to the black coloration of the specimen that could not been removed by centrifugation nor filtration. The results of that day were particularly wrong (two positive results and one negative for RT-ddPCR vs. two invalid results and one negative for RT-qPCR) but still in a favor of RT-ddPCR. An explanation of this observation can be associated with the fact that ddPCR shows increased tolerance to inhibit substances due to the distribution and separation of individual micro-reactions, which mitigates the impact of inhibitors on PCR amplification by retaining discernible positive signal even if moderate PCR inhibition is occurring in a droplet (44). Moreover, ddPCR is considered to be more sensitive than RT-qPCR (45). These phenomena support the role of ddPCR as an attractive alternative to qPCR for diagnostic applications in conditions when increased sensitivity and processivity is necessary.

We have tested whether our protocol setup for SARS-CoV-2 isolation and detection would be functional if frozen samples were processed. The outcome clearly suggested that, even though the possibility of utilization of such stored material would be beneficial, our optimized workflow does not provide satisfactory results in this case.

Similarly, pre-treatment of wastewater by filtration through a 0.45 μm filter was not beneficial when Zymo Environ Water RNA Kit was used. On the contrary, several non-significant trends were observed in the case of Vivaspin ultrafiltration and PEG precipitation; however, we did not further investigate these two methods due to their inefficiency.

In this work, we have optimized protocol for the detection of SARS-CoV-2 RNA in wastewater in the conditions of our region. However, this workflow or its modifications can be utilized in similar environments elsewhere or can serve as a basis for the development of tools for WBE of SARS-CoV-2 or other pathogens that can be found in sewage system.

5. Conclusion

In conclusion:

- Usage of Zymo Environ Water RNA Kit provided superior quality of isolated RNA in comparison with both ultracentrifugation and PEG precipitation.
- RT-ddPCR outperforms RT-qPCR.
- Freezing of wastewater samples significantly reduces the RNA yield.
- Filtering is counterproductive when Zymo Environ Water RNA Kit is used.
- WBE is a useful and cost-effective tool for SARS-CoV-2 pandemic management with great potential for application on other pathogens.
- We have shown that the sensitivity of testing the samples with a nearer detection limit can be improved by selecting the appropriate combination of enrichment, isolation, and detection methods.

Data availability statement

The raw data supporting the conclusions of this article will be made available by the authors, without undue reservation.

Author contributions

VL and MS: conceptualization, investigation, formal analysis, methodology, validation, writing—original draft, review, and editing. TB, EL, ZK, VH, ET, and AH: methodology, validation, and writing—review and editing. TZ: review and editing, methodology, and resources. PP: investigation, methodology, review, and editing. LR: resources, methodology, review, and editing. ZD, EN, RP, AC, and EH: resources, writing—review and editing, and funding acquisition. All authors contributed to the article and approved the submitted version.

Funding

This work was supported by the Integrated Infrastructure Operational Program for the project New possibilities for

laboratory diagnostics and massive screening of SARS-CoV-2 and identification of mechanisms of virus behavior in the human body, ITMS: 313011AUA4, co-financed by the European Regional Development Fund. The present study was supported by the Scientific Grant Agency of the Ministry of Education, Science, Research and Sport of the Slovak Republic VEGA # 1-0261-22.

Acknowledgments

The authors thank employees of RÚVZ (Regional Office of Public Health) Martin for collection of wastewater samples and Michal Pokusa for material aid.

Conflict of interest

The authors declare that the research was conducted in the absence of any commercial or financial relationships that could be construed as a potential conflict of interest.

Publisher's note

All claims expressed in this article are solely those of the authors and do not necessarily represent those of their affiliated organizations, or those of the publisher, the editors and the reviewers. Any product that may be evaluated in this article, or claim that may be made by its manufacturer, is not guaranteed or endorsed by the publisher.

Supplementary material

The Supplementary Material for this article can be found online at: https://www.frontiersin.org/articles/10.3389/fpubh.2023.1116636/full#supplementary-material

References

1. Wang C, Horby PW, Hayden FG, Gao GF. A novel coronavirus outbreak of global health concern. *Lancet.* (2020) 395:470–3. doi: 10.1016/S0140-6736(20)30185-9

2. Jee Y. WHO International Health Regulations Emergency Committee for the COVID-19 outbreak. *Epidemiol Health.* (2020) 42:e2020013. doi: 10.4178/epih.e2020013

3. World Health Organization (WHO). Available online at: https://www.who.int (accessed November 2, 2022).

4. Pavelka M, Van-Zandvoort K, Abbott S, Sherratt K, Majdan M, CMMID COVID-19 Working Group, et al. The impact of population-wide rapid antigen testing on SARS-CoV-2 prevalence in Slovakia. *Science.* (2021) 372:635–41. doi: 10.1126/science.abf9648

5. Dankova Z, Novakova E, Skerenova M, Holubekova V, Lucansky V, Dvorska D, et al. Comparison of SARS-CoV-2 detection by rapid antigen and by three commercial RT-qPCR tests: a study from Martin University Hospital in Slovakia. *Int J Environ Res Public Health.* (2021) 18:7037. doi: 10.3390/ijerph18137037

6. Trottier J, Darques R, Ait Mouheb N, Partiot E, Bakhache W, Deffieu MS, et al. Post-lockdown detection of SARS-CoV-2 RNA in the wastewater of Montpellier, France. *One Health.* (2020) 10:100157. doi: 10.1016/j.onehlt.2020.100157

7. Ahmed W, Angel N, Edson J, Bibby K, Bivins A, O'Brien JW, et al. First confirmed detection of SARS-CoV-2 in untreated wastewater in Australia: a proof of concept for the wastewater surveillance of COVID-19 in the community. *Sci Total Environ.* (2020) 728:138764. doi: 10.1016/j.scitotenv.2020.138764

8. Bivins A, Greaves J, Fischer R, Yinda KC, Ahmed W, Kitajima M, et al. Persistence of SARS-CoV-2 in water and wastewater. *Environ Sci Technol Lett.* (2020) 7:937–42. doi: 10.1021/acs.estlett.0c00730

9. Kocamemi BA, Kurt H, Hacioglu S, Yarali C, Saatci AM, Pakdemirli B. First data-Set on SARS-CoV-2 detection for Istanbul wastewaters in Turkey. *medRXiv.* (2020) 2020.05.03.20089417. doi: 10.1101/2020.05.03.20089417

10. Randazzo W, Truchado P, Cuevas-Ferrando E, Simón P, Allende A, Sánchez G. SARS-CoV-2 RNA in wastewater anticipated COVID-19 occurrence in a low prevalence area. *Water Res.* (2020) 181:115942. doi: 10.1016/j.watres.2020.115942

11. Wu F, Zhang J, Xiao A, Gu X, Lee WL, Armas F, et al. SARS-CoV-2 titers in wastewater are higher than expected from clinically confirmed cases. *mSystems.* (2020) 5:e00614–20. doi: 10.1128/mSystems.00614-20

12. Li X, Zhang S, Sherchan S, Orive G, Lertxundi U, Haramoto E, et al. Correlation between SARS-CoV-2 RNA concentration in wastewater and COVID-19 cases in community: a systematic review and meta-analysis. *J Hazard Mater.* (2023) 441:129848. doi: 10.1016/j.jhazmat.2022.129848

13. Barreto HG, de Pádua Milagres FA, de Araújo GC, Daúde MM, Benedito VA. Diagnosing the novel SARS-CoV-2 by quantitative RT-PCR: variations and opportunities. *J Mol Med (Berl).* (2020) 98:1727–36. doi: 10.1007/s00109-020-01992-x

14. Falzone L, Musso N, Gattuso G, Bongiorno D, Palermo CI, Scalia G, et al. Sensitivity assessment of droplet digital PCR for SARS-CoV-2 detection. *Int J Mol Med.* (2020) 46:957–64. doi: 10.3892/ijmm.2020.4673

15. Burjanivova T, Lukacova E, Lucansky V, Samec M, Podlesniy P, Kolkova Z, et al. Sensitive SARS-CoV-2 detection, air travel Covid-19 testing, variant determination and fast direct PCR detection, using ddPCR and RT-qPCR methods. *Acta Virol.* (2023) 67:3–12. doi: 10.4149/av_2023_101

16. Suo T, Liu X, Feng J, Guo M, Hu W, Guo D, et al. ddPCR: a more accurate tool for SARS-CoV-2 detection in low viral load specimens. *Emerg Microbes Infect.* (2020) 9:1259–68. doi: 10.1080/22221751.2020.1772678

17. Koronavírus a Slovensko. *Koronavírus a Slovensko*. Available online at: https://korona.gov.sk/ (accessed June 23, 2022).

18. Mazumder P, Dash S, Honda R, Sonne C, Kumar M. Sewage surveillance for SARS-CoV-2: molecular detection, quantification, and normalization factors. *Curr Opin Environ Sci Health.* (2022) 28:100363. doi: 10.1016/j.coesh.2022.100363

19. Sellers SC, Gosnell E, Bryant D, Belmonte S, Self S, McCarter MSJ, et al. Building-level wastewater surveillance of SARS-CoV-2 is associated with transmission and variant trends in a university setting. *Environ Res.* (2022) 215:114277. doi: 10.1016/j.envres.2022.114277

20. Medema G, Heijnen L, Elsinga G, Italiaander R, Brouwer A. Presence of SARS-coronavirus-2 RNA in sewage and correlation with reported COVID-19 prevalence in the early stage of the epidemic in The Netherlands. *Environ Sci Technol Lett.* (2020) 7:511–6. doi: 10.1021/acs.estlett.0c00357

21. Heijnen L, Elsinga G, de Graaf M, Molenkamp R, Koopmans MPG, Medema G. Droplet digital RT-PCR to detect SARS-CoV-2 signature mutations of variants of concern in wastewater. *Sci Total Environ.* (2021) 799:149456. doi: 10.1016/j.scitotenv.2021.149456

22. Sridhar J, Parit R, Boopalakrishnan G, Rexliene MJ, Praveen R, Viswananathan B. Importance of wastewater-based epidemiology for detecting and monitoring SARS-CoV-2. *Case Stud Chem Environ Eng.* (2022) 6:100241. doi: 10.1016/j.cscee.2022.100241

23. Peccia J, Zulli A, Brackney DE, Grubaugh ND, Kaplan EH, Casanovas-Massana A, et al. Measurement of SARS-CoV-2 RNA in wastewater tracks community infection dynamics. *Nat Biotechnol.* (2020) 38:1164–7. doi: 10.1038/s41587-020-0684-z

24. Carrillo-Reyes J, Barragán-Trinidad M, Buitrón G. Surveillance of SARS-CoV-2 in sewage and wastewater treatment plants in Mexico. *J Water Process Eng.* (2021) 40:101815. doi: 10.1016/j.jwpe.2020.101815

25. Fuschi C, Pu H, Negri M, Colwell R, Chen J. Wastewater-based epidemiology for managing the COVID-19 pandemic. *ACS ES T Water.* (2021) 2021:acsestwater.1c00050. doi: 10.1021/acsestwater.1c00050

26. Farkas K, Hillary LS, Malham SK, McDonald JE, Jones DL. Wastewater and public health: the potential of wastewater surveillance for monitoring COVID-19. *Curr Opin Environ Sci Health.* (2020) 17:14–20. doi: 10.1016/j.coesh.2020.06.001

27. Fonseca MS, Machado BAS, de Araújo Rolo C, Hodel KVS, dos Santos Almeida E, de Andrade JB. Evaluation of SARS-CoV-2 concentrations in wastewater and river water samples. *Case Stud Chem Environ Eng.* (2022) 6:100214. doi: 10.1016/j.cscee.2022.100214

28. Bar-Or I, Yaniv K, Shagan M, Ozer E, Weil M, Indenbaum V, et al. Regressing SARS-CoV-2 sewage measurements onto COVID-19 burden in the population: a proof-of-concept for quantitative environmental surveillance. *Front Public Health.* (2022) 9:561710. doi: 10.3389/fpubh.2021.561710

29. Mailepessov D, Arivalan S, Kong M, Griffiths J, Low SL, Chen H, et al. Development of an efficient wastewater testing protocol for high-throughput country-wide SARS-CoV-2 monitoring. *Sci Total Environ.* (2022) 826:154024. doi: 10.1016/j.scitotenv.2022.154024

30. Gallardo-Escárate C, Valenzuela-Muñoz V, Núñez-Acuña G, Valenzuela-Miranda D, Benaventel BP, Sáez-Vera C, et al. The wastewater microbiome: a novel insight for COVID-19 surveillance. *Sci Total Environ.* (2021) 764:142867. doi: 10.1016/j.scitotenv.2020.142867

31. Zhang D, Duran SSF, Lim WYS, Tan CKI, Cheong WCD, Suwardi A, et al. SARS-CoV-2 in wastewater: from detection to evaluation. *Mater Today Adv.* (2022) 13:100211. doi: 10.1016/j.mtadv.2022.100211

32. Ahmed W, Bertsch PM, Bivins A, Bibby K, Farkas K, Gathercole A, et al. Comparison of virus concentration methods for the RT-qPCR-based recovery of murine hepatitis virus, a surrogate for SARS-CoV-2 from untreated wastewater. *Sci Total Environ.* (2020) 739:139960. doi: 10.1016/j.scitotenv.2020.139960

33. Sapula SA, Whittall JJ, Pandopulos AJ, Gerber C, Venter H. An optimized and robust PEG precipitation method for detection of SARS-CoV-2 in wastewater. *Sci Total Environ.* (2021) 785:147270. doi: 10.1016/j.scitotenv.2021.147270

34. Ando H, Iwamoto R, Kobayashi H, Okabe S, Kitajima M. The Efficient and Practical virus Identification System with ENhanced Sensitivity for Solids (EPISENS-S): a rapid and cost-effective SARS-CoV-2 RNA detection method for routine wastewater surveillance. *Sci Total Environ.* (2022) 843:157101. doi: 10.1016/j.scitotenv.2022.157101

35. Kevill JL, Lambert-Slosarska K, Pellett C, Woodhall N. Richardson-O'Neill I, Pântea I, et al. Assessment of two types of passive sampler for the efficient recovery of SARS-CoV-2 and other viruses from wastewater. *Sci Total Environ.* (2022) 838:156580. doi: 10.1016/j.scitotenv.2022.156580

36. Adachi Katayama Y, Hayase S, Ando Y, Kuroita T, Okada K, Iwamoto R, et al. A novel high-throughput and highly sensitive method to detect viral nucleic acids including SARS-CoV-2 RNA in wastewater. *Sci Total Environ.* (2023) 856:158966. doi: 10.1016/j.scitotenv.2022.158966

37. Farkas K, Pellett C, Alex-Sanders N, Bridgman MTP, Corbishley A, Grimsley JMS, et al. Comparative assessment of filtration- and precipitation-based methods for the concentration of SARS-CoV-2 and other viruses from wastewater. *Microbiol Spectr.* (2022) 10:e01102–22. doi: 10.1128/spectrum.01102-22

38. Zdenkova K, Bartackova J, Cermakova E, Demnerova K, Dostalkova A, Janda V, et al. Monitoring COVID-19 spread in Prague local neighborhoods based on the presence of SARS-CoV-2 RNA in wastewater collected throughout the sewer network. *Water Res.* (2022) 216:118343. doi: 10.1016/j.watres.2022.118343

39. Flood MT, D'Souza N, Rose JB, Aw TG. Methods evaluation for rapid concentration and quantification of SARS-CoV-2 in raw wastewater using droplet digital and quantitative RT-PCR. *Food Environ Virol.* (2021) 13:303–15. doi: 10.1007/s12560-021-09488-8

40. Torii S, Oishi W, Zhu Y, Thakali O, Malla B, Yu Z, et al. Comparison of five polyethylene glycol precipitation procedures for the RT-qPCR based recovery of murine hepatitis virus, bacteriophage phi6, and pepper mild mottle virus as a surrogate for SARS-CoV-2 from wastewater. *Sci Total Environ.* (2022) 807:150722. doi: 10.1016/j.scitotenv.2021.150722

41. Câmara AB, Bonfante J, da Penha MG, Cassini STA, de Pinho Keller R. Detecting SARS-CoV-2 in sludge samples: a systematic review. *Sci Total Environ.* (2023) 859:160012. doi: 10.1016/j.scitotenv.2022.160012

42. O'Brien M, Rundell ZC, Nemec MD, Langan LM, Back JA, Lugo JN, et al. comparison of four commercially available RNA extraction kits for wastewater surveillance of SARS-CoV-2 in a college population. *Sci Total Environ.* (2021) 801:149595. doi: 10.1016/j.scitotenv.2021.149595

43. Mousazadeh M, Ashoori R, Paital B, Kabdaşli I, Frontistis Z, Hashemi M, et al. Wastewater based epidemiology perspective as a faster protocol for detecting coronavirus RNA in human populations: a review with specific reference to SARS-CoV-2 virus. *Pathogens.* (2021) 10:1008. doi: 10.3390/pathogens10081008

44. Dingle TC, Sedlak RH, Cook L, Jerome KR. Tolerance of droplet-digital PCR versus real-time quantitative PCR to inhibitory substances. *Clin Chem.* (2013) 59:1670–2. doi: 10.1373/clinchem.2013.211045

45. Li J, Lin W, Du P, Liu W, Liu X, Yang C, et al. Comparison of reverse-transcription qPCR and droplet digital PCR for the detection of SARS-CoV-2 in clinical specimens of hospitalized patients. *Diagn Microbiol Infect Dis.* (2022) 103:115677. doi: 10.1016/j.diagmicrobio.2022.115677

frontiers | Frontiers in Public Health

TYPE Perspective
PUBLISHED 21 March 2023
DOI 10.3389/fpubh.2023.1137881

OPEN ACCESS

EDITED BY
Charlene Ranadheera,
Public Health Agency of Canada (PHAC), Canada

REVIEWED BY
Seil Kim,
Korea Research Institute of Standards and Science, Republic of Korea

*CORRESPONDENCE
TEPHI Wastewater Consortium
✉ TEPHIWastewaterConsortium@gmail.com
Anthony W. Maresso
✉ maresso@bcm.edu

†These authors have contributed equally to this work

SPECIALTY SECTION
This article was submitted to Infectious Diseases: Epidemiology and Prevention, a section of the journal Frontiers in Public Health

RECEIVED 04 January 2023
ACCEPTED 09 February 2023
PUBLISHED 21 March 2023

CITATION
Clark JR, Terwilliger A, Avadhanula V, Tisza M, Cormier J, Javornik-Cregeen S, Ross MC, Hoffman KL, Troisi C, Hanson B, Petrosino J, Balliew J, Piedra PA, Rios J, Deegan J, Bauer C, Wu F, Mena KD, Boerwinkle E and Maresso AW (2023) Wastewater pandemic preparedness: Toward an end-to-end pathogen monitoring program. *Front. Public Health* 11:1137881. doi: 10.3389/fpubh.2023.1137881

Wastewater pandemic preparedness: Toward an end-to-end pathogen monitoring program

Justin R. Clark[1,2†], Austen Terwilliger[1,2†], Vasanthi Avadhanula[2†], Michael Tisza[2,3], Juwan Cormier[2,3], Sara Javornik-Cregeen[2,3], Matthew Clayton Ross[2,3], Kristi Louise Hoffman[2,3], Catherine Troisi[4,5], Blake Hanson[4,5,6], Joseph Petrosino[2,3], John Balliew[7], Pedro A. Piedra[2,8], Janelle Rios[4,5], Jennifer Deegan[5,9], Cici Bauer[4,5,10], Fuqing Wu[4,5], Kristina D. Mena[4,5], Eric Boerwinkle[4,5,11] and Anthony W. Maresso[1,2*] on behalf of TEPHI Wastewater Consortium*

[1]TAILOR Labs, Baylor College of Medicine, Houston, TX, United States, [2]Department of Molecular Virology and Microbiology, Baylor College of Medicine, Houston, TX, United States, [3]Alkek Center for Metagenomics and Microbiome Research, CMMR, Baylor College of Medicine, Houston, TX, United States, [4]UTHealth Houston School of Public Health, Houston, TX, United States, [5]Texas Epidemic Public Health Institute (TEPHI), UTHealth Houston, Houston, TX, United States, [6]Center for Infectious Diseases, Department of Epidemiology, Human Genetics and Environmental Sciences, Houston, TX, United States, [7]El Paso Water Utility, El Paso, TX, United States, [8]Pediatrics Department, Baylor College of Medicine, Houston, TX, United States, [9]The University of Texas Health Science Center at Houston, Houston, TX, United States, [10]Department of Biostatistics and Data Science, UTHealth School of Public Health, Houston, TX, United States, [11]Human Genetics Center, Department of Epidemiology, Human Genetics and Environmental Sciences, Houston, TX, United States

Molecular analysis of public wastewater has great potential as a harbinger for community health and health threats. Long-used to monitor the presence of enteric viruses, in particular polio, recent successes of wastewater as a reliable lead indicator for trends in SARS-CoV-2 levels and hospital admissions has generated optimism and emerging evidence that similar science can be applied to other pathogens of pandemic potential (PPPs), especially respiratory viruses and their variants of concern (VOC). However, there are substantial challenges associated with implementation of this ideal, namely that multiple and distinct fields of inquiry must be bridged and coordinated. These include engineering, molecular sciences, temporal-geospatial analytics, epidemiology and medical, and governmental and public health messaging, all of which present their own caveats. Here, we outline a framework for an integrated, state-wide, end-to-end human pathogen monitoring program using wastewater to track viral PPPs.

KEYWORDS

wastewater, virus, pathogens, detection, epidemiologic, public health, early warning system

Historical backdrop

"A sewer is a cynic. It tells everything." Victor Hugo, *Les Miserables* (1892).

In 1939, a plane departed Detroit in route to Connecticut carrying a very unusual piece of cargo. Destined for the laboratories of Drs. John Paul and James Trask at Yale University, the package consisted of several samples of Detroit city sewage. Years earlier, Paul and Trask reasoned that since the virus that causes polio could be found in fecal matter [first reported in 1912 (1)], it may also be shed into city wastewater (2). When macaques were injected with the sewage (there was no PCR at the time and microscopy was still developing) showed signs of poliomyelitis, a result confirmed by researchers in Stockholm (3), it suggested a human virus found in public excrement might report on the state of disease at the population level. However, it was a mentee of Paul, Dr. Joseph Melnick, who showed in the 1940s that polio levels in stool and sewage are associated with the number of severe cases in the population (a result that prompted him to search for viral prevalence based on fecal shedding rates), studies that birthed the field of wastewater-based epidemiology (WBE) (1, 4, 5). This led to the implementation of environmental poliovirus surveillance (EPS) systems in countries where polio cases are still endemic, and the emergence of WBE for poliovirus and other pathogens (6).

Recent SARS-CoV-2 experience—Rebirth

Success of the use of wastewater to monitor SARS-CoV-2 levels, and forecasting future trends aiding in public preparation and hospital-readiness, has reinvigorated viral WBE. Consensus is that similar approaches may be applied to other human viral pathogens, including adenoviruses, enteroviruses, noroviruses, rotavirus, and hepatitis viruses. The Centers for Disease Control and Prevention (CDC) initiated the National Wastewater Surveillance System (NWSS) in September 2020 to track the dispersion of SARS-CoV-2. Our own team's activity began in April of 2020 in the cities of Houston and El Paso, Texas, both of which have implemented a city-wide SARS-CoV-2 wastewater (WW) monitoring program (7–9). Recently, the CDC expanded their SARS-CoV-2 wastewater testing program to include poliovirus after vaccine derived poliovirus was detected in New York state (10). This implies a U.S. readiness to apply such a program and science to other viral pathogens.

SARS-CoV-2 and other respiratory viruses are well-known to cause gastrointestinal (GI) symptoms like diarrhea and vomiting (11–16). The GI manifestations are associated with viral RNA and infectious virus in fecal samples and can be detected throughout the course of infection (17–19). Additionally, histologic studies have shown SARS-CoV-2 virions damaging the GI epithelium (17, 19, 20). SARS-CoV-2 infected persons have peak viral loads 1–3 days before symptom onset and can shed virus for three or more weeks (21, 22). Both symptomatic and asymptomatic individuals can transmit the virus efficiently and can have prolonged viral shedding (23–25). Although it cannot be expected that all human viruses will present with an infection biology and natural history that is conducive to WBE (such as SARS-CoV-2), there is reason to believe many viruses like adenoviruses and enteroviruses with major epidemic potential will be amenable to similar WBE. This is the impetus for the efforts described in this perspective.

To our knowledge, comprehensive province/state or nationwide monitoring of various human pathogens in wastewater has not been implemented anywhere. Even the monitoring of illicit drug use, which was proposed by the U.S. Environmental Protection Agency 2 decades ago (though it is more commonly used in European cities), appears to have no standardized widespread use (26, 27). On the city level, SARS-CoV-2 has been monitored in wastewater in every continent except Antarctica (8, 28–32). The closest any country has come to implementing SARS-CoV-2 wastewater monitoring on the national level may be, as described above, the National Wastewater Surveillance System (NWSS) in the U.S. by the Centers for Disease Control and Prevention and the U.S. Department for Health and Human Services in September 2020 (33). Most of the recently published WBE studies appear to be the work of academic researchers analyzing samples they have been given access to or local health departments (or equivalent) working with academic researchers to monitor SARS-CoV-2. The NWSS was started to coordinate these SARS-CoV-2 wastewater monitoring efforts in the U.S. What started with pilot sites in 8 states in 2020 now has over 1,250 sites covering over 100 million people (33). However, the NWSS Committee on Community Wastewater-Based Infectious Disease Surveillance points out a major shortfall with the NWSS in that it currently "…consists of localities, tribes, and states that were willing and able to participate during the pandemic emergency…" and this pandemic emergency, "…spurred many researchers and utilities to volunteer their labor and donate resources in support of the effort, but the vision of a sustained national wastewater surveillance system necessitates a shift from volunteerism to a strategic national plan with well-defined roles supported by federal investments" (33). Given the success of the NWSS in tracking SARS-CoV-2 and citing success in tracking vaccine-derived polio outbreaks in London and New York, and success in rapidly tracking monkeypox, the aforementioned committee has recommended expanding the NWSS efforts to monitor other human pathogens (10, 33–37).

Reminiscent of the NWSS in the U.S., national and international efforts to track SARS-CoV-2 have recently been made in Israel and the European Union, respectively. In Israel, researchers at the Israel Ministry of Health have described their methods of tracking SARS-CoV-2 and SARS-CoV-2 variants in wastewater using PCR on samples from 13 treatment plants that cover more than 50% of Israel's population (38). In 2021, the European Commission adopted a Recommendation that EU Member States work toward monitoring SARS-CoV-2 in wastewater (39). As of March 2022, more than 1,370 wastewater treatment plants are under surveillance (40). However, to our knowledge, no effort to expand these efforts to other pathogens in a routine manner has been made.

A statewide pandemic preparedness initiative

In the Spring of 2021, the 87th Texas Legislature established the Texas Epidemic Public Health Institute (TEPHI). Housed

within The University of Texas Health Science Center at Houston (UTHealth Houston), TEPHI's mandate is to work collaboratively with state, local, and federal agencies, academic institutions, professional associations, businesses, and community organizations to better prepare the state for public health threats. TEPHI's mission and structure is informed by lessons learned during the Texas response to the COVID-19 pandemic to address gaps in public health organization and infrastructure in order to better inform, train, and protect Texans.

As part of the effort, TEPHI is launching numerous programs to support community preparedness across the state, including a collaboration with Baylor College of Medicine (BCM) and the UTHealth Houston School of Public Health (SPH) to establish a statewide Texas Wastewater Environmental Biomonitoring (TexWEB) network. The TWC (TEPHI Wastewater Consortium) will (1) partner with state utilities and public health departments to promote the virtues of wastewater science; (2) establish standard operating procedures (SOPs) for the detection of viral and/or other pathogen nucleic acid from complex wastewater sludge; (3) incorporate the latest cutting-edge technologies to enhance target detection; (4) serve as the state's real-time and ongoing wastewater pathogen monitoring system (prioritizing disease-causing human viruses in the first stages); (5) generate health department, health care and community data repositories that allow users to assess risks and trends in their counties; and (6) establish an effective chain-of-command reporting network that informs public health departments and state governments concerning levels and trends of viral PPPs in sentinel communities across the state. Charges 5 and 6 are particularly important, specifically for ensuring agreement when a detection event poses an immediate or sustained health concern, and the processes by which stakeholders are notified. This article provides an overview of the planning and effort for the first 6 months of the program, hopefully serving as a guide for other states to consider implementation of similar monitoring endeavors. Figure 1 demonstrates the specific procedural and methodological elements of this program, which are outlined in detail below.

Nucleic acid: The universal viral WBE detection target

The hallmark principle of WBE is to translate the upstream detection of a chemical or biological substance into reasonable public health information or action. Some of the earliest WBE involved monitoring for pollutants in the early 20th century in England (41, 42). Contemporary WBE has expanded to include pesticides (43) macrolide antibiotics (44), organophosphate esters (45), illicit substances (46–55), antibiotic resistance (56–58), and the topic herein, pathogenic viruses. Regardless of what is detected, all detection activities are unified around the assumption that the concentration of a substance, biologic (here a virus) and/or other agent will be proportional to the amount excreted by the population or contaminating the water supplies. The levels of this agent are thought then to be reflective of the relative risk or status of the health of the population that sheds or is exposed to the agent.

To this point, most non-pathogen WBE has been based on chemical analysis of small molecules or chemical substances. Since each substance has its own unique chemical characteristics, the method by which the agent is detected must be tailored to utilize these properties. This dilemma is potentially less of a concern for viral WBE for two main reasons, which, in theory, may facilitate the monitoring of many viruses of concern using a shared or single methodological platform. These features are (1) the universal presence of nucleic acid (DNA and RNA) in all pathogens, including viruses and (2) the invention of oligo-based priming and amplification of said DNA by polymerase chain reaction (PCR) or of RNA by the reverse transcription of RNA into DNA with subsequent amplification of the DNA target (RT-PCR). The first feature simplifies detection technology to a narrow chemical space (nucleic acid, being composed of only four bases, is much more chemically similar to all other nucleic acid, regardless of the source pathogen). The second feature facilitates the massive amplification of trace amounts of this molecule to greater than a trillion times its original concentration, thereby enhancing sensitivity. The high specificity of primers matched to the target in question and the measurement of light-emitting probes bound to amplified products (RT-PCR) generates a highly sensitive DNA/RNA detection system, regardless of pathogen. When also applied to modern DNA sequencing technologies to derive a genetic barcode of the amplified nucleic acid, the unambiguity of sequence information makes identification of the pathogen unequivocal. As such, these principles and technologies are/have been used detect the presence of viral and bacterial pathogens, fecal bacteria, and antibiotic resistance genes (59–65).

The Consortium's methodological approach to viral detection

In the WBE efforts proposed herein, the Consortium has leveraged the above principles to implement two methodological approaches to track human viruses in wastewater (Supplementary Figure 1). The first (so-called "targeted" method) uses RT-PCR and Digital PCR to detect respiratory, gastrointestinal, and blood-borne viruses that are either commonly transmitted in community settings (e.g., SARS-CoV-2, Flu, RSV, norovirus) or are periodically endemic to the Southern part of the U.S. (some arboviruses, including dengue viruses). The advantage of a targeted approach is sensitivity and speed. By using well-designed primers to the virus in question and a validated PCR assay, very low levels of viral nucleic acid can be detected in hours. Digital PCR increases sensitivity by diluting the sample into hundreds to thousands of partitions, thereby ensuring that inhibitors of a reaction may be "diluted out" of some partitions. The technique is useful for detecting nucleic acid that may be in low abundance for one reason or another (see below).

PCR contrasts with the second method, termed by the Consortium "agnostic" or "comprehensive." Past efforts to characterize the virus metagenome (all the genomes of viruses in a sample) have relied on enrichment of virus-like particles, the capture of viral nucleic acid with probe-based pulldowns, or shotgun whole genome sequencing (66–69). The preponderance of plant viruses or phage in these datasets, and/or the use of probes designed for only a subset of human viruses, limits a pan assessment of disease-causing human viruses. The agnostic approach used by this Consortium employs a next-generation

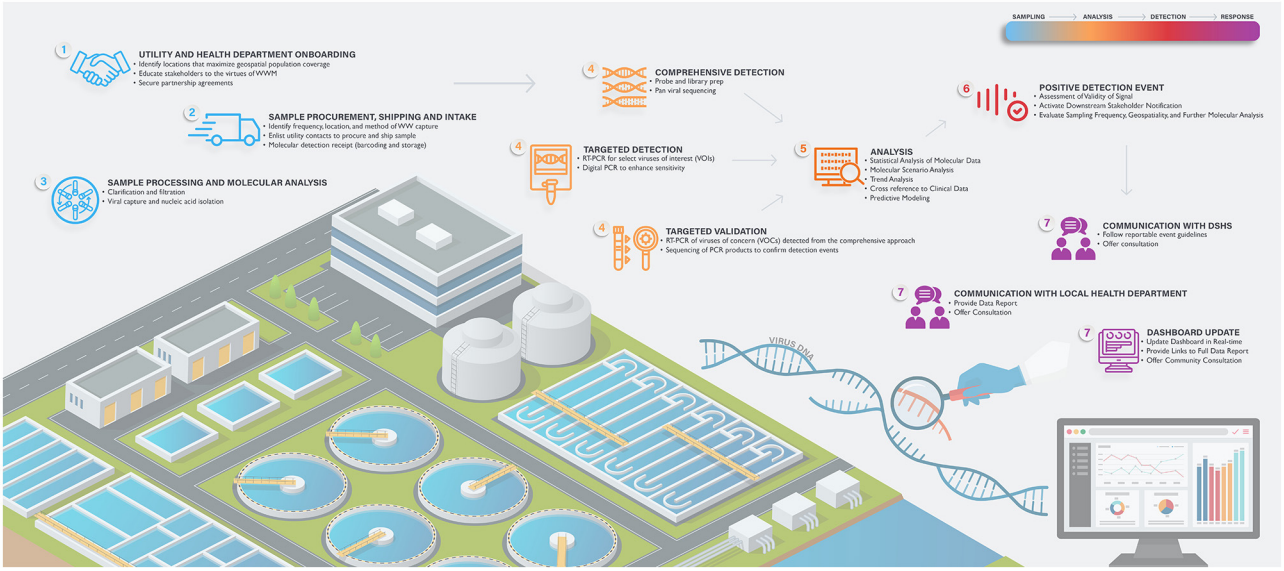

FIGURE 1
Formation of an end-to-end, statewide wastewater viral epidemiology program. Step 1—utility onboarding; Step 2—sample procurement, shipping and intake; Step 3—sample processing and molecular analysis; Step 4—targeted and comprehensive detection with targeted validation; Step 5—analysis; Step 6—positive detection response; Step 7—health department notification, communication to government stakeholders and community data update.

probe-based capture sequencing panel (TWIST Comprehensive Viral Research Panel) capable of detecting over 3,000 human and animal viruses, as well as novel variants of known viruses targeted by the panel. Additionally, while the enrichment step utilized prior to next-generation sequencing vastly lowers the amount of off-target sequencing generated from other WW components, the sheer number of detectable viruses necessitates deep sequencing to achieve both the breadth and depth of reads needed for reliable viral detection. While the cost of sequencing continues to decrease year-over-year, the agnostic approach is more expensive than the targeted approach. Importantly, whereas the agnostic approach might have reduced sensitivity as compared to the targeted approach, its value is that it provides an unbiased "whole virome" analysis of a complex sample. This allows the Consortium to capture "everything else" not covered by the targeted analysis, which may prove useful for hundreds of other viruses that cause human diseases, variants of specific viruses (because sequence information increases specificity), as well as novel emerging viruses that are not yet on any clinical radar. Unlike the targeted approach, the agnostic method takes a few weeks for a full analysis to be finished, incurs additional costs, and requires significant technical expertise. A summary of advantages and disadvantages to each technique outlined here can be found in Supplemental Table 1.

Validation and limitations of current methodological approaches

Although nucleic acid provides for streamlining of the detection pipeline, there are recurring concerns that one must be aware of and require further investigation. We briefly discuss some here so that others who wish to consider this work are informed. Because each virus has its own biology, chemistry, and natural history of infection, each of these attributes will affect viral levels detected in WW. Some overriding determinates are that the virus or its nucleic acid (1) must be shed in human excrement (or enter wastewater in some consistent way); (2) must be relatively stable in raw sewage exposed to a harsh chemically and environmentally-shifting conditions; and (3) be enriched during the viral capture steps. Many viruses have a human infection biology that likely precludes them from excretion into the WW (perhaps their infection tropism has nothing to do with the gastrointestinal or urinary tract). Even if excreted, others have a capsid or membrane structure that is unstable, thereby exposing their sensitive nucleic acid to harmful sludge conditions. Finally, viruses may be excreted and be stable but if the targeted or capture method fails to bind them, they cannot be detected. Thus, any pipeline attempting to provide universal (or even highly targeted) detection may have one or more of these issues affecting the outcome.

When conditions 1–3 above are met, other factors may limit sensitivity or reproducibility. Adding to the list above, these include, but are not limited to; (4) the number of infected people; (5) the amount or frequency of shedding; (6) transit time to the plant; (7) composition of the plant sewage (8) environmental changes such as rainfall or temperature; (9) collection technique and sample transport; (10) storage of sample; (11) capture technique (e.g., size, ionicity); (12) co-purifying inhibitors of the capture or detection methods (including non-specific binding of viral material to wastewater matter or direct inhibition of this matter of downstream processes); (13) whether the liquid or solid phase is examined; and finally (14) sensitivity, specificity, and genome coverage of the probes and primers, homology of the primers to variants and emerging pathogens, and so forth. A summary of limitations and associated reasons that impact viral

and pathogen detections can be found in Supplemental Table 2. Where possible, care should be taken to limit the negative impact of these on the process to limit attrition of signal. In the targeted approach, this is easier to achieve because the emphasis is on a single virus. Use of the targeted virus or its nucleic acid as a proxy ("spike-in") during tests of the pipeline can determine what factors affect levels and signal (attrition). However, in the agnostic approach, because of the sheer magnitude of total viruses surveyed, it is not currently possible to optimize capture, amplification, and detection for every virus. In these cases, a best-fit approach is taken, whereby what works for a subset of key viruses (we use SARS-CoV-2 as a representative constituent) provides confidence that the methodological conditions are conducive to detecting many but not all viruses.

How will detection events be validated? The PCR technology itself has shortcomings in that nucleic acid shearing can reduce priming (false negative), while the lack of primer specificity can produce off-target amplification (false positive). One common method for validating the targeted method (here PCR) is to have the test repeated in a second, independent laboratory (70, 71). However, a second laboratory testing the same corrupted sample may produce the same result. One benefit of using a two-pronged approach (i.e., targeted and agnostic as described above) is the orthogonal nature of verification; if two distinct tests are positive, and detection is achieved *via* different methods, there is strong evidence the signal is real. In time, we hope to add a third assay, so-called "targeted sequencing," which will employ primers that tile across the entire viral genome of the virus in question, to produce sequence information that coverages at or near 100% of the genome. Not only does this provide confidence the detection is real, it also has the value of increasing the ability to identify variants that are present or emerging (72–74).

Onboarding utilities and safety

Successful upstream of viral detection requires public works utilities to gain access to wastewater samples and expertise in wastewater treatment processes and engineering. Specific legal agreements regarding disclosures of sampling sites, use of the information, and general risk assessment may be required between those analyzing the samples and those providing them. There are costs associated with sampling, including personnel, equipment needed for sampling, and shipment of the sample itself. Many utilities already understand the risks associated with working with such material, but detection science may reveal additional pathogens not routinely considered for risk assessment. Quantitative microbial risk assessment (QMRA) is a systematic approach to estimating the probability or likelihood of infection, illness and death from exposure to disease-causing pathogens. The dynamic, four-component framework of hazard identification, dose-response assessment, exposure assessment, and risk characterization defines an iterative process that comprehensively evaluates the pathogen-host interaction (75). The focus of a QMRA is the pathogen, with data generated from field and/or laboratory studies to inform its occurrence in the environment, its survivability and virulence properties, and its transmission pathways. Previous human dose-response studies are available for many pathogens transmitted through environmental sources (such as air, water, food and fomites), and best-fit mathematical models have been developed to represent infection probabilities for specific microorganisms (76).

One of the objectives of our TWC pipeline is to develop a reverse QMRA to public health readiness, for example to estimate the number of infections in a community based on viral levels in WW. The data obtained in a traditional QMRA is pathogen specific with information characterizing the host-pathogen interaction including incubation period, morbidity ratios, range of symptoms, likelihood of secondary transmission, and specific sequelae, such as excretion patterns. By applying the appropriate dose-response model in a reverse QMRA, the number of infections within a community can be estimated based on the microbial composition of the sewage serving that municipality. This QMRA approach can be used to interpret wastewater monitoring trends observed over time, with qualitative characterization revealing unseasonal pathogens due to unexpected community infections and illnesses. Algorithms can then be developed to estimate the number of community infections after a PCR or sequencing result is attained. Through integration, the qualitative and quantitative QMRA output can estimate the likelihood of community transmission, determine whether an outbreak is occurring, or estimate if an epidemic is imminent. At the moment, reverse QMRA seems possible for SARS-CoV-2, influenzae, norovirus, monkeypox, and possibly respiratory syncytial virus (RSV). Such output will address the assumption described earlier that the amount of pathogen detected in sewage is proportional to the amount excreted by the population served by that wastewater system, as well as help estimate the possible number of people infected.

Data analysis and statistics

It has been reported that SARS-CoV-2 detection in wastewater leads case reports by 2–14 days, though it has been argued that a 4-day lead time is the most plausible (8, 77, 78). Estimations of lead times for hospitalizations have been reported to be 4–8 days (79, 80). Though limitations of such WBE lead time calculations have been noted, it has been calculated for other pathogens such as influenza virus A, where wastewater detection led clinical case detection by 17 days, and RSV, where wastewater detection led clinical detection by about 1 week (77, 78, 81). Olesen et al. (77) succinctly argued some of the issues with the currently ill-defined idea of "lead times" in WBE and how the term has been used in different circumstances. They outlined these circumstances as, (1) "qualitative detection of disease presence/absence," (2) "independent, quantitative estimate of community-level disease," and (3) "quantitative estimate of rapid changes in disease incidence" (77). For the purposes of TEPHI, the first circumstance—"qualitative detection of disease presence/absence"—is the initial goal when dealing with non-SARS-CoV-2 pathogens.

Essential to viral WBE is the formation of predictive or forecasting models that provide lead-time warning of outbreaks, transmission, or an ongoing epidemic or pandemic. Formation of such models requires data analysis on historical data with both wastewater and epidemiological/clinical data to establish the relationships between viral nucleic acid detected in the

wastewater and the epidemic severity (e.g., reported case rates), from which models may be further developed for forecasting. As an example, various studies have reported the promising potentials of WBE during the SARS-CoV-2 pandemics, however challenges remain. A recent review by Faraway 2022 made recommendations in building quantitative prediction models using WBE (82), emphasizing key factors that determine the accuracy of any forecasting models including: (1) sampling design; (2) sensitivity and reproducibility of the measurement process; (3) availability of the auxiliary environmental variables; (4) the amount of clinical data to provide for cross correlation; and (5) prior knowledge of the particular disease under study (more difficult for newly emerging pathogens, for example Zika). All of these are being addressed by the TEPHI Wastewater Consortium in some fashion. In addition, we identified other obstacles as: (6) the lack of state and/or countrywide data repositories accessible to interested stakeholders; (7) fragmented clinical data sets that lack metadata; and (8) lack of robust real-time data sharing portals (not only among investigators in the same fields but also in distinct fields, example linking viral PCR data to nasal testing data for SARS-CoV-2).

The Consortium's public health approach to viral WBE

Equally challenging as viral detection is the use of this information for public health action. Although the practice is still developing, some broadly agreed-upon actions are emerging. At this juncture it is important to emphasize the complementary nature of WBE, traditional public health and clinical surveillance. Clinical observation of an infected patient for a rare condition or an increase in frequency of infections in the population for a common condition often proceeds meaningful signal in wastewater at a distant locality. For example, in the recent pandemic, SARS-CoV-2 in Wuhan, China and Lombardy, Italy were examples of what the rest of the world was going to experience. In this context, WBE can then be tailored to look for the appearance of the pathogen in other locations. In our network, for example, El Paso, TX is a border town that, because of its arid location, recycles nearly 100% of its water. It is also a global leader in wastewater technologies and a lead city for the monitoring program mentioned herein. Houston, on the other hand, is a major metropolis with many catchment areas and receives international travelers. In these cases, WBE can be used to catalyze development of a local response plan to an initially "far-off" threat. As the local response plan is initiated, WBE may activate alerts in nearby or more remote cities to initiate, intensify, or expand their monitoring programs. One might think of certain cities as canaries for a country (a good example for the U.S. might be large coastal cities that receive international travelers such as New York and Houston). Another way that WBE can be used following changes in reported cases is to answer the question of how broad the geographic distribution of an early outbreak is. For example, is the recent observation of a paralytic poliomyelitis case in NY a bellwether for reemergence of polio in the United States? Observations from clinical and public health surveillance does not necessarily have to precede WBE, and one reason to continue to improve WBE operations and laboratory sensitivity and specificity is to improve early detection before a local outbreak reaches the clinical horizon. The lead time examples of both polio and SARS-CoV-2 cases serve here to show that detection can significantly precede clinical detection.

Public health surveillance and action need to be seen as complementary and occurring simultaneously. For example, West Nile is a virus being monitored in our program. However, before West Nile is observed in an area, public health activities and educational programs should be working to eliminate standing water and implement other mosquito control measures. Second, what actions must be performed for the detection of less common but very concerning viruses? Following the 2014 occurrence of Ebola in Dallas, TX, protocol development, table-top exercises and personnel training for handling these and similar patients became a regular feature of public health, emergency management, first responders and health care. As we work to better understand how syndromic surveillance, healthcare case trend monitoring, WBE, and public health can better coordinate and communicate, it is important that WBE be included in the preparedness and response process with full knowledge of its strengths and weaknesses. Managing expectations is critical. At the moment, it is not certain if viruses of substantial concern such as Ebola or Smallpox can even be detected in public WW, and, if so, whether it will be a lead indicator of more transmissions.

The Consortium has identified four examples of public health and clinical actions informed by WBE that are of clear benefit, which include: (1) upstaffing in response to a detection event or trend. For example, during the COVID-19 pandemic it was not unusual for health care systems to employ contract nurses to meet surge capacity during a peak of the infection driven either by seasonality or emergence of novel SARS-CoV-2 variants. Similarly, wastewater-based forecasting has been used to aid in planning staffing needs and visitation policies at nursing home facilities; (2) In 2022, the United States had a summer monkeypox outbreak in multiple cities. At the time, vaccine supply was limited, so it was important to quickly develop strategies for getting the most population-benefit from the available orthopox vaccine. Mobile or pop-up vaccine units can be set-up in areas where the virus is present and at-risk individuals frequent; (3) related to 2 above, the Consortium is working to detect vaccine-preventable viruses such as measles and rubella. Given resistance against routine vaccination, it is possible viral WBE may report areas of vaccine fallout (for example, lowered vaccination rates leading to reemergence of vaccine-preventable diseases (of note, it is now reasonable to add SARS-CoV-2 to this list); (4) Finally, WBE can be a sturdy bridge to community engagement and education. An often over-looked but critical communication need is public awareness of WBE is presentation of a complex process into layperson digestible information, and what the information means for the community and its members (relative risk and behavior). For example, the Consortium aims to generate three types of data sets that scale in complexity depending on the stakeholders engaged. The first set will be highly technical, designed mostly for scientists developing the methodologies of detection and downstream analysis. The second will be a slightly less detailed but broad summary of levels aimed for public health and government officials. Finally, the last set includes community interactions (possibilities include

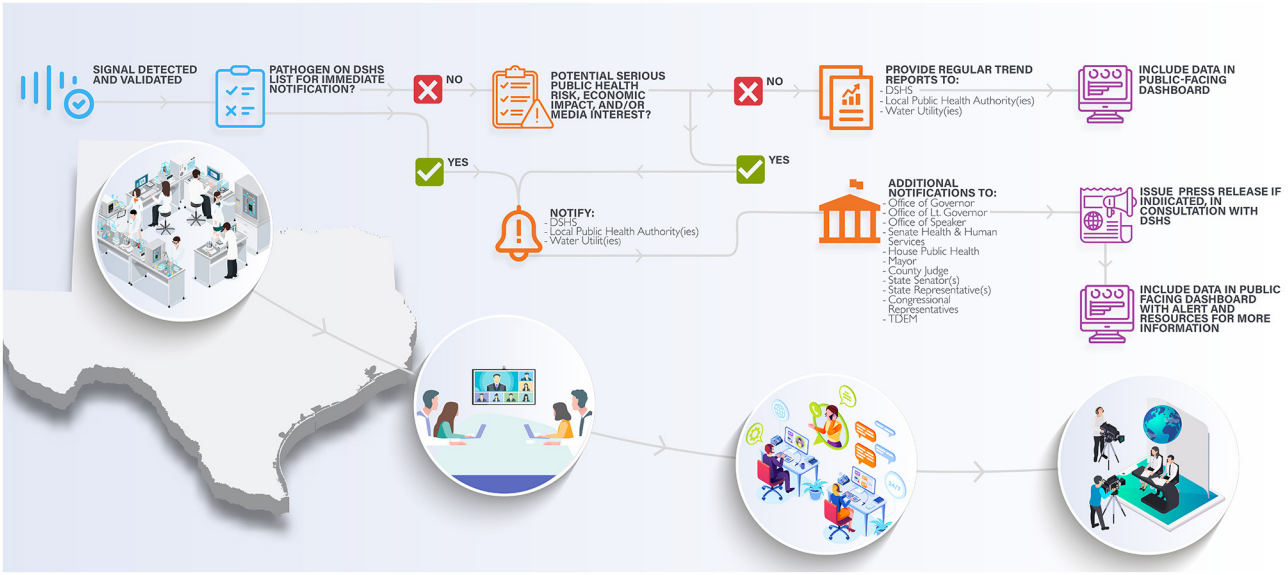

FIGURE 2
The wastewater detection notification scheme and network. Validated viral detection events of concern are assessed first for whether they are on the DSHS immediate notification list. DSHS as well as other stakeholders (local public health experts, state leaders, and/or utilities) are notified with additional action dependent on the threat of the concern (for example, smallpox vs. influenzae). Additional actions such as consultation with stakeholders and/or a press release may be needed. Viruses of seasonal or endemic nature (influenzae, SARS-CoV-2, RSV) are automatically entered into a real-time trend analysis with user-friendly reports provided on a regular basis (dependent on whether the targeted or agnostic method is being used). Long-term goals include a user-friendly community data set segmented in time, space, and viral species or variant detected.

dashboards, togglable links more in-depth information about threat levels or risk, etc) relevant to public health. This final set requires investigation into what is appropriate to report. Community engagement and buy-in (town halls) are critical, as some viruses can be stigmatizing to communities (for example, HIV). A summary of the Consortium's current plan for a public health arm following a validated detection event is shown in Figure 2.

The future

Outside of the clear opportunities and challenges presented above with implementation of the TWC program, there are other exciting areas and challenges to consider as this field evolves and matures. On the detection front, the "what to detect" seems to be ever-changing and is always of importance. The U.S. Environmental Protection Agency has identified many pathogens that might be present in WW, including bacteria (*V. cholera*, *Salmonella typhi*, *enteropathogenic E. coli*, *Campylobacter jejuni*, *shigella dysinteriae*, and *Yersinia entrocolitica*), protozoa (Giardia, Cryptosporidium, *E. histolytica*), and helminths Ascaris, Ancylostoma, Trichuris, and Strongiloides (83). It is absolutely clear that WW harbors bacteria carrying genetic elements that confer resistance to antibiotics. This "silent pandemic" is expected to claim 10 million lives annually by 2050 and, since tracking of the emergence of resistant genes can prepare clinicians for where to provide antibiotic stewardship, WBE may be a useful source of such information. Although currently not considered by the Consortium, one also wonders if a community's immunologic status may be inferable from WBE, especially as it relates to inflammation or neutralizing antibody status to certain pathogens (one application of QMRA). On the public health front, it is clear relaying the information to stakeholders and the downstream steps they take are of substantial priority. This requires integration of utilities and their expertise in wastewater management, molecular scientists and technicians detecting the agents, the statistical and computer scientists analyzing the data, and the liaisons to connect these parties to the public health network, government officials and community. The Consortium is building a unified and integrated program that links these stakeholders in Texas. Finally, one wonders if the principles, pipeline, and program constructed from viral WBE may be applied to other medium monitoring activities, particularly air, which TEPHI plans to expand. Detection of viruses in air samples has already been demonstrated (84–87), but is associated with its own set of challenges, including sampling equipment (pump type, collection media), protocols (sampling volume, time, rate), varying sampling conditions (temperature, humidity), transport and storage conditions, and the type of virus to be detected (88).

In summary, the Consortium has begun efforts to implement a robust, real-time, and reliable viral WBE program across the state of Texas that brings utilities, microbiologists, chemists, clinicians, epidemiologists, statisticians, and public health experts together to identify and appropriately respond to viruses of pandemic potential. Some early success has been realized in utility onboarding, implementation of at least two molecular detection methods, and the creation of an integrated team that span the above fields of inquiry. In time, we hope to report further gains and obstacles in the coming year as the science and programmatic features of viral WBE continue to grow locally, nationally, and internationally.

Data availability statement

The original contributions presented in the study are included in the article/Supplementary material, further inquiries can be directed to the corresponding authors.

Author contributions

AM, JD, and JC conceived of the figures. AM, AT, JRC, VA, MT, BH, EB, KM, JR, CT, JD, and CB contributed to the writing and editing. The consortium designed the pipeline and framework for a statewide program. AM compiled all documents and organized the effort. JRC provided citation formatting. All authors contributed to the article and approved the submitted version.

Funding

S.B. 1780, 87th Legislature, 2021 Reg. Sess. (Texas 2021).

Acknowledgments

The Consortium thanks the El Paso, Lubbock, and Houston water utilities for sample procurement in the first phase of the program. Support is provided by funding from the Texas Legislature under the TEPHI program. A special thanks for Osman Galindo and Leah Ghobrial for expert rendering of the artwork in Figures 1, 2 and Supplemental Figure 1. We also thank Dr. Loren Hopkins at Houston Health for utility support.

Conflict of interest

The authors declare that the research was conducted in the absence of any commercial or financial relationships that could be construed as a potential conflict of interest.

Publisher's note

Supplementary material

The Supplementary Material for this article can be found online at: https://www.frontiersin.org/articles/10.3389/fpubh.2023.1137881/full#supplementary-material

SUPPLEMENTARY FIGURE 1
The molecular platform for viral wastewater detection and epidemiology. Wastewater samples are collected, shipped, and either immediately processed or stored. Large solids are sedimented and cleared supernatants are applied to electronegative filters for viral capture and nucleic acid extraction. Samples are then either tested by RT-PCR ("targeted" approach) or sent for library preparation and sequencing using a comprehensive human virus probe set ("agnostic" approach). The final stages include a statistical analysis of the data, examination of trends, and the production of a data report for health networks and the public.

References

1. Metcalf TG, Melnick JL, Estes MK. Environmental virology: from detection of virus in sewage and water by isolation to identification by molecular biology—a trip of over 50 years. *Annu Rev Microbiol.* (1995) 49:461–87. doi: 10.1146/annurev.mi.49.100195.002333

2. Paul JR, Trask JD, Gard S. Poliomyelitic virus in urban sewage. *J Exp Med.* (1940) 71:765–77. doi: 10.1084/jem.71.6.765

3. Kling C, Olin G, Fahraeus J, Norlin G. Sewage as a carrier and disseminator of poliomyelitis virus. *Acta Med Scand.* (1942) 112:217–49. doi: 10.1111/j.0954-6820.1942.tb13091.x

4. Altman L. *Joseph Melnick, Polio Pioneer, Dies at 86*. New York, NY: The New York Times (2001).

5. Melnick JL. Poliomyelitis virus in urban sewage in epidemic and in non-epidemic times. *Am J Epidemiol.* (1947) 45:240–53. doi: 10.1093/oxfordjournals.aje.a119132

6. Asghar H, Diop OM, Weldegebriel G, Malik F, Shetty S, El Bassioni L, et al. Environmental surveillance for polioviruses in the global polio eradication initiative. *J Infect Dis.* (2014) 210:S294–303. doi: 10.1093/infdis/jiu384

7. Hopkins L, Persse D, Caton K, Ensor K, Schneider R, McCall C, et al. Citywide wastewater SARS-CoV-2 levels strongly correlated with multiple disease surveillance indicators and outcomes over three COVID-19 waves. *Sci Total Environ.* (2023) 855:158967. doi: 10.1016/j.scitotenv.2022.158967

8. Stadler L, Ensor K, Clark J, Kalvapalle P, LaTurner ZW, Mojica L, et al. Wastewater analysis of SARS-CoV-2 as a predictive metric of positivity rate for a major metropolis. *medRxiv.* (2020) 11:6191. doi: 10.1101/2020.11.04.20226191

9. Gitter A, Bauer C, Wu F, Ramphul R, Chavarria C, Zhang K, et al. Assessment of a SARS-CoV-2 wastewater monitoring program in El Paso, Texas, from November 2020 to June 2022. *Int J Environ Health Res.* (2023) 23:1–11. doi: 10.1080/09603123.2022.2159017

10. Link-Gelles R, Lutterloh E, Schnabel Ruppert P, Backenson PB, St George K, Rosenberg ES, et al. Public health response to a case of paralytic poliomyelitis in an unvaccinated person and detection of poliovirus in wastewater—New York, June–August 2022. *MMWR Morb Mortal Wkly Rep.* (2022) 71:1065–8. doi: 10.15585/mmwr.mm7133e2

11. Centers for Disease Control and Prevention. *CDC Planning Wastewater Testing for Polio in Select Communities*. Atlanta: Centers for Disease Control and Prevention (2022). Available online at: https://www.cdc.gov/media/releases/2022/p1130-polio.html (accessed December 04, 2022)

12. Brandal LT, MacDonald E, Veneti L, Ravlo T, Lange H, Naseer U, et al. Outbreak caused by the SARS-CoV-2 omicron variant in Norway, November to December 2021. *Eurosurveillance.* (2021) 26:1147. doi: 10.2807/1560-7917.ES.2021.26.50.2101147

13. Wrapp D, Wang N, Corbett KS, Goldsmith JA, Hsieh C-L, Abiona O, et al. Cryo-EM structure of the 2019-nCoV spike in the prefusion conformation. *Science.* (2020) 367:1260–3. doi: 10.1126/science.abb2507

14. Plante JA, Liu Y, Liu J, Xia H, Johnson BA, Lokugamage KG, et al. Spike mutation D614G alters SARS-CoV-2 fitness. *Nature.* (2021) 592:116–21. doi: 10.1038/s41586-020-2895-3

15. Li M-Y, Li L, Zhang Y, Wang X-S. Expression of the SARS-CoV-2 cell receptor gene ACE2 in a wide variety of human tissues. *Infect Dis Poverty.* (2020) 9:45. doi: 10.1186/s40249-020-00662-x

16. Minodier L, Charrel RN, Ceccaldi P-E, van der Werf S, Blanchon T, Hanslik T, et al. Prevalence of gastrointestinal symptoms in patients with influenza, clinical significance, and pathophysiology of human influenza viruses in faecal samples: what do we know? *Virol J.* (2015) 12:215. doi: 10.1186/s12985-015-0448-4

17. Xiao F, Tang M, Zheng X, Liu Y, Li X, Shan H. Evidence for gastrointestinal infection of SARS-CoV-2. *Gastroenterology.* (2020) 158:1831–3.e3. doi: 10.1053/j.gastro.2020.02.055

18. Nobel YR, Phipps M, Zucker J, Lebwohl B, Wang TC, Sobieszczyk ME, et al. Gastrointestinal symptoms and coronavirus disease 2019: a case-control study from the United States. *Gastroenterology.* (2020) 159:373–5.e2. doi: 10.1053/j.gastro.2020.04.017

19. Guo M, Tao W, Flavell RA, Zhu S. Potential intestinal infection and faecal–oral transmission of SARS-CoV-2. *Nat Rev Gastroenterol Hepatol.* (2021) 18:269–83. doi: 10.1038/s41575-021-00416-6

20. Stein SR, Ramelli SC, Grazioli A, Chung J-Y, Singh M, Yinda CK, et al. SARS-CoV-2 infection and persistence in the human body and brain at autopsy. *Nature.* (2022) 612:758–63. doi: 10.1038/s41586-022-05542-y

21. Hewitt RJ, Lloyd CM. Regulation of immune responses by the airway epithelial cell landscape. *Nat Rev Immunol.* (2021) 21:347–62. doi: 10.1038/s41577-020-00477-9

22. Denney L, Ho L-P. The role of respiratory epithelium in host defence against influenza virus infection. *Biomed J.* (2018) 41:218–33. doi: 10.1016/j.bj.2018.08.004

23. Zhao Z, Wei Y, Tao C. An enlightening role for cytokine storm in coronavirus infection. *Clin Immunol.* (2021) 222:108615. doi: 10.1016/j.clim.2020.108615

24. Gill N, Wlodarska M, Finlay BB. The future of mucosal immunology: studying an integrated system-wide organ. *Nat Immunol.* (2010) 11:558–60. doi: 10.1038/ni0710-558

25. Vareille M, Kieninger E, Edwards MR, Regamey N. The airway epithelium: soldier in the fight against respiratory viruses. *Clin Microbiol Rev.* (2011) 24:210–29. doi: 10.1128/CMR.00014-10

26. Daughton CG. Illicit drugs in municipal sewage. *Pharmaceut Care Prod Environ.* (2001) 791:348–64. doi: 10.1021/bk-2001-0791.ch020

27. Subedi B, Burgard D. *Wastewater-Based Epidemiology as a Complementary Approach to the Conventional Survey-Based Approach for the Estimation of Community Consumption of Drugs*. New York, NY: American Chemical Society (2019). p. 3–21. doi: 10.1021/bk-2019-1319.ch001

28. de Freitas Bueno R, Claro ICM, Augusto MR, Duran AFA, Camillo LMB, Cabral AD, et al. Wastewater-based epidemiology: a Brazilian SARS-CoV-2 surveillance experience. *J Environ Chem Eng.* (2022) 10:108298. doi: 10.1016/j.jece.2022.108298

29. Pillay L, Amoah ID, Kumari S, Bux F. Potential and challenges encountered in the application of wastewater-based epidemiology as an early warning system for COVID-19 infections in South Africa. *ACS ES&T Water.* (2022) 2:2105–13. doi: 10.1021/acsestwater.2c00049

30. Wurtzer S, Marechal V, Mouchel J, Maday Y, Teyssou R, Richard E, et al. Evaluation of lockdown effect on SARS-CoV-2 dynamics through viral genome quantification in waste water, Greater Paris, France, 5 March to 23 April 2020. *Eurosurveillance.* (2020) 25:776. doi: 10.2807/1560-7917.ES.2020.25.50.2000776

31. Kumar M, Joshi M, Patel AK, Joshi CG. Unravelling the early warning capability of wastewater surveillance for COVID-19: a temporal study on SARS-CoV-2 RNA detection and need for the escalation. *Environ Res.* (2021) 196:110946. doi: 10.1016/j.envres.2021.110946

32. LaTurner ZW, Zong DM, Kalvapalle P, Gamas KR, Terwilliger A, Crosby T, et al. Evaluating recovery, cost, and throughput of different concentration methods for SARS-CoV-2 wastewater-based epidemiology. *Water Res.* (2021) 197:117043. doi: 10.1016/j.watres.2021.117043

33. National Academies Press. *Wastewater-Based Disease Surveillance for Public Health Action*. Washington, DC: National Academies Press (2023).

34. de Jonge EF, Peterse CM, Koelewijn JM, van der Drift A-MR, van der Beek RFHJ, Nagelkerke E, et al. The detection of monkeypox virus DNA in wastewater samples in the Netherlands. *Sci Total Environ.* (2022) 852:158265. doi: 10.1016/j.scitotenv.2022.158265

35. Ryerson AB, Lang D, Alazawi MA, Neyra M, Hill DT, George K, et al. Wastewater testing and detection of poliovirus type 2 genetically linked to virus isolated from a paralytic polio case: New York, March 9–October 11, 2022. *MMWR Morb Mortal Wkly Rep.* (2022) 71:1418–24. doi: 10.15585/mmwr.mm7144e2

36. Klapsa D, Wilton T, Zealand A, Bujaki E, Saxentoff E, Troman C, et al. Sustained detection of type 2 poliovirus in London sewage between February and July, 2022, by enhanced environmental surveillance. *Lancet.* (2022) 400:1531–8. doi: 10.1016/S0140-6736(22)01804-9

37. Wise J. Poliovirus is detected in sewage from north and east London. *BMJ.* (2022) 36:1546. doi: 10.1136/bmj.o1546

38. Bar-Or I, Indenbaum V, Weil M, Elul M, Levi N, Aguvaev I, et al. National scale real-time surveillance of SARS-CoV-2 variants dynamics by wastewater monitoring in Israel. *Viruses.* (2022) 14:1229. doi: 10.3390/v14061229

39. European Commission. *COMMISSION RECOMMENDATION of 17.3.2021 on a Common Approach to Establish a Systematic Surveillance of SARS-CoV-2 and Its Variants in Wastewaters in the EU*. Brussels: European Commission (2021). Available online at: https://eur-lex.europa.eu/LexUriServ/LexUriServ.do?uri=CELEX:12012E/TXT:en:PDF (accessed January 31, 2023).

40. Directorate-General for Environment. *Coronavirus Response: Monitoring of Wastewater Contributes to Tracking Coronavirus and Variants Across All EU Countries*. Copenhagen: EU Environment Newsletter (2022).

41. Gracia-Lor E, Castiglioni S, Bade R, Been F, Castrignanò E, Covaci A, et al. Measuring biomarkers in wastewater as a new source of epidemiological information: current state and future perspectives. *Environ Int.* (2017) 99:131–50. doi: 10.1016/j.envint.2016.12.016

42. Calvert HT. The eighth report of the royal commission on sewage disposal. *Lancet.* (1912) 180:1530–1. doi: 10.1016/S0140-6736(01)41378-X

43. Rousis NI, Gracia-Lor E, Zuccato E, Bade R, Baz-Lomba JA, Castrignanò E, et al. Wastewater-based epidemiology to assess pan-European pesticide exposure. *Water Res.* (2017) 121:270–9. doi: 10.1016/j.watres.2017.05.044

44. Loganathan B, Phillips M, Mowery H, Jones-Lepp TL. Contamination profiles and mass loadings of macrolide antibiotics and illicit drugs from a small urban wastewater treatment plant. *Chemosphere.* (2009) 75:70–7. doi: 10.1016/j.chemosphere.2008.11.047

45. O'Brien JW, Thai PK, Brandsma SH, Leonards PEG, Ort C, Mueller JF. Wastewater analysis of Census day samples to investigate per capita input of organophosphorus flame retardants and plasticizers into wastewater. *Chemosphere.* (2015) 138:328–34. doi: 10.1016/j.chemosphere.2015.06.014

46. Bartelt-Hunt SL, Snow DD, Damon T, Shockley J, Hoagland K. The occurrence of illicit and therapeutic pharmaceuticals in wastewater effluent and surface waters in Nebraska. *Environ Pollut.* (2009) 157:786–91. doi: 10.1016/j.envpol.2008.11.025

47. Bones J, Thomas KV, Paull B. Using environmental analytical data to estimate levels of community consumption of illicit drugs and abused pharmaceuticals. *J Environ Monit.* (2007) 9:701. doi: 10.1039/b702799k

48. Mari F, Politi L, Biggeri A, Accetta G, Trignano C, di Padua M, et al. Cocaine and heroin in waste water plants: a 1-year study in the city of Florence, Italy. *Foren Sci Int.* (2009) 189:88–92. doi: 10.1016/j.forsciint.2009.04.018

49. Ort C, Nuijs ALN, Berset J, Bijlsma L, Castiglioni S, Covaci A, et al. Spatial differences and temporal changes in illicit drug use in Europe quantified by wastewater analysis. *Addiction.* (2014) 109:1338–52. doi: 10.1111/add.12570

50. Rodríguez-Álvarez T, Racamonde I, González-Mariño I, Borsotti A, Rodil R, Rodríguez I, et al. Alcohol and cocaine co-consumption in two European cities assessed by wastewater analysis. *Sci Total Environ.* (2015) 536:91–8. doi: 10.1016/j.scitotenv.2015.07.016

51. Thomaidis NS, Gago-Ferrero P, Ort C, Maragou NC, Alygizakis NA, Borova VL, et al. Reflection of socioeconomic changes in wastewater: licit and illicit drug use patterns. *Environ Sci Technol.* (2016) 50:10065–72. doi: 10.1021/acs.est.6b02417

52. Thomas K, Bijlsma L, Castiglioni S, Covaci A, Emke E, Grabic R, et al. Comparing illicit drug use in 19 European cities through sewage analysis. *Sci Total Environ.* (2012) 432:432–9. doi: 10.1016/j.scitotenv.2012.06.069

53. van Nuijs ALN, Castiglioni S, Tarcomnicu I, Postigo C, de Alda ML, Neels H, et al. Illicit drug consumption estimations derived from wastewater analysis: a critical review. *Sci Total Environ.* (2011) 409:3564–77. doi: 10.1016/j.scitotenv.2010.05.030

54. Zuccato E, Chiabrando C, Castiglioni S, Bagnati R, Fanelli R. Estimating community drug abuse by wastewater analysis. *Environ Health Perspect.* (2008) 116:1027–32. doi: 10.1289/ehp.11022

55. Zuccato E, Chiabrando C, Castiglioni S, Calamari D, Bagnati R, Schiarea S, et al. Cocaine in surface waters: a new evidence-based tool to monitor community drug abuse. *Environ Health.* (2005) 4:14. doi: 10.1186/1476-069X-4-14

56. Szczepanowski R, Linke B, Krahn I, Gartemann K-H, Gützkow T, Eichler W, et al. Detection of 140 clinically relevant antibiotic-resistance genes in the plasmid metagenome of wastewater treatment plant bacteria showing reduced susceptibility to selected antibiotics. *Microbiology.* (2009) 155:2306–19. doi: 10.1099/mic.0.028233-0

57. Tennstedt T, Szczepanowski R, Braun S, Pâhler A, Schlâter A. Occurrence of integron-associated resistance gene cassettes located on antibiotic resistance plasmids isolated from a wastewater treatment plant. *FEMS Microbiol Ecol.* (2003) 45:239–52. doi: 10.1016/S0168-6496(03)00164-8

58. Munk P, Brinch C, Møller FD, Petersen TN, Hendriksen RS, Seyfarth AM, et al. Genomic analysis of sewage from 101 countries reveals global landscape of antimicrobial resistance. *Nat Commun.* (2022) 13:7251. doi: 10.1038/s41467-022-34312-7

59. Colomer-Lluch M, Calero-Cáceres W, Jebri S, Hmaied F, Muniesa M, Jofre J. Antibiotic resistance genes in bacterial and bacteriophage fractions of Tunisian and Spanish wastewaters as markers to compare the antibiotic resistance patterns in each population. *Environ Int.* (2014) 73:167–75. doi: 10.1016/j.envint.2014.07.003

60. Heijnen L, Medema G. Surveillance of influenza A and the pandemic influenza A (H1N1) 2009 in sewage and surface water in the Netherlands. *J Water Health.* (2011) 9:434–42. doi: 10.2166/wh.2011.019

61. Laht M, Karkman A, Voolaid V, Ritz C, Tenson T, Virta M, et al. Abundances of tetracycline, sulphonamide and beta-lactam antibiotic resistance genes in conventional wastewater treatment plants (WWTPs) with different waste load. *PLoS ONE.* (2014) 9:e103705. doi: 10.1371/journal.pone.0103705

62. Lee D-Y, Shannon K, Beaudette LA. Detection of bacterial pathogens in municipal wastewater using an oligonucleotide microarray and real-time quantitative PCR. *J Microbiol Methods.* (2006) 65:453–67. doi: 10.1016/j.mimet.2005.09.008

63. Prado T, Fumian TM, Miagostovich MP, Gaspar AMC. Monitoring the hepatitis A virus in urban wastewater from Rio de Janeiro, Brazil. *Trans R Soc Trop Med Hyg.* (2012) 106:104–9. doi: 10.1016/j.trstmh.2011.10.005

64. Rousselon N, Delgenès J-P, Godon J-J, A. new real time PCR (TaqMan® PCR) system for detection of the16S rDNA gene associated with fecal bacteria. *J Microbiol Methods.* (2004) 59:15–22. doi: 10.1016/j.mimet.2004.05.007

65. Shannon KE, Lee D-Y, Trevors JT, Beaudette LA. Application of real-time quantitative PCR for the detection of selected bacterial pathogens during municipal wastewater treatment. *Sci Total Environ.* (2007) 382:121–9. doi: 10.1016/j.scitotenv.2007.02.039

66. Martínez-Puchol S, Rusiñol M, Fernández-Cassi X, Timoneda N, Itarte M, Andrés C, et al. Characterisation of the sewage virome: comparison of NGS tools and occurrence of significant pathogens. *Sci Total Environ.* (2020) 713:136604. doi: 10.1016/j.scitotenv.2020.136604

67. Crits-Christoph A, Kantor RS, Olm MR, Whitney ON, Al-Shayeb B, Lou YC, et al. Genome sequencing of sewage detects regionally prevalent SARS-CoV-2 variants. *MBio.* (2021) 12:20. doi: 10.1128/mBio.02703-20

68. Rothman JA, Loveless TB, Kapcia J, Adams ED, Steele JA, Zimmer-Faust AG, et al. RNA viromics of southern California wastewater and detection of SARS-CoV-2 single-nucleotide variants. *Appl Environ Microbiol.* (2021) 87:e0144821. doi: 10.1128/AEM.01448-21

69. Fernandez-Cassi X, Timoneda N, Martínez-Puchol S, Rusiñol M, Rodriguez-Manzano J, Figuerola N, et al. Metagenomics for the study of viruses in urban sewage as a tool for public health surveillance. *Sci Total Environ.* (2018) 618:870–80. doi: 10.1016/j.scitotenv.2017.08.249

70. Chik AHS, Glier MB, Servos M, Mangat CS, Pang X-L, Qiu Y, et al. Comparison of approaches to quantify SARS-CoV-2 in wastewater using RT-qPCR: Results and implications from a collaborative inter-laboratory study in Canada. *J Environ Sci.* (2021) 107:218–29. doi: 10.1016/j.jes.2021.01.029

71. Pecson BM, Darby E, Haas CN, Amha YM, Bartolo M, Danielson R, et al. Reproducibility and sensitivity of 36 methods to quantify the SARS-CoV-2 genetic signal in raw wastewater: findings from an interlaboratory methods evaluation in the US. *Environ Sci.* (2021) 7:504–20. doi: 10.1039/D0EW00946F

72. Karthikeyan S, Levy JI, de Hoff P, Humphrey G, Birmingham A, Jepsen K, et al. Wastewater sequencing reveals early cryptic SARS-CoV-2 variant transmission. *Nature.* (2022) 609:101–8. doi: 10.1038/s41586-022-05049-6

73. Lin X, Glier M, Kuchinski K, Ross-Van Mierlo T, McVea D, Tyson JR, et al. Assessing multiplex tiling PCR sequencing approaches for detecting genomic variants of SARS-CoV-2 in municipal wastewater. *mSystems.* (2021) 6:21. doi: 10.1128/mSystems.01068-21

74. Nemudryi A, Nemudraia A, Wiegand T, Surya K, Buyukyoruk M, Cicha C, et al. Temporal detection and phylogenetic assessment of SARS-CoV-2 in municipal wastewater. *Cell Rep Med.* (2020) 1:100098. doi: 10.1016/j.xcrm.2020.100098

75. Haas CN, Rose JB, Gerba CP. *Quantitative Microbial Risk Assessment*. 1st edn. New York, NY: John Wiley & Sons Inc. (1999).

76. Haas CN, Rose JB, Gerba CP. *Quantitative Microbial Risk Assessment*. 2nd edn. New York, NY: John Wiley & Sons Inc. (2014). doi: 10.1002/9781118910030

77. Olesen SW, Imakaev M, Duvallet C. Making waves: defining the lead time of wastewater-based epidemiology for COVID-19. *Water Res.* (2021) 202:117433. doi: 10.1016/j.watres.2021.117433

78. Bibby K, Bivins A, Wu Z, North D. Making waves: plausible lead time for wastewater based epidemiology as an early warning system for COVID-19. *Water Res.* (2021) 202:117438. doi: 10.1016/j.watres.2021.117438

79. Galani A, Aalizadeh R, Kostakis M, Markou A, Alygizakis N, Lytras T, et al. SARS-CoV-2 wastewater surveillance data can predict hospitalizations and ICU admissions. *Sci Total Environ.* (2022) 804:150151. doi: 10.1016/j.scitotenv.2021.150151

80. D'Aoust PM, Graber TE, Mercier E, Montpetit D, Alexandrov I, Neault N, et al. Catching a resurgence: Increase in SARS-CoV-2 viral RNA identified in wastewater 48 h before COVID-19 clinical tests and 96 h before hospitalizations. *Sci Total Environ.* (2021) 770:145319. doi: 10.1016/j.scitotenv.2021.145319

81. Mercier E, D'Aoust PM, Thakali O, Hegazy N, Jia J-J, Zhang Z, et al. Municipal and neighbourhood level wastewater surveillance and subtyping of an influenza virus outbreak. *Sci Rep.* (2022) 12:15777. doi: 10.1038/s41598-022-20076-z

82. Faraway J, Boxall-Clasby J, Feil EJ, Gibbon MJ, Hatfield O, Kasprzyk-Hordern B, et al. Challenges in realising the potential of wastewater-based epidemiology to quantitatively monitor and predict the spread of disease. *J Water Health.* (2022) 20:1038–50. doi: 10.2166/wh.2022.020

83. U.S. Environmental Protection Agency. *Guidelines for Water Reuse*. Washington, DC: U.S. Environmental Protection Agency (2012).

84. Kayalar Ö, Ari A, Babuççu G, Konyalilar N, Dogan Ö, Can F, et al. Existence of SARS-CoV-2 RNA on ambient particulate matter samples: a nationwide study in Turkey. *Sci Total Environ.* (2021) 789:147976. doi: 10.1016/j.scitotenv.2021.147976

85. Liu Y, Ning Z, Chen Y, Guo M, Liu Y, Gali NK, et al. Aerodynamic analysis of SARS-CoV-2 in two Wuhan hospitals. *Nature.* (2020) 582:557–60. doi: 10.1038/s41586-020-2271-3

86. Chamseddine A, Soudani N, Kanafani Z, Alameddine I, Dbaibo G, Zaraket H, et al. Detection of influenza virus in air samples of patient rooms. *J Hosp Infect.* (2021) 108:33–42. doi: 10.1016/j.jhin.2020.10.020

87. Lednicky JA, Lauzardo M, Fan ZH, Jutla A, Tilly TB, Gangwar M, et al. Viable SARS-CoV-2 in the air of a hospital room with COVID-19 patients. *Int J Infect Dis.* (2020) 100:476–82. doi: 10.1016/j.ijid.2020.09.025

88. Rahmani AR, Leili M, Azarian G, Poormohammadi A. Sampling and detection of corona viruses in air: a mini review. *Sci Total Environ.* (2020) 740:140207. doi: 10.1016/j.scitotenv.2020.140207

frontiers | Frontiers in Public Health

TYPE Brief Research Report
PUBLISHED 17 May 2023
DOI 10.3389/fpubh.2023.1139423

OPEN ACCESS

EDITED BY
David Champredon,
Public Health Agency of Canada (PHAC), Canada

REVIEWED BY
Hayley Danielle Yaglom,
Translational Genomics Research Institute, United States
Kristina Træholt Franck,
Statens Serum Institut, Denmark

*CORRESPONDENCE
R. Michael McKay
✉ Robert.McKay@uwindsor.ca

RECEIVED 07 January 2023
ACCEPTED 28 April 2023
PUBLISHED 17 May 2023

CITATION
Corchis-Scott R, Geng Q, Al Riahi AM, Labak A, Podadera A, Ng KKS, Porter LA, Tong Y, Dixon JC, Menard SL, Seth R and McKay RM (2023) Actionable wastewater surveillance: application to a university residence hall during the transition between Delta and Omicron resurgences of COVID-19. *Front. Public Health* 11:1139423. doi: 10.3389/fpubh.2023.1139423

Actionable wastewater surveillance: application to a university residence hall during the transition between Delta and Omicron resurgences of COVID-19

Ryland Corchis-Scott[1], Qiudi Geng[1], Abdul Monem Al Riahi[1], Amr Labak[1], Ana Podadera[2], Kenneth K. S. Ng[2], Lisa A. Porter[3], Yufeng Tong[2], Jess C. Dixon[4], Sherri Lynne Menard[5], Rajesh Seth[6] and R. Michael McKay[1]*

[1]Great Lakes Institute for Environmental Research, University of Windsor, Windsor, ON, Canada, [2]Department of Chemistry and Biochemistry, University of Windsor, Windsor, ON, Canada, [3]Department of Biomedical Sciences, University of Windsor, Windsor, ON, Canada, [4]Department of Kinesiology, University of Windsor, Windsor, ON, Canada, [5]Environmental Health and Safety, University of Windsor, Windsor, ON, Canada, [6]Civil and Environmental Engineering, University of Windsor, Windsor, ON, Canada

Wastewater surveillance has gained traction during the COVID-19 pandemic as an effective and non-biased means to track community infection. While most surveillance relies on samples collected at municipal wastewater treatment plants, surveillance is more actionable when samples are collected "upstream" where mitigation of transmission is tractable. This report describes the results of wastewater surveillance for SARS-CoV-2 at residence halls on a university campus aimed at preventing outbreak escalation by mitigating community spread. Another goal was to estimate fecal shedding rates of SARS-CoV-2 in a non-clinical setting. Passive sampling devices were deployed in sewer laterals originating from residence halls at a frequency of twice weekly during fall 2021 as the Delta variant of concern continued to circulate across North America. A positive detection as part of routine sampling in late November 2021 triggered daily monitoring and further isolated the signal to a single wing of one residence hall. Detection of SARS-CoV-2 within the wastewater over a period of 3 consecutive days led to a coordinated rapid antigen testing campaign targeting the residence hall occupants and the identification and isolation of infected individuals. With knowledge of the number of individuals testing positive for COVID-19, fecal shedding rates were estimated to range from 3.70 log10 gc · g feces^{-1} to 5.94 log10 gc · g feces^{-1}. These results reinforce the efficacy of wastewater surveillance as an early indicator of infection in congregate living settings. Detections can trigger public health measures ranging from enhanced communications to targeted coordinated testing and quarantine.

KEYWORDS

COVID-19, RT-qPCR, SARS-CoV-2, wastewater, public health

1. Introduction

SARS-CoV-2 is the virus responsible for COVID-19 (Coronavirus Disease 2019). SARS-CoV-2 infection produces less severe illness than SARS-CoV and MERS-CoV with lower mortality (1, 2). However, the basic reproduction number (R_0) of SARS-CoV-2 is substantially higher than previous coronavirus epidemics (1). Strong evidence of airborne transmission largely explains higher transmissibility of SARS-CoV-2 (3, 4). Additionally, asymptomatic cases of COVID-19 likely promote transmission as individuals can pass the infection without knowing they are contagious (5, 6). Testing populations widely is complicated by the fact that clinical testing is expensive and can overwhelm healthcare resources. Alternate means of ascertaining disease prevalence has emerged as an important public health goal for pandemic management.

SARS-CoV-2 can be shed in the digestive tract of infected individuals and excreted in feces (7, 8). Consequently, SARS-CoV-2 RNA can be detected in untreated wastewater (9) following collection at wastewater treatment facilities (10, 11). Correlations have been found between the amount of SARS-CoV-2 viral material in wastewater and the prevalence of disease within the community served, (12) with many instances demonstrating that wastewater surveillance may provide early warning of increases in clinical cases (12–17).

Testing the footprint of disease within an entire community can help to inform public health decision making (18). However, testing wastewater "upstream" of treatment facilities arguably produces more immediately actionable data that may be used to mitigate disease transmission (19–21). During the COVID-19 pandemic, wastewater surveillance of congregate living settings has been adopted by many universities to assess disease prevalence on campus (22–27). In this setting, it has been shown to be a cost-effective means of detecting cases among individuals in high density housing, especially in comparison with clinical testing protocols (28). Wastewater surveillance can also warn of outbreaks in other congregate living settings. This type of "upstream" monitoring has been implemented in homeless shelters (29) and in long-term care facilities (30) where early detection and mitigation of transmission is especially important as the monitored populations are more susceptible to mortality associated with COVID-19 infection (31).

Upstream sampling modalities can rely on the same methodologies employed to monitor wastewater at centralized wastewater treatment facilities where composite samples are collected by autosampler. This type of sampling does not always lend itself to upstream locations where practical considerations such as autosampler deployment and variable flows can preclude sampling. Passive samplers offer an alternative, especially in logistically challenging settings where they can detect a single case per 10,000 individuals (32). Moore Swabs are a class of passive sampling device composed of absorptive material placed in a flowing medium to continuously filter particulate material for analysis (33). Moore Swabs have been used in wastewater surveillance at broad and fine spatial resolutions (i.e., monitoring upstream and at the community level) and have been shown to be equivalent to or outperform grab and composite sampling (34–36).

In February 2021, the University of Windsor implemented a program to monitor wastewater in a single residence hall on campus. During spring 2021, wastewater surveillance likely averted a COVID-19 outbreak by detecting an infection using passive samplers and analysis by RT-qPCR. The detection led to a public health response which included a testing campaign at the residence and the eventual quarantine of an infected individual and their close contacts (20). The campus monitoring program was expanded at the beginning of the 2021 fall semester to include three residence halls. This report focuses on a second occurrence in which wastewater surveillance may have prevented an outbreak. In addition to resulting in an actionable public health response, data generated provided taxonomic resolution of the variant of SARS-CoV-2 responsible and estimation of fecal shedding rates for the variant.

2. Methods

2.1. Sample collection

Passive samplers were deployed once weekly at three campus residence halls beginning in summer 2021 to establish a baseline prior to students moving to campus. Beginning in fall 2021, sampling frequency was increased to twice weekly. Swabs passively interacted with wastewater for approximately 24 h before they were collected. Once collected, swabs were placed in sealable plastic bags and transported to the laboratory on ice for immediate processing. Samplers consisted of a feminine hygiene product (Tampax Cardboard Tampons, Regular Absorbency, Procter & Gamble, Cincinnati, OH, United States) clipped to a carabiner which was attached to the interior of the rim of a sewer cover via fishing line and a magnet. Duplicate tampons were placed within each monitored sewer lateral to increase the volume of liquid absorbed.

2.2. Sample processing

At the laboratory, liquids and solids were expelled manually by massaging the tampons while still in the sealed plastic bag. A mean volume of 35 mL (SD ± 10) was eluted from each swab. The liquid and suspended solids were decanted into a sterile 50 mL conical polypropylene tube and centrifuged at 4820 × *g* for 40 min at 4°C. The supernatant was collected and passed through a 0.22 µm Sterivex cartridge filter (MilliporeSigma, Burlington, MA, United States). Filters were flash frozen in liquid nitrogen and were stored in liquid nitrogen at −196°C until extraction. RNA was extracted from the filters using the AllPrep PowerViral DNA/RNA kit (Qiagen, Germantown, MD, United States) modified by addition of 5% (v/v) 2-mercaptoethanol to the lysis buffer. RNA was eluted in 50 µL of RNAse-free water.

2.3. RT-qPCR

Template was analyzed undiluted and diluted 1:5 with RNAse-free water to relieve PCR inhibition. RT-qPCR targeted the conserved N1 and N2 regions of the nucleocapsid (N) gene of SARS-CoV-2 (37). RT-qPCR was also performed to evaluate the levels of Pepper Mild Mottled Virus (PMMoV) within the wastewater as an indicator of human fecal matter (38–40) using primers and probes described previously (41). RT-qPCR reactions for SARS-CoV-2 contained 10 µL

of 2× RT-qPCR master mix (Takyon Dry One-Step RT Probe MasterMix No Rox; Eurogentec, Liege, Belgium), 5 µL of template and the remaining 5 µL consisted of forward primer (final concentration of 300 nM), reverse primer (final concentration of 300 nM) and probe (final concentration of 150 nM). All samples were run in technical triplicates for each target assayed. The thermocycling protocol for each of the gene targets was consistent. Reverse transcription was performed for 10 min at 48°C, followed by an enzyme activation step at 95°C for 3 min and 50 cycles of denaturation and annealing/extension at 95°C for 10 s and 60°C for 45 s, respectively. This protocol was carried out using a MA6000 thermocycler (Sansure Biotech, Changsha, China). No template controls were included with each RT-qPCR run and a 7-point standard curve for SARS-CoV-2 derived from serial dilution of a synthetic RNA standard (Exact Diagnostics, Fort Worth, TX, USA) was run with each set of samples. A standard curve for the quantification of PMMoV was generated through serial dilution of a custom Gblock. All standard curves were made in RNAse- free water. No amplification was observed for process controls (extraction blanks) or in no template controls. The LOD of the N1 and N2 assays is 1 copy·µL^{-1} of template, corresponding to a greater than 95% probability of detection. LOD was determined through analysis of 20 replicate 7-point standard curves. Standards for each target met the minimum requirements from Protocol for Evaluations of RT-qPCR Performance Characteristics: Technical Guidance (slope from −3.1 to −3.6 and an R^2 value of at least 0.98) (42).

Samples were also analyzed by RT-qPCR primer extension assay targeting the mutation D63G on the N gene, which is unique to sublineages of the Delta (B.1.617.2) variant of concern (43, 44). RNA extract was diluted 1:5 with RNase-free water and 5 µL of sample was mixed with 10 µL of 2 × RT-qPCR master mix (Eurogentec), 500 nM primers and 125 nM probe in a final reaction volume of 20 µL. Reverse transcription was performed for 10 min at 48°C, this was followed by an enzyme activation step at 95°C for 3 min, 45 cycles of denaturation and annealing/extension at 95°C for 10 s and 55°C for 45 s, respectively. Primer and probe sequences were previously described (45). To quantify the SARS-CoV-2 viral load, a standard curve was generated using a synthesized gblock DNA fragment serially diluted in RNAse-free water (Supplementary Table S1).

2.4. Fecal shedding calculation

Estimation of fecal shedding rates followed an approach previously described (46) adopting modifications made describing a previous outbreak on the University of Windsor campus (20). The formula used to estimate fecal shedding rate was:

$$FS = \frac{(VC \times Q \times h)}{(G \times I)}$$

where *VC* is the estimated concentration of N1 gene found in the wastewater in gene copies·L^{-1}. *Q* is the approximate flow rate of water leaving the residence hall in L·min^{-1} and *h* is a constant that allows the conversion of units. In the denominator, *G* is the median *per capita* wet weight mass of feces from high income countries (47) and *I* is the number of infected individuals contributing to shedding SARS-CoV-2 viral material into the sewer. As in previous work regarding fecal shedding, the absolute gene copies·L^{-1} of N1 was calculated using the median PMMoV (2.32×10^6 gene copies·L^{-1}) from 17 grab samples collected in February and March, 2021 (20). This was necessary since it is challenging to produce accurate estimates of SARS-CoV-2 gene concentration in the sampled water itself using passive samplers. However, an accurate back estimation may be made using the ratio between SARS-CoV-2 and PMMoV gene concentrations found in the material collected by the passive samplers. This assumes that the passive sampling device captures PMMoV and SARS-CoV-2 with equal efficiency. Sample calculations can be found in the Supplementary Material.

Flow rates were determined by examination of the water usage within the residence as recorded by a utilities meter within the building. This method of determining the flow was necessitated by the challenges associated with mounting a flow meter within the sewer and the inconsistent flow, which was often too low to be detected by a flow meter. Since monitoring was conducted at each of the laterals associated with the building but SARS-CoV-2 was only detected in one of the two laterals, flow per resident was calculated and adjusted to reflect the number of residents housed in the north portion of the building (corresponding to the lateral that tested positive for SARS-CoV-2).

2.5. Ethics review

The information on the cases described are considered exempt from ethics review under the Canadian *Tri-Council Policy Statement: Ethical Conduct for Research Involving Humans – TCPS 2 (2018)* Articles 2.4 and 2.5.

3. Results and discussion

3.1. Campus wastewater surveillance

During summer 2021, student residence halls at the University were minimally occupied with ~30 students residing in one building. The occupied building was monitored once weekly over the summer semester with no detections of SARS-CoV-2. The University opened 3 residence halls (hereafter referred to as Residence A, Residence B and Residence C) in late August 2021. In preparation for the resumption of occupancy for these 3 buildings, frequency of wastewater monitoring was increased to twice weekly the week before students resumed occupancy. A total of 526 students inhabited the 3 residence halls at the beginning of the fall semester. As part of the University's Return to Campus initiative, students living in residence halls were required to have at least 1 dose of a vaccine approved by Health Canada.

Wastewater testing yielded no detections of SARS-CoV-2 at residence halls through the beginning of the semester (Figure 1). This trajectory mirrored the low incidence of COVID-19 in the Windsor-Essex region at this time (Supplementary Figure S1). It was likewise consistent with low concentration of SARS-CoV-2 detected in municipal wastewater following an August–September 2021 resurgence due to the Delta variant of concern (VOC) (Supplementary Figure S1). Also contributing to the apparent absence of disease on campus was a relatively low student population housed

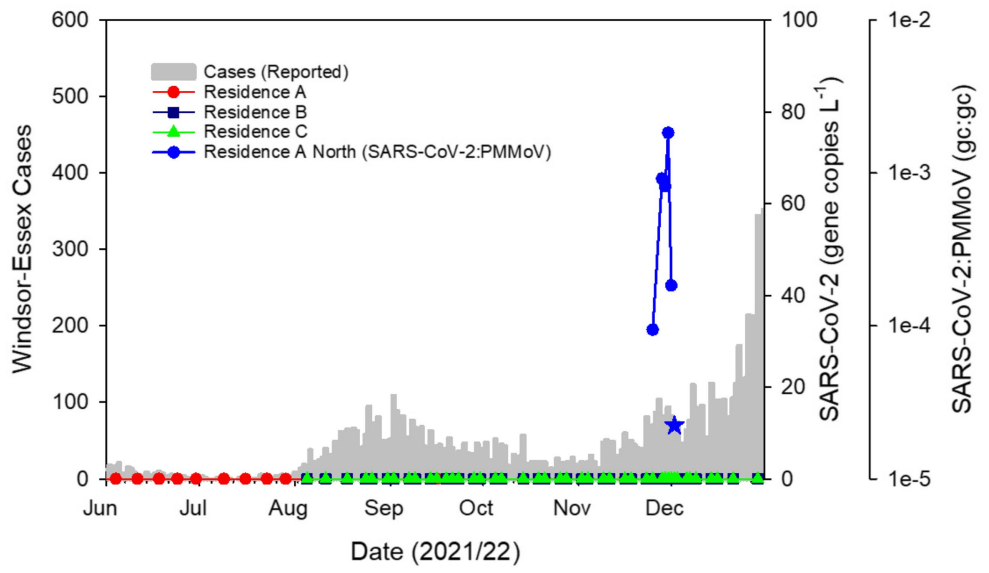

FIGURE 1
SARS-CoV-2 in campus residence hall wastewater plotted as the ratio of gene copies (gc) of SARS-CoV-2:PMMoV against COVID-19 cases in the Windsor-Essex region by reported date. Sampling the wastewater at 3 residence halls with Moore swabs twice weekly over a 12-week period showed no detectable SARS-CoV-2 following which detection related to the outbreak described here commenced with a sample collected on November 25, 2021. SARS-CoV-2 remained detectable through December 2 albeit yielding a weak signal on that date (blue star) and RT-qPCR amplification of only two technical replicates, both yielding Ct values outside the range of the standard curve. Thereafter, SARS-CoV-2 was not detected in campus residence sewer laterals through the remainder of the fall semester.

in residence halls combined with suspension of most in person classes during fall semester. Additionally, the University's vaccination policy for on-campus students likely helped to reduce the chance of an outbreak prior to the November–December infections detailed in this report. Given the regularity in which monitoring was conducted and the duration of passive sampler deployment, it is unlikely that surveillance efforts during the fall semester failed to capture cases of COVID-19 within the residence halls monitored.

Following nearly 3 months of non-detects for SARS-CoV-2, on November 26, 2021, a wastewater sample collected at Residence A tested positive with triplicate technical replicates for the N1 gene region yielding a mean pepper biomarker normalized ratio of 9.4×10^{-5} ($\pm 1.4 \times 10^{-5}$SD; Figure 1). The detection triggered daily sampling of each residence hall and prompted separate sampling of sewer laterals serving distinct wings of Residence A allowing spatial isolation of SARS-CoV-2 signal. Subsequent samples collected from Residence B, Residence C and Residence A South sewer lateral showed no SARS-CoV-2 signal (Figure 1). The initial detect of SARS-CoV-2 was followed by a weak signal from a sample collected the following day where only a single technical replicate amplified for the SARS-CoV-2 N1 gene target. The reasons for this weak signal are unknown but the concentration of fecal biomarker from this sample was also low suggesting that the sample was dilute or that inhibition was present within the wastewater matrix. Alternatively, the initial infected individual(s) may not have contributed to the wastewater sampled either due to irregular defecation patterns (48) and the weak signal caused by residual SARS-CoV-2 material within the sewer lateral. Sample placement, timing and duration are important considerations for accurate monitoring (49). Whatever the reason for the weak detect, this signal invited the possibility that the initial detect was caused by a transient visitor rather than an occupant. Therefore, public health action was paused while a third sample was collected. Passive samplers placed on November 27 were collected the following day. Residence B, Residence C and Residence A South showed no signs of COVID-19 infections. However, the sample collected from Residence A North yielded a robust SARS-CoV-2 signal with a mean pepper-normalized SARS-CoV-2 ratio of 9.2×10^{-4} ($\pm 3.6 \times 10^{-5}$ SD), one order of magnitude higher than the initial detect (Figure 1). The lower Ct values associated with this sample as well as the persistence of the signal over 3 days led to the conclusion that an individual within the building was likely infected with COVID-19. This information was communicated to the University leadership and daily sampling was continued to achieve high temporal resolution monitoring of the sewage leaving the residence hall. A sample collected on November 30 showed a continued upward trend in SARS-CoV-2 signal intensity at Residence A North (N1:PMMoV mean $1.8 \times 10^{-3} \pm 5.9 \times 10^{-4}$) with the biomarker-normalized SARS-CoV-2 ratio having increased by two orders of magnitude over the initial detection (Figure 1). Viral signal was absent at all other monitored sites. Daily testing of the wastewater at all residence halls on campus continued for the next 3 days. The signal at Residence A North waned rapidly to levels that were undetectable by December 3. SARS-CoV-2 was not detected in campus wastewater for the remainder of the semester.

Wastewater monitoring at upstream sites may act as mirrors of trends within the community (Supplementary Figure S2) (50, 51). Additionally, variant-specific assays as well as sequencing of variants within upstream sites can provide insight about variants of SARS-CoV-2 within the larger population. It is easier to resolve variants in upstream sewage than sewage from community level wastewater treatment plants since fewer individuals contribute to the signal. During the outbreak on campus, the Delta VOC was dominant within the southwest region of Ontario as confirmed by variant-specific

RT-qPCR (Supplementary Figure S1), as well as wastewater sequencing and sequencing of a subset of clinically confirmed cases (52). The Delta VOC was characterized by increased transmissibility, higher replication efficiency and viral loads, shorter incubation times and vaccine evasion (53–55). RT-qPCR analysis conducted on RNA extracted from the wastewater sample collected at Residence A North on November 30 showed evidence of the presence of the D63G mutation in the N gene which is diagnostic of the Delta VOC (43, 44). Next-Generation sequencing of this sample confirmed that the strain responsible for the outbreak was likely the Delta sublineage AY.103 (Supplementary Data). Province-wide, this sublineage represented ~20% of reported cases based on sequencing of clinical samples between epi weeks 45–48 (November 7 to December 4, 2021) only trailing sublineage AY.25 as the dominant circulating strain in the province (56). However, within the Windsor-Essex region, sublineage AY.103 was dominant, accounting for 47.9% of the 885 cases reported by the health unit over this same period (56).

Wastewater surveillance also facilitated estimates of fecal shedding rates calculated based on the ratio between gene copies of N1 and PMMoV for each day of the outbreak. Shedding rates were calculated for each sample and with different assumed numbers of infected individuals contributing to the SARS-CoV-2 signal (Table 1). Rates of shedding increased over the first 5 days of the outbreak, likely corresponding to progression in infection and/or new infections. This is consistent with literature indicating that viral shedding peaks 4–6 days following infection, coincident with symptom onset (57–60). In this study we report fecal shedding rates ranging from 3.70 log10 gc · g feces^{-1} to 5.94 log10 gc · g feces^{-1}. This range is lower than expected given reports of higher viral titres for the Delta VOC (53–55) but it is similar to what was calculated in a previous outbreak on the University campus that was attributed to the Alpha VOC (3.93 log10 gc · g feces^{-1} to 5.99 log10 gc · g feces^{-1}) (20). The reported maximum of 5.94 log10 gc·g feces^{-1} likely represents a maximal or near maximal viral load as it was estimated approximately 5 days after the initial SARS-CoV-2 detection (54, 55) and was the peak level measured in the wastewater stream. Estimates of fecal shedding rates were indirectly ascertained based on the ratio of SARS-CoV-2:PMMoV (Supplementary Table S3) in wastewater concentrated from a passive sampling device and must be cautiously interpreted. Further uncertainty in the estimate may be attributed to the flow rates used in the calculation being estimated based on facility water usage. However, estimated fecal shedding rates largely fall within the range produced by direct measurement of stool samples of COVID-19 patients reported in select recent studies, supporting the validity of approximation methods (Supplementary Table S4). Finally, multiple studies have shown that not all infected individuals shed SARS-CoV-2 RNA in stool (58, 61).

The vaccination status of the cases in the present outbreak is unknown but should not influence the viral concentration as the viral loads for vaccinated and unvaccinated individuals infected with the Delta VOC are similar (60, 62, 63).Understanding fecal shedding rates in a more controlled congregate living setting can allow for better interpretation of community level wastewater surveillance data especially in estimating the number of cases associated with the catchment of a particular wastewater treatment plant. This application is especially important as wide-scale clinical testing waned during the emergence of the Omicron VOC, and public health has become more reliant on wastewater data to track the progression of the pandemic (52). Hence, using small scale studies to determine fecal shedding rates may aid in more accurate estimation of SARS-CoV-2 caseloads in the community (64, 65). Some studies have attempted to quantify SARS-CoV-2 shedding rates with a top down approach by using the number of reported cases within a population and back calculating fecal shedding rates by considering the SARS-CoV-2 gene concentrations within the wastewater collected at treatment facilities (66). However, these attempts rely on the assumption that case counts are accurate and do not properly account for loss in signal within the sewershed from adsorption to solids, oxidation and microbial activity (67). Thus, outbreaks in upstream monitoring locations offer better opportunities to calculate fecal shedding rates.

3.2. Public health response

All campus residence hall occupants were messaged on the evening of November 27 notifying them of the positive wastewater results at Residence A and reinforcing University COVID-19 protocols including health self-assessments, physical distancing, hand washing and mask wearing. They were also asked to refrain from receiving visitors from other residence halls. With continued positive wastewater results from Residence A North, residents of this hall were again messaged the morning of November 29 encouraging residents to avail themselves of on-campus COVID-19 rapid testing and informing them of the temporary closure of common areas in the building. The campus testing center received 35 students on November 30 of which one occupant of Residence

TABLE 1 Calculation of fecal shedding rates.

	Fecal shedding rate (log10 gc · g feces^{-1})									
	Persons infected									
Date (2021)	1	2	3	4	5	6	7	8	9	10
11–28	5.62	5.32	5.14	5.02	4.92	4.84	4.78	4.72	4.67	4.62
11–29	5.55	5.25	5.07	4.95	4.85	4.77	4.70	4.64	4.59	4.55
11–30	5.94	5.64	5.46	5.34	5.24	5.16	5.09	5.03	4.98	4.94
12–01	4.93	4.63	4.45	4.33	4.23	4.15	4.09	4.03	3.98	3.93
12–02	4.30	4.00	3.83	3.70	3.60	3.52	3.46	3.40	3.35	3.30

A range of rates were calculated taking into consideration the possible number of infected individuals who contributed to the wastewater stream during this outbreak. Given the immediate rapid decline of wastewater signal following the removal of the 4 infected individuals identified with rapid tests, it is likely that the number of infected individuals contributing to the signal was no larger than 4. In addition, rates were calculated for each day of the outbreak based on the change in SARS-CoV-2 signal intensity.

A North tested positive and was moved, along with a close contact, to a quarantine floor in a separate building by late afternoon. Two additional students reported positive tests on December 1 and were relocated to quarantine by noon that day. Testing was moved on-site at Residence A on December 1 to attract more students for testing but resulted in only 2 additional students submitting to rapid testing. Also on December 1, the Office of Health and Safety issued an update to the University community alerting all students, faculty and staff to the evolving situation. On December 2, an additional positive case was reported who along with 3 close contacts was relocated to quarantine. On December 4, the University released a press statement indicating that a total of 4 cases had been detected and identified wastewater surveillance as the main indicator that triggered the identification of the cases (68). Several close contacts voluntarily isolated off campus and their infection status is unknown. No additional cases of COVID-19 were reported among student residents through to the end of fall semester in contrast to the winter 2022 semester (Supplementary Figure S2).

Rapid communication of monitoring data is critical in using wastewater-based surveillance as a tool to mitigate spread of COVID-19. A wastewater monitoring program implemented by the University of California San Diego focused on high frequency testing and rapid information dissemination to diagnose an estimated 85% of COVID-19 cases on campus early in the course of the disease (69). The authors stressed the importance of timely reporting and coordination between wastewater surveillance campaigns and clinical testing efforts, an opinion echoed across upstream monitoring programs (20, 70). In the present case, once it was confirmed that the SARS-CoV-2 detected within the sewer lateral for Residence A was not an anomaly, action was taken by the University in consultation with the local public health unit. Messaging targeting building occupants encouraged voluntary testing and reinforced COVID-19 protections and protocols in effect at the University. Only ~10% of the Residence A occupants submitted to rapid antigen tests administered on-site. In contrast, a similar incident on the University campus the previous spring resulted in a much higher uptake of testing (27). The lower uptake reported here may be related to pandemic fatigue as adherence to transmission mitigation policies is prone to decline over time (71, 72). Despite the lower test uptake, this study represents the successful implementation of wastewater-based surveillance in coordination with clinical testing to reduce the impact of an outbreak. Without the application of wastewater surveillance, these cases may have infected others on campus and within the larger community (73). Here we demonstrate that wastewater-based surveillance at fine spatial resolution can produce actionable data.

If the population under surveillance is informed about wastewater monitoring and trusts the results, clinical testing may not always be necessary to prevent spread. Instead, promoting awareness of the likely presence of COVID-19 infections and advising the adoption of transmission mitigating practices may be enough to curtail outbreaks. In fact, because of monitoring efforts on campus, signs are now posted within each of the monitored residence halls to inform students of wastewater results. Signs are updated on a weekly basis, are color-coded for easy interpretation, and are designed to encourage behaviors that reduce the likelihood of the transmission of respiratory infections. Continued challenges in the use of wastewater surveillance include variability in the wastewater matrix leading to quantification issues, ensuring continued buy-in from administrators, residents, and public health agencies as well as convalescent shedding that can obscure the relevancy of signals (especially in larger congregate living settings where recovering cases and new infections cohabitate) (74). Despite these challenges, wastewater-based surveillance for monitoring respiratory and other transmissible infections in congregate living settings is a promising direction that can produce highly actionable data for public health agencies and other administrations responsible for the health of residents. Possible extensions of SARS-CoV-2 surveillance include use of these methodologies to monitor other respiratory pathogens such as Respiratory Syncytial Virus (RSV) and Influenza (75, 76).

Data availability statement

The datasets presented in this study can be found in online repositories. The names of the repository/repositories and accession number(s) can be found at: https://www.ncbi.nlm.nih.gov/genbank/, OQ180905.

Author contributions

RC-S: conceptualization, methodology, validation, formal analysis, investigation, and writing- original draft preparation. QG: methodology, validation, formal analysis, investigation, data curation, and writing- reviewing and editing. AA and AL: investigation. AP: formal analysis, investigation, data curation, and writing- reviewing and editing. KN: formal analysis, investigation, resources, writing-reviewing and editing, supervision, and project administration. LP: writing- reviewing and editing, supervision, and project administration. YT, SM, and JD: resources, writing- reviewing and editing, supervision, and project administration. RS: conceptualization, methodology, writing- reviewing and editing, and supervision. RM: conceptualization, resources, writing- reviewing and editing, visualization, supervision, project administration, and funding acquisition. All authors contributed to the article and approved the submitted version.

Funding

Funding in support of the Ontario Wastewater Surveillance Initiative was provided by the Ontario Ministry of Environment, Conservation and Parks. AA and AL were supported by the University of Windsor Outstanding Scholars Program.

Acknowledgments

The authors acknowledge the contributions of the University of Windsor Return to Campus Action Group for their support of the campus wastewater surveillance program. In particular, the authors thank D. Rawlings and J. McGinlay who provided logistical support to access residence hall occupancy data and infrastructure for sampling.

Conflict of interest

The authors declare that the research was conducted in the absence of any commercial or financial relationships that could be construed as a potential conflict of interest.

Publisher's note

All claims expressed in this article are solely those of the authors and do not necessarily represent those of their affiliated organizations, or those of the publisher, the editors and the reviewers. Any product that may be evaluated in this article, or claim that may be made by its manufacturer, is not guaranteed or endorsed by the publisher.

Supplementary material

The Supplementary material for this article can be found online at: https://www.frontiersin.org/articles/10.3389/fpubh.2023.1139423/full#supplementary-material

References

1. Abdelrahman Z, Li M, Wang X. Comparative review of SARS-CoV-2, SARS-CoV, MERS-CoV, and influenza a respiratory viruses. *Front Immunol*. (2020) 11:11. doi: 10.3389/fimmu.2020.552909

2. Zeidler A, Karpinski TM. SARS-CoV, MERS-CoV, SARS-CoV-2 comparison of three emerging coronaviruses. *Jundishapur J Microbiol*. (2020) 13:103744. doi: 10.5812/jjm.103744

3. Jarvis MC. Aerosol transmission of SARS-CoV-2: physical principles and implications. *Front Public Health*. (2020) 8:590041. doi: 10.3389/fpubh.2020.590041

4. Noorimotlagh Z, Jaafarzadeh N, Martínez SS, Mirzaee SA. A systematic review of possible airborne transmission of the COVID-19 virus (SARS-CoV-2) in the indoor air environment. *Environ Res*. (2021) 193:110612. doi: 10.1016/j.envres.2020.110612

5. He X, Lau EHY, Wu P, Deng X, Wang J, Hao X, et al. Temporal dynamics in viral shedding and transmissibility of COVID-19. *Nat Med*. (2020) 26:672–5. doi: 10.1038/s41591-020-0869-5

6. Syangtan G, Bista S, Dawadi P, Rayamajhee B, Shrestha LB, Tuladhar R, et al. Asymptomatic SARS-CoV-2 carriers: a systematic review and Meta-analysis. *Front Public Health*. (2021) 8:8. doi: 10.3389/fpubh.2020.587374

7. Chen Y, Chen L, Deng Q, Zhang G, Wu K, Ni L, et al. The presence of SARS-CoV-2 RNA in the feces of COVID-19 patients. *J Med Virol*. (2020) 92:833–40. doi: 10.1002/jmv.25825

8. Park S, Lee CW, Park DI, Woo HY, Cheong HS, Shin HC, et al. Detection of SARS-CoV-2 in fecal samples from patients with asymptomatic and mild COVID-19 in Korea. *Clin Gastroenterol Hepatol*. (2021) 19:1387–1394.e2. doi: 10.1016/j.cgh.2020.06.005

9. Ahmed W, Angel N, Edson J, Bibby K, Bivins A, O'Brien JW, et al. First confirmed detection of SARS-CoV-2 in untreated wastewater in Australia: a proof of concept for the wastewater surveillance of COVID-19 in the community. *Sci Total Environ*. (2020) 728:138764. doi: 10.1016/j.scitotenv.2020.138764

10. Ahmed W, Bertsch PM, Bibby K, Haramoto E, Hewitt J, Huygens F, et al. Decay of SARS-CoV-2 and surrogate murine hepatitis virus RNA in untreated wastewater to inform application in wastewater-based epidemiology. *Environ Res*. (2020) 191:110092. doi: 10.1016/j.envres.2020.110092

11. Sala-Comorera L, Reynolds LJ, Martin NA, O'Sullivan JJ, Meijer WG, Fletcher NF. Decay of infectious SARS-CoV-2 and surrogates in aquatic environments. *Water Res*. (2021) 201:117090. doi: 10.1016/j.watres.2021.117090

12. Medema G, Heijnen L, Elsinga G, Italiaander R, Brouwer A. Presence of SARS-Coronavirus-2 RNA in sewage and correlation with reported COVID-19 prevalence in the early stage of the epidemic in the Netherlands. *Environ Sci Technol Lett*. (2020) 7:511–6. doi: 10.1021/acs.estlett.0c00357

13. D'Aoust PM, Graber TE, Mercier E, Montpetit D, Alexandrov I, Neault N, et al. Catching a resurgence: increase in SARS-CoV-2 viral RNA identified in wastewater 48 h before COVID-19 clinical tests and 96 h before hospitalizations. *Sci Total Environ*. (2021) 770:145319. doi: 10.1016/j.scitotenv.2021.145319

14. Peccia J, Zulli A, Brackney DE, Grubaugh ND, Kaplan EH, Casanovas-Massana A, et al. Measurement of SARS-CoV-2 RNA in wastewater tracks community infection dynamics. *Nat Biotechnol*. (2020) 38:1164–7. doi: 10.1038/s41587-020-0684-z

15. Randazzo W, Truchado P, Cuevas-Ferrando E, Simón P, Allende A, Sánchez G. SARS-CoV-2 RNA in wastewater anticipated COVID-19 occurrence in a low prevalence area. *Water Res*. (2020) 181:115942. doi: 10.1016/j.watres.2020.115942

16. Sangsanont J, Rattanakul S, Kongprajug A, Chyerochana N, Sresung M, Sriporatana N, et al. SARS-CoV-2 RNA surveillance in large to small centralized wastewater treatment plants preceding the third COVID-19 resurgence in Bangkok, Thailand. *Sci Total Environ*. (2022) 809:151169. doi: 10.1016/j.scitotenv.2021.151169

17. Ahmed W, Tscharke B, Bertsch PM, Bibby K, Bivins A, Choi P, et al. SARS-CoV-2 RNA monitoring in wastewater as a potential early warning system for COVID-19 transmission in the community: a temporal case study. *Sci Total Environ*. (2021) 761:144216. doi: 10.1016/j.scitotenv.2020.144216

18. Hillary LS, Farkas K, Maher KH, Lucaci A, Thorpe J, Distaso MA, et al. Monitoring SARS-CoV-2 in municipal wastewater to evaluate the success of lockdown measures for controlling COVID-19 in the UK. *Water Res*. (2021) 200:117214. doi: 10.1016/j.watres.2021.117214

19. Betancourt WQ, Schmitz BW, Innes GK, Prasek SM, Pogreba Brown KM, Stark ER, et al. COVID-19 containment on a college campus via wastewater-based epidemiology, targeted clinical testing and an intervention. *Sci Total Environ*. (2021) 779:146408. doi: 10.1016/j.scitotenv.2021.146408

20. Corchis-Scott R, Geng Q, Seth R, Ray R, Beg M, Biswas N, et al. Averting an outbreak of SARS-CoV-2 in a university residence hall through wastewater surveillance. *Microbiol Spect*. (2021) 9:e00792–21. doi: 10.1128/Spectrum.00792-21

21. Kotay SM, Tanabe KO, Colosi LM, Poulter MD, Barry KE, Holstege CP, et al. Building-level wastewater surveillance for SARS-CoV-2 in occupied university dormitories as an outbreak forecasting tool: one year case study. *ACS EST Water*. (2022) 2:2094–104. doi: 10.1021/acsestwater.2c00057

22. de Llanos R, Cejudo-Marín R, Barneo M, Pérez-Cataluña A, Barberá-Riera M, Rebagliato M, et al. Monitoring the evolution of SARS-CoV-2 on a Spanish university campus through wastewater analysis: a pilot project for the reopening strategy. *Sci Total Environ*. (2022) 845:157370. doi: 10.1016/j.scitotenv.2022.157370

23. Gibas C, Lambirth K, Mittal N, Juel MAI, Barua VB, Roppolo Brazell L, et al. Implementing building-level SARS-CoV-2 wastewater surveillance on a university campus. *Sci Total Environ*. (2021) 782:146749. doi: 10.1016/j.scitotenv.2021.146749

24. Lu E, Ai Y, Davis A, Straathof J, Halloran K, Hull N, et al. Wastewater surveillance of SARS-CoV-2 in dormitories as a part of comprehensive university campus COVID-19 monitoring. *Environ Res*. (2022) 212:113580. doi: 10.1016/j.envres.2022.113580

25. Mangwana N, Archer E, Muller CJF, Preiser W, Wolfaardt G, Kasprzyk-Hordern B, et al. Sewage surveillance of SARS-CoV-2 at student campus residences in the Western cape, South Africa. *Sci Total Environ*. (2022) 851:158028. doi: 10.1016/j.scitotenv.2022.158028

26. Scott LC, Aubee A, Babahaji L, Vigil K, Tims S, Aw TG. Targeted wastewater surveillance of SARS-CoV-2 on a university campus for COVID-19 outbreak detection and mitigation. *Environ Res*. (2021) 200:111374. doi: 10.1016/j.envres.2021.111374

27. Wang Y, Liu P, Zhang H, Ibaraki M, VanTassell J, Geith K, et al. Early warning of a COVID-19 surge on a university campus based on wastewater surveillance for SARS-CoV-2 at residence halls. *Sci Total Environ*. (2022) 821:153291. doi: 10.1016/j.scitotenv.2022.153291

28. Wright J, Driver EM, Bowes DA, Johnston B, Halden RU. Comparison of high-frequency in-pipe SARS-CoV-2 wastewater-based surveillance to concurrent COVID-19 random clinical testing on a public U.S. university campus. *Sci Total Environ*. (2022) 820:152877. doi: 10.1016/j.scitotenv.2021.152877

29. Akingbola S, Fernandes R, Borden S, Gilbride K, Oswald C, Straus S, et al. Early identification of a COVID-19 outbreak detected by wastewater surveillance at a large homeless shelter in Toronto, Ontario. *Can J Public Health*. (2022) 114:72–9. doi: 10.17269/s41997-022-00696-8

30. Davó L, Seguí R, Botija P, Beltrán MJ, Albert E, Torres I, et al. Early detection of SARS-CoV-2 infection cases or outbreaks at nursing homes by targeted wastewater tracking. *Clin Microbiol Infect*. (2021) 27:1061–3. doi: 10.1016/j.cmi.2021.02.003

31. Hippisley-Cox J, Coupland CA, Mehta N, Keogh RH, Diaz-Ordaz K, Khunti K, et al. Risk prediction of covid-19 related death and hospital admission in adults after covid-19 vaccination: national prospective cohort study. *BMJ*. (2021) 374:n2244. doi: 10.1136/bmj.n2244

32. Li J, Ahmed W, Metcalfe S, Smith WJM, Tscharke B, Lynch P, et al. Monitoring of SARS-CoV-2 in sewersheds with low COVID-19 cases using a passive sampling technique. *Water Res*. (2022) 218:118481. doi: 10.1016/j.watres.2022.118481

33. Sikorski MJ, Levine MM. Reviving the "Moore swab": a classic environmental surveillance tool involving filtration of flowing surface water and sewage water to

recover Typhoidal Salmonella Bacteria. *Appl Environ Microbiol*. (2020) 86:e00060–20. doi: 10.1128/AEM.00060-20

34. Rafiee M, Isazadeh S, Mohseni-Bandpei A, Mohebbi SR, Jahangiri-rad M, Eslami A, et al. Moore swab performs equal to composite and outperforms grab sampling for SARS-CoV-2 monitoring in wastewater. *Sci Total Environ*. (2021) 790:148205. doi: 10.1016/j.scitotenv.2021.148205

35. Schang C, Crosbie ND, Nolan M, Poon R, Wang M, Jex A, et al. Passive sampling of SARS-CoV-2 for wastewater surveillance. *Environ Sci Technol*. (2021) 55:10432–41. doi: 10.1021/acs.est.1c01530

36. Wilson M, Qiu Y, Yu J, Lee BE, McCarthy DT, Pang X. Comparison of auto sampling and passive sampling methods for SARS-CoV-2 detection in wastewater. *Pathogens*. (2022) 11:359. doi: 10.3390/pathogens11030359

37. Lu X, Wang L, Sakthivel SK, Whitaker B, Murray J, Kamili S, et al. US CDC real-time reverse transcription PCR panel for detection of severe acute respiratory syndrome coronavirus 2. *Emerg Infect Dis*. (2020) 26:1654–65. doi: 10.3201/eid2608.201246

38. Rosario K, Symonds EM, Sinigalliano C, Stewart J, Breitbart M. Pepper mild mottle virus as an Indicator of fecal pollution. *Appl Environ Microbiol*. (2009) 75:7261–7. doi: 10.1128/AEM.00410-09

39. Zhang T, Breitbart M, Lee WH, Run JQ, Wei CL, Soh SWL, et al. RNA viral community in human feces: prevalence of plant pathogenic viruses. *PLoS Biol*. (2006) 4:e3. doi: 10.1371/journal.pbio.0040003

40. Kitajima M, Sassi HP, Torrey JR. Pepper mild mottle virus as a water quality indicator. *NPJ Clean Water*. (2018) 1:1–9. doi: 10.1038/s41545-018-0019-5

41. Haramoto E, Kitajima M, Kishida N, Konno Y, Katayama H, Asami M, et al. Occurrence of Pepper mild mottle virus in drinking water sources in Japan. *Appl Environ Microbiol*. (2013) 79:7413–8. doi: 10.1128/AEM.02354-13

42. Chik A, Abbey AM, Flemming C, Fletcher T, Ho J, Oke M, et al. *Ontario MECP, Ontario Clean Water Agency. MECP Wastewater Surveillance Initiative, Protocol for Evaluations of RT-qPCR Performance Characteristics (ISBN 978-1-4868-5481-3 Internal Laboratory Protocol)*. 2021

43. Shiehzadegan S, Alaghemand N, Fox M, Venketaraman V. Analysis of the Delta variant B.1.617.2 COVID-19. *Clin Pract*. (2021) 11:778–84. doi: 10.3390/clinpract11040093

44. Kannan SR, Spratt AN, Cohen AR, Naqvi SH, Chand HS, Quinn TP, et al. Evolutionary analysis of the Delta and Delta plus variants of the SARS-CoV-2 viruses. *J Autoimmun*. (2021) 124:102715. doi: 10.1016/j.jaut.2021.102715

45. D'Aoust PM, Tian X, Towhid ST, Xiao A, Mercier E, Hegazy N, et al. Wastewater to clinical case (WC) ratio of COVID-19 identifies insufficient clinical testing, onset of new variants of concern and population immunity in urban communities. *Sci Total Environ*. (2022) 853:158547. doi: 10.1016/j.scitotenv.2022.158547

46. Schmitz BW, Innes GK, Prasek SM, Betancourt WQ, Stark ER, Foster AR, et al. Enumerating asymptomatic COVID-19 cases and estimating SARS-CoV-2 fecal shedding rates via wastewater-based epidemiology. *Sci Total Environ*. (2021) 801:149794. doi: 10.1016/j.scitotenv.2021.149794

47. Rose C, Parker A, Jefferson B, Cartmell E. The characterization of feces and urine: a review of the literature to inform advanced treatment technology. *Crit Rev Environ Sci Technol*. (2015) 45:1827–79. doi: 10.1080/10643389.2014.1000761

48. Heaton KW, Radvan J, Cripps H, Mountford RA, Braddon FE, Hughes AO. Defecation frequency and timing, and stool form in the general population: a prospective study. *Gut*. (1992) 33:818–24. doi: 10.1136/gut.33.6.818

49. Anderson-Coughlin BL, Shearer AEH, Omar AN, Litt PK, Bernberg E, Murphy M, et al. Coordination of SARS-CoV-2 wastewater and clinical testing of university students demonstrates the importance of sampling duration and collection time. *Sci Total Environ*. (2022) 830:154619. doi: 10.1016/j.scitotenv.2022.154619

50. Bitter LC, Kibbee R, Jiménez GC, Örmeci B. Wastewater surveillance of SARS-CoV-2 at a Canadian university campus and the impact of wastewater characteristics on viral RNA detection. *ACS EST Water*. (2022) 2:2034–46. doi: 10.1021/acsestwater.2c00060

51. Jain N, Hamilton D, Mital S, Ilias A, Brinkmann M, McPhedran K. Long-term passive wastewater surveillance of SARS-CoV-2 for seven university dormitories in comparison to municipal surveillance. *Sci Total Environ*. (2022) 852:158421. doi: 10.1016/j.scitotenv.2022.158421

52. Arts E, Brown S, Bulir D, Charles T, DeGroot C, Delatolla R, et al. *Community surveillance of omicron in Ontario: wastewater-based epidemiology comes of age*. (2022). Available at: https://europepmc.org/article/PPR/PPR468647

53. Bian L, Gao Q, Gao F, Wang Q, He Q, Wu X, et al. Impact of the Delta variant on vaccine efficacy and response strategies. *Expert Rev Vaccines*. (2021) 20:1201–9. doi: 10.1080/14760584.2021.1976153

54. Mlcochova P, Kemp SA, Dhar MS, Papa G, Meng B, Ferreira IATM, et al. SARS-CoV-2 B.1.617.2 Delta variant replication and immune evasion. *Nature*. (2021) 599:114–9. doi: 10.1038/s41586-021-03944-y

55. Wang Y, Chen R, Hu F, Lan Y, Yang Z, Zhan C, et al. Transmission, viral kinetics and clinical characteristics of the emergent SARS-CoV-2 Delta VOC in Guangzhou, China. *EClinicalMedicine*. (2021) 40:101129. doi: 10.1016/j.eclinm.2021.101129

56. Ontario Agency for Health Protection and Promotion (Public Health Ontario). *Epidemiologic summary: SARS-CoV-2 whole genome sequencing in Ontario*. Toronto, ON: Science of The Total Environment. (2021).

57. Cavany S, Bivins A, Wu Z, North D, Bibby K, Perkins TA. Inferring SARS-CoV-2 RNA shedding into wastewater relative to the time of infection. *Epidemiol Infect*. (2022) 150:e21. doi: 10.1017/S0950268821002752

58. Jones TC, Biele G, Mühlemann B, Veith T, Schneider J, Beheim-Schwarzbach J, et al. Estimating infectiousness throughout SARS-CoV-2 infection course. *Science*. (2021) 373:eabi5273. doi: 10.1126/science.abi5273

59. Stankiewicz Karita HC, Dong TQ, Johnston C, Neuzil KM, Paasche-Orlow MK, Kissinger PJ, et al. Trajectory of viral RNA load among persons with incident SARS-CoV-2 G614 infection (Wuhan strain) in association with COVID-19 symptom onset and severity. *JAMA Netw Open*. (2022) 5:e2142796. doi: 10.1001/jamanetworkopen.2021.42796

60. Garcia-Knight M, Anglin K, Tassetto M, Lu S, Zhang A, Goldberg SA, et al. Infectious viral shedding of SARS-CoV-2 Delta following vaccination: a longitudinal cohort study. *PLoS Pathog*. (2022) 18:e1010802. doi: 10.1371/journal.ppat.1010802

61. van Doorn AS, Meijer B, Frampton CMA, Barclay ML, de Boer NKH. Systematic review with meta-analysis: SARS-CoV-2 stool testing and the potential for faecal-oral transmission. *Aliment Pharmacol Ther*. (2020) 52:1276–88. doi: 10.1111/apt.16036

62. Kandel CE, Banete A, Taylor M, Llanes A, McCready J, Crowl G, et al. Similar duration of viral shedding of the severe acute respiratory coronavirus virus 2 (SARS-CoV-2) delta variant between vaccinated and incompletely vaccinated individuals. *Infect Control Hosp Epidemiol*. (2022):1–3. doi: 10.1017/ice.2022.124

63. Jung J, Kim JY, Park H, Park S, Lim JS, Lim SY, et al. Transmission and infectious SARS-CoV-2 shedding kinetics in vaccinated and unvaccinated individuals. *JAMA Netw Open*. (2022) 5:e2213606. doi: 10.1001/jamanetworkopen.2022.13606

64. Pan Y, Zhang D, Yang P, Poon LLM, Wang Q. Viral load of SARS-CoV-2 in clinical samples. *Lancet Infect Dis*. (2020) 20:411–2. doi: 10.1016/S1473-3099(20)30113-4

65. Lescure FX, Bouadma L, Nguyen D, Parisey M, Wicky PH, Behillil S, et al. Clinical and virological data of the first cases of COVID-19 in Europe: a case series. *Lancet Infect Dis*. (2020) 20:697–706. doi: 10.1016/S1473-3099(20)30200-0

66. Prasek SM, Pepper IL, Innes GK, Slinski S, Ruedas M, Sanchez A, et al. Population level SARS-CoV-2 fecal shedding rates determined via wastewater-based epidemiology. *Sci Total Environ*. (2022) 838:156535. doi: 10.1016/j.scitotenv.2022.156535

67. Petala M, Dafou D, Kostoglou M, Karapantsios T, Kanata E, Chatziefstathiou A, et al. A physicochemical model for rationalizing SARS-CoV-2 concentration in sewage. Case study: the city of Thessaloniki in Greece. *Sci Total Environ*. (2021) 755:142855. doi: 10.1016/j.scitotenv.2020.142855

68. News CBC. COVID-19 outbreak declared at UWindsor residence after four positive cases CBC news [internet]. *CBC*. (2021) Available at: https://www.cbc.ca/news/canada/windsor/university-windsor-residence-outbreak-1.6274778

69. Karthikeyan S, Nguyen A, McDonald D, Zong Y, Ronquillo N, Ren J, et al. Rapid, large-scale wastewater surveillance and automated reporting system enable early detection of nearly 85% of COVID-19 cases on a university campus. *mSystems*. (2021) 6:e00793–21. doi: 10.1128/mSystems.00793-21

70. Welling CM, Singleton DR, Haase SB, Browning CH, Stoner BR, Gunsch CK, et al. Predictive values of time-dense SARS-CoV-2 wastewater analysis in university campus buildings. *Sci Total Environ*. (2022) 835:155401. doi: 10.1016/j.scitotenv.2022.155401

71. Delussu F, Tizzoni M, Gauvin L. Evidence of pandemic fatigue associated with stricter tiered COVID-19 restrictions. *PLOS Digit Health*. (2022) 1:e0000035. doi: 10.1371/journal.pdig.0000035

72. Petherick A, Goldszmidt R, Andrade EB, Furst R, Hale T, Pott A, et al. A worldwide assessment of changes in adherence to COVID-19 protective behaviours and hypothesized pandemic fatigue. *Nat Hum Behav*. (2021) 5:1145–60. doi: 10.1038/s41562-021-01181-x

73. Liu Y, Rocklöv J. The reproductive number of the Delta variant of SARS-CoV-2 is far higher compared to the ancestral SARS-CoV-2 virus. *J Travel Med*. (2021) 28:taab124. doi: 10.1093/jtm/taab124

74. Colosi LM, Barry KE, Kotay SM, Porter MD, Poulter MD, Ratliff C, et al. Development of wastewater pooled surveillance of severe acute respiratory syndrome coronavirus 2 (SARS-CoV-2) from congregate living settings. *Appl Environ Microbiol*. (2021) 87:e00433–21. doi: 10.1128/AEM.00433-21

75. Mercier E, D'Aoust PM, Thakali O, Hegazy N, Jia JJ, Zhang Z, et al. Municipal and neighbourhood level wastewater surveillance and subtyping of an influenza virus outbreak. *Sci Rep*. (2022) 12:15777. doi: 10.1038/s41598-022-20076-z

76. Hughes B, Duong D, White BJ, Wigginton KR, Chan EMG, Wolfe MK, et al. Respiratory syncytial virus (RSV) RNA in wastewater settled solids reflects RSV clinical positivity rates. *Environ Sci Technol Lett*. (2022) 9:173–8. doi: 10.1021/acs.estlett.1c00963

frontiers | Frontiers in Public Health

TYPE Original Research
PUBLISHED 02 June 2023
DOI 10.3389/fpubh.2023.1178515

OPEN ACCESS

EDITED BY
David Champredon,
Public Health Agency of Canada (PHAC), Canada

REVIEWED BY
Dustin Hill,
Syracuse University, United States
Saber Soltani,
Tehran University of Medical Sciences, Iran

*CORRESPONDENCE
Irene Xagoraraki
✉ xagorara@msu.edu

†These authors have contributed equally to this work and share first authorship

RECEIVED 02 March 2023
ACCEPTED 12 May 2023
PUBLISHED 02 June 2023

CITATION
Gentry Z, Zhao L, Faust RA, David RE, Norton J and Xagoraraki I (2023) Wastewater surveillance beyond COVID-19: a ranking system for communicable disease testing in the tri-county Detroit area, Michigan, USA.
Front. Public Health 11:1178515.
doi: 10.3389/fpubh.2023.1178515

Wastewater surveillance beyond COVID-19: a ranking system for communicable disease testing in the tri-county Detroit area, Michigan, USA

Zachary Gentry[1†], Liang Zhao[1†], Russell A. Faust[2], Randy E. David[3], John Norton[4] and Irene Xagoraraki[1*]

[1]Department of Civil and Environmental Engineering, Michigan State University, East Lansing, MI, United States, [2]Oakland County Health Division, Pontiac, MI, United States, [3]Wayne State University School of Medicine, Detroit, MI, United States, [4]Great Lakes Water Authority, Detroit, MI, United States

Introduction: Throughout the coronavirus disease 2019 (COVID-19) pandemic, wastewater surveillance has been utilized to monitor the disease in the United States through routine national, statewide, and regional monitoring projects. A significant canon of evidence was produced showing that wastewater surveillance is a credible and effective tool for disease monitoring. Hence, the application of wastewater surveillance can extend beyond monitoring SARS-CoV-2 to encompass a diverse range of emerging diseases. This article proposed a ranking system for prioritizing reportable communicable diseases (CDs) in the Tri-County Detroit Area (TCDA), Michigan, for future wastewater surveillance applications at the Great Lakes Water Authority's Water Reclamation Plant (GLWA's WRP).

Methods: The comprehensive CD wastewater surveillance ranking system (CDWSRank) was developed based on 6 binary and 6 quantitative parameters. The final ranking scores of CDs were computed by summing the multiplication products of weighting factors for each parameter, and then were sorted based on decreasing priority. Disease incidence data from 2014 to 2021 were collected for the TCDA. Disease incidence trends in the TCDA were endowed with higher weights, prioritizing the TCDA over the state of Michigan.

Results: Disparities in incidences of CDs were identified between the TCDA and state of Michigan, indicating epidemiological differences. Among 96 ranked CDs, some top ranked CDs did not present relatively high incidences but were prioritized, suggesting that such CDs require significant attention by wastewater surveillance practitioners, despite their relatively low incidences in the geographic area of interest. Appropriate wastewater sample concentration methods are summarized for the application of wastewater surveillance as per viral, bacterial, parasitic, and fungal pathogens.

Discussion: The CDWSRank system is one of the first of its kind to provide an empirical approach to prioritize CDs for wastewater surveillance, specifically in geographies served by centralized wastewater collection in the area of interest. The CDWSRank system provides a methodological tool and critical information that can help public health officials and policymakers allocate resources. It can be used to prioritize disease surveillance efforts and ensure that public health interventions are targeted at the most potentially urgent threats. The CDWSRank system can be easily adopted to geographical locations beyond the TCDA.

KEYWORDS

wastewater surveillance, communicable disease (CD), ranking system, COVID-19, emerging disease

1. Introduction

Since the beginning of the coronavirus disease 2019 (COVID-19) pandemic, wastewater surveillance has been consistently applied to monitor severe acute respiratory syndrome coronavirus 2 (SARS-CoV-2) viral RNA worldwide (1–10). Wastewater surveillance epidemiology is a translation of the theory that human wastewater can serve as a representative community-composite sample to monitor fluctuations of disease incidence. A pathogen that can be detected in bodily fluids, including excreta, urine, sputum, and saliva, has the potential to be detected and thus, monitored (2, 11–14). Wastewater surveillance and epidemiology has a diverse range of benefits, including (1) circumventing the need for mass clinical testing, (2) conserving health, economic, and societal resources, (3) providing unbiased and unspecific monitoring of disease incidence regardless of symptomatic or asymptomatic conditions, and (4) providing early warnings of impending disease surges (4, 5, 7, 10, 12, 15). Wastewater surveillance has been extraordinarily successful at monitoring multiple pathogens, including SARS-CoV-2 (2, 4–7, 11, 16), hepatitis A and hepatitis E (17), herpesviruses (18), poliovirus (19, 20), and others. Despite its great potential, most wastewater disease monitoring to date has been limited to SARS-CoV-2. Notably, recent exceptions encompass poliovirus (21) and monkeypox virus (22–24). Thus, it is paramount that the adoption and integration of this scientifically-validated methodology is accelerated, particularly among emerging disease, neglected disease, or diseases of high outbreak potential.

Communicable diseases (CDs), for instance, tuberculosis (TB) and sexually transmitted infections (STIs), are among the leading causes of death and disability worldwide, according to the WHO (who.int). CDs are caused by microorganisms including bacteria, viruses, fungi, or various parasites that can be transmitted widely and quickly within human populations (25). Some infectious diseases are transmitted through "bites" from insect vectors, while others can be caused by ingesting contaminated food or water (who.int). The WHO, U.S. NIH, U.S. AID, U.S. CDC, and the international scientific community has long recognized the need to develop a comprehensive education, prediction, and prevention system for CDs (13, 26, 27).

A few studies have developed methodologies for ranking CD threats to the public (28–30). However, these systems have limitations and cannot be directly used by local health department to make decisions regarding appropriate targets for wastewater surveillance. Briefly, they relied heavily on subjective assessments of weights given by experts to multiple parameters. They were lacking critical quantitative information such as incidence of diseases based on clinical data, and basic reproduction numbers of CDs. Besides, most parameters were assigned a value according to the Delphi Method, which consists of gathering expert opinions to weight a disease on a parameter then multiplied by a scale of numbers such as 1–5 (29) or 0–7 (31) in terms of level of importance.

The objective of this study is to develop a comprehensive communicable disease ranking system ("CDWSRank" system) that prioritizes CDs for wastewater surveillance (Figure 1). To this end, we investigated 96 CDs in the Tri-County Detroit Area (TCDA), Michigan, Unites States, reported through the Michigan Disease Surveillance System (MDSS). All CDs were ranked through the CDWSRank system, which involved 2 categories of parameter: binary and quantitative. Binary parameters examine the presence or absence of CDs in the following inventories: (1) CDC National Notifiable Infectious Disease and Conditions List (NNIDCL), (2) Michigan Department of Health and Human Services (MDHHS) Weekly Disease Report, (3) EPA Contaminant Candidate List (CCL), (4) CDC bioterrorism agents list, (5) pathogen's detectability in wastewater or excreta, and (6) association of disease with single or multiple pathogens. Quantitative parameters include: (1) clinical case trend in Michigan, (2) clinical case trend in the TCDA, (3) ratio of clinical case incidence between Michigan and the TCDA (geographic ratio), (4) annual clinical cases in Michigan, (5) annual clinical cases in the TCDA, and (6) the R_0 (basic reproduction number) of the disease.

The CDWSRank system is one of the first of its kind to provide an empirical method for selecting CDs for wastewater surveillance, in geographies serviced by centralized wastewater collection and treatment. To demonstrate the importance of site-specific ranking, CD trends were analyzed for both the TCDA and Michigan as a whole for the period between 2014 and 2021. This manuscript will moreover summarize wastewater sampling methods based on pathogen type. Ultimately, this article should contribute to the reduced impact of CDs by procuring valuable information for public health practitioners, researchers, and medical professionals.

2. Materials and methods

2.1. Communicable disease data acquisition

Weekly reports from the MDSS between 2014 and 2021 were accessed from the MDHHS website (michigan.gov/mdhhs). Data in the weekly reports were provisional, based on current data at the time that the report was published. Communicable disease incidence (per 100,000) for the state of Michigan are shown in Figure 2. Similar data was collected for the TCDA, including City of Detroit, and Wayne, Macomb, and Oakland Counties. Examples of disease trends between 2014 and 2017 are shown in Figures 3–6. MDSS weekly disease reports define the epidemiological "week" in concurrence with the CDC's Morbidity and Mortality Weekly Report (MMWR) (cdc.gov/mmwr), which runs from Sunday (day 1) to Saturday (day 7). All CDs were cross-referenced against multiple regulatory

Abbreviations: CCL, Contaminant Candidate List; CDWSRank system, communicable disease wastewater surveillance ranking system; CDs, communicable diseases; GI, Gastrointestinal Illness; GLWA, Great Lakes Water Authority; HIV/AIDS, Human Immunodeficiency Virus and Acquired Immunodeficiency Syndrome; TCDA, Tri-County Detroit Area; MDHHS, Michigan Department of Health and Human Services; MDSS, Michigan Disease Surveillance System; WDR, MDHHS/MDSS Weekly Disease Report; NNIDCL, National Notifiable Infectious Disease and Conditions List; STDs, sexually transmitted diseases; U.S. EPA, United States Environmental Protection Agency; U.S. AID, United States Agency of International Development; U.S. CDC, United States Centers for Disease Control and Prevention; U.S. NIH, United States National Institutes of Health; WHO, World Health Organization.

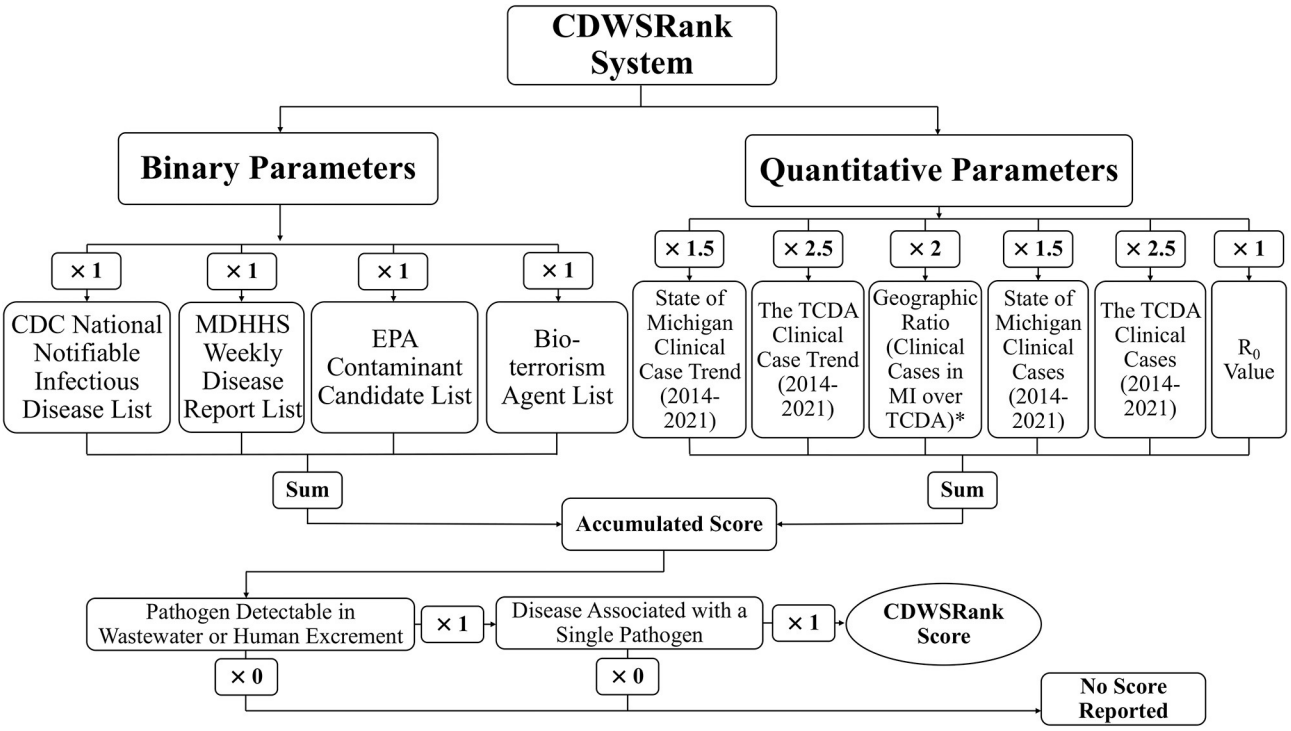

FIGURE 1
Overall schematic of CDWSRank system. *marked parameter indicates that the annual caseload for Michigan from 2014-2021 was divided by the annual caseload for the TCDA, where the average of those was then taken for downstream analyses. The A+1 value was assigned to those CDs with an average ratio of <1.

lists including the U.S. CDC's NNIDCL (cdc.gov/nndss), the U.S. EPA's CCL (epa.gov/ccl), and the U.S. CDC's bioterrorism agents list (cdc.gov/bioterrorism). Additionally, the detectability of the pathogens associated with each CD in human excreta and wastewater, which is crucial evidence for the applicability of wastewater surveillance for monitoring CDs, was investigated through an extensive literature review (Tables 1–4). R_0's were also collected through a literature review and are summarized in Table 5.

2.2. The CDWSRank system

The following sections demonstrate the design of the CDWSRank system and its associated parameters. The presence and absence of all CDs in regulatory lists including NNIDCL, WDR, and CCL, as well as being described as a bioterrorism agent, the association of the disease with a single or multiple pathogens, and detectability of pathogens in human wastewater were modeled as binary parameters. Quantitative parameters include: (1) clinical case trend in Michigan, (2) clinical case trend in the TCDA, (3) ratio of clinical case incidence between Michigan and the TCDA (geographic ratio), (4) annual clinical cases in Michigan, (5) annual clinical cases in the TCDA, and (6) the R_0 (basic reproduction number) of the disease. The overall schematic of the parameters and weighting factors of each parameter is presented in Figure 1.

2.2.1. Binary parameters

The presence or absence of CDs for each binary parameter was treated as a ×1 weighting factor (multiplier) and ×0 weighting factor (multiplier), respectively, which were then summed for the final ranking score. The CDC's NNIDCL provides comprehensive reporting of CDs that occur in the USA. Diseases that are reported in the NNIDCL are considered notifiable, but whether or not they are reported at the state level, varies (cdc.gov). Furthermore, internationally notifiable diseases reported in WHO's International Health Regulations (IHR), such as cholera, are also reportable in NNIDCL (cdc.gov). The IHR covers not only CDs but also other public health concerns including chemical and radiological threats (cdc.gov). All CDs were assessed for whether they are listed on the CDC's NNIDCL, and the corresponding presence or absence was marked with "Y" (presence in NNIDCL) or "N" (absence in NNIDCL). A multiplier of 1 was assigned to any CD's presence on NNIDCL. Similarly, the presence of a CD in the MDHHS Weekly Disease Report (WDR) was given a weighting factor or "multiplier" of 1.

The EPA's CCL includes drinking water contaminants that are recognized or expected to occur in public water systems and are not currently subject to EPA drinking water regulations (epa.gov). The EPA uses the CCL to identify priority contaminants for regulatory decision-making and information gathering (epa.gov). The EPA announced Draft CCL 5 on July 19, 2021, followed by the publication of Final CCL 5 on November 14, 2022 (epa.gov). All CDs were assessed for whether they appear on EPA CCL 5,

10.3389/fpubh.2023.1178515

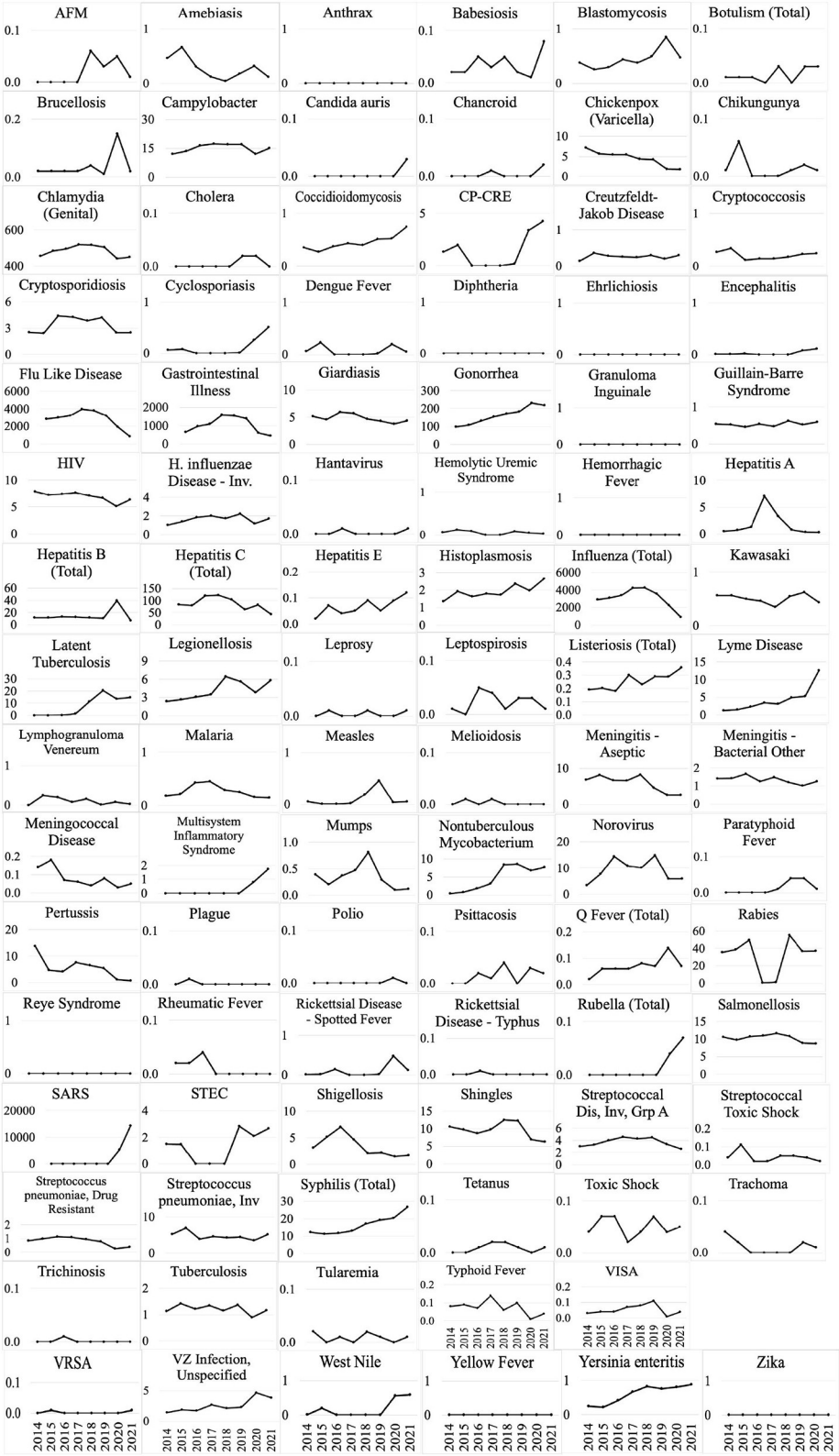

FIGURE 2
Disease incidence (per 100,000) for 95 CDs between 2014 and 2021 in the state of Michigan (Disease incidence for Monkeypox was unavailable during this period).

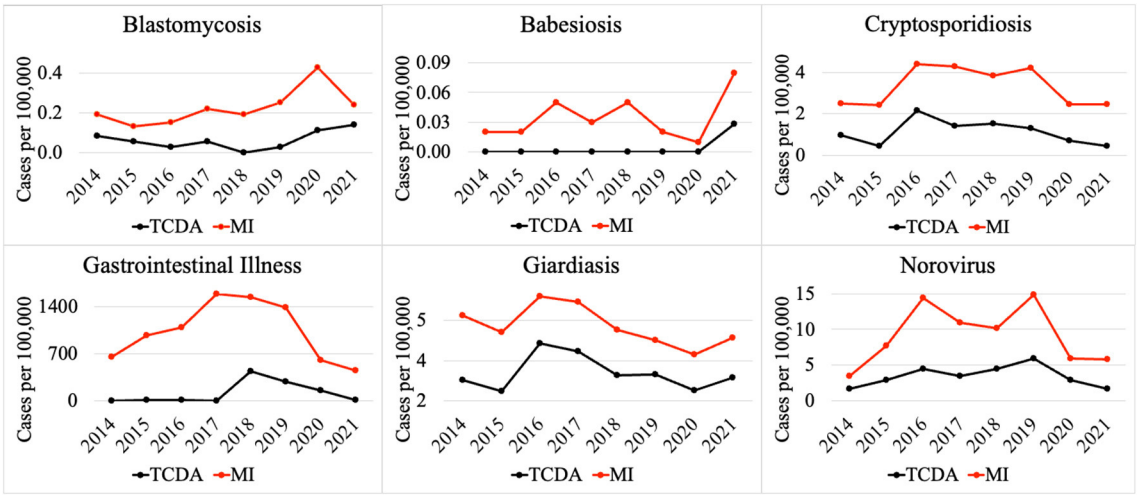

FIGURE 3
Comparison of selected CDs incidences (per 100,000) between TCDA and MI (ratio < 1).

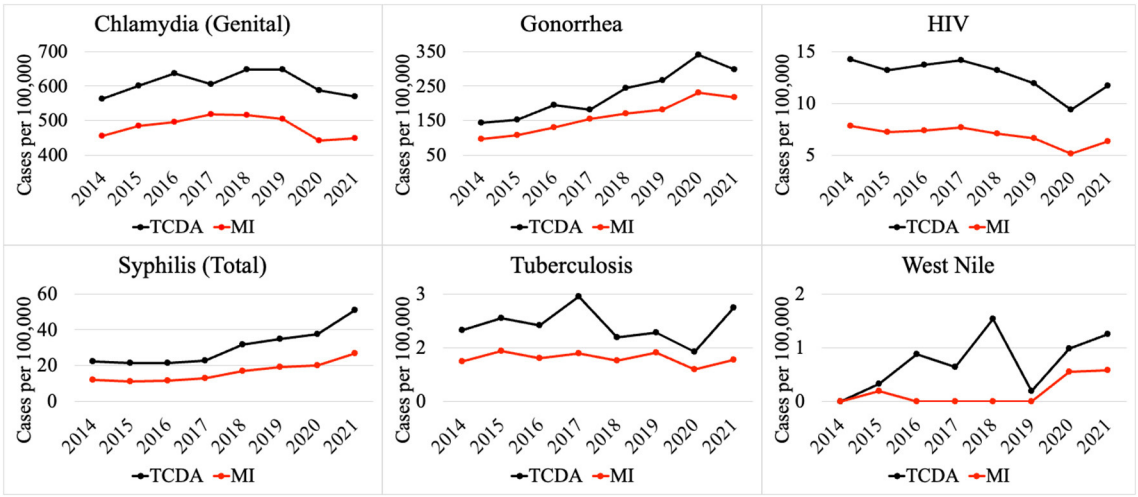

FIGURE 4
Comparison of selected CDs incidences (per 100,000) between TCDA and MI (ratio > 1).

and the corresponding presence or absence was marked with a "Y" (presence in CCL) or "N" (absence in CCL).

The CDC classifies bioterrorism agents into 3 categories, namely, A, B, and C, depending, primarily, on how easily the diseases can be transmitted and the severity of illness (cdc.gov). Agents in category A are considered of the highest risk, as they can be easily transmitted within human populations and can result in high death rates and significant public health impacts. Examples include anthrax and plague. Agents in category B have the second highest priority risk, as they are moderately easy to spread and can result in moderate morbidity rates. Examples include Q fever and typhus fever. Agents in category C are considered the third highest priority risk and they can easily spread among humans and cause health impacts (cdc.gov). Examples include hantavirus and Nipah virus. The presence of CDs as CDC-defined bioterrorism agents was marked with "*" for category A and "**" for category B. A weighting factor or multiplier of 1 was assigned to a CD listed as a CDC bioterrorism agent, regardless of category.

The detectability of pathogens causative of CDs in human wastewater is crucial to the successful implementation of wastewater surveillance. Following extensive literature reviews, the detectability of the causative pathogen in excreta or wastewater was marked with a "Y" (detectable), "N" (non-detectable), or "N/A" (data unavailable) in Tables 1–4. For the final ranking score, a multiplier of 1 or 0 was given to CDs with a causative pathogen that is detectable or non-detectable, respectively, in excreta and/or wastewater.

The binary parameter of disease associated with single or multiple pathogens considers the exact source of a causative pathogen of a CD. In this system, CDs with multiple

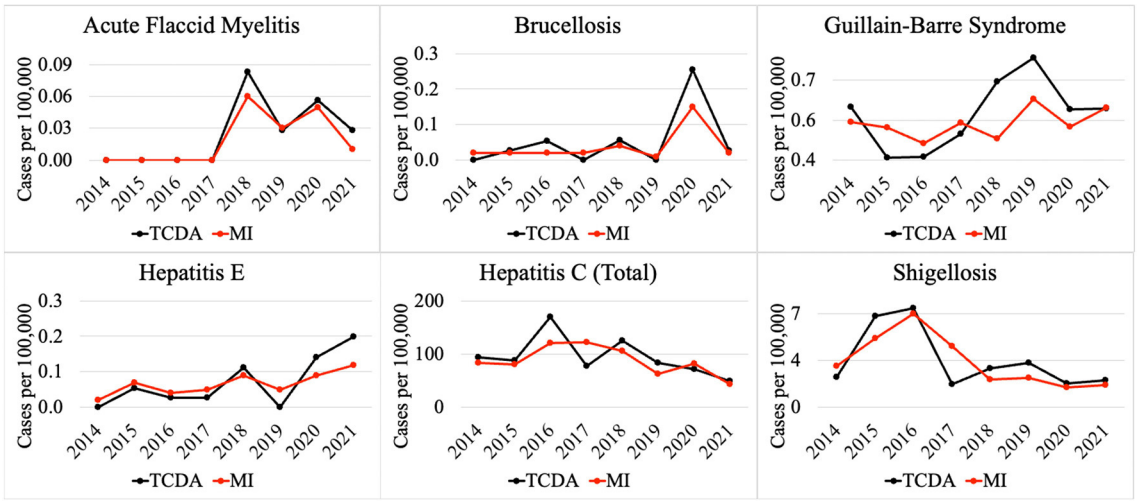

FIGURE 5
Comparison of selected CDs incidences (per 100,000) between TCDA and MI (ratio ≈ 1).

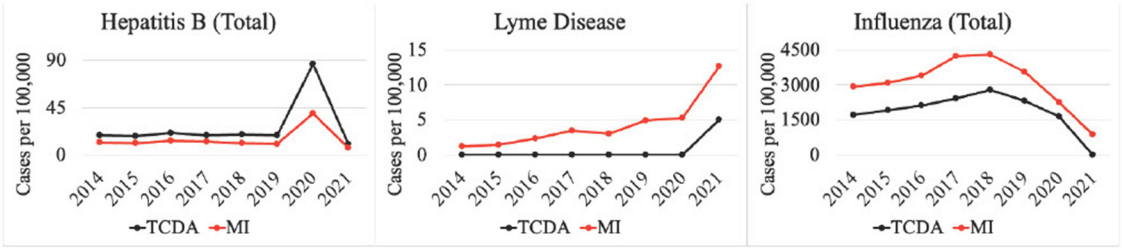

FIGURE 6
Selected CDs incidences potentially affected by the COVID-19 pandemic.

causative pathogens would make them nearly impossible to be determined or detected. Therefore, CDs with multiple causative pathogens were assigned a multiplier of 0 at the final ranking score, to moderate the over-ranking of these CDs. A final ranking multiplier of 1 was assigned to CDs with a single causative pathogen.

2.2.2. Quantitative parameters

Quantitative parameters include: (1) clinical case trend in Michigan, (2) clinical case trend in the TCDA, (3) ratio of clinical case incidence between Michigan and the TCDA (geographic ratio), (4) annual clinical cases in Michigan, (5) annual clinical cases in the TCDA, and (6) the R_0 (basic reproduction number) of the disease. Clinical case trends in Michigan as a whole and in the TCDA specifically, were determined by calculating the correlation R-value between disease incidence (per 100,000) each year (2014 to 2021) and the given year, for all CDs. The weighting factor or multiplier of 1.5 and 2.5 were assigned to clinical case trends in Michigan and the TCDA, respectively, providing greater emphasis on the TCDA.

The ratio of clinical case incidence between Michigan and the TCDA is assessed through calculating case incidence (per 100,000) for each CD, for the state of Michigan, then the TCDA. Next, the ratio of these values is calculated as the quotient of Michigan cases and TCDA cases, done for each year in the study period. Finally, the average of annual ratios was calculated, and each CD was assigned a value of 1 if the average was less than 1 (indicating that the CD was more prevalent in the TCDA than the state of Michigan as a whole). A CD was assigned a value of 0 if the ratio was equal to, or greater than 1. A weighting factor or "multiplier" of 2 was given to this metric.

Clinical cases in Michigan and in the TCDA were determined by computing the decadic log of the average clinical caseload for the years studied. Taking the common logarithm was necessary as clinical caseloads varied greatly in magnitude; this operation, therefore, allowed for the comparison of CDs even with disparate magnitudes of caseloads, while still preserving accurate variation measures. The weighting factor or "multiplier" of 1.5 and 2.5 were assigned to clinical cases in Michigan and the TCDA, respectively, providing greater emphasis on the TCDA.

The R_0 of CDs were determined through literature investigation (Table 5). This parameter was included to increase the ranking score of CDs that can be transmitted efficiently, through person-to-person contact (167). This parameter prioritizes CDs that have the potential to spread rapidly. This parameter was given a weighting factor of 1.

10.3389/fpubh.2023.1178515

TABLE 1 MDHHS-reported conditions associated with viruses that can potentially be monitored with wastewater surveillance.

Disease name	Virus potentially associated with the disease	Found in excrement	Found in wastewater	CDC NNIDCL?	EPA CCL?
Acute flaccid myelitis (AFM)	West Nile, enteroviruses, other viruses	Yes	Yes	N	Y
Chickenpox (Varicella)	Varicella-Zoster Virus	Yes	Yes	Y	N
Chikungunya	Chikungunya Virus	Yes	N/A	Y	N
Coronavirus disease 2019 (COVID-19)	Severe acute respiratory syndrome coronavirus 2 (SARS-CoV-2)	Yes	Yes	Y	N
Dengue fever	Dengue Virus	Yes	Yes	Y	N
Flu like disease	Multiple viruses	N/A	Yes	N	N
Gastrointestinal illness	Multiple viruses, bacteria, parasites	Yes	Yes	Y	N
Hepatitis A	Hepatitis A Virus	N/A	Yes	Y	Y
Hepatitis B	Hepatitis B Virus	Yes	Yes	Y	N
Hepatitis C	Hepatitis C Virus	Yes	Yes	Y	N
Hepatitis E	Hepatitis E Virus	Yes	Yes	N	N
Human Immunodeficiency Virus (HIV) Infection	HIV virus	Yes	Yes	Y	N
Influenza	Influenza virus	N/A	Yes	Y	N
Measles	Measles virus	Yes	Yes	Y	N
Meningitis - Aseptic	Several kinds of viruses. Most Commonly nonpolio enteroviruses	N/A	Yes	N	N
Monkeypox	Monkeypox virus	Yes	Yes	N	N
Mumps	Mumps virus	Yes	N/A	Y	N
Norovirus	Norovirus	Yes	Yes	N	Y
Polio	Poliovirus	Yes	Yes	Y	N
Rubella	Rubella virus	N/A	Yes	Y	N
Shingles	Varicella-Zoster virus	Yes	Yes	N	N
VZ Infection, Unspecified	Varicella-Zoster virus	Yes	Yes	Y	N
West Nile Virus	West Nile virus	Yes	Yes	N	N
Yellow Fever	Yellow fever virus	Yes	N/A	Y	N
Zika	Zika virus	Yes	Yes	Y	N

MDHHS, Michigan Department of Health and Human Services; NNIDCL, National Notifiable Infectious Disease and Conditions List; CCL, Contaminant Candidate List. N/A indicates the information was unavailable at the time that the study was conducted. Data sources: (4–7, 13, 24, 32–55).

2.2.3. Overall CDWSRank system ranking score

An overall ranking score (R_{CD}) of the CDWSRank system for CDs is calculated using the following Eq. (1), where R_{CD} is the overall ranking score of the i^{th} CD, W_i is the weighting factor for binary parameters, N_i is the weighting factor for quantitative parameters, B_i represents binary parameters, Q_i represents quantitative parameters, D_i represents the detectability of causative pathogens in human excreta or wastewater, and M_i represents the association of a CD with a single or multiple pathogens.

$$R_{\mathrm{CD}} = (W_i \sum_{i=1}^{n} B_i + N_i \sum_{i=1}^{m} Q_i) \times D_i \times M_i \quad (1)$$

An equation for calculating an overall rank score of the i^{th} CD with all binary and quantitative parameters displayed, can be expressed as follows:

R_{CD} = [1 × (NNIDCL) + 1 × (WDR) + 1 × (CCL) + 1 × (Bioterrorism) + 2 × (Geographic ratio) + 1.5 × (Clinical case trend in Michigan) + 2.5 × (Clinical case trend in the TCDA) + 1.5 × (Clinical case in Michigan) + 2.5 × (Clinical case in TCDA) + 1 × (R_0)] × [1 × (Detectability in human excreta or wastewater)] × [1 × (Association of disease with single or multiple pathogens)] (2)

For example, an overall rank score of SARS-CoV-2 can be computed as: [1 × (1) + 1 × (1) + 1 × (0) + 1 × (0) + 2 × (1) + 1.5 × (0.57) + 2.5 × (0.6) + 1.5 × (5.39) + 2.5 × (4.98) + 1 × (2.11)] × (1) × (1) = 29.

10.3389/fpubh.2023.1178515

TABLE 2 MDHHS-reported conditions associated with bacteria that can potentially be monitored with wastewater surveillance.

Disease name	Bacteria potentially associated with the disease	Found in excrement	Found in wastewater	CDC NNIDCL?	EPA CCL?
Anthrax*	Bacillus anthracis	N/A	Yes	Y	N
Botulism*	Clostridium (botulinum, butyricum, baratii)	Yes	N/A	Y	N
Brucellosis**	Brucella spp.	N/A	Yes	Y	N
Campylobacter	Campylobacter spp.	Yes	Yes	Y	Y^
Chlamydia (Genital)	Chlamydia trachomatis	Yes	N/A	Y	N
Cholera**	Vibrio cholerae	Yes	N/A	Y	N
CP-CRE	Enterobacter resistant to carbapenem	Yes	Yes	Y	Y
Gonorrhea	Neisseria gonorrhoeae	Yes	N/A	Y	N
Guillain-Barre Syndrome	Campylobacter jejuni, several viruses	N/A	Yes	N	Y
H. Influenzae Disease - Inv.	Haemophilus influenzae	Yes	N/A	Y	N
Legionellosis	Legionella pneumophila	Yes	Yes	Y	Y
Leprosy	Mycobacterium leprae	Yes	N/A	N	N
Leptospirosis	Leptospira spp.	Yes	N/A	Y	N
Listeriosis	Listeria monocytogenes	N/A	Yes	Y	N
Lymphogranuloma Venereum	Chlamydia trachomatis L1, L2, L3	Yes	N/A	Y	N
Nontuberculous Mycobacterium	Mycobacteria spp.	Yes	Yes	N	N
Paratyphoid Fever	Salmonella Paratyphii A, B, and C	Yes	Yes	N	N
Plague*	Yersinia pesits	N/A	Yes	Y	N
Psittacosis	Chlamydia psittaci	Yes	N/A	Y	N
Q Fever**	Coxiella burnetti	N/A	Yes	Y	N
Salmonellosis	Salmonella	Yes	Yes	Y	Y
Shiga Toxin-producing Escherichia Coli (STEC)	E. coli	N/A	Yes	Y	Y
Shigellosis	Shigella	Yes	Yes	Y	Y
Streptococcus Pneumoniae, Drug Resistant	Streptococcus pneumoniae	Yes	N/A	N	N
Streptococcus Pneumoniae, Inv	Streptococcus pneumoniae	Yes	N/A	N	N
Syphilis	Treponema pallidum	Yes	N/A	Y	N
Toxic Shock	Staphylococcus and streptococcus bacteria	N/A	Yes	Y	N
Trachoma	Chlamydia trachomatis	Yes	N/A	Y	N
Tuberculosis	Mycobacterium tuberculosis	Yes	Yes	Y	N
Typhoid Fever	Salmonella typhii	Yes	Yes	Y	N
VISA/VRSA	Staphylococcus aureus	N/A	Yes	Y	N

MDHHS, Michigan Department of Health and Human Services; NNIDCL, National Notifiable Infectious Disease and Conditions List; CCL, Contaminant Candidate List. N/A indicates the information was unavailable at the time that the study was conducted. *indicates bioterrorism category A. **indicates bioterrorism category B. Data sources: (56–86).

TABLE 3 MDHHS-reported conditions associated with parasites that can potentially be monitored with wastewater surveillance.

Disease name	Parasite(s) potentially associated with the disease	Found in excrement	Found in wastewater	CDC NNIDCL?	EPA CCL?
Amebiasis	Entamoeba histolytica	Yes	Yes	N	N
Cryptosporidiosis**	Cryptosporidium parvum	Yes	Yes	Y	N
Cyclosporiasis	Cyclospora cayetanensis	Yes	Yes	Y	N
Giardiasis	Giardia duodenalis	Yes	Yes	Y	N
Malaria	Plasmodium falciparum	Yes	N/A	Y	N

MDHHS, Michigan Department of Health and Human Services; NNIDCL, National Notifiable Infectious Disease and Conditions List; CCL, Contaminant Candidate List. N/A indicates the information was unavailable at the time that the study was conducted. **indicates bioterrorism category B. The parasitic category is designated for pathogens caused by parasitic organisms, excluding fungal, bacterial, and viral pathogens. Data sources: (87–95).

TABLE 4 MDHHS-reported conditions associated with fungi that can potentially be monitored with wastewater surveillance.

Disease name	Fungus potentially associated with the disease	Found in excrement	Found in wastewater	CDC NNIDCL?	EPA CCL?
Blastomycosis	Blastomyces dermatitidis and gilchristii	Yes	N/A	N	N
Candida auris	Candida auris	Yes	Yes	Y	N
Cryptococcosis	Cryptococcus neoformans	N/A	Yes	N	N

MDHHS, Michigan Department of Health and Human Services; NNIDCL, National Notifiable Infectious Disease and Conditions List; CCL, Contaminant Candidate List. N/A indicates the information was unavailable at the time that the study was conducted. Data sources: (96–99).

2.3. Wastewater surveillance concentration methods based on pathogen type

In addition to the development of the CDWSRank system, a comprehensive literature review was conducted to summarize appropriate wastewater sample concentration surveillance methods based pathogen type, namely: bacterial, fungal, parasitic, and viral (Table 6).

3. Results

3.1. Classification of CDs

Tables 1–3 present viruses, bacteria, parasites and fungi that are detectable in human excrement or wastewater, indicating their potential to be monitored by wastewater surveillance. Notably, some of the listed pathogens were successfully detected in worldwide wastewater samples, with disease incidence monitored using wastewater surveillance. These include dengue virus (32), hepatitis B (33), monkeypox virus (22–24), norovirus (168, 169), Poliovirus (19, 20), SARS-CoV-2 (2, 4–7, 10, 16), yellow fever virus, and zika virus (32).

Twenty-five CDs are associated with viral pathogens, including chickenpox, COVID-19, monkeypox, norovirus, West Nile fever and so on (Table 1). The viruses that are associated with the diseases are also summarized in Table 1. For instance, varicella-zoster virus is the causative agent of chickenpox. Notably, only 3 of the 25 viruses, including acute flaccid myelitis-related enterovirus, hepatitis A, and norovirus, appear on the EPA's CCL. Some viral diseases can be found on the CDC's NNIDCL, including COVID-19, HIV/AIDS, and Zika. No viral CDs in the list are classified as CDC bioterrorism agents. Table 2 shows 31 CDs associated with bacterial pathogens, including anthrax, cholera, gonorrhea, plague, syphilis, and so forth. The bacteria that are potentially associated with the diseases were also summarized in Table 2. For instance, clostridium (botulinum, butyricum, baratii) is the potential causative agent associated with botulism. Seven of the 31 bacteria are listed on the EPA's CCL, including chlamydia, CP-CRE, Guillain-Barre syndrome, legionellosis, salmonellosis, STEC, and shigellosis. And 25 of the 31 of the bacterial-related CDs are listed on the CDC's NNIDCL. Six of 31 bacterial-related CDs are not listed on the CDC's NNIDCL, including Guillain-Barre syndrome, leprosy, non-tuberculous mycobacterium, paratyphoid fever, and streptococcus pneumoniae. Among all bacterial CDs, anthrax, botulism, and plague are listed in bioterrorism category A, while brucellosis, cholera, and Q fever are listed in bioterrorism category B. Table 3 includes 5 parasitic CDs that can be detected in either human excreta or wastewater. The potentially causative agents of these diseases were also summarized in Table 3. For instance, cryptosporidium parvum is the parasite associated with cryptosporidiosis. None of pathogens related to parasitic CDs are listed on the EPA's CCL, and 4 of them are listed on the CDC's NNIDCL, including cryptosporidiosis, cyclosporiasis, giardiasis, and malaria, expect for amebiasis. Cryptosporidiosis is listed in the CDC's bioterrorism category B. Lastly, Table 4 shows 3 fungal-related CDs, including blastomycosis, cryptococcosis, and candidiasis. The fungi associated with the diseases are summarized in Table 4. For instance, blastomyces dermatitidis and gilchristii are the potential causes of blastomycosis. None of them are listed on the EPA's CCL and only candidiasis (candida auris) was listed on the CDC's NNIDCL (Table 4).

10.3389/fpubh.2023.1178515

TABLE 5 R_0 values for 96 CDs.

Disease name	R_0 Value	Source
Acute flaccid myelitis (AFM)	0	N/A
Amebiasis	7	(100)
Anthrax	1.251	(101)
Babesiosis++	1.56	(102)
Blastomycosis	0	N/A
Botulism (Total)	0	N/A
Brucellosis	0	N/A
Campylobacter	0	N/A
Candida auris	0	N/A
Chancroid	0	N/A
Chickenpox (Varicella)	11	(rcpi.ie)
Chikungunya	3.4	(103)
Chlamydia (Genital)	0.55	(104)
Cholera	2.15	(105)
Coccidioidomycosis	0	N/A
CP-CRE	0	N/A
Creutzfeldt-Jakob Disease	0	N/A
Cryptococcosis	0	N/A
Cryptosporidiosis	0	(106)
Cyclosporiasis	0	N/A
Dengue Fever	10	(107)
Diphtheria	7.2	(108)
Ehrlichiosis	0	N/A
Encephalitis	0	N/A
Flu Like Disease	1.5	(vdh.virginia.gov)
Gastrointestinal Illness	0	N/A
Giardiasis	4.181	(109)
Gonorrhea	0.89	(110)
Granuloma Inguinale	0	N/A
Guillain-Barre Syndrome	0	N/A
HIV	3.5	(netec.org)
H. influenzae Disease - Inv.	0	N/A
Hantavirus	0	N/A
Hemolytic Uremic Syndrome	0	N/A
Hemorrhagic Fever	1.62	(111)
Hepatitis A	0	N/A
Hepatitis B (Total)	9.175	(112)
Hepatitis C (Total)	2.12	(113)
Hepatitis E	6.5	(114)
Histoplasmosis	0	N/A
Influenza (Total)	1.5	(vdh.virginia.gov)

(Continued)

TABLE 5 (Continued)

Disease name	R_0 Value	Source
Kawasaki	0	N/A
Latent Tuberculosis	0	N/A
Legionellosis	0	N/A
Leprosy	2.75	(115)
Leptospirosis	1.52	(116)
Listeriosis (Total)	0	N/A
Lyme Disease	0	N/A
Lymphogranuloma venereum	3.5	(netec.org)
Malaria	0	N/A
Measles	15	(117)
Melioidosis	0	N/A
Meningitis - Aseptic	1.048	(118)
Meningitis - Bacterial Other	1.048	(118)
Meningococcal Disease	1.36	(119)
Monkeypox	2.1	(120)
Multisystem Inflammatory Syndrome	0	N/A
Mumps	11	(health.gov.au)
Nontuberculous Mycobacterium	9	(121)
Norovirus	2	(122)
Paratyphoid Fever	2.8	(123)
Pertussis	5.5	(124)
Plague	1.45	(125)
Polio	12	(126)
Psittacosis	0	N/A
Q Fever (Total)	0	N/A
Rabies	0	N/A
Reye Syndrome	0	N/A
Rheumatic Fever	0	N/A
Rickettsial Disease - Spotted Fever	1.7	(127)
Rickettsial Disease - Typhus	0	N/A
Rubella (Total)	6.6	(128)
Salmonellosis	0	N/A
SARS	2.11	(129)
STEC	1.5	(130)
Shigellosis	1.29	(131)
Shingles	0	N/A
Streptococcal Dis, Inv, Grp A	0	N/A
Streptococcal Toxic Shock	0	N/A
Streptococcus pneumoniae, Drug Resistant	1.5	(132)

(Continued)

TABLE 5 (Continued)

Disease name	R_0 Value	Source
Streptococcus pneumoniae, Inv	1.5	(132)
Syphilis (Total)	1.5	(133)
Tetanus	0	N/A
Toxic Shock	0	N/A
Trachoma	2.8	(134)
Trichinosis	0	N/A
Tuberculosis	8	(115)
Tularemia	1.57	(135)
Typhoid Fever	2.8	(123)
VISA	0	N/A
VRSA	0	N/A
VZ Infection, Unspecified	6.5	(136)
West Nile	0	N/A
Yellow Fever	0	N/A
Yersinia enteritis	0	N/A
Zika	3.8	(137)

N/A indicates the information was unavailable at the time that the study was conducted. Those pathogens for which the Ro is unknown will have zero (0) added to their cumulative score.

TABLE 6 Concentration methods for wastewater surveillance by pathogen type.

Pathogen type	Concentration methods	Reference
Bacterial	Centrifugation	(138–141)
	Membrane filtration	(142, 143)
	Precipitation and filtration	(144)
Fungal	Centrifugation and culture	(145, 146)
	Plate culture growth	(147–149)
Parasitic	Centrifugation	(150–156)
	Filtration and centrifugation	(157, 158)
Viral	Aluminum-driven flocculation	(159)
	Concentrator instrument	(2)
	Centrifugation	(160, 161)
	Electronegative membrane vortex	(162)
	Filtration	(160, 163)
	Membrane adsorption	(159, 164)
	Organic flocculation	(163)
	PEG	(5, 160, 162, 163)
	Precipitation	(164)
	Ultracentrifugation	(164)
	Ultrafiltration	(8, 11, 160–162, 164, 165)
	VIRADEL	(4–8, 17, 165, 166)
	Without pre-treatment/concentration	(16)

3.2. Observations of CDs' incidence and trend

3.2.1. Comparison of CD incidence in the TCDA vs. the state of Michigan

All CD incidences (per 100,000) from 2014 to 2021 in Michigan are demonstrated in Figure 2. Influenza, "influenza-like" or "flu-like" diseases, chlamydia, gonorrhea, and gastrointestinal illness (GI) have among the highest average incidences in Michigan.

Notably, multiple CDs presented lower incidences (per 100,000) in the TCDA than in broader Michigan (Figure 3). GI presented much higher cases per 100,000 in Michigan than in TCDA. Between 2017 and 2019, more than 1,400 incidences per 100,000 were observed in Michigan. In contrast, during the same period, approximate 400 incidences per 100,000 were observed in TCDA (Figure 3). Likewise, incidences per 100,000 of cryptosporidiosis, giardiasis, and norovirus were observed as much as twice higher in Michigan than in TCDA.

On the contrary, multiple CDs presented higher incidences (per 100,000) in the TCDA than in broader Michigan (Figure 4). CDs, such as gonorrhea, which can cause severe and permanent health issues (cdc.gov), has increased continuously and dramatically from 5,245 cases in 2014 to 12,034 cases in 2020 (and slightly decreased to 10,483 cases in 2021) in the TCDA. Gonorrhea incidence in TCDA is approximately five times higher than the rest of Michigan (Michigan.gov). Likewise, sextually transmitted diseases such as HIV, syphilis, and chlamydia were observed with consistent higher incidences per 100,000 in TCDA than in statewide Michigan (Figure 4). Also, West Nile fever incidences per 100,000 have increased dramatically in TCDA from 2019 to 2020 (Figure 4).

Figure 5 demonstrates selected CDs with approximately the same disease incidence (per 100,000), between the TCDA and Michigan, including AFM, brucellosis, Guillain-Barre syndrome, hepatitis E and C, as well as shigellosis.

3.2.2. Potential impact of COVID-19 pandemic on CDs

Multiple CDs were potentially affected by the COVID-19 pandemic (Figure 6). For instance, cases of hepatitis B surged from 675 (Michigan) and 1,081 (TCDA) in 2019, to 3,064 (Michigan) and 4,007 (TCDA) in 2020, during the inchoate stages of the COVID-19 pandemic. Afterwards, incidences in both Michigan and the TCDA decreased significantly, during COVID-19 stabilization, suggesting that a pandemic could cause an impact on disease incidence. The pandemic also affected the incidence of several vector-borne diseases, for example Lyme disease. Lyme disease surged in both Michigan as a whole and the TCDA between 2020 and 2021 (Figure 6). The incidence of influenza per 100,000 individuals in both TCDA and Michigan has been consistently decreasing since 2018. However, the decrease has been particularly significant from 2020 to 2021, concurring with the global spread of COVID-19.

This may suggest that the health control measures implemented in response to the COVID-19 pandemic, such as shelter-in-place orders and social distancing, have had a positive impact on reducing the incidence of influenza.

3.3. Overall ranking

Figure 7 presents the final ranking (top 30 out of 96 CDs) generated from the CDWSRank system, prioritizing wastewater surveillance target applications in the TCDA. Several CDs caused by viruses that are detectable in human excreta or wastewater were among the top 30 listed. These include COVID-19 (ranked 1st), hepatitis B (ranked 2nd), measles (ranked 3rd), influenza (ranked 6th), hepatitis C (ranked 8th), polio (ranked 18th), HIV/AIDS (ranked 19st), hepatitis E (ranked 21st), and norovirus (ranked 27th). Among the top 30 ranked CDs, some did not present relatively high incidences but were prioritized upon using the CDWSRank system. Examples include measles, polio, HIV/AIDS, hepatitis E, and norovirus, suggesting that such CDs require significant attention by wastewater surveillance practitioners, despite their relatively low incidence rates in the geographic study area in recent years.

Though not unexpected, the highest ranked CDs are those that do not spread solely by direct contact with animals, but rather those that are transmitted from person to person or from food or fomites. Only one vector-borne disease appears within the top 30, which is West Nile fever (ranked 29th). Over 50% (16/30) of CDs in the top 30 are either foodborne or STIs.

It is worth noting that 4 of the top 30 ranked CDs are known to health agencies to be vaccine preventable, highlighting the need for surveillance to warn against conditions that are not easily preventable, or those that could be particularly devastating to those not able to be immunized, such as infants or the immunodeficient. One CD ranked by this system was assigned a negative R_{CD}, melioidosis. This indicates that, though detectable using wastewater surveillance methods, this disease has been trending downward in the geographic areas and timeframe of this study, precluding it as a priority for monitoring.

Additionally, certain CDs (mentioned in Sections 3.2.1 and 3.2.2) received a ranking score of 0 since a multiplier of 0 for binary parameters was assigned. Lyme disease, for example, received a score of 0 since the detectability of Lyme disease in excreta or wastewater was set to 0. It was set to 0 because at the time of this study there were no published reports available indicating the ability to detect the bacteria (*Borrelia burgdorferi* and *Borrelia mayonii*) that causes Lyme disease in excreta or wastewater. As research efforts of the scientific community progress this may change.

4. Discussion

4.1. Differences of CDs in TCDA and state of Michigan

Differences in incidence among CDs in the TCDA vs. the state of Michigan demonstrate epidemiological trends that differ, possibly due to population density, wildlife/ecology, climate, socioeconomic and racial inequities, cultural or behavioral differences, age distribution, and access to healthcare and/or medical insurance (170–174). The ranking system results focus on TCDA which is an urban area with high-density population. However, as of 2021 (175), approximately 1.8 million residents, which accounts for nearly 20 percent of Michigan's population, live in rural areas. Consequently, Michiganders as a whole face a relatively elevated risk of contracting CDs such as cryptosporidiosis, giardiasis, and norovirus (Figure 3).

Residents in rural areas may have limited accessibility to medical care for diseases that require extensive or sophisticated care regimens (176). A study demonstrated possible causes for disparities between urban and rural areas by comparing outdoor time, where longer outdoor time were spent by rural residents than their urban counterparts (174), potentially creating an elevated risk of being infected by zoonotic pathogens. In rural areas, zoonotic diseases are of particular concern for farm workers, especially those working with livestock (177). In addition to zoonotic disease, residents of rural areas of Michigan are of great concern for vector-borne diseases, such as babesiosis (Figure 3), and others (178). It is important to note that human behavior, such as water related human activities, can also impact the transmission of vector-borne diseases, in addition to the effects of a warming climate in Michigan, especially the TCDA area (179). For example, higher average incidence of West Nile fever in the TCDA than in statewide Michigan can be attributed to both factors (180, 181).

Multiple CDs presented higher incidences per 100,000 in TCDA than in statewide Michigan, such as HIV and syphilis. This could possibly be related to a limited access to healthcare among the socioeconomically disadvantaged and racial minorities in TCDA (182). There are multiple causes of higher disease incidence of HIV and other STIs in TCDA, such as gonorrhea and syphilis (Figure 4). Briefly, a recent investigation indicated that elevated HIV prevalence in the TCDA was associated with minorities, gay and bisexual populations up to 29 years old, and the socioeconomically disadvantaged, such as those experiencing homelessness, poverty, and unemployment (170). It is worth noting that this trend is observed nationwide (183, 184). Researchers have also found that TCDA had a TB incidence twice than that of Michigan, affected by both racial inequity and places of interaction (185).

4.2. Impact of COVID-19 pandemic on CDs in TCDA and state of Michigan

Incidences per 100,000 of diseases such as hepatitis B, influenza and others, in both Michigan and the TCDA changed significantly, during COVID-19 inception, suggesting that a pandemic could cause an impact on disease incidence (Figure 7). This was corroborated in recent studies (186–188), and has been shown in countless epidemics worldwide (189, 190). Interestingly, several CDs whose incidences fell during the pandemic were those that traditionally rose in the other reported years, such as influenza. It is likely that reduced human contact and heightened hygiene in response to COVID-19 may have caused the dramatic decrease

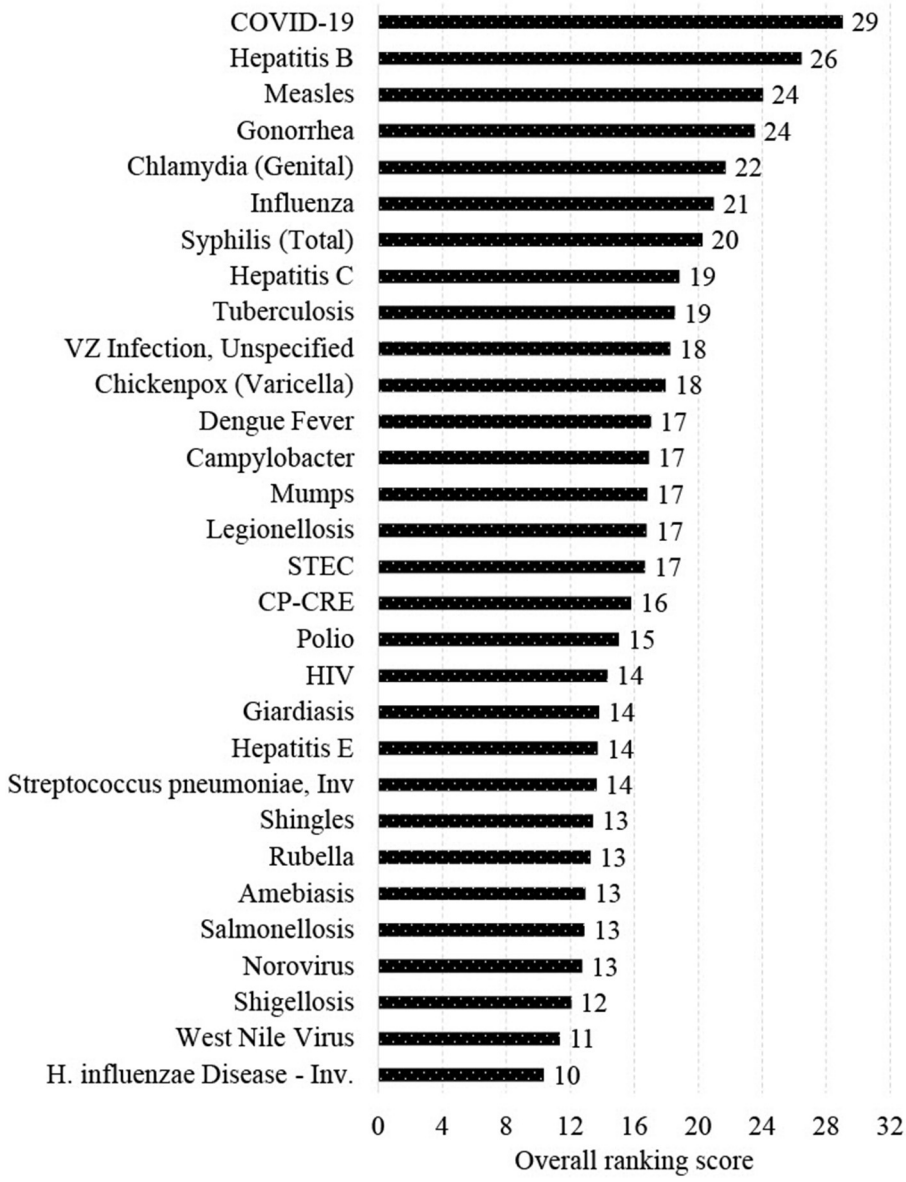

FIGURE 7
Top 30 CDs by CDWSRank system for prospective wastewater surveillance in the TCDA.

(191). On the contrary, Lyme disease surged in both Michigan as a whole and the TCDA between 2020 and 2021 (Figure 6). This may be attributable to an increasing number of outdoor recreational activities as result of diminished indoor options, due to COVID-19 social distancing restrictions (192). Another potential explanation for the pandemic's effect on CD incidence is that some CDs are caused by opportunistic pathogens that reactivate in a host when an individual's immune response is weakened, often by another pathogenic condition (193). The renewed prevalence of these CDs can be a direct effect of COVID-19 disease, creating the conditions of pathogen reactivation or new infections (194).

Studies have investigated the impact of the COVID-19 pandemic on sexually transmitted infections (STIs), such as syphilis (Figure 4) (195, 196). The disease incidence (per 100,000) of syphilis increased significantly between 2020 and 2021 in both the TCDA and broader Michigan, amid the pandemic (Figure 4). Potential causes may include the diversion of funding and health resources from STI programs, shutdown of STI clinics, less available treating physicians, a reticence to appear in-office to meet clinicians, and longer laboratory turnaround times (195). It is worth noting that during the COVID-19 pandemic, many health reporting systems faced challenges due to the increased workload and limited resources in the public health workforce (197). This

may have led to delays in reporting some diseases or with lower-quality data. However, it is important to note that COVID-19 has also resulted in improvements in health reporting systems in some areas, as public health agencies and governments have recognized the importance of timely and accurate reporting of disease data (198). The impact on health reporting systems by COVID-19 pandemic varied depending on the region, the disease, and the public health response to the pandemic.

4.3. Wastewater surveillance for viral CDs

CDWSRank placed 16 viral CDs in the top 30 for wastewater surveillance (Figure 7). Hepatitis B, for example, ranked 2nd (Figure 7). Recently, researchers conducted wastewater surveillance to monitor hepatitis B in 19 cities across China, after clinical cases had increased dramatically (33). The wastewater surveillance results were consistent with the prevalence reported in surveys, indicating that estimating Hepatitis B prevalence through wastewater surveillance is feasible in large cities in Southern China. Hepatitis C ranked 8th in CDWSRank for the TCDA region. Its RNA was detected and quantified in human fecal specimens in multiple studies, suggesting a significant potential for using wastewater monitoring as a tool for detecting hepatitis C virus (199). Chickenpox (ranked 11th) has been persistent in the statewide Michigan between 2014 and 2021, as shown in Figure 2. A few studies have attempted to test human bodily fluids, particularly urine, for monitoring varicella-zoster virus (which causes chickenpox and shingles), and other similar pathogens, such as in the Poxviridae family (34, 200). Notably, belonging to the same orthopoxvirus genus as varicella-zoster (201), the monkeypox virus has been spreading worldwide (outside of its traditional range) since May 2022. The virus has been detected in wastewater in Rome, Italy (23), and California, USA (24), showcasing the immense potential of wastewater surveillance as a tool for monitoring viruses in the Poxviridae family (200).

Viral pathogens, such as measles virus (measles is ranked 3rd) and varicella-zoster (shingles is ranked 23rd) were detected in urine specimens, indicating their potential to be monitored through wastewater surveillance as well (35, 202). Influenza, which ranked 6th on CDWSRank, was investigated in previous studies regarding the potential of wastewater surveillance (203).

Notably, polio ranks 18th in our CDWSRank system primarily due to its high R_0 value, indicating that it has the potential to spread widely and quickly. Although polio cases have not been identified in Michigan between 2014–2021, the disease can have severe health consequences and can be dangerous if it emerges. It is worth noting that the data published by the MDHHS is subject to yearly review. New information and inclusion of recent data could potentially affect the ranking of polio or any other CDs in our CDWSRank system. Polio's inclusion in our system is based on its potential to pose a significant public health threat, highlighting the importance of ongoing disease surveillance efforts to prevent the resurgence of CDs like polio. Overall, our CDWSRank system is designed to indicate which diseases should be prioritized in the context of wastewater surveillance for TCDA based on local clinical data and other parameters such as R_0.

4.4. Wastewater surveillance for bacterial, fungal, and parasitic CDs

CDWSRank placed 12 bacterial CDs ranked in the top 30 (Figure 7). These include tuberculosis (ranked 9th), CP-CRE (ranked 17th), legionellosis (ranked 15th), salmonellosis (ranked 26th), and shigellosis (ranked 28th), all detecteble both in human excreta and wastewater. Also, campylobacter (ranked 13th) was identified as a highly-sensitive pathogen for wastewater surveillance (204). Bacterial pathogens, such as *Chlamydia trachomatis* can be detected in wastewater (205). Despite being detectable in human excreta and wastewater, paratyphoid fever, Q fever, and typhoid fever were not ranked among the top 30 CDs.

Only two parasitic CDs, giardiasis (ranked 20th) and amebiasis (ranked 25th) ranked among the top 30. No fungal CDs were ranked among the top 30 CDs. Despite this, fungal CDs, including blastomycosis and cryptococcosis have great potential to be monitored using wastewater, as they can be detected in either human excreta or wastewater (Table 4).

4.5. Strengths and limitations of CDWSRank system

The goal of this study is to develop a quantitative prioritization system for wastewater surveillance of CDs in the TCDA. Several studies have developed methodologies to rank the threat of CDs with different scopes and methodologies (28–31). However, these studies have many limitations in their ranking systems which were refined and improved by the CDWSRank system.

Firstly, these ranking systems did not include parameters such as actual disease cases and basic reproduction numbers (R_0) for CDs (28–31). For instance, Balabanova et al., applied criteria such as incidence rate to prioritize 127 CDs in Germany (28). However, the study did not include the actual annual incidence number of the CDs. Instead, the importance of incidence for each disease was evaluated by weights given by experts. In our CDWSRank system, the actual disease incidence data between 2014 and 2021 for 96 CDs were extensively investigated and included in the system. Besides, in this study we investigated the R_0 for 96 CDs and incorporated them in the system when available.

Secondly, existing ranking systems relied heavily on experts' opinions on weighting the parameters when ranking the diseases (28–31). For instance, Cardoen et al., proposed a ranking system for 51 zoonotic agents which replied on scores given by 35 scientific experts in the field of animal and public health, food, clinical microbiology, and epidemiology (30). Likewise, Humblet et al., applied multicriteria decision-making methodologies based on expert opinions and data to rank 100 infectious diseases, in a system that included 57 criteria and 5 categories encompassing epidemiology, economy, public health, society, and prevention/control (31). The systems are affected by individual opinions of experts evaluating qualitative parameters. Experts' opinions could be subject to bias, which can affect the final ranking results. The subjective nature of weighting parameters by individuals for some criteria, such as public health impact, animal health impact, and food impact, can lead to

uncertainty and variation in final ranking scores depending on individual interpretations of these parameters (30). In contrast, to circumvent the bias of subjective opinions of experts, we designed the CDWSRank system based on a data-driven approach that considers critical factors including quantitative parameters of disease incidence and trend, geographical ratio, and R_0 for all CDs. In this way, the proposed ranking system differs from existing systems that are primarily based on the subjective, albeit expert, opinions. Besides, the weights given by experts for the specific locations can be hardly applied to other areas. However, by replacing the quantitative parameters in CDWSRank system, it can be applied beyond TCDA to other locations with accessible data. For instance, the clinical case trend in the State of Michigan and TCDA can be replaced by clinical disease databases based on different geographical information, henceforth enhancing the CDWSRank system's potential for wider applications.

Thirdly, the ranking systems in previous studies were designed for specific events or areas, which can be hardly applied beyond their scope. For instance, Balabanova et al. (28) included notifiable diseases in Germany and reportable diseases within the European Union. Likewise, Economopoulou et al. (29) focused only on the risk of CDs associated with the hosting of the London 2012 Olympic Games. To circumvent those biases, the 96 CDs included in CDWSRank system were selected based on U.S. CDC reportable disease lists and other governmental lists including the EPA CCL and CDC Bio-terrorism List, and local disease report lists including MDHHS WDR, which distinguishes it from all previous ranking systems for ranking CDs (28–31). This proposed ranking system is highly adaptable to other regions, especially those with similar reporting models which most states in the United Sates have, as a result of the CDC National Notifiable Disease Surveillance System requirements. Furthermore, to the best of our knowledge, there have been no published studies ranking CDs of public health importance that can be monitored using wastewater surveillance.

The goal of this study was to develop a prioritization system for wastewater surveillance of CDs in the TCDA. Limitations of this study are expounded below. Firstly, a multiplier of 0 was applied to a given CD if their causative pathogen has not been detected in wastewater or human excreta according to published studies thus far. This excludes potentially harmful CDs which can result in severe public health consequences, such as anthrax, hantavirus, and plague. Secondly, the weighting factors or multipliers for both binary and quantitative parameters were determined by researchers of this study and specifically designed with an emphasis on the TCDA. Nonetheless, weighting factors are adjustable and can vary across studies and regions with dissimilar research emphases. Thirdly, data unavailability limited the parameter types that could be involved in the proposed ranking system. For instance, mortality rate, case fatality, or incidence rate of some CDs could not be located in any published studies or publicly-available datasets for the TCDA. Additionally, due to a lack of R_0 information on some CDs, the ranking system may have disregarded diseases that are potentially harmful to human health but that do not yet have an established, specific R_0. R_0 values are situation-dependent and can significantly affect the rank (167). Besides, the CDWSRank system is limited since it does not explore the connection between severity and economic impact of the diseases ranked in this study. The severity of the disease in many instances would vary significantly with access to health care and the economic impact would vary with the severity. Despite the researchers' initial attempts to include parameters of mortality rate and severity, very few studies were found that adequately quantified these values in the TCDA region. It is, however, possible to include these parameters when adapting the CDWSRank system for a different locale if those data are available in the new area studied. Another significant limitation on the CDWSRank system is its reliance on case data being publicly and readily available. The implications of this limitation become particularly salient in locations where clinical data and information for reportable diseases are unavailable. However, as the CDWSRank system did produce a ranking score for Monkeypox, a disease without the case numbers published at the time of study, it is evident that the system can still create a ranking based on the other parameters. Hence, the CDWSRank system retains its utility in settings where access to data is restricted.

Social determinants of health such as socioeconomic status, environment, race and ethnicity, gender, culture, and access to health care would be other parameters for future development of the CDWSRank system. However, measuring and quantifying these factors for all 96 CDs in TCDA pose significant challenges, given the limited availability and accessibility of relevant data. Nonetheless, the insights generated by the CDWSRank system can be particularly valuable for guiding wastewater surveillance of emerging CDs which is beneficial for socioeconomically disadvantaged communities with limited healthcare access or traditional surveillance systems. Nevertheless, it is critical to note that as the aforementioned constraints become known, updating the CDWSRank system becomes necessary.

It is worth noting that some of the diseases of concern are seasonal (such as influenza) or rare (such as polio) and therefore only occasional surveillance may be recommended. In addition, some CDs, such as chlamydia, gonorrhea, and HIV, prioritized by CDWSRank system in TCDA are associated not only with urban areas, but also with socioeconomical and racial inequality, which can skew statistical designs. Social determinants of health, such as poverty, poor housing conditions, lack of access to healthcare, can disproportionately affect certain racial or ethnic groups and increase their risk of contracting and transmitting communicable diseases (170–173). For example, individuals living in crowded and unsanitary conditions are more likely to contract infectious diseases like TB or hepatitis A (206, 207). Therefore, surveillance of specific regions of concern may be recommended.

4.6. Future directions

In the State of Michigan, as in multiple other regions across the nation, the COVID-19 pandemic prompted the creation of wastewater surveillance networks. As the primary health focus shifts away from COVID-19 these currently available networks and their infrastructure and resources can be adapted to monitor other emerging diseases. This study offers a tool for transitioning to wastewater surveillance programs beyond COVID-19. By identifying and ranking the CDs that pose the most significant risk to public health in TCDA, the CDWSRank system provides a methodological tool and critical information that can help public health officials and policymakers allocate resources more

effectively. This information can be used to prioritize disease surveillance efforts and ensure that public health interventions are targeted at the most potentially urgent threats.

Furthermore, with regards to the extension of the CDWSRank system's applicability beyond the TCDA region, it is worth noting that the quantitative parameters heavily rely on local clinical data, while the binary parameters are primarily developed from regulatory lists obtained from local health departments as well as from U.S. governmental agencies. It is worth mentioning that all states in the U.S. are mandated to report to the C.D.C. and have their respective local health departments responsible for reporting notifiable diseases. Therefore, extending the application of the CDWSRank system to other regions within the U.S. would be relatively straightforward.

5. Conclusion

In this study, we developed a comprehensive and effective ranking system (CDWSRank) of wastewater surveillance prioritization for 96 CDs in the Tri-County Detroit Area (TCDA), Michigan, USA. The CDWSRank system comprises 6 binary and 6 quantitative parameters, with CDs classified into four groups: viral, bacterial, fungal, and parasitic. Critical regulatory lists, including the CDC's NNIDCL, MDHHS's WDR, EPA's CCL, and CDC's bioterrorism agents list were incorporated into the CDWSRank system. Disease incidences and trends of reportable CDs in the TCDA and broader state of Michigan were also incorporated into the system. Disparities in incidences of CDs were identified between the TCDA and state of Michigan, indicating epidemiological differences. Appropriate sampling and sample concentration methods for wastewater surveillance application were summarized as per our four categories, viral, bacterial, fungal, and parasitic.

The CDWSRank system is one of the first of its kind with the potential to prioritize resources and efforts toward monitoring and preventing the spread of CDs through wastewater surveillance. It helps researchers and public health practitioners to identify CDs that at a higher risk of disease transmission and prioritize monitoring efforts to mitigate their spread. The CDWSRank system provides an evidence- and data-based approach to decision making, ensuring the resources are allocated for wastewater surveillance beyond the COVID-19 pandemic. Ultimately, the development and implementation of the CDWSRank system for CDs can help reduce the impact of CDs on public health and promote broader applications of wastewater surveillance for public health benefits. CDWSRank can and should be adopted for ranking CDs in other geographical locations, with updated etiological and epidemiological information.

Data availability statement

The original contributions presented in the study are included in the article/supplementary material, further inquiries can be directed to the corresponding author.

Author contributions

ZG and LZ: methodology, investigation, data acquisition, data curation, formal analysis, visualization, writing—original draft, writing—review and editing, and are co-led manuscript development. RF and RD: writing—review and editing. JN: funding acquisition and writing—review and editing. IX: conceptualization, funding acquisition, methodology, investigation, project administration, resources, supervision, and writing—review and editing. All authors contributed to the article and approved the submitted version.

Funding

This study was funded by the Michigan Department of Health and Human Services (MDHHS) and the Great Lakes Water Authority (GLWA).

Acknowledgments

We acknowledge the support from operators, the laboratory team, and managers of the Wastewater Resource Recovery Facility at the Great Lakes Water Authority. We furthermore thank CDM Smith for supporting this work.

Conflict of interest

The authors declare that the research was conducted in the absence of any commercial or financial relationships that could be construed as a potential conflict of interest.

Publisher's note

References

1. Ahmed W, Tscharke B, Bertsch PM, Bibby K, Bivins A, Choi P, et al. SARS-CoV-2 RNA monitoring in wastewater as a potential early warning system for COVID-19 transmission in the community: A temporal case study. *Sci Total Environ.* (2021) 761:144216. doi: 10.1016/j.scitotenv.2020.144216

2. Ahmed W, Bivins A, Simpson SL, Bertsch PM, Ehret J, Hosegood I, et al. Wastewater surveillance demonstrates high predictive value for COVID-19 infection on board repatriation flights to Australia. *Environ Int.* (2022) 158:106938. doi: 10.1016/j.envint.2021.106938

3. Ahmed W, Bertsch PM, Angel N, Bibby K, Bivins A, Dierens L, et al. Detection of SARS-CoV-2 RNA in commercial passenger aircraft and cruise ship wastewater: a surveillance tool for assessing the presence of COVID-19 infected travellers. *J Travel Med*. (2020) 27:taaa116. doi: 10.1093/jtm/taaa116

4. Li Y, Miyani B, Zhao L, Spooner M, Gentry Z, Zou Y, et al. Surveillance of SARS-CoV-2 in nine neighborhood sewersheds in Detroit Tri-County area, United States: Assessing per capita SARS-CoV-2 estimations and COVID-19 incidence. *Sci Total Environ.* (2022) 851:158350. doi: 10.1016/j.scitotenv.2022.158350

5. Zhao L, Zou Y, Li Y, Miyani B, Spooner M, Gentry Z, et al. Five-week warning of COVID-19 peaks prior to the Omicron surge in Detroit, Michigan using wastewater surveillance. *Sci Total Environ.* (2022) 844:157040. doi: 10.1016/j.scitotenv.2022.157040

6. Miyani B, Fonoll X, Norton J, Mehrotra A, Xagoraraki I. SARS-CoV-2 in Detroit Wastewater. *J Environ Eng.* (2020) 146:06020004. doi: 10.1061/(ASCE)EE.1943-7870.0001830

7. Miyani B, Zhao L, Spooner M, Buch S, Gentry Z, Mehrotra A, et al. Early Warnings of COVID-19 Second Wave in Detroit. *J Environ Eng.* (2021) 147:06021004. doi: 10.1061/(ASCE)EE.1943-7870.0001907

8. Sherchan SP, Shahin S, Ward LM, Tandukar S, Aw TG, Schmitz B, et al. First detection of SARS-CoV-2 RNA in wastewater in North America: A study in Louisiana, USA. *Sci Total Environ.* (2020) 743:140621. doi: 10.1016/j.scitotenv.2020.140621

9. Medema G, Heijnen L, Elsinga G, Italiaander R, Brouwer A. Presence of SARS-Coronavirus-2 RNA in Sewage and Correlation with Reported COVID-19 Prevalence in the Early Stage of the Epidemic in the Netherlands. *Environ Sci Technol Lett.* (2020) 7:511–6. doi: 10.1021/acs.estlett.0c00357

10. Zhao L, Zou Y, David RE, Withington S, McFarlane S, Faust RA, et al. Simple methods for early warnings of COVID-19 surges: Lessons learned from 21 months of wastewater and clinical data collection in Detroit, Michigan, United States. *Sci Total Environ.* (2022) 864:161152. doi: 10.1016/j.scitotenv.2022.161152

11. Ahmed W, Angel N, Edson J, Bibby K, Bivins A, O'Brien JW, et al. First confirmed detection of SARS-CoV-2 in untreated wastewater in Australia: A proof of concept for the wastewater surveillance of COVID-19 in the community. *Sci Total Environ.* (2020) 728:138764. doi: 10.1016/j.scitotenv.2020.138764

12. Bibby K, Bivins A, Wu Z, North D. Making waves: Plausible lead time for wastewater based epidemiology as an early warning system for COVID-19. *Water Res.* (2021) 202:117438. doi: 10.1016/j.watres.2021.117438

13. Xagoraraki I, O'Brien E. Wastewater-based epidemiology for early detection of viral outbreaks. In: O'Bannon DJ, editor. *Women in Water Quality: Investigations by Prominent Female Engineers*. Cham: Springer International Publishing; (2020). p. 75–97. doi: 10.1007/978-3-030-17819-2_5

14. Xagoraraki I. Can we predict viral outbreaks using wastewater surveillance? *J Environ Eng.* (2020) 146:1820003. doi: 10.1061/(ASCE)EE.1943-7870.0001831

15. Kitajima M, Ahmed W, Bibby K, Carducci A, Gerba CP, Hamilton KA, et al. SARS-CoV-2 in wastewater: State of the knowledge and research needs. *Sci Total Environ.* (2020) 739:139076. doi: 10.1016/j.scitotenv.2020.139076

16. Ahmed W, Bivins A, Bertsch PM, Bibby K, Gyawali P, Sherchan SP, et al. Intraday variability of indicator and pathogenic viruses in 1-h and 24-h composite wastewater samples: Implications for wastewater-based epidemiology. *Environ Res.* (2021) 193:110531. doi: 10.1016/j.envres.2020.110531

17. McCall C, Wu H, O'Brien E, Xagoraraki I. Assessment of enteric viruses during a hepatitis outbreak in Detroit MI using wastewater surveillance and metagenomic analysis. *J Appl Microbiol.* (2021) 131:1539–54. doi: 10.1111/jam.15027

18. Miyani B, McCall C, Xagoraraki I. High abundance of human herpesvirus 8 in wastewater from a large urban area. *J Appl Microbiol.* (2021) 130:1402–11. doi: 10.1111/jam.14895

19. Hovi T, Shulman L, Van Der Avoort H, Deshpande J, Roivainen M, De Gourville E. Role of environmental poliovirus surveillance in global polio eradication and beyond. *Epidemiol Infect.* (2012) 140:1–13. doi: 10.1017/S095026881000316X

20. Roberts L. Israel's silent polio epidemic breaks all the rules. *Science.* (2013) 342:679–80. doi: 10.1126/science.342.6159.679

21. Link-Gelles R, Lutterloh E, Schnabel Ruppert P, Backenson PB, George K, Rosenberg ES, et al. Public health response to a case of paralytic poliomyelitis in an unvaccinated person and detection of poliovirus in wastewater — New York. *MMWR Morb Mortal Wkly Rep.* (2022) 71:1065–8. doi: 10.15585/mmwr.mm7133e2

22. de Jonge EF, Peterse CM, Koelewijn JM, van der Drift AMR, van der Beek RFHJ, Nagelkerke E, et al. The detection of monkeypox virus DNA in wastewater samples in the Netherlands. *Sci Total Environ.* (2022) 852:158265. doi: 10.1016/j.scitotenv.2022.158265

23. la Rosa G, Mancini P, Veneri C, Bonanno Ferraro G, Lucentini L, Iaconelli M, et al. Detection of Monkeypox virus DNA in the wastewater of an airport in Rome, Italy: expanding environmental surveillance to emerging threats. medRxiv. (2022). doi: 10.1101/2022.08.18.22278932

24. Wolfe MK, Duong D, Hughes B, Chan-Herur V, White BJ, Boehm AB. Detection of monkeypox viral DNA in a routine wastewater monitoring program. *medRxiv*. (2022). doi: 10.1101/2022.07.25.22278043

25. van Seventer JM, Hochberg NS. Principles of Infectious Diseases: Transmission, Diagnosis, Prevention, and Control. In: *International Encyclopedia of Public Health*. Elsevier (2017). p. 22–39. doi: 10.1016/B978-0-12-803678-5.00516-6

26. Morse SS, Mazet JA, Woolhouse M, Parrish CR, Carroll D, Karesh WB, et al. Prediction and prevention of the next pandemic zoonosis. *Lancet.* (2012) 380:1956–65. doi: 10.1016/S0140-6736(12)61684-5

27. Chharia A, Jeevan G, Jha RA, Liu M, Berman JM, Glorioso C. Accuracy of US CDC COVID-19 Forecasting Models. *medRxiv*. (2022). doi: 10.1101/2022.04.20.22274097

28. Balabanova Y, Gilsdorf A, Buda S, Burger R, Eckmanns T, Gärtner B, et al. Communicable Diseases Prioritized for Surveillance and Epidemiological Research: Results of a Standardized Prioritization Procedure in Germany. *PLoS ONE.* (2011) 6:e25691. doi: 10.1371/journal.pone.0025691

29. Economopoulou A, Kinross P, Domanovic D, Coulombier D. Infectious diseases prioritisation for event-based surveillance at the European Union level for the 2012 Olympic and Paralympic Games. *Eurosurveillance.* (2014) 19:20770. doi: 10.2807/1560-7917.ES2014.19.15.20770

30. Cardoen S, van Huffel X, Berkvens D, Quoilin S, Ducoffre G, Saegerman C, et al. Evidence-Based Semiquantitative Methodology for Prioritization of Foodborne Zoonoses. *Foodborne Pathog Dis.* (2009) 6:1083–96. doi: 10.1089/fpd.2009.0291

31. Humblet MF, Vandeputte S, Albert A, Gosset C, Kirschvink N, Haubruge E, et al. Multidisciplinary and Evidence-based Method for Prioritizing Diseases of Food-producing Animals and Zoonoses. *Emerg Infect Dis.* (2012) 18:e1. doi: 10.3201/eid1804.111151

32. Chandra F, Lee WL, Armas F, Leifels M, Gu X, Chen H, et al. Persistence of Dengue (Serotypes 2 and 3), Zika, Yellow Fever, and Murine Hepatitis Virus RNA in Untreated Wastewater. *Environ Sci Technol Lett.* (2021) 8:785–91. doi: 10.1021/acs.estlett.1c00517

33. Hou C, Hua Z, Xu P, Xu H, Wang Y, Liao J, et al. Estimating the prevalence of hepatitis B by wastewater-based epidemiology in 19 cities in China. *Sci Total Environ.* (2020) 740:139696. doi: 10.1016/j.scitotenv.2020.139696

34. McCall C, Wu H, Miyani B, Xagoraraki I. Identification of multiple potential viral diseases in a large urban center using wastewater surveillance. *Water Res.* (2020) 184:116160. doi: 10.1016/j.watres.2020.116160

35. Rota PA, Khan AS, Durigon E, Yuran T, Villamarzo YS, Bellini WJ. Detection of measles virus RNA in urine specimens from vaccine recipients. *J Clin Microbiol.* (1995) 33:2485–8. doi: 10.1128/jcm.33.9.2485-2488.1995

36. Faleye TOC, Adewumi MO, Japhet MO, David OM, Oluyege AO, Adeniji JA, et al. Non-polio enteroviruses in faeces of children diagnosed with acute flaccid paralysis in Nigeria. *Virol J.* (2017) 14:175. doi: 10.1186/s12985-017-0846-x

37. Leung J, Harpaz R, Baughman AL, Heath K, Loparev V, Vázquez M, et al. Evaluation of Laboratory Methods for Diagnosis of Varicella. *Clin Infect Dis.* (2010) 51:23–32. doi: 10.1086/653113

38. Musso D, Teissier A, Rouault E, Teururai S, de Pina JJ, Nhan TX. Detection of chikungunya virus in saliva and urine. *Virol J.* (2016) 13:102. doi: 10.1186/s12985-016-0556-9

39. Lamb LE, Bartolone SN, Tree MO, Conway MJ, Rossignol J, Smith CP, et al. Rapid Detection of Zika Virus in Urine Samples and Infected Mosquitos by Reverse Transcription-Loop-Mediated Isothermal Amplification. *Sci Rep*. (2018) 8:3803. doi: 10.1038/s41598-018-22102-5

40. Jain S, Su YH, Su YP, McCloud S, Xue R, Lee TJ, et al. Characterization of the hepatitis B virus DNA detected in urine of chronic hepatitis B patients. *BMC Gastroenterol.* (2018) 18:40. doi: 10.1186/s12876-018-0767-1

41. Numata N, Ohori H, Hayakawa Y, Saitoh Y, Tsunoda A, Kanno A. Demonstration of hepatitis C virus genome in saliva and urine of patients with type C hepatitis: Usefulness of the single round polymerase chain reaction method for detection of the HCV genome. *J Med Virol.* (1993) 41:120–8. doi: 10.1002/jmv.1890410207

42. Aggarwal R, McCaustland KA. Hepatitis E virus RNA detection in serum and feces specimens with the use of microspin columns. *J Virol Methods.* (1998) 74:209–13. doi: 10.1016/S0166-0934(98)00049-4

43. Beyer S, Szewzyk R, Gnirss R, Johne R, Selinka HC. Detection and Characterization of Hepatitis E Virus Genotype 3 in Wastewater and Urban Surface Waters in Germany. *Food Environ Virol.* (2020) 12:137–47. doi: 10.1007/s12560-020-09424-2

44. Kevill JL, Lambert-Slosarska K, Pellett C, Woodhall N, Richardson-O'Neill I, Pântea I, et al. Assessment of two types of passive sampler for the efficient recovery of SARS-CoV-2 and other viruses from wastewater. *Sci Total Environ.* (2022) 838:156580. doi: 10.1016/j.scitotenv.2022.156580

45. Krause CH, Eastick K, Ogilvie MM. Real-time PCR for mumps diagnosis on clinical specimens—Comparison with results of conventional methods of virus detection and nested PCR. *J Clin Virol.* (2006) 37:184–9. doi: 10.1016/j.jcv.2006.07.009

46. Baek SH, Kim MW, Park CY, Choi CS, Kailasa SK, Park JP, et al. Development of a rapid and sensitive electrochemical biosensor for detection of human norovirus via novel specific binding peptides. *Biosens Bioelectron.* (2019) 123:223–9. doi: 10.1016/j.bios.2018.08.064

47. Kitajima M, Haramoto E, Phanuwan C, Katayama H, Ohgaki S. Detection of genogroup IV norovirus in wastewater and river water in Japan. *Lett Appl Microbiol.* (2009) 49:655–8. doi: 10.1111/j.1472-765X.2009.02718.x

48. Kim JM, Kim HM, Lee EJ, Jo HJ, Yoon Y, Lee NJ, et al. Detection and Isolation of SARS-CoV-2 in Serum, Urine, and Stool Specimens of COVID-19 Patients from the Republic of Korea. *Osong Public Health Res Perspect.* (2020) 11:112–7. doi: 10.24171/j.phrp.2020.11.3.02

49. Lago PM, Gary HE, Pérez LS, Cáceres V, Olivera JB, Puentes RP, et al. Poliovirus detection in wastewater and stools following an immunization campaign in Havana, Cuba. *Int J Epidemiol.* (2003) 32:772–7. doi: 10.1093/ije/dyg185

50. Gdoura M, Fares W, Bougatef S, Inoubli A, Touzi H, Hogga N, et al. The value of West Nile virus RNA detection by real-time RT-PCR in urine samples from patients with neuroinvasive forms. *Arch Microbiol.* (2022) 204:238. doi: 10.1007/s00203-022-02829-6

51. Domingo C, Yactayo S, Agbenu E, Demanou M, Schulz AR, Daskalow K, et al. Detection of Yellow Fever 17D Genome in Urine. *J Clin Microbiol.* (2011) 49:760–2. doi: 10.1128/JCM.01775-10

52. Peiró-Mestres A, Fuertes I, Camprubí-Ferrer D, Marcos MÁ, Vilella A, Navarro M, et al. Frequent detection of monkeypox virus DNA in saliva, semen, and other clinical samples from 12 patients, Barcelona, Spain. *Eurosurveillance.* (2022) 27:2200503. doi: 10.2807/1560-7917.ES.2022.27.28.2200503

53. Battistone A, Buttinelli G, Fiore S, Amato C, Bonomo P, Patti AM, et al. Sporadic isolation of sabin-like polioviruses and high-level detection of non-polio enteroviruses during sewage surveillance in seven italian cities, after several years of inactivated poliovirus vaccination. *Appl Environ Microbiol.* (2014) 80:4491–501. doi: 10.1128/AEM.00108-14

54. Palmer CJ, Bonilla GF, Tsai YL, Lee MH, Javier BJ, Siwak EB. Analysis of sewage effluent for human immunodeficiency virus (HIV) using infectivity assay and reverse transcriptase polymerase chain reaction. *Can J Microbiol.* (1995) 41:809–15. doi: 10.1139/m95-111

55. Li JJ, Huang YQ, Poiesz BJ, Zaumetzger-Abbot L, Friedman-Kien AE. Detection of human immunodeficiency virus type 1 (HIV-1) in urine cell pellets from HIV-1-seropositive individuals. *J Clin Microbiol.* (1992) 30:1051–5. doi: 10.1128/jcm.30.5.1051-1055.1992

56. Wattiau P, Klee SR, Fretin D, van Hessche M, Ménart M, Franz T, et al. Occurrence and genetic diversity of *Bacillus anthracis* strains isolated in an active wool-cleaning factory. *Appl Environ Microbiol.* (2008) 74:4005–11. doi: 10.1128/AEM.00417-08

57. Kalb SR, Moura H, Boyer AE, McWilliams LG, Pirkle JL, Barr JR. The use of Endopep–MS for the detection of botulinum toxins A, B, E, and F in serum and stool samples. *Anal Biochem.* (2006) 351:84–92. doi: 10.1016/j.ab.2006.01.027

58. LaGier MJ, Joseph LA, Passaretti T, Musser KA, Cirino NM, A. real-time multiplexed PCR assay for rapid detection and differentiation of *Campylobacter jejuni* and *Campylobacter coli*. *Mol Cell Probes.* (2004) 18:275–82. doi: 10.1016/j.mcp.2004.04.002

59. Bonetta S, Pignata C, Lorenzi E, de Ceglia M, Meucci L, Bonetta S, et al. Detection of pathogenic Campylobacter, E coli O157:H7 and Salmonella spp in wastewater by PCR assay. *Environ Sci Pollut Res.* (2016) 23:15302–9. doi: 10.1007/s11356-016-6682-5

60. Gaydos CA, Theodore M, Dalesio N, Wood BJ, Quinn TC. Comparison of Three Nucleic Acid Amplification Tests for Detection of *Chlamydia trachomatis* in Urine Specimens. *J Clin Microbiol.* (2004) 42:3041–5. doi: 10.1128/JCM.42.7.3041-3045.2004

61. Rahman M, Sack DA, Mahmood S, Hossain A. Rapid diagnosis of cholera by coagglutination test using 4-h fecal enrichment cultures. *J Clin Microbiol.* (1987) 25:2204–6. doi: 10.1128/jcm.25.11.2204-2206.1987

62. Galler H, Feierl G, Petternel C, Reinthaler FF, Haas D, Grisold AJ, et al. KPC-2 and OXA-48 carbapenemase-harbouring Enterobacteriaceae detected in an Austrian wastewater treatment plant. *Clin Microbiol Infect.* (2014) 20:O132–4. doi: 10.1111/1469-0691.12336

63. Akduman D, Ehret JM, Messina K, Ragsdale S, Judson FN. Evaluation of a Strand Displacement Amplification Assay (BD ProbeTec-SDA) for Detection of *Neisseria gonorrhoeae* in Urine Specimens. *J Clin Microbiol.* (2002) 40:281–3. doi: 10.1128/JCM.40.1.281-283.2002

64. Riera L. Detection of Haemophilus influenzae type b antigenuria by Bactigen and Phadebact kits. *J Clin Microbiol.* (1985) 21:638–40. doi: 10.1128/jcm.21.4.638-640.1985

65. Murdoch DR, Walford EJ, Jennings LC, Light GJ, Schousboe MI, Chereshsky AY, et al. Use of the polymerase chain reaction to detect legionella DNA in urine and serum samples from patients with pneumonia. *Clin Infect Dis.* (1996) 23:475–80. doi: 10.1093/clinids/23.3.475

66. Catalan V, Garcia F, Moreno C, Vila MJ, Apraiz D. Detection of Legionella pneumophila in wastewater by nested polymerase chain reaction. *Res Microbiol.* (1997) 148:71–8. doi: 10.1016/S0923-2508(97)81902-X

67. Caleffi KR, Hirata RDC, Hirata MH, Caleffi ER, Siqueira VLD, Cardoso RF. Use of the polymerase chain reaction to detect Mycobacterium leprae in urine. *Brazilian J Med Biol Res.* (2012) 45:153–7. doi: 10.1590/S0100-879X2012007500011

68. Mérien F, Amouriaux P, Perolat P, Baranton G, Girons I. Polymerase chain reaction for detection of Leptospira spp in clinical samples. *J Clin Microbiol.* (1992) 30:2219–24. doi: 10.1128/jcm.30.9.2219-2224.1992

69. Moreno Y, Ballesteros L, García-Hernández J, Santiago P, González A, Ferrús MA. Specific detection of viable Listeria monocytogenes in Spanish wastewater treatment plants by Fluorescent In Situ Hybridization and PCR. *Water Res.* (2011) 45:4634–40. doi: 10.1016/j.watres.2011.06.015

70. Lee DY, Lauder H, Cruwys H, Falletta P, Beaudette LA. Development and application of an oligonucleotide microarray and real-time quantitative PCR for detection of wastewater bacterial pathogens. *Sci Total Environ.* (2008) 398:203–11. doi: 10.1016/j.scitotenv.2008.03.004

71. Guo F, Zhang T, Li B, Wang Z, Ju F, Liang Y. Mycobacterial species and their contribution to cholesterol degradation in wastewater treatment plants. *Sci Rep.* (2019) 9:836. doi: 10.1038/s41598-018-37332-w

72. Amalina ZN, Khalid MF, Rahman SF, Ahmad MN, Ahmad Najib M, Ismail A, et al. Nucleic Acid-Based Lateral Flow Biosensor for Salmonella Typhi and Salmonella Paratyphi: A Detection in Stool Samples of Suspected Carriers. *Diagnostics.* (2021) 11:700. doi: 10.3390/diagnostics11040700

73. Liu P, Ibaraki M, Kapoor R, Amin N, Das A, Miah R, et al. Development of Moore Swab and Ultrafiltration Concentration and Detection Methods for Salmonella Typhi and Salmonella Paratyphi A in Wastewater and Application in Kolkata, India and Dhaka, Bangladesh. *Front Microbiol.* (2021) 15:12. doi: 10.3389/fmicb.2021.684094

74. Branley JM, Roy B, Dwyer DE, Sorrell TC. Real-time PCR detection and quantitation of Chlamydophila psittaci in human and avian specimens from a veterinary clinic cluster. *Eur J Clin Microbiol Infect Dis.* (2008) 27:269–73. doi: 10.1007/s10096-007-0431-0

75. Schets FM, de Heer L, de Roda Husman AM. Coxiella burnetii in sewage water at sewage water treatment plants in a Q fever epidemic area. *Int J Hyg Environ Health.* (2013) 216:698–702. doi: 10.1016/j.ijheh.2012.12.010

76. Araj GF, Chugh TD. Detection of Salmonella spp. in clinical specimens by capture enzyme-linked immunosorbent assay. *J Clin Microbiol.* (1987) 25:2150–3. doi: 10.1128/jcm.25.11.2150-2153.1987

77. Cohen D, Orr N, Robin G, Slepon R, Ashkenazi S, Ashkenazi I, et al. Detection of antibodies to Shigella lipopolysaccharide in urine after natural Shigella infection or vaccination. *Clin Diagn Lab Immunol.* (1996) 3:451–5. doi: 10.1128/cdli.3.4.451-455.1996

78. Pant A, Mittal AK. New Protocol for the Enumeration of *Salmonella* and *Shigella* from Wastewater. *J Environ Eng.* (2008) 134:222–6. doi: 10.1061/(ASCE)0733-9372(2008)134:3(222)

79. Domanguez J, Gal N, Blanco S, Pedroso P, Prat C, Matas L, et al. Detection of Streptococcus pneumoniae Antigen by a Rapid Immunochromatographic Assay in Urine Samples. *Chest.* (2001) 119:243–9. doi: 10.1378/chest.119.1.243

80. Wang C, Zheng X, Guan Z, Zou D, Gu X, Lu H, et al. Quantified Detection of Treponema pallidum DNA by PCR Assays in Urine and Plasma of Syphilis Patients. *Microbiol Spectr.* (2022) 10:e01772–21. doi: 10.1128/spectrum.01772-21

81. Gómez P, Lozano C, Benito D, Estepa V, Tenorio C, Zarazaga M, et al. Characterization of staphylococci in urban wastewater treatment plants in Spain, with detection of methicillin resistant Staphylococcus aureus ST398. *Environ Pollut.* (2016) 212:71–6. doi: 10.1016/j.envpol.2016.01.038

82. Bulterys MA, Wagner B, Redard-Jacot M, Suresh A, Pollock NR, Moreau E, et al. Point-Of-Care Urine LAM Tests for Tuberculosis Diagnosis: A Status Update. *J Clin Med.* (2019) 9:111. doi: 10.3390/jcm9010111

83. Mtetwa HN, Amoah ID, Kumari S, Bux F, Reddy P. Molecular surveillance of tuberculosis-causing mycobacteria in wastewater. *Heliyon.* (2022) 8:e08910. doi: 10.1016/j.heliyon.2022.e08910

84. Bahl MI, Rosenberg K. High abundance and diversity of Bacillus anthracis plasmid pXO1-like replicons in municipal wastewater. *FEMS Microbiol Ecol.* (2010) 74:241–7. doi: 10.1111/j.1574-6941.2010.00922.x

85. Al-Gheethi AAS, Abdul-Monem MO, AL-Zubeiry AHS, Efaq AN, Shamar AM, Al-Amery RMA. Effectiveness of selected wastewater treatment plants in Yemen for reduction of faecal indicators and pathogenic bacteria in secondary effluents and sludge. *Water Pract Technol.* (2014) 9:293–306. doi: 10.2166/wpt.2014.031

86. Berendes D, Kirby A, Brown J, Wester AL. Human faeces-associated extended-spectrum β-lactamase-producing Escherichia coli discharge into sanitation systems in 2015 and 2030: a global and regional analysis. *Lancet Planet Health.* (2020) 4:e246–55. doi: 10.1016/S2542-5196(20)30099-1

87. Stark D, van Hal S, Fotedar R, Butcher A, Marriott D, Ellis J, et al. Comparison of Stool Antigen Detection Kits to PCR for Diagnosis of Amebiasis. *J Clin Microbiol.* (2008) 46:1678–81. doi: 10.1128/JCM.02261-07

88. Srikanth R, Naik D. Health Effects of Wastewater Reuse for Agriculture in the Suburbs of Asmara City, Eritrea. *Int J Occup Environ Health.* (2004) 10:284–8. doi: 10.1179/oeh.2004.10.3.284

89. Guy RA, Payment P, Krull UJ, Horgen PA. Real-Time PCR for Quantification of *Giardia* and *Cryptosporidium* in Environmental Water Samples and Sewage. *Appl Environ Microbiol.* (2003) 69:5178–85. doi: 10.1128/AEM.69.9.5178-5185.2003

90. Dixon BR, Bussey JM, Parrington LJ, Parenteau M. Detection of *Cyclospora cayetanensis* Oocysts in Human Fecal Specimens by Flow Cytometry. *J Clin Microbiol.* (2005) 43:2375–9. doi: 10.1128/JCM.43.5.2375-2379.2005

91. Sturbaum GD, Ortega YR, Gilman RH, Sterling CR, Cabrera L, Klein DA. Detection of *Cyclospora cayetanensis* in Wastewater. *Appl Environ Microbiol.* (1998) 64:2284–6. doi: 10.1128/AEM.64.6.2284-2286.1998

92. Johnston SP, Ballard MM, Beach MJ, Causer L, Wilkins PP. Evaluation of Three Commercial Assays for Detection of *Giardia* and *Cryptosporidium* Organisms in Fecal Specimens. *J Clin Microbiol.* (2003) 41:623–6. doi: 10.1128/JCM.41.2.623-626.2003

93. Mayer CL, Palmer CJ. Evaluation of PCR, nested PCR, and fluorescent antibodies for detection of Giardia and Cryptosporidium species in wastewater. *Appl Environ Microbiol.* (1996) 62:2081–5. doi: 10.1128/aem.62.6.2081-2085.1996

94. Jirku M, Pomajbíková K, PetrŽelková KJ, Huzová Z, Modrý D, Lukeš J. Detection of *Plasmodium* spp. *in Human Feces Emerg Infect Dis.* (2012) 18:634. doi: 10.3201/eid1804.110984

95. Khurana S, Chaudhary P. Laboratory diagnosis of cryptosporidiosis. *Trop Parasitol.* (2018) 8:2. doi: 10.4103/tp.TP_34_17

96. Jia S, Zhang X. Biological HRPs in wastewater. In: *High-Risk Pollutants in Wastewater*. Elsevier; (2020). p. 41–78. doi: 10.1016/B978-0-12-816448-8.00003-4

97. Kauffman CA, Pappas PG, Sobel JD, Dismukes WE. *Essentials of Clinical Mycology*. New York, NY: Springer. (2011). doi: 10.1007/978-1-4419-6640-7

98. Mataraci-Kara E, Ataman M, Yilmaz G, Ozbek-Celik B. Evaluation of antifungal and disinfectant-resistant Candida species isolated from hospital wastewater. *Arch Microbiol.* (2020) 202:2543–50. doi: 10.1007/s00203-020-01975-z

99. Walchak RC, Buckwalter SP, Zinsmaster NM, Henn KM, Johnson KM, Koelsch JM, et al. Candida auris direct detection from surveillance swabs, blood, and urine using a laboratory-developed PCR method. *J Fungi.* (2020) 6:224. doi: 10.3390/jof6040224

100. Hategekimana F, Saha S, Chaturvedi A. Dynamics of amoebiasis transmission: stability and sensitivity analysis. *Mathematics.* (2017) 5:58. doi: 10.3390/math5040058

101. van den Driessche P. Reproduction numbers of infectious disease models. *Infect Dis Model.* (2017) 2:288–303. doi: 10.1016/j.idm.2017.06.002

102. Dunn J. *The mathematical epidemiology of human babesiosis in the North-Eastern United States*. Doctoral dissertation, RMIT University. (2014).

103. Haider N, Vairo F, Ippolito G, Zumla A, Kock RA. Basic reproduction number of chikungunya virus transmitted by aedes mosquitoes. *Emerg Infect Dis.* (2020) 26:2429. doi: 10.3201/eid2610.190957

104. Potterat JJ, Zimmerman-Rogers H, Muth SQ, Rothenberg RB, Green DL, Taylor JE, et al. Chlamydia transmission: concurrency, reproduction number, and the epidemic trajectory. *Am J Epidemiol.* (1999) 150:1331–9. doi: 10.1093/oxfordjournals.aje.a009965

105. Phelps M, Perner ML, Pitzer VE, Andreasen V, Jensen PKM, Simonsen L. Cholera epidemics of the past offer new insights into an old enemy. *J Infect Dis.* (2018) 217:641–9. doi: 10.1093/infdis/jix602

106. Tien JH, Earn DJD. Multiple transmission pathways and disease dynamics in a waterborne pathogen model. *Bull Math Biol.* (2010) 72:1506–33. doi: 10.1007/s11538-010-9507-6

107. Nishiura H. *Mathematical and statistical analyses of the spread of Dengue*. (2006).

108. Matsuyama R, Akhmetzhanov AR, Endo A, Lee H, Yamaguchi T, Tsuzuki S, et al. Uncertainty and sensitivity analysis of the basic reproduction number of diphtheria: a case study of a Rohingya refugee camp in Bangladesh. *PeerJ.* (2018) 6:e4583. doi: 10.7717/peerj.4583

109. Mpeshe S, Nyerere N. A human-animal model of giardiasis infection in contaminated environment. *Int J Adv Appl Mathem Mech.* (2021) 8:37–47.

110. Jolly AM, Wylie JL. Gonorrhoea and chlamydia core groups and sexual networks in Manitoba. *Sex Transm Infect.* (2002) 78:i145–51. doi: 10.1136/sti.78.suppl_1.i145

111. Khan A, Naveed M, Dur-e-Ahmad M, Imran M. Estimating the basic reproductive ratio for the Ebola outbreak in Liberia and Sierra Leone. *Infect Dis Poverty.* (2015) 4:1–8. doi: 10.1186/s40249-015-0043-3

112. Hung HF, Wang YC, Yen AMF, Chen HH. Stochastic model for hepatitis B virus infection through maternal (vertical) and environmental (horizontal) transmission with applications to basic reproductive number estimation and economic appraisal of preventive strategies. *Stochastic Environ Res Risk Assess.* (2014) 28:611–25. doi: 10.1007/s00477-013-0776-0

113. Pybus OG, Charleston MA, Gupta S, Rambaut A, Holmes EC, Harvey PH, et al. The epidemic behavior of the hepatitis C virus. *Science.* (1979) 292:2323–5. doi: 10.1126/science.1058321

114. Dalton HR, Hunter JG, Bendall RP. Hepatitis e. *Curr Opin Infect Dis.* (2013) 26:471–8. doi: 10.1097/01.qco.0000433308.83029.97

115. Lietman T, Porco T, Blower S. Leprosy and tuberculosis: the epidemiological consequences of cross-immunity. *Am J Public Health.* (1997) 87:1923–7. doi: 10.2105/AJPH.87.12.1923

116. Engida HA, Theuri DM, Gathungu D, Gachohi J, Alemneh HT. A mathematical model analysis for the transmission dynamics of leptospirosis disease in human and rodent populations. *Comput Math Methods Med.* (2022) 2022:1806585. doi: 10.1155/2022/1806585

117. Guerra FM, Bolotin S, Lim G, Heffernan J, Deeks SL, Li Y, et al. The basic reproduction number (R0) of measles: a systematic review. *Lancet Infect Dis.* (2017) 17:e420–8. doi: 10.1016/S1473-3099(17)30307-9

118. Opoku NKDO, Borkor RN, Adu AF, Nyarko HN, Doughan A, Appiah EM, et al. Modelling the Transmission Dynamics of Meningitis among High and Low-Risk People in Ghana with Cost-Effectiveness Analysis. In: *Abstract and Applied Analysis Hindawi.* (2022). doi: 10.1155/2022/9084283

119. Trotter CL, Gay NJ, Edmunds WJ. Dynamic models of meningococcal carriage, disease, and the impact of serogroup C conjugate vaccination. *Am J Epidemiol.* (2005) 162:89–100. doi: 10.1093/aje/kwi160

120. Grant R, Nguyen LBL, Breban R. Modelling human-to-human transmission of monkeypox. *Bull World Health Organ.* (2020) 98:638. doi: 10.2471/BLT.19.242347

121. Caley P, Hone J. Assessing the host disease status of wildlife and the implications for disease control: Mycobacterium bovis infection in feral ferrets. *J Appl Ecol.* (2005) 42:708–19. doi: 10.1111/j.1365-2664.2005.01053.x

122. Gaythorpe KAM, Trotter CL, Lopman B, Steele M, Conlan AJK. Norovirus transmission dynamics: a modelling review. *Epidemiol Infect.* (2018) 146:147–58. doi: 10.1017/S0950268817002692

123. Pitzer VE, Bowles CC, Baker S, Kang G, Balaji V, Farrar JJ, et al. Predicting the impact of vaccination on the transmission dynamics of typhoid in South Asia: a mathematical modeling study. *PLoS Negl Trop Dis.* (2014) 8:e2642. doi: 10.1371/journal.pntd.0002642

124. Kretzschmar M, Teunis PFM, Pebody RG. Incidence and reproduction numbers of pertussis: estimates from serological and social contact data in five European countries. *PLoS Med.* (2010) 7:e1000291. doi: 10.1371/journal.pmed.1000291

125. Sichone J, Simuunza MC, Hang'ombe BM, Kikonko M. Estimating the basic reproduction number for the 2015 bubonic plague outbreak in Nyimba district of Eastern Zambia. *PLoS Negl Trop Dis.* (2020). 14:e0008811. doi: 10.1371/journal.pntd.0008811

126. Eichner M, Dietz K. Eradication of poliomyelitis: when can one be sure that polio virus transmission has been terminated? *Am J Epidemiol.* (1996) 143:816–22. doi: 10.1093/oxfordjournals.aje.a008820

127. Polo G, Labruna MB, Ferreira F. Basic reproduction number for the Brazilian Spotted Fever. *J Theor Biol.* (2018) 458:119–24. doi: 10.1016/j.jtbi.2018.09.011

128. Sfikas N, Greenhalgh D, Lewis F. The basic reproduction number and the vaccination coverage required to eliminate rubella from England and Wales. *Math Popul Stud.* (2007) 14:3–29. doi: 10.1080/08898480601090634

129. Khan MA, Atangana A. Mathematical modeling and analysis of COVID-19: A study of new variant Omicron. *Physica A.* (2022) 599:127452. doi: 10.1016/j.physa.2022.127452

130. Chen S, Sanderson MW, Lee C, Cernicchiaro N, Renter DG, Lanzas C. Basic reproduction number and transmission dynamics of common serogroups of enterohemorrhagic Escherichia coli. *Appl Environ Microbiol.* (2016) 82:5612–20. doi: 10.1128/AEM.00815-16

131. Joh RI, Hoekstra RM, Barzilay EJ, Bowen A, Mintz ED, Weiss H, et al. Dynamics of shigellosis epidemics: estimating individual-level transmission and reporting rates from national epidemiologic data sets. *Am J Epidemiol.* (2013) 178:1319–26. doi: 10.1093/aje/kwt122

132. Obolski U, Lourenço J, Thompson C, Thompson R, Gori A, Gupta S. Vaccination can drive an increase in frequencies of antibiotic resistance among nonvaccine serotypes of Streptococcus pneumoniae. *Proc Nat Acad Sci.* (2018) 115:3102–7. doi: 10.1073/pnas.1718712115

133. Garnett GP, Aral SO, Hoyle D, Cates W, Anderson RM. The natural history of syphilis: implications for the transmission dynamics and control of infection. *Sex Transm Dis.* (1997) 24:185–200. doi: 10.1097/00007435-199704000-00002

134. Martin DL, Wiegand R, Goodhew B, Lammie P, Black CM, West S, et al. Serological measures of trachoma transmission intensity. *Sci Rep.* (2015) 5:1–5. doi: 10.1038/srep18532

135. Dobay A, Pilo P, Lindholm AK, Origgi F, Bagheri HC, König B. Dynamics of a tularemia outbreak in a closely monitored free-roaming population of wild house mice. *PLoS ONE.* (2015) 10:e0141103. doi: 10.1371/journal.pone.0141103

136. Marangi L, Mirinaviciute G, Flem E, Scalia Tomba G, Guzzetta G, Freiesleben de Blasio B, et al. The natural history of varicella zoster virus infection in Norway: Further insights on exogenous boosting and progressive immunity to herpes zoster. *PLoS ONE.* (2017) 12:e0176845. doi: 10.1371/journal.pone.0176845

137. Towers S, Brauer F, Castillo-Chavez C, Falconar AKI, Mubayi A, Romero-Vivas CME. Estimate of the reproduction number of the 2015 Zika virus outbreak in Barranquilla, Colombia, and estimation of the relative role of sexual transmission. *Epidemics.* (2016) 17:50–5. doi: 10.1016/j.epidem.2016.10.003

138. Lemarchand K, Berthiaume F, Maynard C, Harel J, Payment P, Bayardelle P, et al. Optimization of microbial DNA extraction and purification from raw wastewater

samples for downstream pathogen detection by microarrays. *J Microbiol Methods.* (2005) 63:115–26. doi: 10.1016/j.mimet.2005.02.021

139. Volkmann H, Schwartz T, Kirchen S, Stofer C, Obst U. Evaluation of inhibition and cross-reaction effects on real-time PCR applied to the total DNA of wastewater samples for the quantification of bacterial antibiotic resistance genes and taxon-specific targets. *Mol Cell Probes.* (2007) 21:125–33. doi: 10.1016/j.mcp.2006.08.009

140. Shannon KE, Lee DY, Trevors JT, Beaudette LA. Application of real-time quantitative PCR for the detection of selected bacterial pathogens during municipal wastewater treatment. *Sci Total Environ.* (2007) 382:121–9. doi: 10.1016/j.scitotenv.2007.02.039

141. Caldwell JM, Levine JF. Domestic wastewater influent profiling using mitochondrial real-time PCR for source tracking animal contamination. *J Microbiol Methods.* (2009) 77:17–22. doi: 10.1016/j.mimet.2008.11.007

142. Moges F, Endris M, Belyhun Y, Worku W. Isolation and characterization of multiple drug resistance bacterial pathogens from waste water in hospital and non-hospital environments, Northwest Ethiopia. *BMC Res Notes.* (2014) 7:215. doi: 10.1186/1756-0500-7-215

143. Kumaraswamy R, Amha YM, Anwar MZ, Henschel A, Rodríguez J, Ahmad F. Molecular analysis for screening human bacterial pathogens in municipal wastewater treatment and reuse. *Environ Sci Technol.* (2014) 48:11610–9. doi: 10.1021/es502546t

144. Weidhaas JL, Macbeth TW, Olsen RL, Sadowsky MJ, Norat D, Harwood VJ. Identification of a *Brevibacterium* marker gene specific to poultry litter and development of a quantitative PCR assay. *J Appl Microbiol.* (2010) 109:334–47. doi: 10.1111/j.1365-2672.2010.04666.x

145. Ezeonuegbu BA, Abdullahi MD, Whong CMZ, Sohunago JW, Kassem HS, Yaro CA, et al. Characterization and phylogeny of fungi isolated from industrial wastewater using multiple genes. *Sci Rep.* (2022) 12:2094. doi: 10.1038/s41598-022-05820-9

146. Zhang H, Feng J, Chen S, Li B, Sekar R, Zhao Z, et al. Disentangling the drivers of diversity and distribution of fungal community composition in wastewater treatment plants across spatial scales. *Front Microbiol.* (2018) 18:9. doi: 10.3389/fmicb.2018.01291

147. Dalecka B, Oskarsson C, Juhna T, Kuttava Rajarao G. Isolation of Fungal Strains from Municipal Wastewater for the Removal of Pharmaceutical Substances. *Water (Basel).* (2020) 12:524. doi: 10.3390/w12020524

148. Guest RK, Smith DW. Isolation and screening of fungi to determine potential for ammonia nitrogen treatment in wastewater. *J Environ Eng Sci.* (2007) 6:209–17. doi: 10.1139/s06-050

149. Ali EAM, Sayed MA, Abdel-Rahman TMA, Hussein R. Fungal remediation of Cd(ii) from wastewater using immobilization techniques. *RSC Adv.* (2021) 11:4853–63. doi: 10.1039/D0RA08578B

150. Zhou L, Singh A, Jiang J, Xiao L. Molecular surveillance of *Cryptosporidium* spp. in raw wastewater in milwaukee: implications for understanding outbreak occurrence and transmission dynamics. *J Clin Microbiol.* (2003) 41:5254–7. doi: 10.1128/JCM.41.11.5254-5257.2003

151. Li N, Xiao L, Wang L, Zhao S, Zhao X, Duan L, et al. Molecular Surveillance of Cryptosporidium spp, Giardia duodenalis, and Enterocytozoon bieneusi by Genotyping and Subtyping Parasites in Wastewater. *PLoS Negl Trop Dis.* (2012) 6:e1809. doi: 10.1371/journal.pntd.0001809

152. Berglund B, Dienus O, Sokolova E, Berglind E, Matussek A, Pettersson T, et al. Occurrence and removal efficiency of parasitic protozoa in Swedish wastewater treatment plants. *Sci Total Environ.* (2017) 598:821–7. doi: 10.1016/j.scitotenv.2017.04.015

153. Martins FDC, Ladeia WA, Toledo R, dos Garcia JL, Navarro IT, Freire RL. Surveillance of Giardia and Cryptosporidium in sewage from an urban area in Brazil. *Rev Brasil Parasitol Veter.* (2019) 28:291–7. doi: 10.1590/s1984-29612019037

154. Ulloa-Stanojlović FM, Aguiar B, Jara LM, Sato MIZ, Guerrero JA, Hachich E, et al. Occurrence of Giardia intestinalis and Cryptosporidium sp. in wastewater samples from São Paulo State, Brazil, and Lima, Peru. *Environ Sci Pollut Res.* (2016) 23:22197–205. doi: 10.1007/s11356-016-7537-9

155. Wang Y, Liu P, Zhang H, Ibaraki M, VanTassell J, Geith K, et al. Early warning of a COVID-19 surge on a university campus based on wastewater surveillance for SARS-CoV-2 at residence halls. *Sci Total Environ.* (2022) 821:153291. doi: 10.1016/j.scitotenv.2022.153291

156. ben Ayed L, Yang W, Widmer G, Cama V, Ortega Y, Xiao L. Survey and genetic characterization of wastewater in Tunisia for Cryptosporidium spp., Giardia duodenalis, Enterocytozoon bieneusi, Cyclospora cayetanensis and Eimeria spp. *J Water Health.* (2012) 10:431–44. doi: 10.2166/wh.2012.204

157. Stensvold CR, Lebbad M, Hansen A, Beser J, Belkessa S, O'Brien Andersen L, et al. Differentiation of Blastocystis and parasitic archamoebids encountered in untreated wastewater samples by amplicon-based next-generation sequencing. *Parasite Epidemiol Control.* (2020) 9:e00131. doi: 10.1016/j.parepi.2019.e00131

158. Ajonina C, Buzie C, Otterpohl R. The Detection of *Giardia* Cysts in a Large-Scale Wastewater Treatment Plant in Hamburg, Germany. *J Toxicol Environ Health A.* (2013) 76:509–14. doi: 10.1080/15287394.2013.785208

159. Randazzo W, Cuevas-Ferrando E, Sanjuán R, Domingo-Calap P, Sánchez G. Metropolitan wastewater analysis for COVID-19 epidemiological surveillance. *Int J Hyg Environ Health.* (2020) 230:113621. doi: 10.1016/j.ijheh.2020.113621

160. Kaya D, Niemeier D, Ahmed W, Kjellerup B. Evaluation of multiple analytical methods for SARS-CoV-2 surveillance in wastewater samples. *Sci Total Environ.* (2022) 808:152033. doi: 10.1016/j.scitotenv.2021.152033

161. O'Brien M, Rundell ZC, Nemec MD, Langan LM, Back JA, Lugo JN, et al. comparison of four commercially available RNA extraction kits for wastewater surveillance of SARS-CoV-2 in a college population. *Sci Total Environ.* (2021) 801:149595. doi: 10.1016/j.scitotenv.2021.149595

162. Torii S, Furumai H, Katayama H. Applicability of polyethylene glycol precipitation followed by acid guanidinium thiocyanate-phenol-chloroform extraction for the detection of SARS-CoV-2 RNA from municipal wastewater. *Sci Total Environ.* (2021) 756:143067. doi: 10.1016/j.scitotenv.2020.143067

163. Hjelmsø MH, Hellmér M, Fernandez-Cassi X, Timoneda N, Lukjancenko O, Seidel M, et al. Evaluation of Methods for the Concentration and Extraction of Viruses from Sewage in the Context of Metagenomic Sequencing. *PLoS ONE.* (2017) 12:e0170199. doi: 10.1371/journal.pone.0170199

164. Zheng X, Deng Y, Xu X, Li S, Zhang Y, Ding J, et al. Comparison of virus concentration methods and RNA extraction methods for SARS-CoV-2 wastewater surveillance. *Sci Total Environ.* (2022) 824:153687. doi: 10.1016/j.scitotenv.2022.153687

165. Sherchan SP, Shahin S, Patel J, Ward LM, Tandukar S, Uprety S, et al. Occurrence of SARS-CoV-2 RNA in six municipal wastewater treatment plants at the early stage of COVID-19 pandemic in The United States. *Pathogens.* (2021) 10:798. doi: 10.3390/pathogens10070798

166. Ahmed W, Bivins A, Metcalfe S, Smith WJM, Verbyla ME, Symonds EM, et al. Evaluation of process limit of detection and quantification variation of SARS-CoV-2 RT-qPCR and RT-dPCR assays for wastewater surveillance. *Water Res.* (2022) 213:118132. doi: 10.1016/j.watres.2022.118132

167. Yadav AK, Kumar S, Singh G, Kansara NK. Demystifying R naught: Understanding what does it hide? *Indian J Commun Med.* (2021) 46:7. doi: 10.4103/ijcm.IJCM_989_20

168. Kazama S, Masago Y, Tohma K, Souma N, Imagawa T, Suzuki A, et al. Temporal dynamics of norovirus determined through monitoring of municipal wastewater by pyrosequencing and virological surveillance of gastroenteritis cases. *Water Res.* (2016) 92:244–53. doi: 10.1016/j.watres.2015.10.024

169. Fioretti JM, Fumian TM, Rocha MS, dos Santos I de AL, Carvalho-Costa FA, de Assis MR, et al. Surveillance of Noroviruses in Rio De Janeiro, Brazil: Occurrence of New GIV Genotype in Clinical and Wastewater Samples. *Food Environ Virol.* (2018) 10:1–6. doi: 10.1007/s12560-017-9308-2

170. Bauermeister J, Eaton L, Stephenson R. A multilevel analysis of neighborhood socioeconomic disadvantage and transactional sex with casual partners among young men who have sex with men living in metro Detroit. *Behav Med.* (2016) 42:197–204. doi: 10.1080/08964289.2015.1110560

171. Bayeh R, Yampolsky MA, Ryder AG. The social lives of infectious diseases: Why culture matters to COVID-19. *Front Psychol.* (2021) 12:648086. doi: 10.3389/fpsyg.2021.648086

172. Du WY, Yin CN, Wang HT, Li ZW, Wang WJ, Xue FZ, et al. Infectious diseases among elderly persons: Results from a population-based observational study in Shandong province, China, 2013-2017. *J Glob Health.* (2021) 11:08010. doi: 10.7189/jogh.11.08010

173. Greene SK, Levin-Rector A, Hadler JL, Fine AD. Disparities in reportable communicable disease incidence by census tract-level poverty, New York City, 2006–2013. *Am J Public Health.* (2015) 105:e27–34. doi: 10.2105/AJPH.2015.302741

174. Thulin CG, Malmsten J, Ericsson G. Opportunities and challenges with growing wildlife populations and zoonotic diseases in Sweden. *Eur J Wildl Res.* (2015) 61:649–56. doi: 10.1007/s10344-015-0945-1

175. Wright N, Scherdt M, Aebersold ML, McCullagh MC, Medvec BR, Ellimoottil C, et al. Rural Michigan farmers' health concerns and experiences: a focus group study. *J Prim Care Commun Health.* (2021) 12:21501327211053520. doi: 10.1177/21501327211053519

176. Lin YH, Tseng YH, Chen YC, Lin MH, Chou LF, Chen TJ, et al. The rural-urban divide in ambulatory care of gastrointestinal diseases in Taiwan. *BMC Int Health Hum Rights.* (2013) 13:1–7. doi: 10.1186/1472-698X-13-15

177. LeJeune J, Kersting A. Zoonoses: an occupational hazard for livestock workers and a public health concern for rural communities. *J Agric Saf Health.* (2010) 16:161–79. doi: 10.13031/2013.32041

178. Parola P, Paddock CD. Travel and tick-borne diseases: Lyme disease and beyond. *Travel Med Infect Dis.* (2018) 26:1–2. doi: 10.1016/j.tmaid.2018.09.010

179. Vanos JK, Kalkstein LS, Sanford TJ. Detecting synoptic warming trends across the US Midwest and implications to human health and heat-related mortality. *Int J Climatol.* (2015) 35:85–96. doi: 10.1002/joc.3964

180. Filho WL, Scheday S, Boenecke J, Gogoi A, Maharaj A, Korovou S. Climate change, health and mosquito-borne diseases: trends and implications to the pacific region. *Int J Environ Res Public Health.* (2019) 16:5114. doi: 10.3390/ijerph16245114

181. Vora N. Impact of anthropogenic environmental alterations on vector-borne diseases. *Medscape J Med.* (2008) 10:238.

182. Bowen VB, Braxton J, Davis DW, Flagg EW, Grey J, Grier L, et al. *Sexually transmitted disease surveillance 2018*. Annual report. (2019). doi: 10.15620/cdc.59237

183. Denning P, DiNenno E. Communities in crisis: is there a generalized HIV epidemic in impoverished urban areas of the United States. In: *XVIII International AIDS Conference*. (2010).

184. Pellowski JA, Kalichman SC, Matthews KA Adler N, A. pandemic of the poor: Social disadvantage and the US HIV epidemic. *Am Psychol.* (2013) 68:197–209. doi: 10.1037/a0032694

185. Noppert GA, Clarke P, Hicken MT, Wilson ML. Understanding the intersection of race and place: the case of tuberculosis in Michigan. *BMC Public Health.* (2019) 19:1669. doi: 10.1186/s12889-019-8036-y

186. Kang SH, Cho DH, Choi J, Baik SK, Gwon JG, Kim MY. Association between chronic hepatitis B infection and COVID-19 outcomes: A Korean nationwide cohort study. *PLoS ONE.* (2021). 16:e0258229. doi: 10.1371/journal.pone.0258229

187. Kondili LA, Buti M, Riveiro-Barciela M, Maticic M, Negro F, Berg T, et al. Impact of the COVID-19 pandemic on hepatitis B and C elimination: An EASL survey. *JHEP Reports.* (2022) 4:100531. doi: 10.1016/j.jhepr.2022.100531

188. Pley CM, McNaughton AL, Matthews PC, Lourenço J. The global impact of the COVID-19 pandemic on the prevention, diagnosis and treatment of hepatitis B virus (HBV) infection. *BMJ Glob Health.* (2021) 6:e004275. doi: 10.1136/bmjgh-2020-004275

189. Formenti B, Gregori N, Crosato V, Marchese V, Tomasoni LR, Castelli F. The impact of COVID-19 on communicable and non-communicable diseases in Africa: a narrative review. *Infez Med.* (2022) 30:30. doi: 10.53854/liim-3001-4

190. Latini A, Magri F, Donà MG, Giuliani M, Cristaudo A, Zaccarelli M. Is COVID-19 affecting the epidemiology of STIs? The experience of syphilis in Rome. *Sex Transm Infect.* (2021) 97:78–78. doi: 10.1136/sextrans-2020-054543

191. Chiu NC, Chi H, Tai YL, Peng CC, Tseng CY, Chen CC, et al. Impact of wearing masks, hand hygiene, and social distancing on influenza, enterovirus, and all-cause pneumonia during the coronavirus pandemic: retrospective national epidemiological surveillance study. *J Med Internet Res.* (2020) 22:e21257. doi: 10.2196/21257

192. Pal M. Lyme disease-an emerging metazoonosis of public health concern. *J Clin Immunol Microbiol.* (2021) 2:1–4. doi: 10.46889/JCIM.2021.2110

193. Mahalaxmi I, Jayaramayya K, Venkatesan D, Subramaniam MD, Renu K, Vijayakumar P, et al. Mucormycosis: An opportunistic pathogen during COVID-19. *Environ Res.* (2021) 201:111643. doi: 10.1016/j.envres.2021.111643

194. Maldonado MD, Romero-Aibar J, Pérez-San-Gregorio MA. COVID-19 pandemic as a risk factor for the reactivation of herpes viruses. *Epidemiol Infect.* (2021) 149:e145. doi: 10.1017/S0950268821001333

195. Wright SS, Kreisel KM, Hitt JC, Pagaoa MA, Weinstock HS, Thorpe PG. Impact of the COVID-19 pandemic on centers for disease control and prevention–funded sexually transmitted disease programs. *Sex Transm Dis.* (2022) 49:e61–3. doi: 10.1097/OLQ.0000000000001566

196. Stanford KA, Almirol E, Schneider J, Hazra A. Rising syphilis rates during the COVID-19 pandemic. *Sex Transm Dis.* (2021) 48:e81–3. doi: 10.1097/OLQ.0000000000001431

197. Willis K, Ezer P, Lewis S, Bismark M, Smallwood N. "Covid Just Amplified the Cracks of the System": Working as a Frontline Health Worker during the COVID-19 Pandemic. *Int J Environ Res Public Health.* (2021) 18:10178. doi: 10.3390/ijerph181910178

198. Schønning K, Dessau RB, Jensen TG, Thorsen NM, Wiuff C, Nielsen L, et al. Electronic reporting of diagnostic laboratory test results from all healthcare sectors is a cornerstone of national preparedness and control of COVID-19 in Denmark. *Apmis.* (2021) 129:438–51. doi: 10.1111/apm.13140

199. Beld M, Sentjens R, Rebers S, Weel J, Wertheim-van Dillen P, Sol C, et al. Detection and Quantitation of Hepatitis C Virus RNA in Feces of Chronically Infected Individuals. *J Clin Microbiol.* (2000) 38:3442–4. doi: 10.1128/JCM.38.9.3442-3444.2000

200. Vaidya SR, Tilavat SM, Kumbhar NS, Kamble MB. Chickenpox outbreak in a tribal and industrial zone from the Union Territory of Dadra and Nagar Haveli, India. *Epidemiol Infect.* (2018) 146:476–80. doi: 10.1017/S0950268818000201

201. Delhon G. Poxviridae. In: *Veterinary Microbiology*. (2022). p. 522–32. doi: 10.1002/9781119650836.ch53

202. Sims N, Kasprzyk-Hordern B. Future perspectives of wastewater-based epidemiology: Monitoring infectious disease spread and resistance to the community level. *Environ Int.* (2020) 139:105689. doi: 10.1016/j.envint.2020.105689

203. Lee WL, Gu X, Armas F, Leifels M, Wu F, Chandra F, et al. Monitoring human arboviral diseases through wastewater surveillance: Challenges, progress and future opportunities. *Water Res.* (2022) 223:118904. doi: 10.1016/j.watres.2022.118904

204. Guo Y, Sivakumar M, Jiang G. Decay of four enteric pathogens and implications to wastewater-based epidemiology: Effects of temperature and wastewater dilutions. *Sci Total Environ.* (2022) 819:152000. doi: 10.1016/j.scitotenv.2021.152000

205. Marques PX, Wand H, Nandy M, Tan C, Shou H, Terplan M, et al. Serum antibodies to surface proteins of *Chlamydia trachomatis* as candidate biomarkers of disease: results from the Baltimore Chlamydia Adolescent/Young Adult Reproductive Management (CHARM) cohort. *FEMS Microbes.* (2022) 17:3. doi: 10.1093/femsmc/xtac004

206. Tanir G, Kiliçarslan F, Göl N, Arslan Z. Age-spesific seroprevalence and associated risk factors for hepatitis A in children in Ankara, Turkey. *J Ankara Med School.* (2003) 25:81–8. doi: 10.1501/Jms_0000000048

207. Dhanaraj B, Papanna MK, Adinarayanan S, Vedachalam C, Sundaram V, Shanmugam S, et al. Prevalence and Risk Factors for Adult Pulmonary Tuberculosis in a Metropolitan City of South India. *PLoS ONE.* (2015) 10:e0124260. doi: 10.1371/journal.pone.0124260

frontiers | Frontiers in Medicine

TYPE Original Research
PUBLISHED 26 June 2023
DOI 10.3389/fmed.2023.1148688

OPEN ACCESS

EDITED BY
David Champredon,
Public Health Agency of Canada (PHAC), Canada

REVIEWED BY
Mir Muhammad Nizamani,
Guizhou University, China
Areti Strati,
National and Kapodistrian University of Athens, Greece

*CORRESPONDENCE
Mallika Lavania
✉ mallikalavania@gmail.com

†These authors have contributed equally to this work

RECEIVED 20 January 2023
ACCEPTED 09 June 2023
PUBLISHED 26 June 2023

CITATION
Shinde M, Lavania M, Rawal J, Chavan N and Shinde P (2023) Evaluation of droplet digital qRT-PCR (dd qRT-PCR) for quantification of SARS CoV-2 RNA in stool and urine specimens of COVID-19 patients.
Front. Med. 10:1148688.
doi: 10.3389/fmed.2023.1148688

Evaluation of droplet digital qRT-PCR (dd qRT-PCR) for quantification of SARS CoV-2 RNA in stool and urine specimens of COVID-19 patients

Manohar Shinde†, Mallika Lavania*†, Jatin Rawal, Nutan Chavan and Pooja Shinde

Enteric Viruses Group, ICMR-National Institute of Virology, Pune, Maharashtra, India

Introduction: There have been a few reports of viral load detection in stool and urine samples of patients with coronavirus disease 2019 (COVID-19), and the transmission of the virus through faecal oral route. For clinical diagnosis and treatment, the widely used reverse transcription-polymerase chain reaction (qRT-PCR) method has some limitations.

Methods: The aim of our study to assess the presence and concentration of SARS CoV-2 RNA in stool and urine samples from COVID-19 patients with mild, moderate, and severe disease, we compared a traditional qRT-PCR approach with a ddPCR. ddPCR and qRT-PCR-based target gene analysis were performed on 107 COVID-19-confirmed patients paired samples (N1 and N2). The MagMax magnetic beads base method was used to isolate RNA. Real-time qRT-PCR and dd PCR were performed on all patients.

Results and Discussion: The average cycle threshold (Ct) of qRT-PCR was highly correlated with the average copy number of 327.10 copies/l analyzed in ddPCR. In ddPCR, urine samples showed 27.1% positivity while for stool it was 100%.

Conclusion: This study's findings not only show that SARS CoV-2 is present in urine and faeces, but also suggest that low concentrations of the viral target ddPCR make it easier to identify positive samples and help resolve for cases of inconclusive diagnosis.

KEYWORDS

droplet digital PCR, N-gene, real time qRT-PCR, SARS-CoV-2, stool, urine

1. Introduction

On December 31, 2019, China reported the first cases of pneumonia from an unidentified source to the World Health Organization (WHO), and on March 11, 2020, WHO declared the coronavirus disease of 2019 (COVID-19) as a pandemic. Over 6.4 million fatalities and 605 million confirmed cases of COVID-19 infections had been documented globally as of September 11th, 2022 (1). It has been almost 3 years since the COVID-19 pandemic started and it continues to affect the global population, as new strains of the virus keep emerging. In spite of developing newer treatment and diagnostic modalities, including very effective vaccines, the disease remains one of the major challenges countries across the globe face today. The World

health organization estimates that till now about 400 million people have had the disease and 5 million have died because of its complications. This large number indicates the rapid transmission of this disease, which has been proven to spread through more than one route. It is known that the SARS CoV-2 presents differently in infected people, it can range from asymptomatic or mild respiratory infection to severe pneumonia with acute respiratory distress syndrome or multi organ failure, which might have a fatal outcome. Among those who develop symptoms the majority present with symptoms of fever, cough, fatigue, myalgia and rhinitis. A significant proportion of infected people also present with gastrointestinal symptoms including diarrhoea, abdominal pain, and vomiting. Occasional observation of dominance of gastro-intestinal symptoms without any respiratory symptoms have also been noted, the possible reason proposed for this finding is the circulation of two types of SARS CoV-2, one with gut tropism and another with lung tropism.

The gold standard method to assess genomic or complimentary DNA levels is quantitative PCR (qPCR), but without proper sample and primer validation and verification, the resulting data might be very varied, false, and impossible to reproduce. Poor data quality has its origins in the insufficient dilution of chemical and protein impurities that, in varying degrees, block Taq polymerase and primer annealing. The samples with the lowest expression differences of twofold or less and the least numerous targets are the most vulnerable, frustrating, and frequently most intriguing. In this study, Droplet Digital PCR (ddPCR) and quantitative PCR (qPCR) systems were directly compared for the detection of gene expression in well-characterized samples utilizing small amounts of pure, synthetic DNA under the same reaction conditions. Quantitative Real-time reverse transcriptase polymerase chain reaction (qRT-PCR) detection of SARS CoV-2 RNA in nasopharyngeal swabs is used to diagnose the majority of COVID-19 cases (The qRT-PCR technology has two advantages: high throughput and sensitivity). Numerous testing platforms have received FDA and CE IVD approval and have been clinically used to diagnose SARS CoV-2 infection as of the first quarter of 2021. These point-of-care tests are quick, but many of them have low sensitivity and high false-negative rates, as a disadvantage or better which limit their use (2). qRT-PCR technology may detect small amounts of virus with high throughput, although faint positives Ct > 35 may be challenging to separate from technical artifacts. The current gold standard for the etiological diagnosis of COVID-19 is viral nucleic acid detection by reverse transcription PCR (RT-PCR) which targets viral genes such ORF1a/b, E, S, and N genes. The sensitivity and accuracy of RT-PCR, however, have been questioned because some patients who had a high degree of clinical suspicion for the disease based on their exposure history and clinical presentation had negative results as well as positive findings in some confirmed cases after recovery (3, 4). Additionally, the RT-PCR technique is unable to assess the efficacy of antiviral medications and has limitations on viral load analysis for determining disease progression and prognosis. Droplet digital PCR (ddPCR) has the benefit of absolute quantification and is more sensitive for virus identification than RT-PCR, according to a number of studies (5, 6).

ddPCR is an orthogonal technique that can be used to detect and measure accurate nucleic acid copy numbers as well as incredibly low amounts of nucleic acid. Several investigations have shown that ddPCR could detect SARS CoV-2 RNA in various body fluids, such as plasma (7, 8).

ddPCR is a very sensitive PCR technique for absolute nucleic acid quantification without the need for a reference curve. Although ddPCR utilization in research labs has grown over the past 10 years, this method is rarely employed in clinical labs, mostly because of its high cost (9).

In order to assess the presence and concentration of SARS CoV-2 RNA in stool and urine samples from COVID-19 patients with mild, moderate, and severe disease, we compared a traditional qRT-PCR approach typically used in clinical microbiology laboratories with a ddPCR.

2. Materials and methods

2.1. Patients and sampling

All of the registered patients were recruited from the different hospitals in the Pune, Deenanath Mangeshkar, Jehangir, and Lokmaanya hospitals in Pune, Western India, between May 2020 and August 2021. Real-time reverse transcription polymerase chain reaction (**qRT-PCR**) results on oro/nasopharyngeal swab samples showed that all of the registered patients were positive for SARS CoV-2 RNA. The study was approved by the Institutional Ethics Committee of ICMR-National Institute of Virology, Pune, Maharashtra, India (No. NIV/IEC/June/2020/D-14 dated 24th June 2020). Workflow for the molecular diagnosis of SARS CoV-2 from stool and urine specimens was represented in Figure 1.

In total, 107 patients were enrolled in the study. Patients who had been diagnosed with COVID-19 in a lab had their faeces and urine samples taken. Prior to being tested for SARS CoV-2, all hospital samples were transported to the ICMR-National Institute of Virology in Pune and stored at −20°C. Samples were stored at −20°C for up to 3 days and subsequently transferred to −80°C until analysis. We included twenty normal samples as a control to check the specificity of assay.

2.2. Sample processing

To remove debris, 30% faecal suspensions in 0.01 M phosphate buffered saline (PBS), pH 7.4, were centrifuged at 4000 rpm (Hettich Universal 320R centrifuge) for 10 min. 10 mL of urine sample was collected in a 15 mL sterile tube. Centrifugation was performed at 500 g for 20 min at 4°C. The supernatant was removed, and the pellet was used to extract RNA (Figure 1).

2.3. RNA extraction

The viral RNA was extracted from 30% (w/v) suspensions of faecal and urine samples using spin columns and the Qiagen Viral RNA extraction Kit (Cat No52904) as directed by the manufacturer (Qiagen, Hilden, Germany).

2.4. Construction of RNA standards

Forward primers with a T7 promoter tag at the 5′ end were created to amplify full-length E gene and N gene sections because the whole SARS CoV-2 genome was taken from the public database and primers

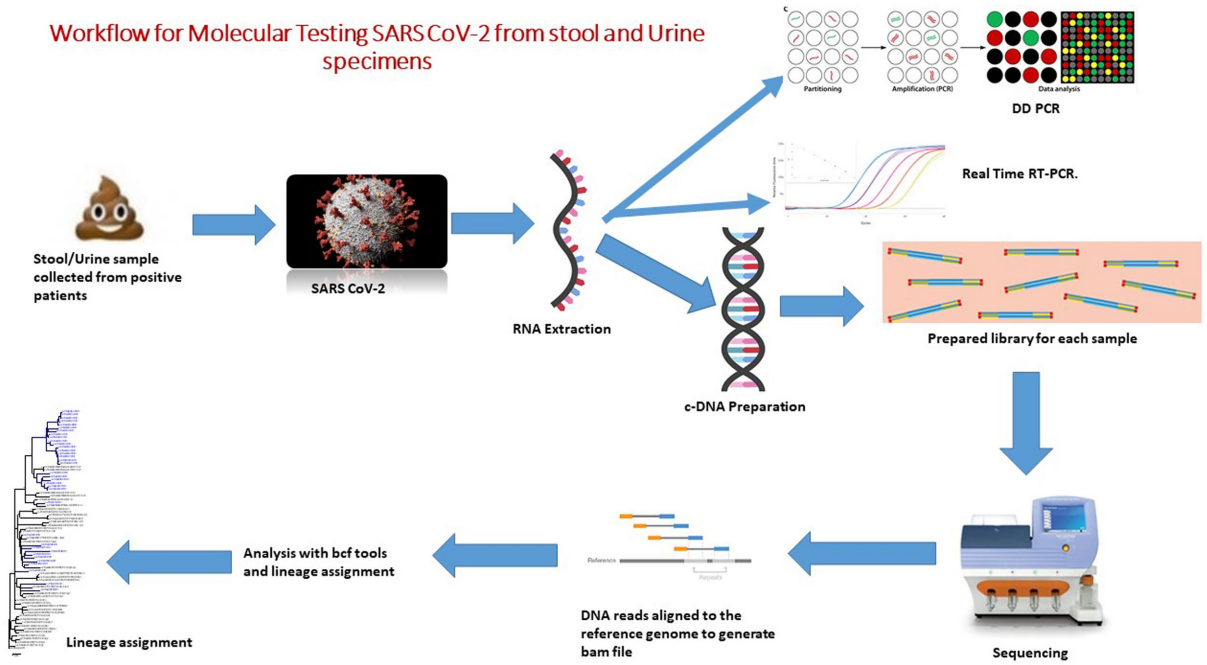

FIGURE 1
Workflow for molecular testing SARS CoV-2 from stool and urine specimens.

were designed. To obtain the desired PCR result, gene-specific PCR was conducted. Amplicons were cleaned by using Qiagen direct PCR purification kit (Cat No- 28104 Qiagen, Hilden, Germany). *In Vitro* Transcribed (IVT) RNA was synthesized using T7 Riboprobe® Systems (Cat No: P1440, Promega, United States) in accordance with the kit's instructions. Each IVT RNA product was serially diluted 10 times before being tested for specific detection and determination of limit of detection using the appropriate gene primer probe sets (10).

The concentration of synthetic fragment of transcribed RNA was measured by fluorometric analysis (Qubit, Thermo Scientific), and then standard curve was constructed by using tenfold serial dilutions of RNA. The copy numbers of the standard RNAs ranged from 2.5 to 2.5 x 10^8/xuL, were used for the consctruction of standard curve for absolute quantification in qRT-PCR. After standardizing the qRT-PCR data using the standard curve in the instrument software (CFX96™ thermocycler), the Ct value for both genes was determined (Bio-Rad, Hercules, California, United States). For data comparison, the Ct of each analysis was taken into consideration.

2.5. Real-time qRT-PCR assay based on N1 and N2 gene

Using a CFX96™ thermocycler and the Qiagen SARS CoV-2 N1 + N2 assay kit (Cat. No. 222015, Qiagen, Germany), qRT-PCR was carried out with 5 µL of total RNA isolated from stool and urine samples (Qiacuity QX-200, Qiagen, Germany). The N1 and N2 genes, which code for the viral nucleocapsid, the E gene, which codes for the viral envelop, as well as the RNAse P gene as an internal control, are all detected by this kit. In accordance with the manufacturer's recommendations, samples were deemed positive for SARS CoV-2 if any of the genes (E or N) it detects had a Ct value below 37.

All the twenty normal samples showed negative results by using Q-PCR targeting this multiplex N1 + N2 assay kit.

2.6. Droplet digital qRT-PCR (dd qRT-PCR) assay based on N1 and N2 gene

SARS CoV-2 RNA was detected and quantified in 5 µL of total RNA obtained from stool and urine specimens using the SARS CoV-2 N1 + N2 assay kit according to manufacturer's instructions on a QX-200 ddPCR platform (Qiacuity QX-200, Qiagen, Germany) and a recent published literature on waste water (11). The SARS CoV-2 CoV-2 N1 + N2 Assay is a mixture of four primers and two probes purified by HPLC at a 20x concentration. These four primers are based on the CDC design, targeting the regions N1 and N2 of the viral genome. The two probes are coupled with FAM as a reporter dye and use ZEN™ quenchers for enhanced sensitivity. For the N1 and N2 assays, the concentrations of the primer and probe, as well as the annealing temperature and duration, were optimized. N1 and N2 assays were carried out in 40 µL reaction mixtures using the QIAcuity One-Step Viral qRT-PCR Kit (Cat no. 1123145, Qiagen) on 26,000 24-well Nanoplates under ideal circumstances (catalog no. 250001, Qiagen). The microfluidic dPCR plates 26,000 QIAcuity 24-well Nanoplates enable 24 samples to be run with up to 26,000 partitions/well. Each partition has a volume of 0.91 nL and the PCR takes place within each partition.

2.7. Statistical analysis

The Mann–Whitney U test was used to make comparisons between the two groups. The Spearman correlation test was used to

examine the relationship between the Ct values of qRT-PCR and the viral load determined by ddPCR. Statistical significance was defined as a p value less than 0.05 (two sided). The analyzes described above were carried out with either Prism 7.0 (GraphPad, La Jolla, CA, United States) software.

3. Results

3.1. Baseline demographic characteristics of patients

In this study, 107 COVID-19 positive patients confirmed by real time qRT-PCR from all age groups who were admitted in different COVID Care Center of Pune District were enrolled, in which 40 (37%) were female, & 67 (63%) were male. The demographic and clinical details of the patients are described in Figure 2. According to the age distribution, the median age was 32 years, with 16 participants belonging to the 0–17 age range, 42 participants to the 18–35 age range, 26 participants to the 36–53 age range, 20 participants to the 54–71 age range, and 3 participants to the 72–89 age range. Most of the participants (68 patients) who had COVID-19 infection were in the 18–35, 36–53, and 0–17 age range.

At the time of admission, fever (78.50%), cough (58.88%), loss of taste or smell (43.93%), diarrhoea (33.64%), sore throat (27.10%), nausea and vomiting (26.17%), runny nose (24.30%), bloody sputum (16.82%), chest discomfort (14.95%), and abdominal pain (14.02%) were the signs and symptoms that were most prominent. Among these 107 participants, 19 (18%) participants were in close contact with known positive case of COVID-19 patient, while 88 (82%) were not having any close contact with known case in last 14 days.

After admission to the COVID Care Center, stool & urine specimens were collected from the patient from day 0, i.e., day on which patient was admitted, while maximum number of specimens were collected on Day 1, 2, 3, and 6.

3.2. Performance of the assays

The quantification for the N1 and N2 qRT-PCR standard curves ranged from 2.5×10^8 to 2.5 gene copies/reaction. The approach revealed a strong linear correlation (R2 = 0.999) between predicted and actual SARS CoV-2 measurement (Figure 3).

The amplification efficiencies, y-intercepts and the correlation coefficient (r^2) were 88.3%, 49.73 and 0.999 for N gene assay (Figure 3). The qRT-PCR assay limits of detection was 1.8-gene copies/reaction for N1 + N2 assay.

3.3. Comparative analysis of qRT-PCR and ddPCR in stool and urine specimens

A total of 214-paired samples from the 107 confirmed patients were tested by both qRT-PCR and ddPCR, including stool and urine sample. According to the qRT-PCR results, 106 samples were positive for stool and one for urine by N-gene. The ddPCR results of the 106 positive stool samples were also positive, and the Ct value of qRT-PCR was highly correlated with the copy number determined by ddPCR (N-gene, R2 = 0.89; N, R 2 = 0.20). In 107 patients, all the stool samples showed 99.06% positive concordance by both methods. Among the 106 negative urine samples identified by qRT-PCR, 77 (72.6%) samples were negative by ddPCR, and 29 samples were positive (Table 1). The median for ddPCR of the copy number for stool and urine samples was 11.30 and 0 respectively, whereas lowest copy number detected in ddPCR for both stool & urine sample was 0.048 copies/μL. Statistically difference was observed in urine specimens by using two tailed analysis [$p < 0.0001$] (Figure 4).

Our findings demonstrated that whereas ddPCR performed better at detecting samples with low viral loads, like urine, qRT-PCR was equally as accurate and reliable in the identification of viruses from stool samples.

FIGURE 2
Baseline demographic and clinical characteristics of the study population.

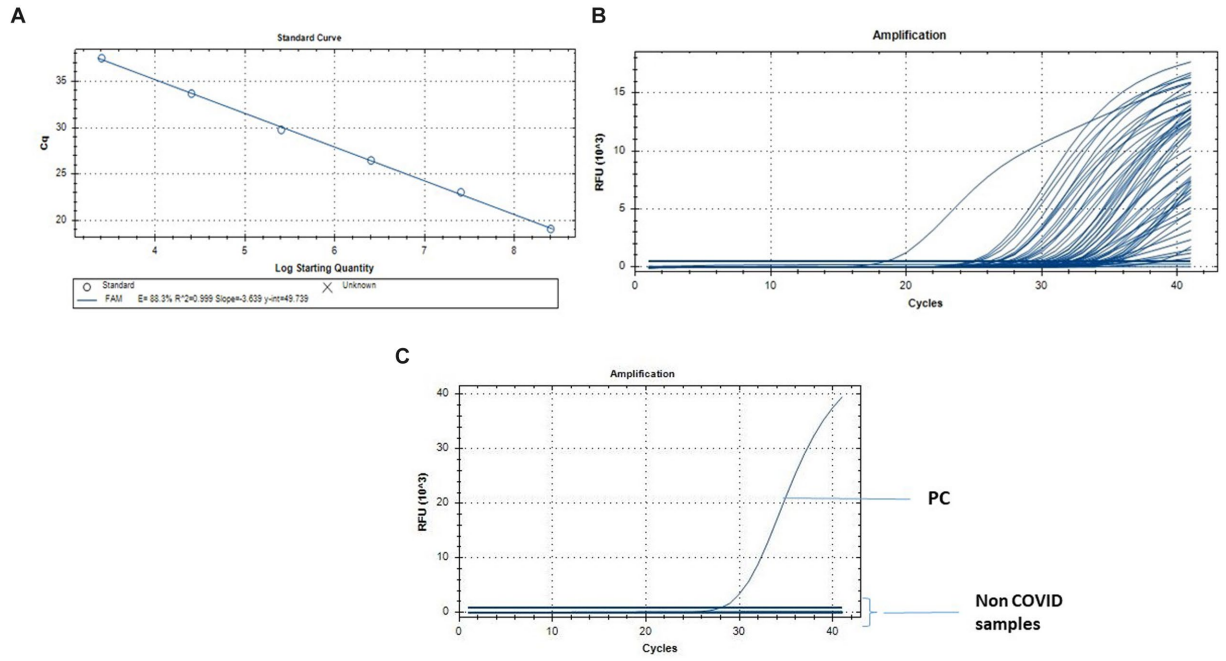

FIGURE 3
Quantification of SARS-CoV-2 by qRT-PCR. **(A)** Standard curve for the real-time PCR targeting N gene. The X-axis represents copies of the plasmids, and the Y-axis represents the cycle threshold (Cq). The assays were linear from 2.5×10^8 to 2.5 gene copies/reaction. **(B)** q-RT PCR results from the fecal and urine specimens of the individuals infected with SARS CoV-2\u00B0C. q-RT PCR from the Non COVID-19 normal individuals for the specificity of the assay.

TABLE 1 Comparative analysis of DD PCR and q-PCR in both stool and urine specimens from SARS CoV-2 positive patients.

	Stool		Urine	
	qRT PCR	DD-PCR	qRT PCR	DD-PCR
Positive	106	107	1	29
Negative	1	0	106	78

4. Discussion

From the beginning of the pandemic, qRT-PCR was used all over the world for the detection of the virus. During the most recent pandemic, qRT-PCR was regarded as the gold standard for virus detection. However, the failure of qRT-PCR in some cases in detecting the genes encoding the spike protein is a matter of concern. Besides that, qRT-PCR is also unable to quantify the viral load from borderline samples. Recent study showed that detection of COVID-19 virus form wastewater treatment by targeting the N1 and N2 coding genes showed positive results (11). Studies of viral load detection from plasma (12), nasopharyngeal swab (13), and sputum (14) showed that ddPCR is more sensitive in detecting the virus in comparision to qRT-PCR. However, this type of comparative studies until have not been reported from stool or urine samples.

The COVID-19 pandemic caused by the SARS CoV-2 virus motivates a variety of diagnostic strategies because of the novel causing pathogen, poorly known clinical consequence, and the limitation of testing resources. Furthermore, although the presence of SARS CoV-2 RNA in wastewater effluents has been established, viral infectivity of positive samples in cell cultures has not yet been established (15). SARS CoV-2 infectivity is sustained for more than 3 h in experimentally produced aerosols (16), and respiratory droplets and aerosols may contain high titers of virus particles (17–19). It should be noted that several research looking at viral shedding and faecal PCR in COVID-19 patients revealed a weak connection between positive stool PCR and level of gastrointestinal symptoms or disease activity (20). Furthermore, it is not yet known whether each stool PCR positive sample contains a live virus or only RNA pieces that have been discharged from the GI tract. Because of the variability in viral load across and within patients, it is crucial for diagnosis and surveillance to directly quantify absolute viral load from crude lysate. Here, in our study we look at the possibility of measuring SARS CoV-2 viral load using digital droplet PCR (ddPCR) directly from faecal and urine specimens. Using many partitioned reactions, digital droplet PCR quantifies the target nucleic acid sequences. Unlike qRT-PCR, which determines concentrations by comparing amplification rates to a standard curve, ddPCR cycles the sample to the endpoint and then counts target molecules directly by counting positive droplets. In comparison to qRT-PCR, this method offers a number of benefits, such as more accurate measurements and absolute quantification without the requirement for a standard curve (21, 22). The human immunodeficiency virus (HIV) (23), the cytomegalovirus (CMV) (24) and the human herpes virus 6 (HHV-6) (25) can all was detected using ddPCR. Purified RNA extracts used in ddPCR of COVID-19 patients show advantages for diagnosis and monitoring, especially in those with low viral loads (26–28).

One hundred and seven COVID-19 confirmed patients were tested to assess the viral load of SARS CoV-2 in stool and urine sample, and to measure the effectiveness of ddPCR in detecting the virus. For samples with high viral loads, we observed that both qRT-PCR and

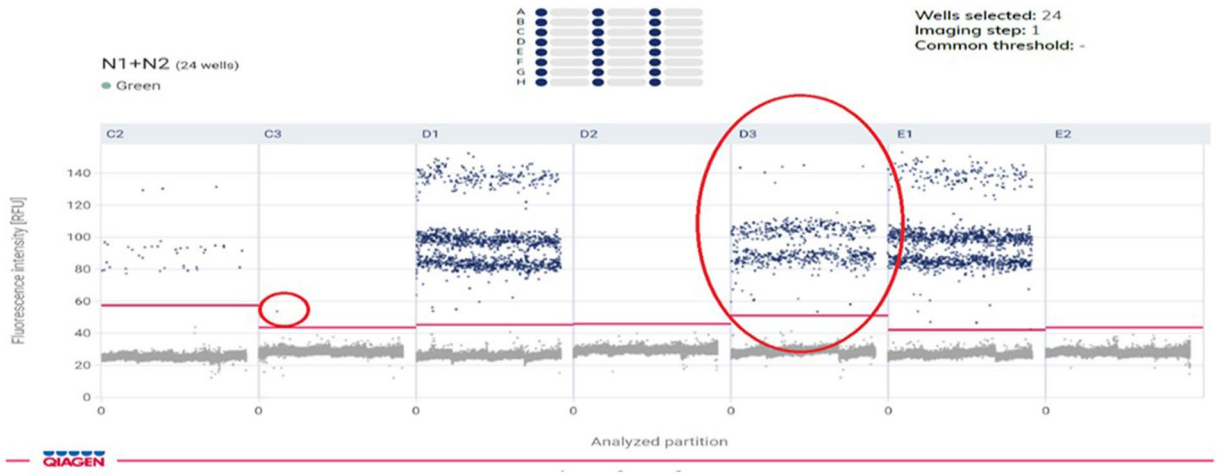

FIGURE 4
Amplitude signal of SARS-CoV-2 Ngene positive droplets obtained with DD-PCR.

ddPCR provided reliable results; however, ddPCR performed better for those with low viral loads. It has been observed that the faeces contain higher viral load than the urine samples. Analyzing the stool and urine samples from 107 COVID-19 positive patients, we observed that ddPCR detects the virus with 100% concordance with qRT-PCR in the case of fecal specimens. While 29 urine samples out of 107 (27.1%) urine samples showed positive results in ddPCR, but qRT-PCR shows positive result for only two (1.86%) patients sample. These observations support that ddPCR is more sensitive in detecting the virus as compared to qRT-PCR. Although reverse transcription-PCR is sensitive and trustworthy, low-viral-load samples were more effectively detected by ddPCR in low viral load condition. Studies across the globe have identified the presence of live infective SARS CoV2 RNA particles in untreated sewage samples thus emphasizing the need for continuous environmental surveillance. Furthermore, it was observed that there is an association between the SARS CoV-2 RNA concentrations found in the water samples and the number of clinical cases reported in a particular area, thus implying that the surveillance of RNA concentrations of virus can be used as a potential early warning system to tract the community spread of the disease. There are several studies on the wastewater-based epidemiology (WBE) reported across the globe after the COVID-19 pandemic. WBE is being used globally to track SARS CoV-2 infections at the community level to aid public health responses to COVID-19. Regarding the sensitivity of WBE and its application in low prevalence situations, concerns still exist. Therefore, such assays will be good for monitoring infectious diseases, such as COVID-19, in the communities in the early stage. However, doing routine surveillance will not be an easy and cost effective task, since a huge number of pathogens are to be monitored regularly. The development of novel techniques in meta-genomics can be used in this regard for the simultaneous environmental surveillance of multiple pathogens, thus reducing the cost of such surveillance in resource poor settings.

The study was constrained by the small sample size for various types of samples and the fact that some patients did not have access to specific clinical information, which prevented results from being connected with symptoms or illness history. It is necessary to conduct further research on individuals who have comprehensive temporal and symptoms data as well as specimens that were collected sequentially from several sites.

5. Conclusion

Due to the diarrhoea symptom, stool is a more accurate signal of viral replication in the body along with throat and nasal swabs, and the viral load in stool samples tends to rise and then fall during the course of the illness. The COVID-19 pandemic spurred caused by the SARS CoV-2 virus sparks a variety of diagnostic strategies because of the novel causing pathogen, poorly known clinical consequence, and the limitation of testing resources. Because of the variability in viral load across and within patients, it is crucial for diagnosis and surveillance to directly quantify absolute viral load from crude lysate. Here, in our study we look at the possibility of measuring SARS CoV-2 viral load using digital droplet PCR (ddPCR) directly from fecal and urine specimens. Our study fills a gap of detection or the presence of SARS CoV-2 viral particles in urine samples that is a much easier specimen to get from patients than stools. We demonstrate that SARS CoV-2 standards can be properly quantified by ddPCR using pure RNA and a variety of sample matrices, including the widely used viral transport medium (VTM).

Data availability statement

The raw data supporting the conclusions of this article will be made available by the authors, without undue reservation.

Ethics statement

The studies involving human participants were reviewed and approved by ICMR-National Institute of Virology, Institutional Ethics Committee. The patients/participants provided their written informed consent to participate in this study.

Author contributions

ML and MS contributed in the conceptualization and experimentation of the study. All the experimentation was done by MS, JR, NC, and PS. ML and JR did the data curation and analysis. MS and JR contributed in recruiting the patients. ML did manuscript writing, reviewing, and editing. ML also did supervision and project administration. All authors contributed to the article and approved the submitted version.

Funding

This research was funded by ICMR-National Institute of Virology, Pune, Maharashtra, India.

Acknowledgments

The authors thank all patients involved in the study. Authors thank Prof. Dr. Priya Abraham, Director ICMR-NIV, Pune for the support during the study. The assistance provided by Mr. P. S. Jadhav, and other nursing staff of the hospitals during sample collection from the hospital are duly acknowledged. Authors thank Ms. Shweta Bhosale for compiling the information from all the patients.

Conflict of interest

The authors declare that the research was conducted in the absence of any commercial or financial relationships that could be construed as a potential conflict of interest.

Publisher's note

All claims expressed in this article are solely those of the authors and do not necessarily represent those of their affiliated organizations, or those of the publisher, the editors and the reviewers. Any product that may be evaluated in this article, or claim that may be made by its manufacturer, is not guaranteed or endorsed by the publisher.

References

1. WHO (2022). Weekly epidemiological update on COVID-19-14 September 2022. Edition 109, 14 September 2022 emergency situational updates. Available at: https://www.who.int/publications/m/item/weekly-epidemiological-update-on-covid-19---14-september-2022 (assessed November 21, 2022).

2. Mitchell SL, George KS. Evaluation of the COVID19 ID NOW EUA assay. *J Clin Virol*. (2020) 128:104429. doi: 10.1016/j.jcv.2020.104429

3. Winichakoon P, Chaiwarith R, Liwsrisakun C, Salee P, Goonna A, Limsukon A, et al. Negative nasopharyngeal and Oropharyngeal swabs do not rule out COVID-19. *J Clin Microbiol*. (2020) 58:e00297–20. doi: 10.1128/JCM.00297-20

4. Wu J, Liu J, Zhao X, Liu C, Wang W, Wang D, et al. Clinical characteristics of imported cases of coronavirus disease 2019 (COVID-19) in Jiangsu Province: a multicenter descriptive study. *Clin Infect Dis*. (2020) 71:706–12. doi: 10.1093/cid/ciaa199

5. Huang JT, Liu YJ, Wang J, Xu ZG, Yang Y, Shen F, et al. Next generation digital PCR measurement of hepatitis B virus copy number in formalin-fixed paraffin-embedded hepatocellular carcinoma tissue. *Clin Chem*. (2015) 61:290–6. doi: 10.1373/clinchem.2014.230227

6. Gupta RK, Abdul-Jawad S, McCoy LE, Mok HP, Peppa D, Salgado M, et al. HIV-1 remission following CCR5Delta32/Delta32 haematopoietic stem-cell transplantation. *Nature*. (2019) 568:244–8. doi: 10.1038/s41586-019-1027-4

7. Chen N, Zhou M, Dong X, Qu J, Gong F, Han Y, et al. Epidemiological and clinical characteristics of 99 cases of 2019 novel coronavirus pneumonia in Wuhan, China: a descriptive study. *Lancet*. (2020) 395:507–13. doi: 10.1016/S0140-6736(20)30211-7

8. Gutmann C, Takov K, Burnap SA, Singh B, Ali H, Theofilatos K, et al. SARS-CoV-2 RNAemia and proteomic trajectories inform prognostication in COVID-19 patients admitted to intensive care. *Nat Commun*. (2021) 12:3406. doi: 10.1038/s41467-021-23494-1

9. Hindson CM, Chevillet JR, Briggs HA, Gallichotte EN, Ruf IK, Hindson BJ, et al. Absolute quantification by droplet digital PCR versus analog real-time PCR. *Nat Methods*. (2013) 10:1003–5. doi: 10.1038/nmeth.2633

10. Choudhary ML, Vipat V, Jadhav S, Basu A, Cherian S, Abraham P, et al. Development of in vitro transcribed RNA as positive control for laboratory diagnosis of SARS-CoV-2 in India. *Indian J Med Res*. (2020) 151:251–4. doi: 10.4103/ijmr.IJMR_671_20

11. Ahmed W, Smith WJM, Metcalfe S, Jackson G, Choi PM, Morrison M, et al. Comparison of QQRT-PCR and RT-dPCR platforms for the trace detection of SARS-CoV-2 RNA in wastewater. *ACS ES T Water*. (2022) 2:1871–80. doi: 10.1021/acsestwater.1c00387

12. Tedim AP, Almansa R, Domínguez-Gil M, González-Rivera M, Micheloud D, Ryan P, et al. Comparison of real-time and droplet digital PCR to detect and quantify SARS-CoV-2 RNA in plasma. *Eur J Clin Investig*. (2021) 51:e13501. doi: 10.1111/eci.13501

13. Alteri C, Cento V, Antonello M, Colagrossi L, Merli M, Ughi N, et al. Detection and quantification of SARS-CoV-2 by droplet digital PCR in real-time PCR negative nasopharyngeal swabs from suspected COVID-19 patients. *PLoS One*. (2020) 15:e0236311. doi: 10.1371/journal.pone.0236311

14. Yu F, Yan L, Wang N, Yang S, Wang L, Tang Y, et al. Quantitative detection and viral load analysis of SARS-CoV-2 in infected patients. *Clin Infect Dis*. (2020) 71:793–8. doi: 10.1093/cid/ciaa345

15. Tran HN, Le GT, Nguyen DT, Juang RS, Rinklebe J, Bhatnagar A, et al. SARS-CoV-2 coronavirus in water and wastewater: a critical review about presence and concern. *Environ Res*. (2021) 193:110265. doi: 10.1016/j.envres.2020.110265

16. van Doremalen N, Bushmaker T, Morris DH, Holbrook MG, Gamble A, Williamson BN, et al. Aerosol and surface stability of SARS-CoV-2 as compared with SARS-CoV-1. *N Engl J Med*. (2020) 382:1564–7. doi: 10.1056/NEJMc2004973

17. Li X, Li J, Ge Q, Du Y, Li G, Li W, et al. Detecting SARS-CoV-2 in the breath of COVID-19 patients. *Front Med*. (2021) 8:604392. doi: 10.3389/fmed.2021.604392

18. Coleman KK, Tay DJW, Tan KS, Ong SWX, Than TS, Koh MH, et al. Viral load of SARS-CoV-2 in respiratory aerosols emitted by COVID-19 patients while breathing, talking, and singing. *Clin Infect Dis*. (2021) 74:1722–8. doi: 10.1093/CID/CIAB691

19. Edwards DA, Ausiello D, Salzman J, Devlin T, Langer R, Beddingfield BJ, et al. Exhaled aerosol increases with COVID-19 infection, age, and obesity. *Proc Natl Acad Sci U S A*. (2021) 118:e2021830118. doi: 10.1073/pnas.2021830118

20. Syed A, Khan A, Gosai F, Asif A, Dhillon S. Gastrointestinal pathophysiology of SARS-CoV2- a literature review. *J Community Hosp Intern Med Perspect*. (2020) 10:523–8. doi: 10.1080/20009666.2020.1811556

21. Vogelstein B, Kinzler KW. Digital PCR. *Proc Natl Acad Sci U S A*. (1999) 96:9236–41. doi: 10.1073/pnas.96.16.9236

22. Kuypers J, Jerome KR. Applications of digital PCR for clinical microbiology. *J Clin Microbiol*. (2017) 55:1621–8. doi: 10.1128/JCM.00211-17

23. Strain MC, Lada SM, Luong T, Rought SE, Gianella S, Terry VH, et al. Highly precise measurement of HIV DNA by droplet digital PCR. *PLoS One*. (2013) 8:e55943. doi: 10.1371/journal.pone.0055943

24. Sedlak RH, Cook L, Cheng A, Magaret A, Jerome KR. Clinical utility of droplet digital PCR for human cytomegalovirus. *J Clin Microbiol*. (2014) 52:2844–8. doi: 10.1128/JCM.00803-14

25. Sedlak RH, Cook L, Huang ML, Magaret A, Zerr DM, Boeckh M, et al. Identification of chromosomally integrated human herpesvirus 6 by droplet digital PCR. *Clin Chem*. (2014) 60:765–72. doi: 10.1373/clinchem.2013.217240

26. Suo T, Liu X, Feng J, Guo M, Hu W, Guo D, et al. ddPCR: a more accurate tool for SARS-CoV-2 detection in low viral load specimens. *Emerg Microbes Infect*. (2020) 9:1259–68. doi: 10.1080/22221751.2020.1772678

27. van Doorn AS, Meijer B, Frampton CMA, Barclay ML, de Boer NKH. Systematic review with meta-analysis: SARS-CoV-2 stool testing and the potential for faecal-oral transmission. *Aliment Pharmacol Ther*. (2020) 52:1276–88. doi: 10.1111/apt.16036

28. Liu X, Feng J, Zhang Q, Guo D, Zhang L, Suo T, et al. Analytical comparisons of SARS-COV-2 detection by qRT-PCR and ddPCR with multiple primer/probe sets. *Emerg Microbes Infect*. (2020) 9:1175–9. doi: 10.1080/22221751.2020.1772679

frontiers | Frontiers in Public Health

TYPE Original Research
PUBLISHED 30 June 2023
DOI 10.3389/fpubh.2023.1141097

OPEN ACCESS

EDITED BY
Charlene Ranadheera,
Public Health Agency of Canada (PHAC), Canada

REVIEWED BY
Vincenzo Marcotrigiano,
Azienda Sanitaria Locale BT Della Provincia di Barletta-Andria-Trani, Italy
Aarthy C. Vallur,
InBios International, United States
Madhvi Joshi,
Gujarat Biotechnology Research Centre (GBRC), India

*CORRESPONDENCE
Colleen C. Naughton
✉ cnaughton2@ucmerced.edu

RECEIVED 10 January 2023
ACCEPTED 08 June 2023
PUBLISHED 30 June 2023

CITATION
Kadonsky KF, Naughton CC, Susa M, Olson R, Singh GL, Daza-Torres ML, Montesinos-López JC, Garcia YE, Gafurova M, Gushgari A, Cosgrove J, White BJ, Boehm AB, Wolfe MK, Nuño M and Bischel HN (2023) Expansion of wastewater-based disease surveillance to improve health equity in California's Central Valley: sequential shifts in case-to-wastewater and hospitalization-to-wastewater ratios.
Front. Public Health 11:1141097.
doi: 10.3389/fpubh.2023.1141097

Expansion of wastewater-based disease surveillance to improve health equity in California's Central Valley: sequential shifts in case-to-wastewater and hospitalization-to-wastewater ratios

Krystin F. Kadonsky[1], Colleen C. Naughton[1]*, Mirjana Susa[2], Rachel Olson[3], Guadalupe L. Singh[1], Maria L. Daza-Torres[2], J. Cricelio Montesinos-López[2], Yury Elena Garcia[2], Maftuna Gafurova[4], Adam Gushgari[4], John Cosgrove[4], Bradley J. White[5], Alexandria B. Boehm[6], Marlene K. Wolfe[7], Miriam Nuño[2] and Heather N. Bischel[3]

[1]Department of Civil and Environmental Engineering, University of California, Merced, Merced, CA, United States, [2]Department of Public Health Sciences, University of California, Davis, Davis, CA, United States, [3]Department of Civil and Environmental Engineering, University of California, Davis, Davis, CA, United States, [4]Eurofins Environment Testing US, West Sacramento, CA, United States, [5]Verily Life Sciences, South San Francisco, CA, United States, [6]Department of Civil & Environmental Engineering, School of Engineering and Doerr School of Sustainability, Stanford University, Stanford, CA, United States, [7]Gangarosa Department of Environmental Health, Rollins School of Public Health, Emory University, Atlanta, GA, United States

Introduction: Over a third of the communities (39%) in the Central Valley of California, a richly diverse and important agricultural region, are classified as disadvantaged—with inadequate access to healthcare, lower socio-economic status, and higher exposure to air and water pollution. The majority of racial and ethnic minorities are also at higher risk of COVID-19 infection, hospitalization, and death according to the Centers for Disease Control and Prevention. Healthy Central Valley Together established a wastewater-based disease surveillance (WDS) program that aims to achieve greater health equity in the region through partnership with Central Valley communities and the Sewer Coronavirus Alert Network. WDS offers a cost-effective strategy to monitor trends in SARS-CoV-2 community infection rates.

Methods: In this study, we evaluated correlations between public health and wastewater data (represented as SARS-CoV-2 target gene copies normalized by pepper mild mottle virus target gene copies) collected for three Central Valley communities over two periods of COVID-19 infection waves between October 2021 and September 2022. Public health data included clinical case counts at county and sewershed scales as well as COVID-19 hospitalization and intensive care unit admissions. Lag-adjusted hospitalization:wastewater ratios were also evaluated as a retrospective metric of disease severity and corollary to hospitalization:case ratios.

Results: Consistent with other studies, strong correlations were found between wastewater and public health data. However, a significant reduction in case:wastewater ratios was observed for all three communities from the first to the second wave of infections, decreasing from an average of 4.7 $\pm$ 1.4 over the first infection wave to 0.8 $\pm$ 0.4 over the second.

Discussion: The decline in case:wastewater ratios was likely due to reduced clinical testing availability and test seeking behavior, highlighting how WDS can fill data gaps associated with under-reporting of cases. Overall, the hospitalization:wastewater ratios remained more stable through the two waves of infections, averaging 0.5 ± 0.3 and 0.3 ± 0.4 over the first and second waves, respectively.

KEYWORDS

SARS-CoV-2, COVID-19, environmental surveillance, wastewater clinical case ratios, health metrics

1. Introduction

California experienced approximately ten million infections and 100,000 deaths between January 2020 and December 2022 from the coronavirus disease (COVID-19) pandemic, caused by severe acute respiratory syndrome coronavirus 2 (SARS-CoV-2) (1). Individuals infected with SARS-CoV-2 often shed viral particles and associated ribonucleic acid (RNA) in their feces regardless of experiencing gastrointestinal symptoms (2). Fecal shedding dominates the total SARS-CoV-2 RNA load in community-level wastewater surveillance compared to other viral shedding routes such as respiratory fluids, saliva, and urine (3). The strong presence of SARS-CoV-2 RNA in wastewater settled solids allows for wastewater-based disease surveillance (WDS) to be utilized as a highly sensitive method to track the environmental persistence and community transmissivity of the virus (along with other highly infectious diseases) (4–6).

WDS involves collection of community-pooled samples of uninfected, asymptomatic, pre-symptomatic, and symptomatic infected individuals from centralized wastewater treatment plants (WWTPs), or, less often, from sewer collection systems (7). Traditional epidemiological monitoring through clinical surveillance is dependent upon infected individuals seeking clinical testing and the availability of clinical tests. WDS offers a less biased mechanism to track viral outbreaks and community infections and can serve as an early indicator of increased COVID-19 community transmission by detecting the virus before symptom onset (8).

Communities around the world rapidly implemented WDS early on in the pandemic. COVIDPoops19, a global ArcGIS dashboard, monitored the growth of WDS implementation since September 2020, including in California (9). Approximately 90% of California's population is serviced by publicly owned centralized WWTPs, with the remaining population serviced by onsite septic systems (10). As of August 2021, 48 of 384 WWTPs in California were monitoring for SARS-CoV-2 RNA in their communities. The majority of WDS programs (70%), at the time, were located in urban areas of Coastal and Southern California. Only 30% of WDS programs were located in rural areas of Central and Northern California (11). Most WWTPs in California are small or moderate in size (10), and more likely to lack the necessary resources and funding to support WDS programs.

Healthy Central Valley Together (HCVT) was launched in the summer of 2021 to expand WDS as a public health tool for greater health equity in rural and disadvantaged communities (DACs). The Central Valley is located in the heart of California, encompassing communities in nineteen counties (12). Over a third of the Central Valley communities (39%) are classified as DACs by CalEnviroScreen 4.0, compared to 31% of communities in California that are DACs overall (13). Approximately 40% of the population in the Central Valley are located within a DAC, compared to 29% of the overall population in California that live in a DAC (13). Of the 10 WDS programs located in California's DACs as of August 2021, one was in the Central Valley. The racial and ethnic demographics of DACs in the Central Valley are as follows: 43% Hispanic or Latino, 35% White, 12% Asian, 7% Black or African American, 2% American Indian and Alaska Native, and 1% Native Hawaiian and Other Pacific Islander (compared to the national averages: 19%, 59%, 6.1%, 14%, 1.3%, and 0.3%) (14).

As of September 2022, ethnic minorities (Hispanic or Latino, Asian, Black or African American, and American Indian or Alaska Native) all had higher risk of COVID-19 cases, hospitalizations, and deaths compared to White, Non-Hispanic persons according to the Centers for Disease Control and Prevention (CDC) (15). Moreover, from 2019–2021 the life expectancy decreased by 5.74 years for Hispanic or Latino, 3.84 years for Black or African American, 3.04 years for Asian, and 1.90 years among White, Non-Hispanic populations due to the COVID-19 pandemic in California (16). Historically, residents of the Central Valley have suffered from a disparity in health care access. Specifically, DACs in this region have access to 1.01 hospitals and medical centers on average per 100 k population while the state averages 2.55 hospitals and medical centers per 100 k population (14, 17). The Central Valley is predicted to experience an 18.7% shortage in primary care physicians by 2025 (18).

HCVT established and supports WDS in disadvantaged and rural communities in California's Central Valley through partnerships with local public health departments, wastewater municipalities, and analytical laboratory partners. HCVT is an extension of WDS implemented in Davis, California through Healthy Davis Together (HDT) (19, 20) in partnership with the Sewer Coronavirus Alert Network (SCAN) (21). WWTPs were selected from communities with high COVID-19 infection rates, below average vaccination rates (based on fully vaccinated individuals), and from public health department recommendations. The present study describes the initial phase of HCVT in three counties (Merced, Stanislaus, and Yolo). We compare temporal trends between SARS-CoV-2 RNA levels in wastewater settled solids and key health metrics collected in each region, and we report on an inter-laboratory comparison of wastewater settled solids analysis. Correlations amongst WDS and health metrics were

TABLE 1 Comparison of percent population fully vaccinated, cumulative cases per 100k population, and total number of hospitals and medical centers between Merced, Stanislaus, and Yolo Counties to statewide metrics from January 1st, 2021 to June 30th, 2021 (1, 17, 23, 24).

Health metrics in June 2021	Merced County	Stanislaus County	Yolo County	Statewide
Percent population fully vaccinated	35%	39%	55%	52%
Cumulative cases per 100 k population	3,859	3,599	2,267	3,015
Hospitals and medical centers	2	7	2	383

analyzed for two surges of COVID-19 infections in the region, the first caused by the Omicron BA.1 variant and the second attributed to the BA.2, BA.4, and BA.5 variants (22). We hypothesized that: (1) correlations between wastewater and health metric data in Central Valley communities would remain strong even with lower access to health resources such as clinical testing and hospitals, (2) changes in testing availability and test-seeking behaviors would lead to changes in case:wastewater ratios observed through time, and (3) hospitalization:wastewater ratios would be more stable through time than case:wastewater ratios.

2. Materials and methods

2.1. Partner engagement and facility onboarding

Merced and Stanislaus Counties were identified as counties of interest due to lower than state average vaccination rates (35% and 39%, respectively, compared to 52% statewide) as of June 2021 (Table 1) (1, 23). Yolo County was selected as a continuation of WDS launched in 2020 through the HDT and SCAN partnership. Vaccination rates by demographic for each county are shown in Supplementary Table S1. Public health departments were consulted to help determine cities for which WDS data would provide value for tracking COVID-19 burden within each county. Figure 1 displays the locations of partner WWTPs in Merced (southernmost location), Modesto (middle location), and Davis (northernmost location) as well as hospital and medical centers in each associated county (1, 17). The Davis WWTP in Yolo County served as an inter-laboratory control for two analytical laboratories used in this study (referred to as Lab 1 and Lab 2) from May through September 2022. Table 2 provides a summary of the sample type and collection frequency, approximate population served (provided by the WWTP), WWTP capacity (MGD), and percentage of industrial input for each treatment plant. Supplementary Table S2 displays city-level data for percent population fully vaccinated, cumulative cases per 100 k population, and total number of hospitals and medical centers (1, 17, 23, 24).

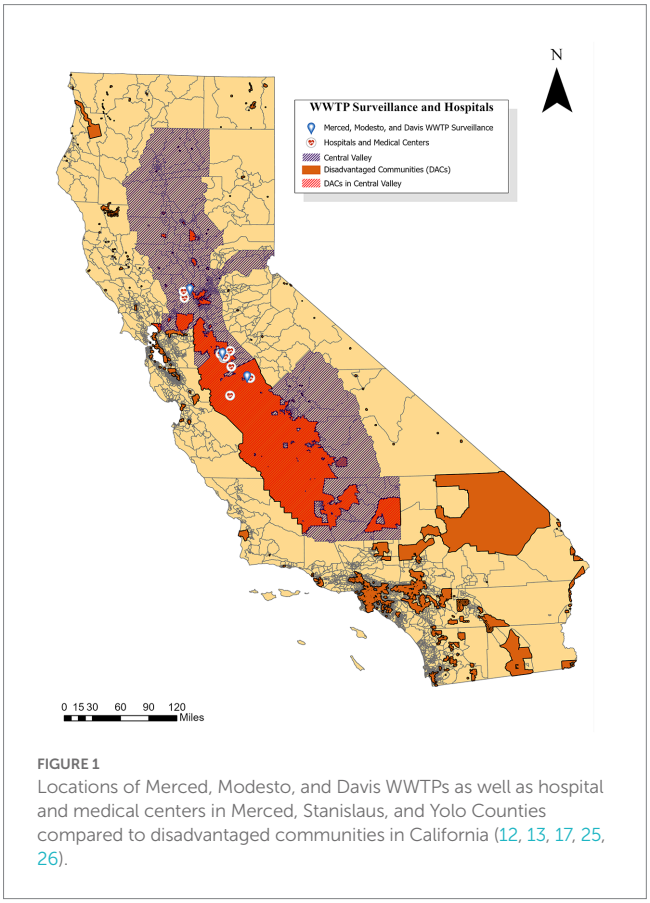

FIGURE 1
Locations of Merced, Modesto, and Davis WWTPs as well as hospital and medical centers in Merced, Stanislaus, and Yolo Counties compared to disadvantaged communities in California (12, 13, 17, 25, 26).

2.2. Sample collection and handling

This study used wastewater solids for wastewater monitoring. Viral nucleic acids and/or viral particles have been shown to preferentially adsorb to the solids in wastewater in a number of studies. Their concentrations in solids have been shown to be higher by three orders of magnitude compared to wastewater influent (27–32). Wastewater solids represent natural concentrators of viral nucleic-acids, and therefore a useful matrix for carrying out WDS. The study period occurred from October 20, 2021 through September 29, 2022.

2.2.1. Sample processing for lab 1

Samples were handled and processed by commercial partner Lab 1 for Merced and Modesto samples collected prior to May 1, 2022 and for samples collected for Davis throughout the entirety of the study period (Table 2). At each location, grab samples of settled solids processed by Lab 1 were collected 7 days per week directly from the primary clarifier sludge outlet. Methodology followed by Lab 1 for wastewater sample preparation, RNA extraction and droplet digital reverse transcriptase polymerase chain reaction (ddRT-PCR) are described in detail elsewhere (6, 33–35). In short, solids were dewatered using centrifugation and then suspended in a buffer, containing added bovine coronavirus (BCoV) vaccine at 10,000 copies/mL. The solids concentration in that solution was ~75 mg/mL. That solution was then homogenized using bead beating, and then centrifuged, and nucleic acids were extracted from the supernatant. All details for these and additional sample processing steps are precisely

TABLE 2 Characteristics of wastewater treatment plants (WWTPs) and primary clarifier sludge samples collected in this study.

Name of WWTP	Sample Type	Population served	WWTP capacity (MGD)	Industrial input (%)	Samples collected for Lab 1 (date range)	Samples collected for Lab 2 (date range)
Davis WWTP	Primary sludge	70,717	7.5	0	7 days per week (10/20/21–9/29/2022)	4–5 days per week (05/01/22–9/29/2022)
Merced WWTP	Primary sludge	91,000	12	12.5	7 days per week (10/20/21–4/30/2022)	4–5 days per week (05/01/22–9/29/2022)
Modesto WWTP	Primary sludge	230,000	19.1	51.3	7 days per week (10/20/21–4/30/2022)	4–5 days per week (05/01/22–9/29/2022)

provided in other peer-reviewed publications (6) and on protocols.io (33, 34), including the methods for determining the dry weight of solids.

The only modification of sample processing implemented by Lab 1 compared to published methods was a 10-fold dilution of extracts from the city of Modesto implemented from December 30, 2021 to May 1, 2022. Extract dilution was necessary to mitigate inhibition. BCoV was used as a process control and was greater than 10% in all samples. Supplementary Figure S1 shows box-and-whisker plots of the fractional recovery of BCoV. The centerline of the box represents the median value (1.05 for Lab 1). The lower detection limit using these methods is 500–1,000 copies/g dry weight solids for Merced and 5,000–10,000 copies/g dry weight for Modesto after the 1:10 template dilution. The exact value within the range depends on the dry weight of solids which varied.

2.2.2. Sample processing for lab 2

Samples were handled and processed by commercial partner Lab 2 for Merced and Modesto samples collected after May 1, 2022 and for duplicate samples from Davis also collected after May 1, 2022 for an inter-laboratory comparison (Table 2). Lab 2 closely followed the methodology and protocols developed and reported by Lab 1 (33, 36), with sample processing, RNA extraction, and ddRT-PCR methods and modifications detailed in this and the following sections. At each location, grab samples of settled solids for Lab 2 were collected 4 or 5 days per week directly from the primary clarifier sludge outlet in 250-mL HDPE bottles (Environmental Sampling Supply, San Leandro, CA). Reduction in sampling frequency to 4 or 5 days per week from daily allowed for the project to expand sampling to more sites in the region. Chan et al. (37) and Schoen et al. (38) found that a minimum sampling frequency of four or five samples per week was sufficient for acceptable trend analysis. Once collected, samples were immediately stored on ice and transported to Lab 2. If samples could not be immediately transported to the laboratory (i.e., due to weekend sample collection), samples were stored at 5°C on site until laboratory transportation. Samples were processed immediately upon arrival and all laboratory processes were completed within 24 h.

Settled solids samples were homogenized by inverting the HDPE bottle multiple times to mix, and a 50 mL aliquot was transferred to a 50 mL conical tube. Settled solids were dewatered by centrifugation at 24,000 × g for 30 min at 4°C. A stock solution of BCoV (BCoV, Calf-Guard Cattle Vaccine, PBS Animal Health) in DNA/RNA Shield (Zymo Research Corporation, Irvine, CA) was prepared at a concentration of 500,000 genome copies/mL. For samples processed prior to July 29, 2022, four or five aliquots of approximately 75 mg of dewatered solids were transferred into new 50 mL conical tubes, weighed, and an appropriate amount of the BCoV solution was pipetted into each tube to achieve 1 mL DNA/RNA shield per 75 mg dewatered solids. For samples processed from July 29, 2022 onwards, a single 750 mg aliquot of dewatered solids was diluted to the same final ratio of DNA/RNA shield to settled solids mass.

RNA was extracted from dewatered solids using the MagMAX™ Microbiome Ultra Nucleic Acid Isolation Kit (Applied Biosystems by Thermo Fisher Scientific) following manufacturer protocols (Pub. No. MAN0018071 Rev. C.0). This protocol deviates from the published methods from Lab 1 by use of KingFisher Flex in place of the Perkin Elmer Chemagic 360. Positive extraction controls (BCoV spike, SARS-CoV-2 genomic RNA: ATCC VR-1986D™ and PolyA: Roche 10108626001) and negative extraction controls (nuclease-free water) were included to check for process validity and to ensure no contamination. RNA extraction was immediately followed by PCR inhibitor removal using the Zymo™ OneStep-96 PCR Inhibitor Removal Kit (Zymo Research Corporation, Irvine, CA) following manufacturer protocols, with minor modifications. In the sample preparation stage, silicone plates were prepared by centrifuging for 10 min at 2576 g. After samples were added, the plates were spun again for 6 minutes at 2576 g. The RNA extracts were stored on ice for same-day ddRT-PCR reactions and transferred to −80°C for long-term storage. The median fractional recovery of BCoV was 0.96 for Lab 2 (Supplementary Figure S1).

2.3. Digital droplet reverse transcriptase PCR (ddRT-PCR)

The following assays were performed to quantify total SARS-CoV-2 concentrations in wastewater samples: N-gene, BCoV, and pepper mild mottle virus (PMMoV). The design and validation of these assays are described by Wolfe et al. (35) and Topol et al. (34). ddRT-PCR protocols implemented by Lab 1 are described in the preceding references. PMMoV is abundant in human fecal matter and its quantified measurements are used to normalize observed SARS-CoV-2 gene target quantitative measurements (6, 39).

The following information describes methods implemented by Lab 2. Primers and probes were purchased from Integrated DNA Technologies (IDT[1]) and positive controls were purchased from American Type Culture Collection (ATCC), Twist Biosciences and IDT. N-gene was run as a triplex assay along with a SARS-CoV-2 S-gene target and an additional variant-specific mutation target (data not included in this analysis). BCoV and PMMoV were run as a duplex assay. ddRT-PCR was performed in 22.5 µL reaction volumes which included 5.5 µL template, 5.5 µL ddPCR

1 https://www.idtdna.com

One-Step RT-ddPCR Advanced Kit for Probes (1,864,021, Bio-Rad, Hercules, CA), 2.2 µL reverse transcriptase, and 1.1 µL 300 mM dithiothreitol (DTT). Duplex assays included 2.2 µL primer probe mix and 5.5 µL nuclease-free water. Triplex assays included 3.3 µL primer probe mix and 4.4 µL nuclease-free water. The final concentration of primers and probes in the reactions was 900 nM and 250 nM, respectively (35). Reactions were performed in sets of four replicates for samples collected between May 2, 2022 and May 29, 2022, and subsequently performed in sets of five replicates from May 30, 2022 forward.

Droplets were generated using the AutoDG automated droplet generator from Bio-Rad. PCR was performed on the C1000 Touch Thermal Cycler (Bio-Rad): the cycling conditions were reverse transcription at 50°C for 60 min, enzyme activation at 95°C for 10 min, followed by 40 two-step cycles of denaturation at 94°C for 30 s and anneal/extension at 58°C (for SARS-CoV-2, PMMoV, and BCoV targets) for 1 min. This was followed by enzyme deactivation at 98°C for 10 min, droplet stabilization at 4°C for 30 min, and indefinite hold at 4°C. Droplets were analyzed using the QX200 droplet reader from Bio-Rad. Thresholding was performed on QX Manager (Bio-Rad: QX Manager Software Regulatory Edition Version 1.2) (6). Concentrations of assay targets were calculated as copies per gram of dry weight, details of which are described by Wolfe et al. (35). Calculation of the limit of detection for the ddRT-PCR assay implemented by Lab 2 followed protocols recommended by Bio-Rad Laboratories and with further details are included in the supplementary information (Supplementary Table S3) (35, 40).

2.4. County health metrics

California county clinical data for Merced, Stanislaus, and Yolo Counties from October 20, 2021 to September 29, 2022 were downloaded from the Official California State Government website which provided the COVID-19 data from the California Health & Human Services Agency (CHHS). The data accessed included fully vaccinated individuals, hospitalization, and county cases. Fully vaccinated data are defined as follows: "2 Pfizer doses > = 17 days apart, 2 Moderna doses > = 24 days apart, 1 dose of J&J, a combination of Pfizer and Moderna doses > = 17 days apart, three or more vaccination records, or only one dose in IRIS labeled as dose number 2" (23).

Hospitalization data used for this analysis included COVID-19 confirmed patients and ICU COVID-19 confirmed patients. The hospitalized COVID-19 confirmed patients are identified as all inpatients, in ICUs and Medical/Surgical units, with laboratory-confirmed COVID-19 results (excluding patients in affiliated clinics, outpatient departments, emergency departments, and overflow locations awaiting an inpatient bed) (41). The ICU COVID-19 confirmed patients are defined as patients in the ICU at the hospital with a laboratory confirmed positive COVID-19 result which includes neonatal intensive care unit (NICU), pediatric intensive care unit (PICU), and adult (41). Hospitalized and ICU patient data are reported based on the county and zip code the hospital is located in, and does not include the county or zip code of residence for each individual patient. To capture as accurately as possible the number of facilities only housing COVID-19 inpatients, the hospital and medical center data used to calculate the number of hospitals and medical centers in each county excludes rehabilitation centers and specialty hospitals. The hospitalization data is dependent upon the number of hospital beds per inpatient facility, and this was not accounted for in the analysis (42).

County case numbers are defined as laboratory-confirmed COVID-19 cases at dates determined by the date of symptom onset, and represent the county of residence for each case (24). Percentage of positive cases in a population were calculated by dividing the number of positive cases from the data by the population count provided by Merced County (population of 287,420), Stanislaus County (population of 562,303), and Yolo County (223,612). The population values in the data collected were taken from the California Department of Finance (DOF) estimates for January 2022 (23, 24, 41). The data for the number of hospitals and medical centers in each county were collected from CHHS and DOF (17). For additional information on how categories were defined, see the data dictionary for individual data sets provided in reference material (23, 24, 41).

2.5. Statistical analysis

A 10-day moving average was applied (the mean of the current day and the previous 9 days) to wastewater data to reduce uncertainty and minimize daily fluctuations of the normalized N gene metric. The cases, hospitalization, and ICU in each figure represent the 7-day moving average at the county-level per 100 k population, accessed from the CHHS dataset (17).

It is expected that a patient who is hospitalized will likely be admitted several days after a confirmed COVID-19 diagnosis or the onset of viremia. Therefore, the number of hospitalizations reported on a specific day will lag cases reported and wastewater data. A correlation analysis was performed with the smoothed data to find the lag between wastewater and each of the metrics analyzed (cases, hospitalizations, and ICU). The lag that provided the highest correlation between these metrics and the wastewater data using a grid search was chosen (Supplementary Table S4). Analyses were carried out for the time period of Wave 1, specified for each county, using the R function "cor" to determine the Pearson correlation between county cases, ICU patients, hospitalizations, and wastewater data.

A Pearson correlation coefficient (r) and line of best fit (linear regression, R^2) was calculated and analyzed between health metrics (county-level hospitalization, county-level ICU confirmed patients, county-case data, and the California Department of Public Health provided sewershed case data) and WDS data (the normalized N-gene/PMMoV unitless metric and the non-normalized N-gene concentration in gene copies per gram dry weight). The statistical analysis was conducted between seven different time periods: entire sample collection, Wave 1, Peak 1, Wave 2, Peak 2, and Lab 1 and Lab 2 sample collection periods. The start and end dates for each "wave" (Table 3)

TABLE 3 Time periods for COVID-19 Central Valley wastewater statistical analysis.

Treatment plant	Analysis period	Start	Peak	End
All	Full Sampling Period	10/20/2021		09/29/2022
Merced	Wave 1	12/19/2021	01/17/2021	03/08/2022
	Wave 2	05/02/2022	07/14/2022	09/29/2022
Modesto	Wave 1	12/28/2021	01/23/2022	02/26/2022
	Wave 2	05/14/2022	07/13/2022	09/29/2022
Davis	Wave 1	12/19/2021	01/09/2022	03/15/2022
	Wave 2	04/27/2022	06/24/2022	09/29/2022

were defined by visually identifying surges in infections for each city and selecting boundaries for the minimum wastewater concentrations surrounding a given "peak." Each "peak" date corresponded to the local maximum N/PMMoV from the 10-day moving average. Correlations assessed for waves included data from the start to end dates indicated for each city. Correlations assessed for peaks used data between the start date and peak date within each wave. Rates of full vaccination were also compiled for each analysis period (Table 4).

2.6. Limitations

We note several limitations of this study. First, wastewater surveillance data at the sewershed or city-level was compared to health metrics at the county-level. The wastewater data from one city may not be representative of that county. We selected the largest population centers in each county (Modesto population ~ 230,000, Merced ~ 90,000, and Davis ~ 70,000) to help mitigate this concern. Second, case data and wastewater data are subject to different sources of variability and bias. For instance, case data captures the population with access to healthcare testing and/or infected individual seeking healthcare, while wastewater data is not subject to this bias. Wastewater concentrations are dependent upon fecal shedding of SARS-CoV-2 RNA, and fecal shedding rates are variable per infected individual, while case counts are less impacted by this variability. Third, hospitalization and ICU data is based on individuals admitted and not separated by county of residence. Therefore, individuals seeking care from other counties may result in an overcount of cases in the county with the hospital and an undercount in their county of residence. Our study used the CHHS database, which receives data from the California Hospital Association and reports based on the county of hospitalization (41). Nevertheless, when the patient is at a hospital, they will be shedding SARS-CoV-2 in feces collected by the local treatment plant, which is not necessarily the same WWTP for their residence.

3. Results

3.1. Trends in health metrics over the study period

Merced, Stanislaus, and Yolo County health metric data are co-plotted with 10-day moving averages of N-gene/PMMoV wastewater concentrations from November 1, 2021 to September 29, 2022 for the corresponding WWTP monitored in each county (Figures 2–4). Supplementary Figure S2 includes the Davis data for only Lab 1. Wastewater data collected from each treatment plant captured two distinct waves of infections. The first wave of infections during the study period occurred from approximately December 2021 to March 2022 (referred to herein as Wave 1), and corresponds to a surge in infections predominantly from the Omicron BA.1 variant in the region (43). The second wave of infections during the study period occurred from April 2022 to September 2022 (referred to herein as Wave 2), and corresponds to the surge in infections predominantly from the BA.2, BA.4, and BA.5 variants in the region (43).

Throughout Wave 1, Yolo County exhibited a somewhat greater number of cases, but lower levels in ICU patients and hospitalizations, compared to Merced and Stanislaus Counties. Stanislaus County experienced higher hospitalizations and ICU patients, and similar county case counts, compared to Merced County. The local maxima of N/PMMoV determined by Lab 1 for Wave 1 were similar amongst the three treatment facilities (0.00043 for Merced, 0.00047 for Modesto, and 0.00043 for Davis). In Wave 2, there were much fewer cases, hospitalization, and ICU patients in all three counties. Wastewater levels also declined overall for both Merced and Modesto in Wave 2 compared to Wave 1. However, the local maximum of N/PMMoV for Davis increased for Wave 2 compared to Wave 1.

For visualization of correlations amongst health and wastewater data, hospitalizations and ICU patient counts are shifted in Figures 2–4 by the lag period identified to maximize correlations with wastewater data. For Merced County, hospitalizations exhibited a 14-day lag and a 9-day lag for ICU patients. In Stanislaus County, a 10-day lag in hospitalizations and a 15-day lag for ICU patients was identified compared to the wastewater data. Yolo County exhibited a 14-day lag for hospitalizations, and a 15-day lag for ICU patients compared to the wastewater data. There was no lead or lag identified for wastewater data compared to clinical case data reported by the date of symptom onset.

3.2. Inter-laboratory comparison for analysis of settled solids

Wastewater settled solids samples collected by Davis during Wave 2 were processed by both Lab 1 and Lab 2 using highly similar analytical methods (modifications of Lab 1 methods that were implemented by Lab 2 are detailed in the methods). N/PMMoV data from the two labs were strongly correlated, with a near 1:1 linear relationship (Figure 5). Lab 2 results yielded somewhat lower concentrations of both N and PMMoV gene copies compared to Lab 1, and similar recovery of BCoV (Supplementary Figures S1, S3-S7). Reporting the normalized statistic (N/PMMoV) helps correct for laboratory variations by using PMMoV as an internal process control (44). The N/PMMoV results determined by Lab 2 were somewhat higher on average than corresponding measurements by Lab 1 (Figure 5). Results indicate overall agreement

TABLE 4 Percent of the population fully vaccinated across all three counties at the start and end of Waves 1 and 2 with the percent increase in vaccination after each wave (23).

Estimated Wave time periods	Start Wave 1 (11/30/21)	End Wave 1 (03/01/22)	Percent change Wave 1	Start Wave 2 (04/05/22)	End Wave 2 (09/27/22)	Percent change Wave 2
Merced	48%	53%	10%	53%	55%	2.8%
Stanislaus	52%	56%	7.6%	57%	58%	2.2%
Yolo	65%	71%	7.8%	71%	73%	2.2%

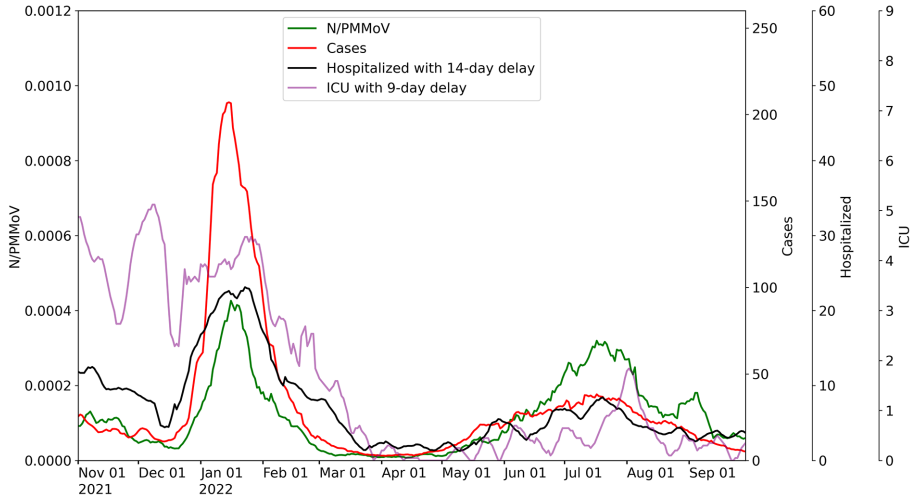

FIGURE 2
City of Merced wastewater concentrations for 10-day average for N/PMMoV compared to weekly average of Merced County cases per 100k population, weekly average county hospitalizations with 14-day lag, and weekly average county ICU patients with 9-day lag.

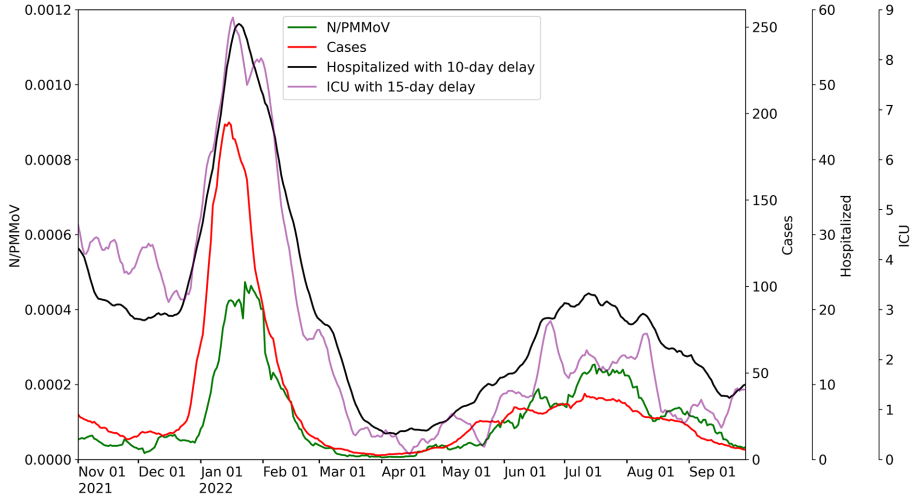

FIGURE 3
City of Modesto wastewater concentrations for 10-day average for N/PMMoV compared to weekly average of Stanislaus County cases per 100k population, weekly average county hospitalizations with 10-day lag, and weekly average county ICU patients with 15-day lag.

in trends observed during Wave 2 and demonstrate similar correlations with the health metric data acquired (Figure 6).

3.3. Relationships between wastewater and health metric data for successive surges

From visual inspection of Figures 2–4, it is apparent that the relative magnitudes of wastewater results compared to the health metric data changed from Wave 1 to Wave 2. The relationships between the wastewater data and health metric data were thus assessed: (1) over the full study period, (2) for each full wave of infection separately, and (3) using only data on the run-up to each maxima for Wave 1 and Wave 2 (referred to herein as Peak 1 and Peak 2, respectively). Correlations between wastewater data and health metric data were evaluated using linear regressions. Correlations were assessed separately at the county-level and within each WWTP sewershed. The Pearson correlation coefficient (r), lag-time delay, and analysis periods for each county for each analysis period are available in Supplementary Table S5. Lines of best fit (coefficient of determination, R^2) between wastewater data and health metric data for each wave of infection are displayed in Figures 6–8. Figures 9–11 show the relationships between N/PMMoV to county and sewershed cases for Peak 1 and 2 (including only data leading up to the maxima of each wave of infection). Correlation plots for wastewater to hospitalization and ICU patient data are in Supplementary Figures S8–S19.

As expected from visual inspection, correlations between health metrics and wastewater data were stronger overall within each wave of infection compared to data assessed over the full study period. The

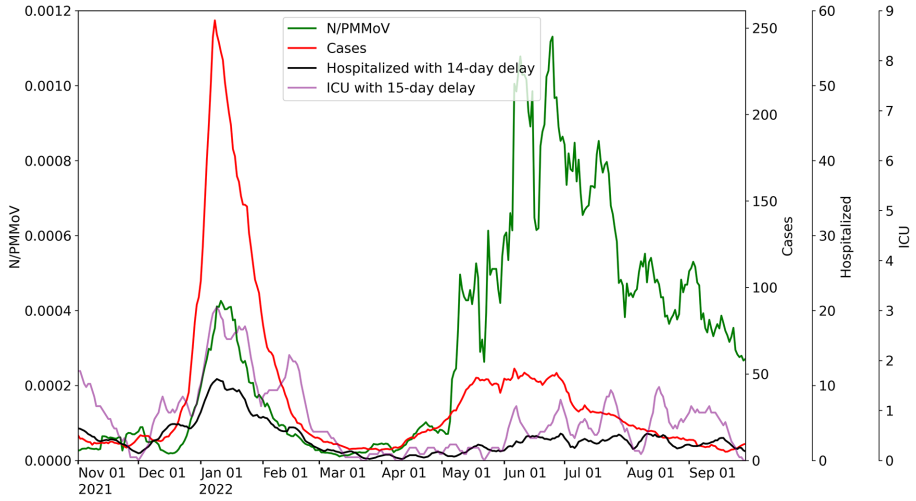

FIGURE 4
City of Davis wastewater concentrations for 10-day average for N/PMMoV compared to weekly average of Yolo County cases per 100k population, weekly average county hospitalizations with 14-day lag, and weekly average county ICU patients with 15-day lag.

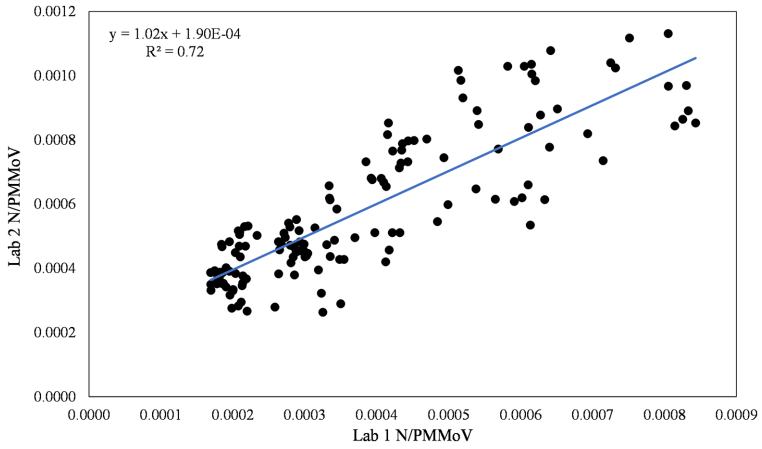

FIGURE 5
Inter-lab comparison of N/PMMoV between Lab 1 and Lab 2 for the city of Davis.

strongest correlations observed were between wastewater data and case data compiled at either the county or sewershed scale. The slopes of the linear relationships for each infection wave were used to determine case:wastewater, hospitalization:wastewater, and ICU:wastewater ratios (Supplementary Table S5, Figures S8–S19). The health metric:wastewater ratios decreased for all counties from Wave 1 to Wave 2 (by 14 to 94%), with the most significant declines generally observed for case:wastewater ratios.

R^2 values displayed in Figures 6–11 exhibit the percentage variation in y values that is explained by x, signifying the variability between each parameter. Notably for Modesto, lower correlation coefficients (and high variability) within Wave 1 (Figure 8) and high correlation coefficients (low variability) within Peak 1 (Figure 10) signified that wastewater and health metric data increased together, but the metrics were more decoupled on the decline from a peak. Since the slope impacts R^2 values, systematic declines in the coefficient of determination from Wave 1 to Wave 2 are largely statistical artifacts as the slope deviated further from 1:1. The relationships between N/PMMoV to county and sewershed cases are also represented in Supplementary Table S5 through the Pearson correlation coefficient (r), the degree of relationship between the two parameters. The Pearson r between wastewater data and health data were generally high, demonstrating strong relationships between health metric and wastewater data (Supplementary Table S5).

4. Discussion

Case:wastewater ratios (regression slopes) consistently declined for all three counties from the first surge in infections observed in this study to the second. The average case:wastewater ratio of 4.7 ± 1.4 over the first wave (calculated using county case data) declined to 0.8 ± 0.4 over the second wave. Factors that may lead to systematic

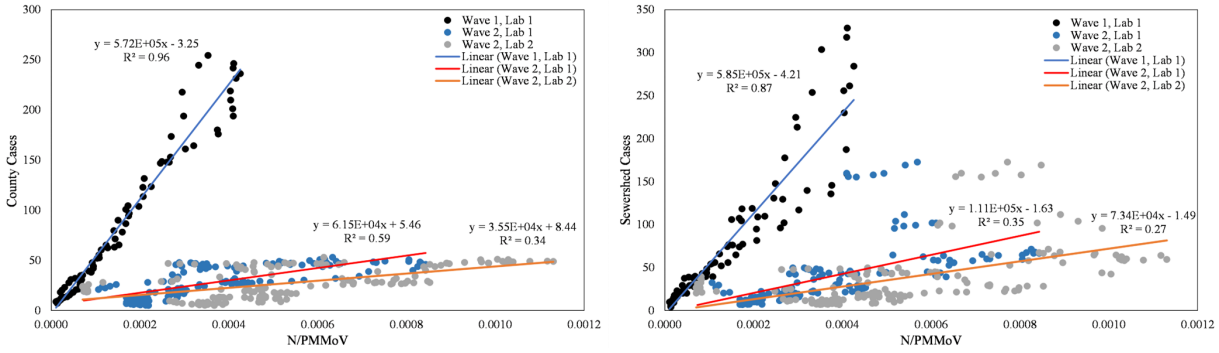

FIGURE 6
City of Davis N/PMMoV vs. Yolo County cases per 100k population (left) and city of Davis N/PMMoV vs. sewershed cases per 100k population (right) between Wave 1 (all Lab 1) and Wave 2 (Lab 1 and Lab 2 separate).

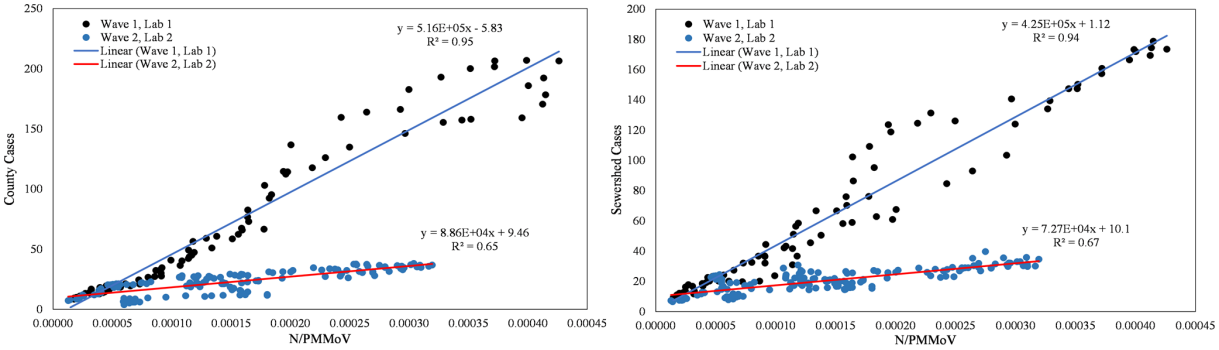

FIGURE 7
City of Merced N/PMMoV vs. Merced County cases per 100k population (left) and city of Merced N/PMMoV vs. sewershed cases per 100k population (right) between Wave 1 (Lab 1) and Wave 2 (Lab 2).

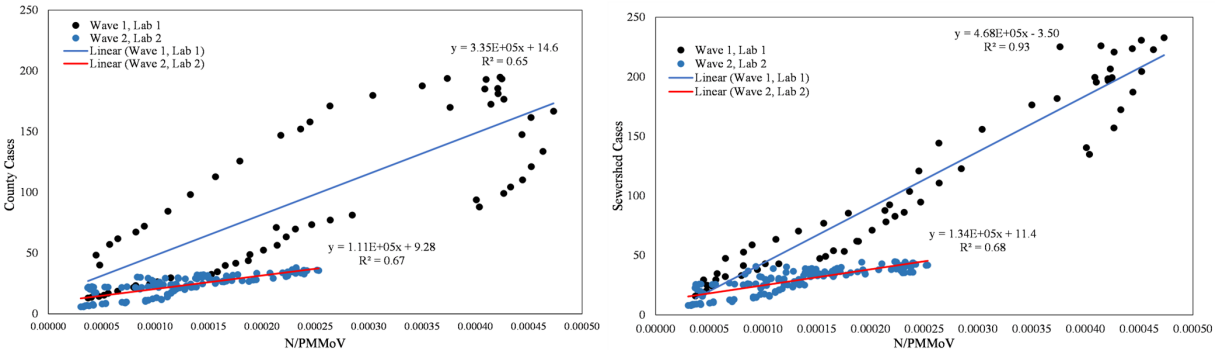

FIGURE 8
City of Modesto N/PMMoV vs. Stanislaus County cases per 100k population (left) and city of Modesto N/PMMoV vs. sewershed cases per 100k population (right) between Wave 1 (Lab 1) and Wave 2 (Lab 2).

declines in case:wastewater ratios include: (1) reduced clinical testing availability and/or participation, (2) replacement of clinical tests by increased use of at-home tests, for which data are not reported to public health officials (45), and (3) changes in the duration or magnitude of fecal shedding (e.g., due to increased rates of vaccination, acquired immunity, new variants, etc.), although little information is available to quantitatively assess this factor (46). Of these factors, we suspect that an increased use of at-home tests and/or changes in test-seeking behavior were especially strong drivers for the declines observed in case:wastewater ratios. While the number of at-home tests conducted in lieu of clinical tests cannot be discerned, discussions with HCVT public health partners affirmed this change

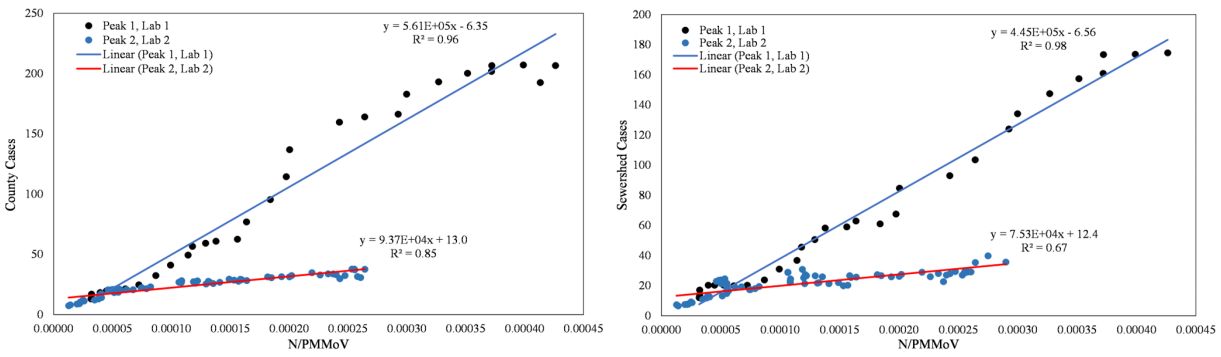

FIGURE 9
City of Merced N/PMMoV vs. Merced County cases per 100k population (left) and city of Merced N/PMMoV vs. sewershed cases per 100k population (right) between Peak 1 (Lab 1) and Peak 2 (Lab 2).

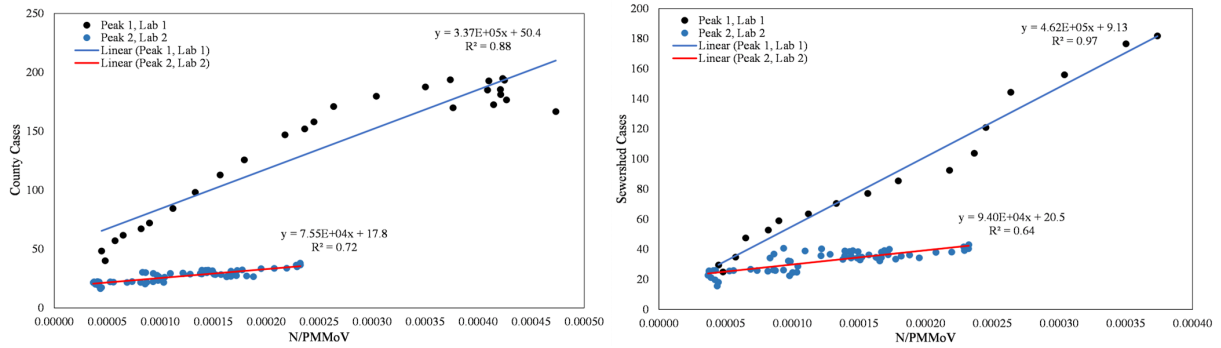

FIGURE 10
City of Modesto N/PMMoV vs. Stanislaus County cases per 100k population (left) and city of Modesto N/PMMoV vs. sewershed cases per 100k population (right) between Peak 1 (Lab 1) and Peak 2 (Lab 2).

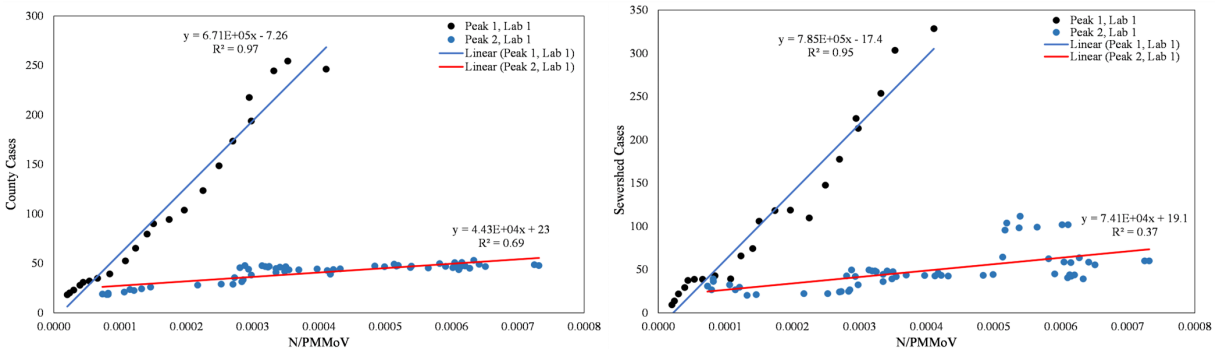

FIGURE 11
City of Davis N/PMMoV vs. Yolo County cases per 100k population (left) and city of Davis N/PMMoV vs. sewershed cases per 100k population (right) between Peak 1 (Lab 1) and Peak 2 (Lab 2).

in testing behaviors over the study period. More information is needed to fully assess the contribution of fecal shedding dynamics towards changes in case:wastewater ratios through time.

Unlike the case:wastewater ratios, the hospitalization:wastewater ratios and ICU:wastewater ratios (adjusted for lags) remained relatively more stable over the two surges in infections monitored in both Merced and Stanislaus counties. The average hospitalization:wastewater ratio was 0.5 ± 0.3 over the first wave and 0.3 ± 0.4 over the second wave. Hospitalizations are known to be a more reliable indicator of severity of infections and, like wastewater

data, are less susceptible to individual choice than test-seeking behaviors. However, hospitalization data within each county is less likely than clinical testing data to be geographically aligned with wastewater data, as patients commonly receive hospital services outside of their residential or workplace jurisdictions. Notwithstanding challenges associated with geographic alignment of wastewater and hospitalization data, the hospitalization:wastewater ratio may be a useful retrospective metric to assess disease severity of an illness, especially when reduced reporting of cases compromises the accuracy of case counts. Wastewater measurements capture information from asymptomatic, mild, and moderate cases, filling data gaps that lead to overestimated hospitalization:case ratios when such cases are counted inaccurately (47).

Three notable differences were observed for Yolo County compared to Merced and Stanislaus Counties. First, a greater number of cases were counted in Yolo County in Wave 1 compared to Merced and Stanislaus Counties. From November 2020 through June 2022, Yolo County and the city of Davis offered community-wide, free clinical testing services through Healthy Yolo Together (HYT) and HDT (19). Participation in each program was high, even for asymptomatic individuals, leading to more comprehensive case counts. Retrospective assessments demonstrated the efficacy of the programs at reducing transmission in the county. The timing of the second infection wave corresponded to the end of the HDT and HYT testing programs (June 30, 2022). The change in programming resulted in dramatic reductions in clinical tests performed in Yolo County.

Second, Yolo County exhibited higher vaccination rates overall. Sixty-five percent of Yolo County was fully vaccinated at the start of the Omicron wave compared to Merced (48%) and Stanislaus (52%) Counties (Table 4). Vaccination rates had increased in each county by 7.8%, 10%, and 7.6% in Yolo, Merced, and Stanislaus Counties, respectively, by the end of the estimated first wave of infections (March 1, 2022).

Third, the hospitalization rates were lower in Yolo County compared to Merced and Stanislaus Counties. On average during the first wave of infections, there were approximately 5 hospitalizations per 100 k population in Yolo County, compared to approximately 15 in Merced County and 41 in Stanislaus County. The approximate average number of ICU admittance per 100 k population for the first wave were more similar amongst the counties, but still lowest in Yolo County (2 in Yolo, 3 in Merced, and 6 in Stanislaus). Hospitalizations and ICU admittance declined in all three counties during Wave 2 compared to Wave 1, with Yolo County maintaining lower rates than Merced and Stanislaus (Supplementary Table S6). Higher vaccination rates in Yolo County for 65+ populations (Supplementary Table S7) may have contributed to the lower ICU admittance and hospitalizations (Supplementary Table S6) observed for Yolo County compared to Merced and Stanislaus Counties. Approximately 93% of the 65+ population in Yolo County was fully vaccinated at the start of the first Omicron wave compared to 78% in Merced, and 83% in Stanislaus Counties.

The results from this study correspond well with other wastewater solids analysis in other locations. Wolfe et al. (6), found strong correlations between SARS-CoV-2 RNA wastewater settled solids concentrations and COVID-19 sewershed cases in eight publicly owned, Northern Californian treatment works from December 2020–March 2021. Wolfe et al. (21) further expanded their analysis to treatment plants in New York and Illinois, and still found strong correlations with COVID-19 cases. The waves of infection captured in our study also have similar timing to the decline in the BA.1 variant in March and emergence of BA.2 in another Californian wastewater solids study (48). Outside of the United States, Hegazy et al. (49) analyzed composite primary clarifier sludge from two treatment plants in Ontario, Canada. They found strong correlations to COVID-19 case rates during the Omicron BA.1 surge (49). Hegazy et al. (49) observed poorer correlations between wastewater data and COVID-19 cases during the Delta wave (July–December 2021), potentially due to higher immunity from vaccinations and prior infection. These findings were similar to the decrease in COVID-19 case correlations observed in Wave 2 (BA.2, BA.4, BA.5) in our study, alongside corresponding increases in vaccinations, boosters, and acquired immunity. Another wastewater solids study that included seven Canadian cities reported changing wastewater to clinical case ratios for different "waves" or dominant variants during the pandemic (50). Similar to our results, Hegazy et al. (49) observed strong correlations with hospitalizations and ICU admissions.

Analysis of wastewater data against health metric data compiled at both the county and city scales offers one strategy to assess population mobility and regional reporting. Wastewater data collected is inherently place-based, while health metrics may be reported in other regions depending on place of residency, place of work, and access to medical centers and hospitals, amongst a myriad of factors. Public health authorities partnered with the HCVT project offered Merced County as one example whereby the closest medical center for residents located in the northern part of the county lies across the county border in Stanislaus County. Further evaluation of wastewater data collected from additional cities across each county is likely to provide insights into disease dynamics across the rural and agricultural communities characteristic of the Central Valley. Integration of wastewater data at regional scales and use of the CalREDIE database (51, 52) for hospitalizations based on county of residence may also offer more representative hospitalization:wastewater ratios when using data from hospitals that serve populations traveling from sewersheds in multiple counties. The California Department of Public Health (CDPH), for instance, assesses population-weighted wastewater data for five public health regions (53) in the state, complementing wastewater data reported at the county and sewershed scales from the CDPH wastewater surveillance network (54).

WDS provides vital public health information to communities by filling gaps in public health data that result from reductions in clinical testing availability, test-seeking behavior, and reporting of test results. WDS data is critical to public health decision-makers in regions where access to and/or utilization of public health resources is inadequate. The HCVT project applied a health equity framework in the selection and implementation of new WDS sites, prioritizing underrepresented regions in California that also exhibited relatively lower vaccination rates, and where higher proportions of the population are identified as disadvantaged. This study demonstrated that WDS still has high correlations with health metric data in areas with lower health care access and reporting. HCVT had open communication on WDS data with public health departments, wastewater treatment plant staff, and city officials from Merced, Stanislaus, and Yolo Counties through weekly email updates, a public website, and bi-weekly meetings throughout the duration of the project. From this communication, public health departments informed local hospitals and skilled nursing facilities of increasing and decreasing wastewater levels. As WDS programs become

further integrated into long-term public health decision-making criteria, a critical assessment of WDS using equity metrics should be considered (e.g., evaluating proportional access to WDS data based on racial and ethnic demographics, disadvantaged community status, and access to public health resources). Integration of equity-based WDS program criteria into public health policies will help support initiatives for greater health equity.

Data availability statement

The datasets analyzed for this study can be found in the Dryad Digital Repository: https://doi.org/10.6071/M3168G.

Ethics statement

The studies involving human participants were reviewed and approved by University of California, Davis and Stanford University. Written informed consent for participation was not required for this study in accordance with the national legislation and the institutional requirements.

Author contributions

KK, CN, and HB: contributed to conception and design of the study. KK, CN, GS, MS, RO, MG, AG, JC, BW, AB, MW, and HB: managed and implemented wastewater sample analysis, data collection and sharing, and quality assurance/quality control. KK and GS: contributed to collecting the health metric data for the data analysis of this project and organized the database from each data source. KK, MD-T, JM-L, YG and MN: performed the statistical analysis. CN, HB, MN, AB, MW, MD-T, and JM-L: reviewed each iteration of the manuscript and provided feedback. KK: assembled and wrote much of the first draft of the manuscript and addressed revision comments. KK, CN, HB, RO, GS, MD-T, MG, AG, and JM-L: wrote sections of the manuscript. KK, MD-T, JM-L, RO, and HB: provided tables and figures. RO, AG, and HB: provided equations. All authors contributed to the article and approved the submitted version.

Funding

The analyses conducted through SCAN were supported by a gift from the CDC-Foundation to AB. Additional research support for HCVT was provided through a philanthropic gift to the University of California, Davis.

Acknowledgments

This work and research would not be possible without our wastewater treatment plant (Merced, Modesto, and Davis) and public health partners (Merced County Department of Public Health, Stanislaus County Department of Public Health, Yolo County Department of Public Health, and California Department of Public Health). We also thank the staff of our commercial lab partners.

Conflict of interest

MG, AG, and JC are employed by Eurofins Environment Testing US. BW is employed by Verily Life Sciences.

The remaining authors declare that the research was conducted in the absence of any commercial or financial relationships that could be construed as a potential conflict of interest.

Publisher's note

Supplementary material

The Supplementary material for this article can be found online at: https://www.frontiersin.org/articles/10.3389/fpubh.2023.1141097/full#supplementary-material

References

1. California State Government. (2022). Tracking COVID-19 in California. Available at: https://covid19.ca.gov/state-dashboard/ (Accessed November 7, 2022).

2. Cheung KS, Hung IFN, Chan PPY, Chan K-H, Yuen K-Y, Leung WK. Gastrointestinal manifestations of SARS-CoV-2 infection and virus load in fecal samples from a Hong Kong cohort: systematic review and Meta-analysis. *Gastroenterology*. (2020) 159:81–95. doi: 10.1053/j.gastro.2020.03.065

3. Crank K, Chen W, Bivins A, Lowry S, Bibby K. Contribution of SARS-CoV-2 RNA shedding routes to RNA loads in wastewater. *Sci Total Environ*. (2021) 806:150376. doi: 10.1016/j.scitotenv.2021.150376

4. Boehm AB, Hughes B, Doung D, Chan-Herur V, Buchman A, Wolfe MK, et al. Wastewater concentrations of human influenza, metapneumovirus, parainfluenza, respiratory syncytial virus, rhinovirus, and seasonal coronavirus nucleic-acids during the COVID-19 pandemic: a surveillance study. *The Lancet Microbe*. (2023) 4:E340–48. doi: 10.1101/2022.09.22.22280218

5. Peccia J, Zulli A, Brackney DE, Grubaugh ND, Kaplan EH, Casanovas-Massana A, et al. Measurement of SARS-CoV-2 RNA in wastewater tracks community infection dynamics. *Nat Biotechnol*. (2020) 38:1164–7. doi: 10.1038/s41587-020-0684-z

6. Wolfe MK, Topol A, Knudson A, Simpson A, White B, Vugia DJ, et al. High-frequency, high-throughput quantification of SARS-CoV-2 RNA in wastewater settled solids at eight publicly owned treatment works in northern California shows strong association with COVID-19 incidence. *mSystems*. (2021) 6:e0082921. doi: 10.1128/mSystems.00829-21

7. Wu F, Xiao A, Zhang J, Moniz K, Endo N, Armas F, et al. SARS-CoV-2 RNA concentrations in wastewater foreshadow dynamics and clinical presentation of new COVID-19 cases. *Sci Total Environ*. (2021) 805:150121. doi: 10.1016/j.scitotenv.2021.150121

8. Medema G, Heijnen L, Elsinga G, Italiaander R, Brouwer A. Presence of SARS-Coronavirus-2 RNA in sewage and correlation with reported COVID-19 prevalence in the early stage of the epidemic in the Netherlands. *Environ Sci Technol Lett*. (2020) 7:511–6. doi: 10.1021/acs.estlett.0c00357

9. Naughton CC, Roman FA, Tariqi AQ, Kadonsky KF. (2021). COVIDPoops19 summary of global SARS-CoV-2 wastewater monitoring efforts by UC Merced researchers. ArcGIS Online Dashboard. Available at: https://arcg.is/1aummW (Accessed November 7, 2022).

10. American Society of Civil Engineers. (2019). Report card for California's infrastructure. Available at: https://infrastructurereportcard.org/wp-content/uploads/2021/07/FullReport-CA_051019.pdf (Accessed November 7, 2022).

11. Medina C, Kadonsky KF, Roman FA, Tariqi AW, Sinclair RG, D'Aoust PM, et al. The need of an environmental justice approach for wastewater based epidemiology for rural and disadvantaged communities: a review in California. *Curr Opin Environ Sci Health*. (2022) 27:100348. doi: 10.1016/j.coesh.2022.100348

12. Tariqi AQ, Naughton CC. Water, health, and environmental justice in California: geospatial analysis of nitrate contamination and thyroid Cancer. *Environ Eng Sci*. (2021) 38:377–88. doi: 10.1089/ees.2020.0315

13. California Office of Environmental Health Hazard Assessment (OEHHA). (2022). California climate investments to benefit disadvantaged communities. Available at: http://calepa.ca.gov/EnvJustice/GHGInvest/ (Accessed November 7, 2022).

14. United States Census Bureau. (2021). QuickFacts. Available at: https://www.census.gov/quickfacts/fact/table/US/PST04522 (Accessed November 7, 2022).

15. Centers for Disease Control and Prevention (CDC). (2022). Risk for COVID-19 infection, hospitalization, and death by race/ethnicity. Available at: https://www.cdc.gov/coronavirus/2019-ncov/covid-data/investigations-discovery/hospitalization-death-by-race-ethnicity.html (Accessed November 7, 2022).

16. Schwandt H, Currie J, Von Wachter T, Kowarski J, Chapman D, Woolf SH. Changes in the relationship between income and life expectancy before and during the COVID-19 pandemic, California, 2015-2021. *JAMA*. (2022) 328:360–6. doi: 10.1001/jama.2022.10952

17. California Health & Human Services Agency (CHHS). (2022). Hospital building data (CSV). Available at: https://data.chhs.ca.gov/dataset/hospital-building-data/resource/d97adf28-ebaf-4204-a29e-bb6bdb7f96b9 (Accessed November 7, 2022).

18. Spetz J, Coffman J, Geyn I. (2017). California's primary care workforce: Forecasted supply, demand, and pipeline of trainees, 2016–2030. Available at: https://healthforce.ucsf.edu/publications/californias-primary-care-workforce-forecasted-supply-demand-and-pipeline-trainees-2016 (Accessed November 7, 2022).

19. Pollock BH, Bergheinmer CL, Nesbitt TS, Stoltz T, Belafsky SR, Burtis KC, et al. Healthy Davis together: creating a model for community control of COVID-19. *Am J Public Health*. (2022) 112:1142–6. doi: 10.2105/AJPH.2022.306880

20. Safford H, Zuniga-Montanez RE, Kim M, Wu X, Wei L, Sharpnack J, et al. Wastewater-based epidemiology for COVID-19: handling qPCR nondetects and comparing spatially granular wastewater and clinical data trends. *Environ Sci Technol Water*. (2022) 2:2114–24. doi: 10.1021/acsestwater.2c00053

21. Wolfe MK, Archana A, Catoe D, Coffman MM, Dorevich S, Graham KE, et al. Scaling of SARS-CoV-2 RNA in settled solids from multiple wastewater treatment plants to compare incidence rates of laboratory-confirmed COVID-19 in their Sewersheds. *Environ Sci Technol Lett*. (2021b) 8:398–404. doi: 10.1021/acs.estlett.1c00184

22. Centers for Disease Control and Prevention (CDC). (2022). CDC Museum COVID-19 Timeline. COVID Data Tracker. Available at: https://www.cdc.gov/museum/timeline/covid19.html (Accessed December 8, 2022).

23. California Health and Human Services Open Data Portal. COVID-19 vaccines administered by demographics by county. (2022). Available at: https://data.chhs.ca.gov/dataset/vaccine-progress-dashboard/resource/71729331-2f09-4ea4-a52f-a2661972e146 (Accessed October 1, 2022).

24. California Health and Human Services Open Data Portal. (2022). Statewide COVID-19 cases deaths tests. Available at: https://data.chhs.ca.gov/dataset/covid-19-time-series-metrics-by-county-and-state/resource/046cdd2b-31e5-4d34-9ed3-b48cdbc4be7a (Accessed October 1, 2022).

25. California Department of Forestry and Fire Protection. (2022). California County boundaries. Available at: https://gis.data.ca.gov/datasets/CALFIRE-Forestry::california-county-boundaries/explore?location=36.585288%2C-115.353505%2C5.80 (Accessed November 7, 2022).

26. California Health and Human Services Geodata. (2019). Medical service study areas. Available at: https://gis.data.ca.gov/datasets/CHHSAgency::medical-service-study-areas/about (Accessed November 7, 2022).

27. Wolfe MK, Duong D, Bakker KM, Ammerman M, Mortenson L, Hughes B, et al. Wastewater-based detection of two influenza outbreaks. *Environ Sci Technol Lett*. (2022) 9:687–92. doi: 10.1021/acs.estlett.2c00350

28. Wolfe MK, Yu AT, Duong D, Rane MS, Hughes B, Chan-Herur V, et al. Use of wastewater for Mpox outbreak surveillance in California. *N Engl J Med*. (2023) 388:570–2. doi: 10.1056/NEJMc2213882

29. Yin Z, Voice TC, Tarabara V, Xagoraraki I. Sorption of human adenovirus to wastewater solids. *J Environ Eng*. (2018) 144:11. doi: 10.1061/(ASCE)EE.1943-7870.0001463

30. Kim S, Kennedy LC, Wolfe MK, Criddle CS, Duong DH, Topol A, et al. SARS-CoV-2 RNA is enriched by orders of magnitude in primary settled solids relative to liquid wastewater at publicly owned treatment works. *Environ Sci (Camb)*. (2022) 8:757–70. doi: 10.1039/D1EW00826A

31. Mercier E, D'Aoust PM, Thakali O, Hegazy N, Jia J-J, Zhang Z, et al. Municipal and neighbourhood level wastewater surveillance and subtyping of an influenza virus outbreak. *Sci Rep*. (2022) 12:15777. doi: 10.1038/s41598-022-20076-z

32. Ye Y, Ellenberg RM, Graham KE, Wigginton KR. Survivability, partitioning, and recovery of enveloped viruses in untreated municipal wastewater. *Environ Sci Technol*. (2016) 50:5077–85. doi: 10.1021/acs.est.6b00876

33. Topol A, Wolfe M, White B, Wigginton K, Boehm AB. *High throughput pre-analytical processing of wastewater settled solids for SARS-CoV-2 RNA analyses V.2. Protocols.io*. (2021).

34. Topol A, Wolfe M, White B, Wigginton K, Boehm AB. *High throughput SARS-COV-2, PMMOV, and BCoV quantification in settled solids using digital RT-PCR V.5. Protocols.io*. (2022).

35. Wolfe MK, Hughes B, Duong D, Chan-Herur V, Wigginton KR, White BJ, et al. Detection of SARS-CoV-2 variants mu, Beta, gamma, lambda, Delta, alpha, and omicron in wastewater settled solids using mutation-specific assays is associated with regional detection of variants in clinical samples. *Appl Environ Microbiol*. (2022) 88:e0004522. doi: 10.1128/aem.00045-22

36. Loeb S, Graham K, Wolfe M, Wigginton K, Boehm AB. *Extraction of RNA from wastewater primary solids using a direct extraction method for downstream SARS-CoV-2 RNA quantification. Protocols.io*. (2020).

37. Chan EMG, Kennedy LC, Wolfe MK, Boehm AB. Identifying trends in SARS-CoV-2 RNA in wastewater to infer changing COVID-19 incidence: Effect of sampling frequency. *PLOS Water*. (2022) 2:e0000088. doi: 10.1371/journal.pwat.0000088

38. Schoen ME, Wolfe MK, Li L, Doung D, White BJ, Hughes B, et al. SARS-CoV-2 RNA wastewater settled solids surveillance frequency and impact on predicted COVID-19 incidence using a distributed lag model. *ACS EST Water*. (2022) 2:2167–74. doi: 10.1021/acsestwater.2c00074

39. Melvin RG, Hendrickson EN, Chaudhry N, Georgewill O, Freese R, Schacker TW, et al. A novel wastewater-based epidemiology indexing method predicts SARS-CoV-2 disease prevalence across treatment facilities in metropolitan and regional populations. *Sci Rep*. (2021) 11:21368–9. doi: 10.1038/s41598-021-00853-y

40. Bio-Rad. *Droplet Digital PCR Applications Guide*. Available at: https://www.bio-rad.com/webroot/web/pdf/lsr/literature/Bulletin_6407.pdf (Accessed October 1, 2022).

41. California Health and Human Services Open Data Portal. (2022). COVID-19 hospitalizations by county data. Available at: https://data.chhs.ca.gov/dataset/covid-19-hospital-data/resource/47af979d-8685-4981-bced-96a6b79d3ed5 (Accessed October 1, 2022).

42. Montesinos-Lopez JC, Daza-Torres ML, Garcia YE, Barboza LA, Sanchez F, Schmidt AJ, et al. The role of SARS-CoV-2 testing on hospitalizations in California. *Life (Basel)*. (2021) 11:1336. doi: 10.3390/life11121336

43. Centers for Disease Control and Prevention (CDC). (2022). COVID data tracker variant proportions. Available at: https://covid.cdc.gov/covid-data-tracker/#variant-proportions (Accessed December 8, 2022).

44. Simpson A, Topol A, White BJ, Wolfe MK, Wigginton KR, Boehm AB. Effect of storage conditions on SARS-CoV-2 RNA quantifications in wastewater solids. *PeerJ*. (2021) 9:e11933. doi: 10.7717/peerj.11933

45. Ritchey MD, Rosenblum HG, del Guercio K, Humbard M, Santos S, Hall J, et al. COVID-19 self-test data: challenges and opportunities – United States, October 31, 2021-June 11, 2022. *MMWR Morb Mortal Wkly Rep*. (2022) 71:1005–10. doi: 10.15585/mmwr.mm7132a1

46. Zhang Y, Cen M, Hu M, Du L, Hu W, Kim JJ, et al. Prevalence and persistent shedding of fecal SARS-CoV-2 RNA in patients with COVID-19 infection: a systematic review and Meta-analysis. *Clin Transl Gastroenterol*. (2021) 12:E0343. doi: 10.14309/ctg.0000000000000343

47. Menachemi N, Dixon BE, Wools-Kaloustian KK, Yiannoutsos CT, Havlerson PK. How many SARS-CoV-2-infected people require hospitalization? Using random sample testing to better inform preparedness efforts. *J Public Health Mang Pract*. (2021) 27:246–50. doi: 10.1097/PHH.0000000000001331

48. Boehm AB, Hughes B, Wolfe MK, White BJ, Duong D, Chan-Herur V. Regional replacement of SARS-CoV-2 variant omicron BA.1 and BA.2 as observed through wastewater surveillance. *Environ Sci Technol Lett*. (2022b) 9:575–80. doi: 10.1021/acs.estlett.2c00266

49. Hegazy N, Cowan A, D'Aoust PM, Mercier E, Towhid ST, Jia J-J, et al. Understanding the dynamic relation between wastewater SARS-CoV-2 signal and clinical metrics throughout the pandemic. *Sci Total Environ*. (2022) 853:158458. doi: 10.1016/j.scitotenv.2022.158458

50. D'Aoust PM, Tian X, Towhid ST, Xiao A, Mercier E, Hegazy N, et al. Wastewater to clinical case (WC) ratio of COVID-19 identifies insufficient clinical testing, onset of new variants of concern and population immunity in urban communities. *Sci Total Environ*. (2022) 853:158547. doi: 10.1016/j.scitotenv.2022.158547

51. California Department of Public Health. (2022). California reportable disease information exchange (CalREDIE). Available at: https://www.cdph.ca.gov/Programs/CID/DCDC/Pages/CalREDIE.aspx (Accessed December 1, 2022).

52. California Hospital Association. (2021). Streamlining COVID-19 data. Available at: https://calhospital.org/streamlining-data/ (Accessed October 1, 2022).

53. California Department of Public Health. (2022). Public health order questions & answers: Hospital & Health Care System Surge. Available at: https://www.cdph.ca.gov/Programs/CID/DCDC/Pages/COVID-19/Order-of-the-State-Public-Health-Officer-Hospital-Health-Care-System-Surge-FAQ.aspx (Accessed November 7, 2022).

54. California Department of Public Health. (2022). CDPH wastewater surveillance network dashboard. Available at: https://www.cdph.ca.gov/Programs/CID/DCDC/Pages/COVID-19/CalSuWers-Dashboard.aspx (Accessed November 7, 2022).

frontiers | Frontiers in Public Health

TYPE Original Research
PUBLISHED 20 July 2023
DOI 10.3389/fpubh.2023.1140441

OPEN ACCESS

EDITED BY
David Champredon,
Public Health Agency of Canada (PHAC), Canada

REVIEWED BY
Niti B. Jadeja,
University of Virginia, United States
Hyatt Green,
SUNY College of Environmental Science and Forestry, United States
Madhvi Joshi,
Gujarat Biotechnology Research Centre (GBRC), India

*CORRESPONDENCE
Irene Xagoraraki
✉ xagorara@msu.edu

RECEIVED 09 January 2023
ACCEPTED 30 June 2023
PUBLISHED 20 July 2023

CITATION
Zhao L, Geng Q, Corchis-Scott R, McKay RM, Norton J and Xagoraraki I (2023) Targeting a free viral fraction enhances the early alert potential of wastewater surveillance for SARS-CoV-2: a methods comparison spanning the transition between delta and omicron variants in a large urban center.
Front. Public Health 11:1140441.
doi: 10.3389/fpubh.2023.1140441

Targeting a free viral fraction enhances the early alert potential of wastewater surveillance for SARS-CoV-2: a methods comparison spanning the transition between delta and omicron variants in a large urban center

Liang Zhao[1], Qiudi Geng[2], Ryland Corchis-Scott[2], Robert Michael McKay[2,3], John Norton[4] and Irene Xagoraraki[1]*

[1]Department of Civil and Environmental Engineering, Michigan State University, East Lansing, MI, United States, [2]Great Lakes Institute for Environmental Research, University of Windsor, Windsor, ON, Canada, [3]Great Lakes Center for Fresh Waters and Human Health, Bowling Green State University, Bowling Green, OH, United States, [4]Great Lakes Water Authority, Detroit, MI, United States

Introduction: Wastewater surveillance has proven to be a valuable approach to monitoring the spread of SARS-CoV-2, the virus that causes Coronavirus disease 2019 (COVID-19). Recognizing the benefits of wastewater surveillance as a tool to support public health in tracking SARS-CoV-2 and other respiratory pathogens, numerous wastewater virus sampling and concentration methods have been tested for appropriate applications as well as their significance for actionability by public health practices.

Methods: Here, we present a 34-week long wastewater surveillance study that covers nearly 4million residents of the Detroit (MI, United States) metropolitan area. Three primary concentration methods were compared with respect to recovery of SARS-CoV-2 from wastewater: Virus Adsorption-Elution (VIRADEL), polyethylene glycol precipitation (PEG), and polysulfone (PES) filtration. Wastewater viral concentrations were normalized using various parameters (flow rate, population, total suspended solids) to account for variations in flow. Three analytical approaches were implemented to compare wastewater viral concentrations across the three primary concentration methods to COVID-19 clinical data for both normalized and non-normalized data: Pearson and Spearman correlations, Dynamic Time Warping (DTW), and Time Lagged Cross Correlation (TLCC) and peak synchrony.

Results: It was found that VIRADEL, which captures free and suspended virus from supernatant wastewater, was a leading indicator of COVID-19 cases within the region, whereas PEG and PES filtration, which target particle-associated virus, each lagged behind the early alert potential of VIRADEL. PEG and PES methods may potentially capture previously shed and accumulated SARS-CoV-2 resuspended from sediments in the interceptors.

Discussion: These results indicate that the VIRADEL method can be used to enhance the early-warning potential of wastewater surveillance applications although drawbacks include the need to process large volumes of wastewater to concentrate sufficiently free and suspended virus for detection. While lagging the

VIRADEL method for early-alert potential, both PEG and PES filtration can be used for routine COVID-19 wastewater monitoring since they allow a large number of samples to be processed concurrently while being more cost-effective and with rapid turn-around yielding results same day as collection.

KEYWORDS

wastewater surveillance, SARS-CoV-2, COVID-19, virus adsorption-elution, polyethylene glycol precipitation, filtration, lead/lag time, dynamic time warping

1. Introduction

Wastewater surveillance has been widely adopted by researchers and health agencies as an effective tool for tracking Severe Acute Respiratory Syndrome Coronavirus 2 (SARS-CoV-2) in wastewater amid the Coronavirus Disease 2019 (COVID-19) pandemic (1–13). SARS-CoV-2 was first identified in Wuhan, Hubei, China, and was designated a Public Health Emergency of International Concern on January 30th, 2020, by the World Health Organization (WHO). COVID-19 was later declared a pandemic on March 11th, 2020 (who.int). Numerous studies have demonstrated that SARS-CoV-2 can be shed from the gastrointestinal tract of infected individuals and its viral RNA can persist and be detected in wastewater (14–18). To increase the sensitivity of the assay used to detect viral RNA in wastewater, samples are routinely concentrated prior to quantification (19–21).

Methods used in published studies to recover and concentrate SARS-CoV-2 viral RNA from wastewater encompass a wide range of techniques including Virus Adsorption-Elution (VIRADEL), polyethylene glycol precipitation (PEG), ultrafiltration, ultracentrifugation, concentrating pipette, filtration and so forth. Some of the methods, such as VIRADEL, exclude large solids and focus on free and suspended viral particles in supernatant wastewater. Other methods, such as PEG precipitation and filtration, target particulate matter and the associated viruses that are sorbed onto solids. Notably, this fraction may preferentially settle within the sewer when flow is reduced and likewise is susceptible to resuspension when flows are elevated (3, 22).

The recovery efficiencies of concentration methods are variable, differing between method, virus type and conditioning of the wastewater sample. Notably, VIRADEL was found to be effective for concentrating viruses from water samples with recovery efficiencies of more than 90% for poliovirus (23, 24), 54.4% for murine norovirus (MNV) (25), 51% for echovirus (26), 35% for enteric virus (27), and 4.7% for adenovirus (28). Likewise, PEG was found to be effective for concentrating viruses in water samples, with recovery efficiencies of 89.5% for echovirus (29), 86% for hepatitis A virus (30), 68% for poliovirus (30), and 56.7% (31) and 26.4% (32) for SARS-CoV-2. Filtration was reported to recover virus from wastewater samples with recovery efficiencies ranging from 26.7 to 65.7% for murine hepatitis virus (33), and 90% for human betacoronavirus OC43 (34).

Applying different concentration methods can achieve different goals. For instance, use of VIRADEL to concentrate SARS-CoV-2 can provide early warnings of impending COVID-19 cases (1, 3, 13). PEG precipitation is an economical and widely adopted method that allows a large number of samples to be processed concurrently and it is suitable for routine COVID-19 wastewater monitoring (22, 35). Likewise, filtration presents a cost-effective and simple approach commonly applied to recover cells and viral particles from environmental samples for nucleic acid extraction (36), which has also been applied to recovery of SARS-CoV-2 from wastewater (12, 35, 37, 38).

Here we present a comparison of three primary concentration methods (VIRADEL, PEG and filtration) to detect SARS-CoV-2 viral RNA in wastewater, in relation to COVID-19 cases amid the transition from Delta to Omicron Variants of Concerns (VOCs) circulating in the Detroit, MI metropolitan area. Similarities and correlations were examined among the three concentration methods with both normalized and non-normalized data. The lead/lag time of each method in relation to the total COVID-19 cases was also assessed. The results presented in this study will assist researchers and public health practitioners to select appropriate primary concentration methods for the recovery of SARS-CoV-2 from wastewater for different wastewater surveillance practices.

2. Materials and methods

Untreated wastewater samples were collected weekly from the Water Resource Recovery Facility (WRRF) of the Great Lakes Water Authority (GLWA) located in Detroit, MI, United States, between October 1, 2021, and May 31, 2022. The WRRF serves the needs of Detroit and 76 area communities with a service area of more than 2,450 square kilometers serving nearly 4 million people. WRRF collects and treats stormwater, as well as residential, industrial, and commercial waste, depending on service areas, with its semi-combined sewershed system. WRRF receives wastewater via three main interceptors including the Detroit River Interceptor (DRI), the North Interceptor-East Arm (NIEA), and the Oakwood-Northwest-Wayne County Interceptor (ONWI) (Figure 1), serving the City of Detroit as well as the three largest Michigan counties by population: Wayne, Oakland, and Macomb. Composite samples collected over 24-h were used to compare the polyethylene glycol (PEG) precipitation and filtration methods, however, the larger volumes required by the virus adsorption-elution (VIRADEL) method necessitated a targeted approach with samples collected between 15:30 to 18:00 each afternoon. The samples were collected from the three interceptors at the point of discharge into the WRRF and maintained chilled on ice during transport to the lab for primary concentration and sample analysis.

2.1. Virus adsorption-elution method

The United States Environmental Protection Agency virus adsorption-elution (VIRADEL) method employing electropositive or electronegative filters was reported to recover and concentrate viruses from wastewater samples previously (1–4, 13, 20, 35). Electronegative filters require preconditioning such as adjusting the pH, prior to downstream concentration processes. Electropositive filters do not

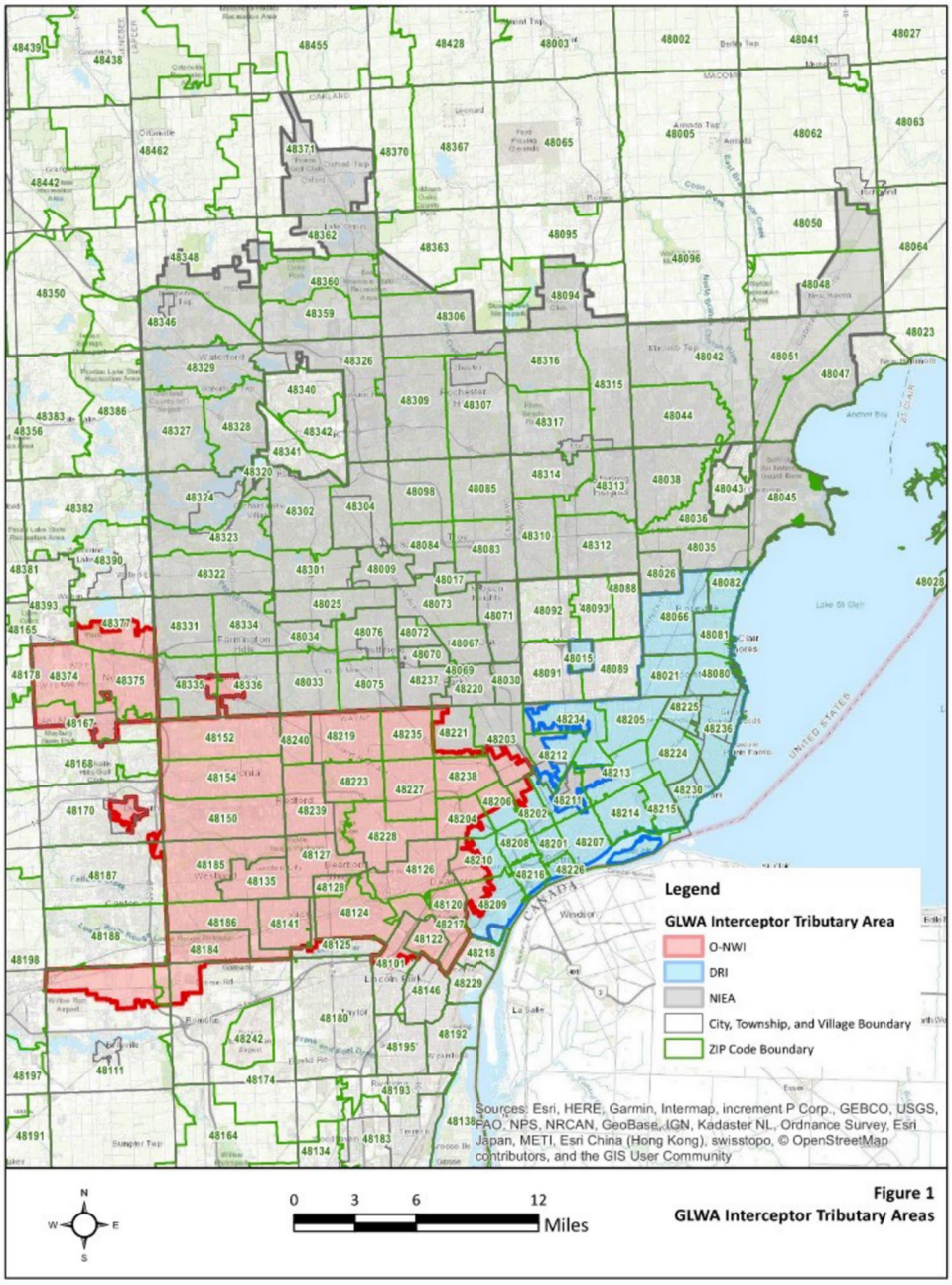

FIGURE 1
GLWA interceptor tributary map.

require any preconditioning (20, 35). In this study, depending on the quantity of suspended solids in the wastewater, 10 to 50 L of untreated wastewater (grab sample) was passed through NanoCeram electropositive cartridge filters (Argonide, Sanford, FL, United States) at a rate less than 11 L/min using a previously described method (1–4). Flow meter readings were tracked at the beginning and end of each sampling event to measure the total volume of wastewater passing through the filters. Following sampling, the NanoCeram filters were transported on ice to the lab for sample analysis within 24 h. The elution process releases viral particles captured by the filters (20). Viruses were eluted using 1.5% beef extract containing 0.05 M glycine, based on a previously described method (1–4). Subsequently, the eluates containing viruses were flocculated by adjusting the pH, following multiple centrifugations and resuspension of particles in sodium phosphate. Afterwards, supernatants containing viruses were separated by adjusting the pH and centrifugation. Finally, the supernatants containing viruses were passed through 0.45 µm and 0.22 µm Millipore filters (MilliporeSigma, Burlington, MA, United States), which were followed by aliquoting and storage of the final aliquots at -80°C for downstream molecular analysis (1–4, 20). Bacteriophage Phi6 was applied as a proxy virus to estimate the recovery efficiency during virus concentration (3, 29, 39). Figure 2 demonstrates the workflow of the VIRADEL method.

2.2. Polyethylene glycol precipitation method

From a 24-h composite sample of untreated wastewater collected in a 1 L Nalgene bottle, 100 mL samples were mixed with 0.2 M sodium chloride and 8% polyethylene glycol (w/v). Samples were mixed gently on a magnetic stirrer at 4°C for 2 h, followed by centrifugation at 4700 × *g* for 45 min at 4°C. The supernatant was removed, and the pellet was resuspended in the remaining liquid (approximately 2-3 mL). The final concentrate volumes were between 1 to 6 mL. All sample concentrates were then subjected to downstream analysis including RNA extraction and RT-ddPCR (Figure 3).

2.3. Filtration method

Composite samples of raw wastewater collected as for the PEG method were concentrated by filtering 50-120 mL through 0.22 µm Sterivex PES cartridge filters (MilliporeSigma, Burlington, MA, United States) using a 50 mL syringe fitted into a caulking gun. Immediately following filtration, the filters were sealed and flash-frozen through immersion in liquid nitrogen as described previously (38). Subsequently, filters were subjected to downstream processes including RNA extraction and RT-qPCR (Figure 4).

2.4. RNA extraction, RT-ddPCR, RT-qPCR

Following VIRADEL and PEG methods, viral RNA was extracted using the QIAamp Viral RNA kit (Qiagen, Germantown, MD, United States), following the manufacturer's protocol modified by use of 140 µL elution buffer to extract the viral RNA (1–4). RT-ddPCR was performed on a QX200 AutoDG Droplet Digital PCR system (Bio-Rad, Hercules, CA, United States), using the One-step RT-ddPCR Advanced Kit for Probes (Bio-Rad, Hercules, CA, United States) as described previously (2, 3). United States Centers for Disease Control and Prevention (US CDC) primers and probes that target the N1 and N2 genes of SARS-CoV-2 were used (2, 3, 13). N1 N2 gene Duplex Assay Reaction Mixture was reported previously (2, 3, 13). Following the preparation of the Duplex Mixture and oil droplets generation, samples were run on a C1000 Touch Thermal Cycler (Bio-Rad, Hercules, CA, United States) using the thermocycling conditions which were reported previously (2, 3, 13). Subsequently, the measurement of fluorescence was performed on a QX200 Droplet Reader (Bio-Rad, Hercules, CA, United States). For each RT-ddPCR run, positive controls (PTCs), negative controls (NTCs), and process negative controls were included, which were described previously (3). All samples were run in triplicate. The Limit of Detection (LOD) and Limit of Blank (LOB) for RT-ddPCR were described and determined previously (2, 3, 13).

Following the filtration method, filters were thawed, and RNA was extracted from the filters using the AllPrep PowerViral DNA/RNA kit (Qiagen, Germantown, MD, United States) modified by addition of 5% 2-mercaptoethanol (v/v). RNA was eluted in 50 µL of RNAse free water. Samples were not treated with DNase upon extraction. Assays for SARS-CoV-2 targeted regions of the nucleocapsid (N) gene using US CDC primers and probes for the N1 and N2 regions (40). Reagents were supplied by Integrated DNA Technologies (Coralville, IA, United States). Reactions contained 5 µL of RNA template mixed with 10 µL of 2 × RT-qPCR master mix (Takyon TM Dry One-Step RT Probe MasterMix No Rox, Eurogentec, Liège, Belgium) and primers and probes in a final reaction volume of 20 µL. Reaction inhibition was

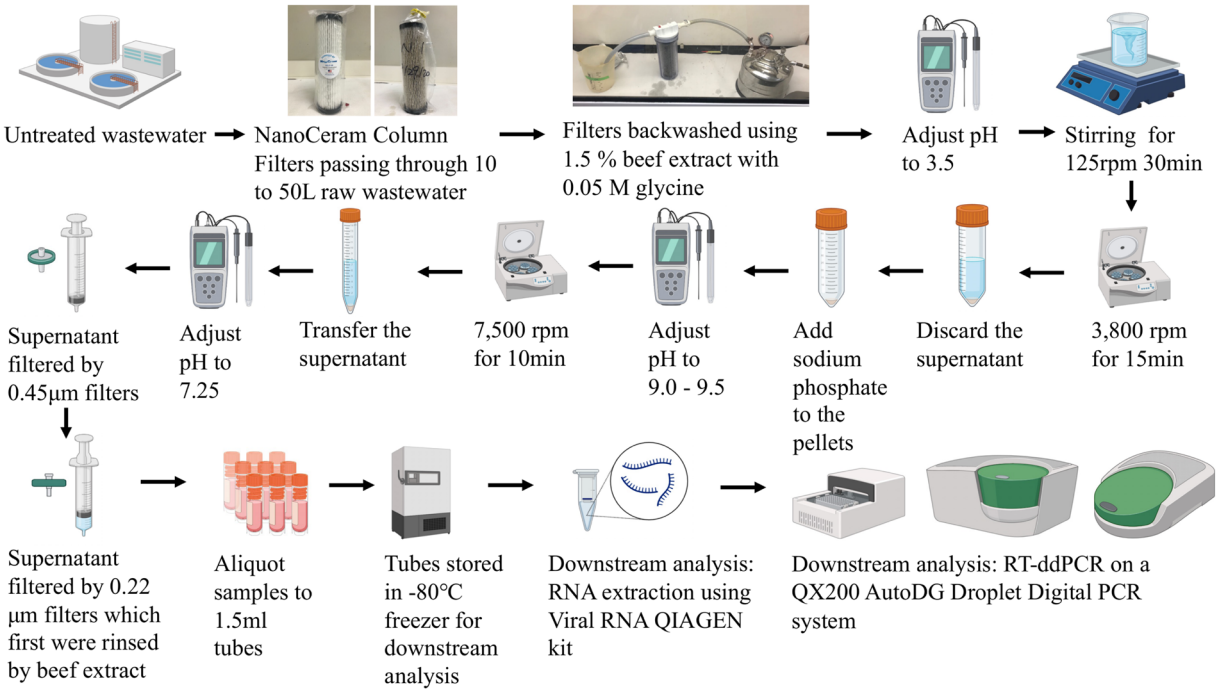

FIGURE 2
Illustrative flowchart of the VIRADEL concentration method and downstream analysis.

10.3389/fpubh.2023.1140441

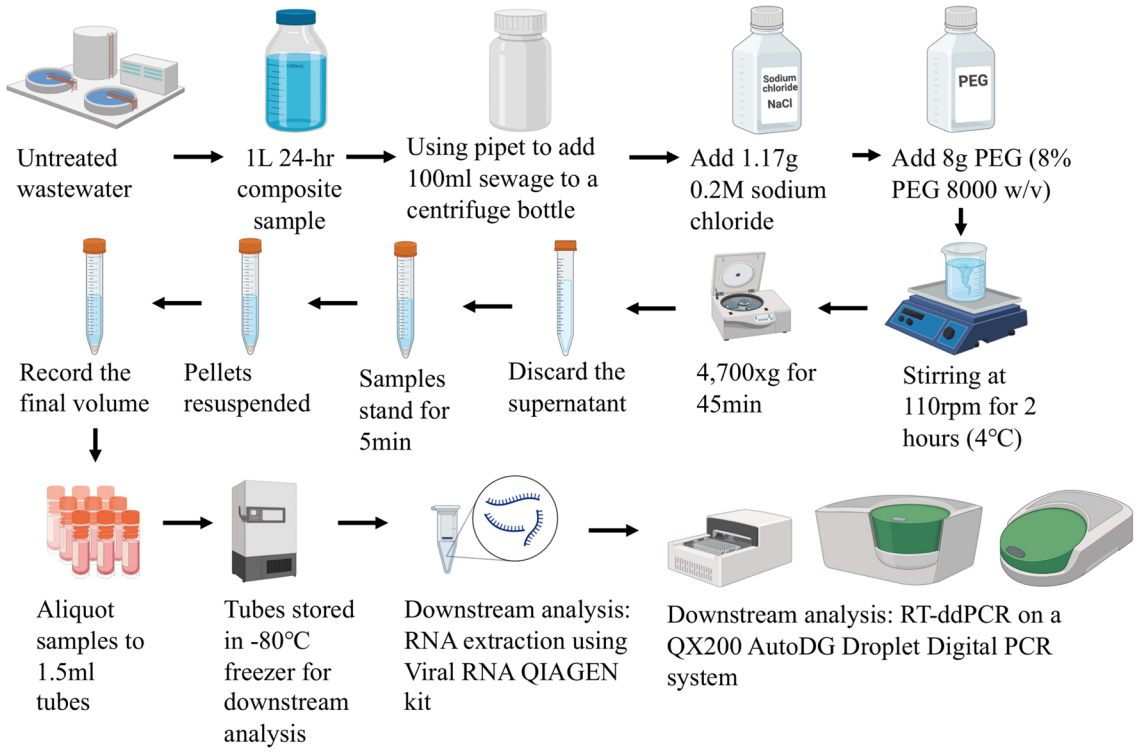

FIGURE 3
Illustrative flowchart of the PEG concentration method and downstream analysis.

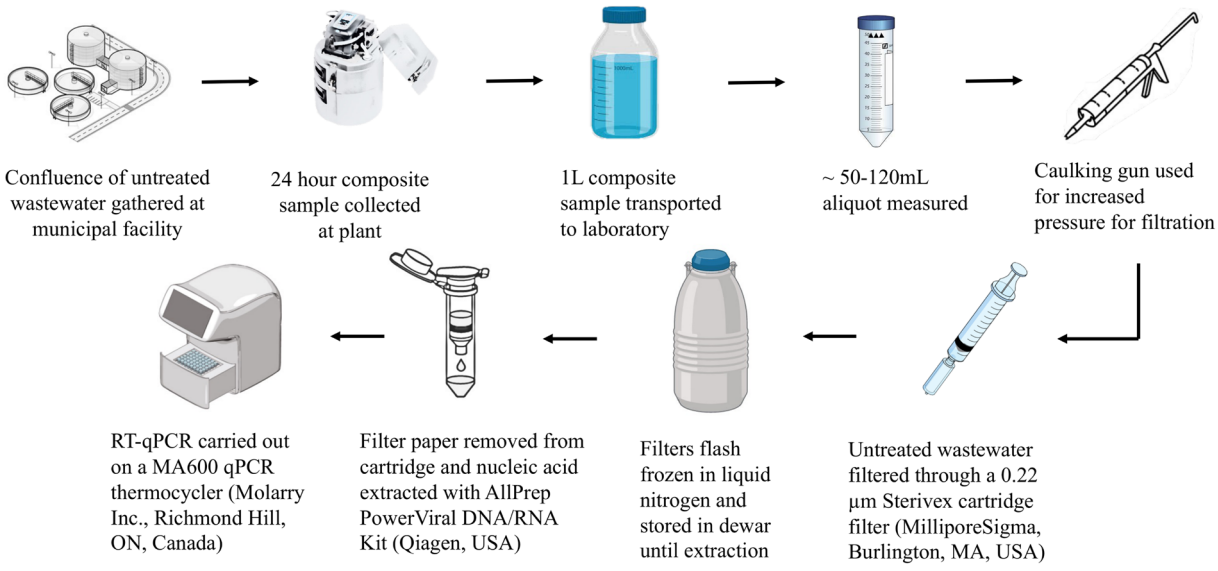

FIGURE 4
Illustrative flowchart of the filtration concentration method and downstream analysis.

assessed using VetMAX XENO Internal Positive Control RNA (Applied Biosystems Corp., Waltham, MA, United States). Due to repeated incidence of inhibition with wastewater samples processed by filtration, template was diluted 1:5 in all reactions. Technical triplicates were run for detection of gene targets. Thermal cycling was performed using a MA6000 qPCR thermocycler (Sansure Biotech, Changsha, China). RT was performed at 48°C for 10 min, followed by polymerase activation at 95°C for 3 min, and 50 cycles of denaturation, annealing/extension at 95°C for 10 s, then 60°C for 45 s, respectively. The EDX SARS-CoV-2 synthetic RNA standard (Exact Diagnostics, Fort Worth, TX, United States) was used to create a 7-point standard curve to quantify N1 and N2 gene targets. No template controls

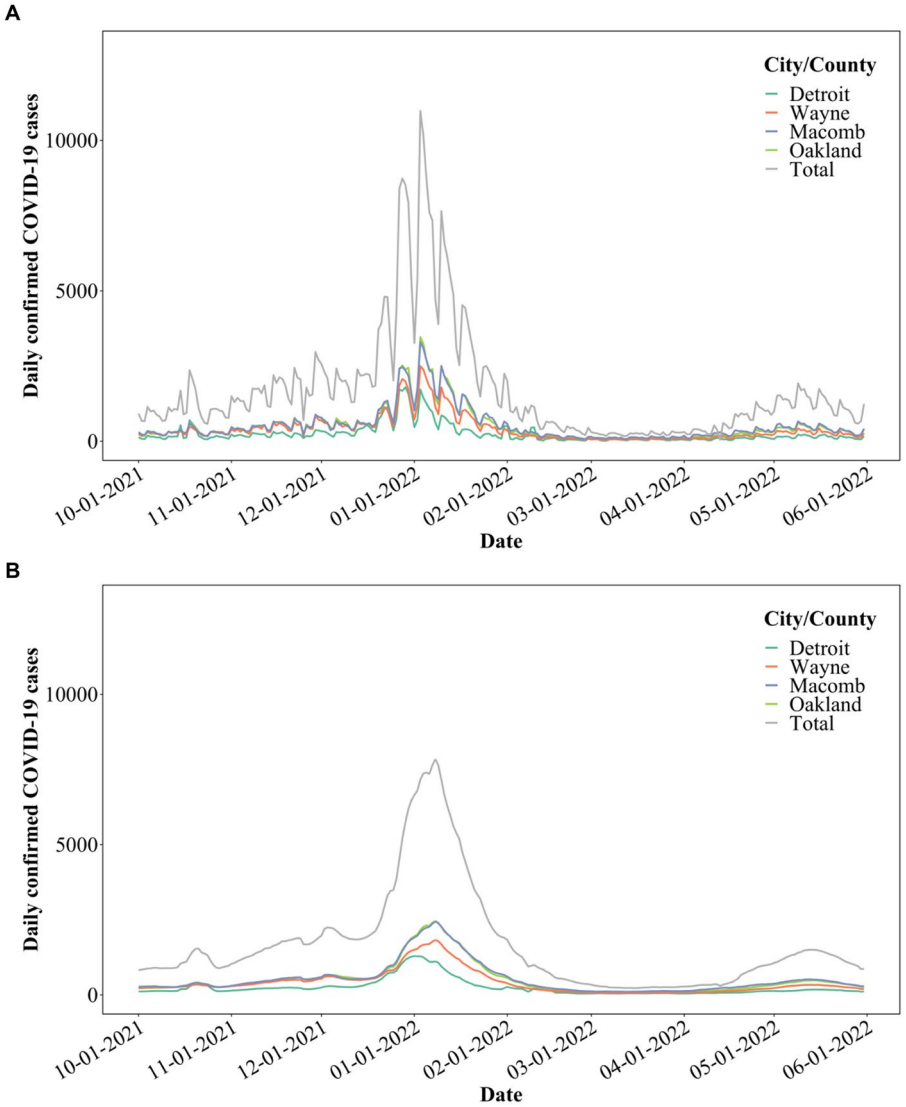

FIGURE 5
(A) COVID-19 cases in the City of Detroit, as well as Wayne, Macomb, and Oakland counties; **(B)** 7-day moving average of the COVID-19 cases.

yielded no amplification, and we report a limit of detection of 5 gene copies of N1 and N2 per reaction containing 5 µL of template RNA for RT-qPCR.

2.5. COVID-19 clinical data

Publicly available clinical data were accessed on August 22, 2022, for the period between October 1, 2021, and May 31, 2022, for the city of Detroit, as well as Wayne, Macomb, and Oakland counties (Figure 5A).[1] Clinical data with a 7-day moving average (3, 41, 42) was used for further statistical analysis (Figure 5B). COVID-19 clinical data were only available per city/county for the Detroit metropolitan area. Each interceptor received wastewater from portions of each city/county. Therefore, only the total SARS-CoV-2 concentrations can be correlated to the total COVID-19 cases of each city/county (3, 13).

2.6. Data analysis and visualization

Data were tracked and organized using Microsoft Excel version 16.66.1. R version 4.1.3 was applied to perform data analysis including Pearson and Spearman correlations, Dynamic Time Warping (DTW), Time Lagged Cross Correlation (TLCC) and peak synchrony, depending primarily on ggplot2 package for visualization, and packages including dtw, synchrony, dplyr, and ggpubr. Missing data from samples were filled using linear interpolation for further analysis (3, 13, 43). For VIRADEL samples, 128 genes concentrations were measured for both N1 and N2 genes between 10/1/21 and 5/31/22. For PEG samples, 88 gene concentrations were measured for both N1 and

1 michigan.gov/coronavirus/stats

N2 genes between 10/1/21 and 5/31/22. For filtration samples, 66 gene concentrations were measured for both N1 and N2 genes between 10/1/21 and 5/31/22. To perform correlation analysis between weekly gene concentrations and daily clinical cases, linear interpolation was conducted to generate daily data based on weekly measurements. The number of interpolated daily gene concentrations were 179, 199, and 210 for VIRADEL, PEG, and filtration, respectively.

To account for the changing flow in wastewater, dilution events, and variability in the solids portion of the wastewater, four approaches (flow rate, flow rate/population, TSS, flow rate×TSS) of normalizing the N1 and N2 gene concentrations (gc/L) were implemented using Eq. (1), Eq. (2), Eq. (3), and Eq. (4) (3, 44, 45). TSS, or "Total Suspended Solids," is an estimate of the entire solids in wastewater in contrast to the liquid fraction or dissolved matter (45). In addition, other parameters, including sanitary percentage and Biological Oxygen Demand (BOD), proved ineffective for normalizing N1 and N2 gene concentrations for the Detroit area and other areas, thus, they were not considered in the current study (3, 9). SARS-CoV-2 gene concentrations measured in the wastewater following VIRADEL, PEG, and filtration methods are reported as gene copies per L (gc/L). The units after normalization using flow rate, flow rate/population, TSS, and flow rate×TSS, are gene copies per day (gc/day), gene copies per day per person (gc/day/person), gene copies per mg TSS (gc/mg TSS), and gene copies per L per pounds/day {gc/[L(pounds/day)]}, respectively.

$$C_{(1)} = C_{N1or\,N2\,gene} * V * f \tag{1}$$

$$C_{(2)} = \frac{C_{(1)}}{P} \tag{2}$$

$$C_{(3)} = \frac{C_{N1or\,N2\,gene}}{TSS} \tag{3}$$

$$C_{(4)} = \frac{C_{N1or\,N2\,gene}}{V * f * k * TSS} \tag{4}$$

$C_{(1)}$ is the normalized concentration of SARS-CoV-2 in gc/day. $C_{(2)}$ is the normalized concentration of SARS-CoV-2 in gc/day/person. $C_{(3)}$ is the normalized concentration of SARS-CoV-2 in gc/mg TSS. $C_{(4)}$ is the normalized concentration of SARS-CoV-2 in gc/[L(pounds/day)]. V is the volume of wastewater flowing into WWTP interceptors during sampling events (MGD). f is the conversion factor between L and MGD. k is the conversion factor between mg and pounds. P is the total population in the Detroit metropolitan area served by WRRF's interceptors including ONWI, NIEA, and DRI. TSS represents the total suspended solids (mg/L).

2.6.1. Correlations among N1 and N2 gene concentrations by VIRADEL, PEG, and filtration

Multiple studies investigated the applications of both Pearson and Spearman correlations on analyzing the relationship between wastewater viral concentrations of SARS-CoV-2 and COVID-19 clinical cases as well as the relationship among wastewater viral concentrations by different genes or methods (9, 46, 47). In this study, Pearson and Spearman correlations were performed among N1 and N2 gene concentrations {gc/L, gc/day, gc/day/person, gc/mg TSS, gc/(L[pounds/day)]} by VIRADEL, PEG, and filtration methods. The Pearson correlation measures how two time series among VIRADEL, PEG, and filtration gene concentrations covary during the study period, and indicate their linear relationships. The Spearman correlation coefficient is a simple and straightforward approach to analyze the degree of associations between two time series (48).

2.6.2. Dynamic time warping

One commonly used algorithm for quantifying the similarities/dissimilarities between time series data is the Euclidean distance (ED), but numerous studies demonstrated that ED is insensitive to time shifting and patterns between time series since it compares the data points of time series in a settled sequence and cannot consider time shifting or patterns (49, 50). Dynamic time warping (DTW) is a well-established algorithm that circumvents the limitations of ED and compares two time series by computing dynamic distances between them considering regional distortions, time shifting, and the optimal warping that best aligns the time series between each other (50, 51). Therefore, similar patterns that occur at different times between time series can be considered as matching, thus, the similarity of time series can be evaluated considering their time shifting and shapes by DTW algorithm (50). The DTW algorithm was proposed previously (51).

The outcome of DTW analysis indicates two time series with the most similar patterns by calculating the minimum overall dissimilarity or the DTW minimum distance where data points on one time series best align data points on another time series (51). Multiple studies investigated the similarities between time series using DTW algorithm (50, 52, 53). However, to our knowledge, this is the first study to apply DTW algorithm to compare the similarities between wastewater gene concentrations data by three concentration methods (VIRADEL, PEG, and filtration), as well as comparing the similarities between wastewater gene concentrations data and COVID-19 clinical data. In this study, package dtw and related packages in R (version 4.1.3) were implemented to calculate DTW for the normalized {gc/day, gc/day/person, gc/mg TSS, and gc/[L(pounds/day)]} and non-normalized (gc/L) data to analyze the similarities/dissimilarities between VIRADEL, PEG, and filtration methods.

One limitation is that the minimum DTW distance can be affected by the scaling factor of time series data. For instance, the minimum DTW distance between PEG (gc/day/person) and COVID-19 cases can be smaller than the distance between VIRADEL (gc/day/person) and cases, indicating that PEG presents higher similarity to cases than VIRADEL. However, this was affected by the population factor which is a constant number but is not dynamic time series data. Using flow/population normalization including a constant factor intentionally changed the similarities among time series data. Therefore, the minimum DTW distance with flow/population normalized data was not considered for further discussions.

2.6.3. Time lagged cross correlation and peak synchrony

To estimate the leading or lagging relationships between wastewater viral concentrations by three concentration methods (VIRADEL, PEG, and filtration) and total COVID-19 cases, TLCC

10.3389/fpubh.2023.1140441

and peak synchrony were performed where the total COVID-19 cases were shifted over time and correlated with wastewater viral concentrations for each concentration method. TLCC refers to correlations between two time series shifted relatively in time. It can identify the direction and relationship between two time series, for instance, a leader-follower relationship, where the leader time series develop a pattern which is repeated by the follower time series (54). TLCC is widely applied in analyzing time series especially delay, lead/lag time, and lagged cross correlation and so forth (44, 54–56). TLCC is an effective approach to estimate the dynamic relationships between two time series and demonstrate how they shift over time (44).

In this study, TLCC is measured by gradually shifting total COVID-19 cases between -20 days (lagging) and + 20 days (leading), and constantly calculating the Pearson's correlation coefficients between two time series for each shifting. Peak synchrony occurs when the peak correlation is observed. For instance, if the peak correlation is observed at the center where the lag time or offset is 0 day, this condition indicates that the time series are most synchronized at day 0 demonstrating no shifting or lag time. However, the peak correlation can be at a different offset if one time series is leading or lagging another one. R package "synchrony," "devtools," and related packages were implemented to calculate the TLCC and peak synchrony between gene concentrations (both normalized and non-normalized data, by VIRADEL, PEG, and filtration methods) and 7-day moving average total COVID-19 cases.

3. Results

3.1. SARS-CoV-2 viral RNA concentrations in wastewater derived by three concentration methods spanning the transition between delta and omicron VOCs

RT-ddPCR (VIRADEL and PEG samples) and RT-qPCR (filtration samples) targeting the N1 and N2 genes was used to quantify SARS-CoV-2 RNA concentrations in wastewater samples collected at GLWA's WRRF over 34 weeks. The study period captured the third major resurgence of COVID-19 cases in the region corresponding to the transition from SARS-CoV-2 Delta (B.1.617.2) variant to Omicron (B.1.1.529) variant (3, 44).

Filtered samples yielded N1 and N2 gene concentrations higher than those of VIRADEL but lower than those of PEG, for both normalized and non-normalized data (Table 1). Filtered samples yielded mean N1 and N2 gene concentrations of 3.22E+04 and 1.50E+04 gc/L, respectively. VIRADEL samples yielded mean N1 and N2 gene concentrations of 1.61E+03 and 1.63E+03 gc/L, respectively. PEG samples yielded mean N1 and N2 gene concentrations of 1.61E+05 and 1.50E+05 gc/L, respectively. The overall observed trends of the VIRADEL total N1 and N2 gene concentrations increased steeply from early December 2021 and reached a peak in late December 2021 (Figure 6A), which heralded the major wave of COVID-19 cases in late December 2021 and early January 2022. Likewise, VIRADEL N1 and N2 gene concentrations increased in early April 2022, which preceded a resurgence of COVID-19 cases later in mid-April 2022.

TABLE 1 Total N1 and N2 gene concentrations measured in wastewater samples by VIRADEL, PEG, and filtration methods.

Gene	Methods			
		VIRADEL	PEG	Filtration
N1 (gc/L)	Maximum	5.64E+03	7.02E+05	1.12E+05
	Minimum	9.01E+02	3.18E+04	5.12E+02
	Mean	1.61E+03	1.61E+05	3.22E+04
N2 (gc/L)	Maximum	4.95E+03	5.48E+05	7.34E+04
	Minimum	9.01E+02	2.97E+04	3.13E+02
	Mean	1.63E+03	1.50E+05	1.50E+04
N1 (gc/day)	Maximum	5.24E+12	4.07E+14	7.40E+13
	Minimum	5.39E+11	2.36E+13	4.12E+11
	Mean	1.35E+12	1.18E+14	2.52E+13
N2 (gc/day)	Maximum	4.62E+12	3.18E+14	4.77E+13
	Minimum	5.84E+11	2.21E+13	2.93E+11
	Mean	1.37E+12	1.12E+14	1.14E+13
N1 (gc/day/person)	Maximum	1.69E+00	1.31E+02	2.38E+01
	Minimum	1.74E-01	7.58E+00	1.32E-01
	Mean	4.34E-01	3.79E+01	8.11E+00
N2 (gc/day/person)	Maximum	1.49E+00	1.02E+02	1.54E+01
	Minimum	1.88E-01	7.12E+00	9.43E-02
	Mean	4.41E-01	3.59E+01	3.65E+00
N1 (gc/mg TSS)	Maximum	5.82E+01	5.72E+03	1.19E+03
	Minimum	6.85E+00	2.20E+02	2.91E+00
	Mean	1.69E+01	1.53E+03	2.97E+02
N2 (gc/mg TSS)	Maximum	5.21E+01	4.66E+03	6.60E+02
	Minimum	6.71E+00	1.99E+02	3.84E+00
	Mean	1.69E+01	1.44E+03	1.41E+02
N1 (gc/(L(pounds/day)))	Maximum	2.94E-02	4.96E+00	8.83E-01
	Minimum	2.00E-03	6.48E-02	1.77E-03
	Mean	9.83E-03	1.01E+00	1.89E-01
N2 (gc/(L(pounds/day)))	Maximum	2.70E-02	4.01E+00	4.84E-01
	Minimum	1.96E-03	5.90E-02	2.06E-03
	Mean	9.84E-03	9.37E-01	9.27E-02

Previous reports have demonstrated that the VIRADEL method can serve as a leading indicator of COVID-19 cases (1, 3, 13). By contrast, PEG measured N1 and N2 gene concentrations were more variable and increased significantly in January 2022, lagging the major wave of COVID-19 infections (Figure 6B). PEG N1 and N2 gene concentrations increased simultaneously with the surge of COVID-19 cases in mid-April 2022, into May 2022. N1 and N2 gene concentrations yielded by the filtration approach increased in early November 2021 and decreased in early December 2021. Thereafter, gene concentrations rapidly increased starting in mid-December 2021, peaking in mid-January 2022, which later significantly decreased to a low level in February 2022 (Figure 6C). Notably, the peak in SARS-CoV-2 measured in wastewater by this approach was staggered, lagging the major wave of COVID-19 cases.

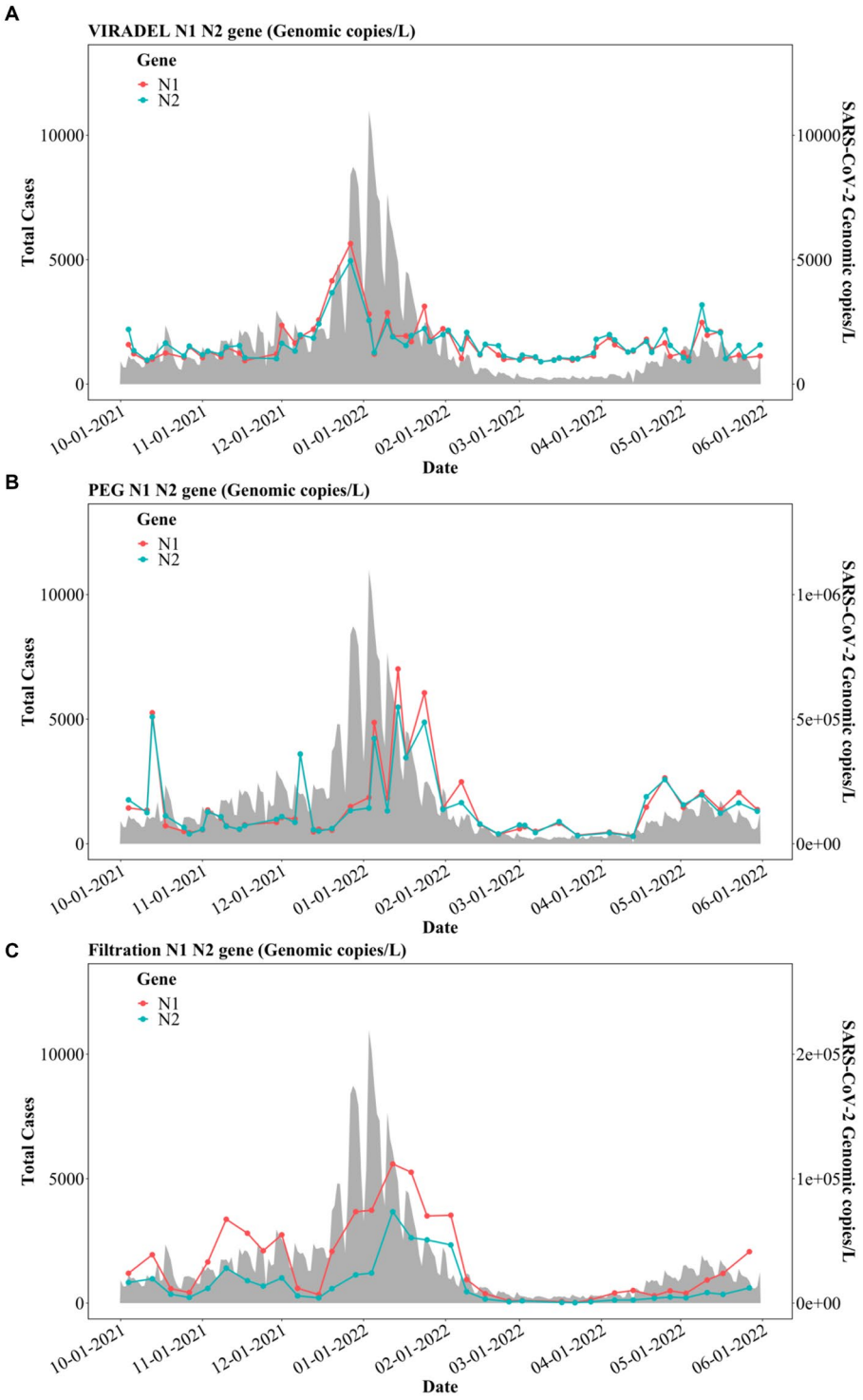

FIGURE 6
N1 and N2 gene concentrations (gc/L) by three concentration methods: **(A)** VIRADEL, **(B)** PEG, **(C)** Filtration, plotted against total COVID-19 cases.

3.2. Correlations and similarity analysis among three concentration methods

3.2.1. Correlations of N1 and N2 gene concentrations among three concentration methods

Multiple studies have applied Pearson and Spearman correlations to analyze the relationships between wastewater SARS-CoV-2 gene concentrations and COVID-19 cases (3, 9, 46), as well as the relationships among gene concentrations of SARS-CoV-2 in wastewater (47, 57). In this study, we tested the Pearson and Spearman correlations among N1 and N2 gene concentrations by VIRADEL, PEG, and filtration with normalized and non-normalized data (Table 2). A value of p that is less than 0.05 is considered statistically significant. For the non-normalized data

(gc/L), the highest correlation was observed between PEG and filtration with N2 gene concentration (Pearson's $r = 0.67$, Spearman's $r = 0.6$). The lowest correlation was found between VIRADEL and PEG for N2 gene concentration (Pearson's $r = 0.12$, Spearman's $r = 0.34$). For non-normalized data (gc/L), the correlations between PEG and filtration were stronger than the correlations between VIRADEL and filtration, which in turn was stronger than the correlations between VIRADEL and PEG. For normalized data, the highest correlation was found between PEG and filtration for N1 (Pearson's $r = 0.73$, Spearman's $r = 0.66$) and N2 (Pearson's $r = 0.76$, Spearman's $r = 0.64$) gene concentrations in gc/[L(pounds/day)]. Significant correlations (Pearson coefficient > 0.63, Spearman coefficient > 0.6) were observed between PEG and filtration in gc/L, gc/mg TSS and gc/(L(pounds/day)) (Table 2). VIRADEL has stronger correlation to filtration than to PEG for both normalized and non-normalized data.

Normalizations using flow rate and flow rate/population reduced the correlations of gene concentrations among VIRADEL, PEG, and filtration compared to the correlations using the non-normalized data (gc/L) (Table 2). For instance, both Pearson and Spearman correlation coefficients between PEG and filtration were reduced from 0.67 (N2, Pearson, gc/L) and 0.6 (N2, Spearman, gc/L) to 0.45 (N2, Pearson, gc/day) and 0.5 (N2, Spearman, gc/day), respectively (Table 2). Conversely, normalizations using TSS and flow rate×TSS enhanced the correlations of gene concentrations among the three methods. For instance, higher correlation coefficients (Pearson's r ranged from 0.73 (N1 gene) to 0.76 (N2 gene), Spearman's r ranged from 0.64 (N2 gene) to 0.66 (N1 gene), all $p < 0.05$) were observed between PEG and filtration gene concentrations after normalization using flow rate×TSS compared to the correlation coefficients for non-normalized data (gc/L) (Pearson's r ranged from 0.63 (N1 gene) to 0.67 (N2 gene), Spearman's $r = 0.6$ (both N1 and N2 gene), all $p < 0.05$).

3.2.2. Dynamic time warping of N1 and N2 gene concentrations among three concentration methods

Detecting patterns and comparing similarities of gene concentration time series data are critical for comparing the concentration methods. Dynamic time warping (DTW) identifies the most similar patterns and the optimal warping match between two time series by calculating the minimum DTW distance (51, 53, 58). Shorter DTW distances indicate higher degree of similarity in patterns/shapes between two time series (59, 60). Table 3 presents the DTW minimum distances among the N1 and N2 gene concentrations by VIRADEL, PEG, and filtration methods. Smallest DTW distances were observed between VIRADEL and filtration for both non-normalized and normalized data, which indicated that VIRADEL has a higher degree of similarity with filtration than with PEG. Largest DTW distances were observed between VIRADEL and PEG for both non-normalized and normalized data, indicating that VIRADEL and PEG have the least similarity. This finding was consistent with the sampling and concentration mechanisms since VIRADEL targets free and suspended viral particles in the dissolved phase of wastewater, whereas PEG targets particle-associated viruses, some of which may represent previously shed and accumulated viruses in the sewer stream (3, 22).

Normalization using flow rate decreased the similarity among methods. For instance, the DTW distance between VIRADEL and filtration increased significantly after normalizing using flow rate (gc/day), indicating that the similarity between VIRADEL and filtration was reduced after normalization (Table 3). Conversely, normalization using TSS and flow rate×TSS strengthened the similarity among methods. For instance, the DTW distances decreased in gc/mg TSS and gc/(L(pounds/day)) comparing to the DTW distance in gc/L among the methods, indicating the

TABLE 2 Correlation coefficients among gene concentrations by VIRADEL, PEG, and filtration methods.

Methods (Unit)	Gene (Correlation)			
	N1 (Pearson)	N1 (Spearman)	N2 (Pearson)	N2 (Spearman)
V-P (gc/L)	0.17	0.36	0.12	0.34
V-P (gc/day)	0.10	0.17	0.11	0.13
V-P (gc/day/person)	0.10	0.17	0.11	0.13
V-P (gc/mg TSS)	0.29	0.41	0.27	0.46
V-P (gc/(L(pounds/day)))	0.46	0.58	0.43	0.62
V-F (gc/L)	0.41	0.46	0.23	0.40
V-F (gc/day)	0.26	0.13	0.04	0.05
V-F (gc/day/person)	0.26	0.13	0.04	0.05
V-F (gc/mg TSS)	0.49	0.47	0.27	0.39
V-F (gc/(L(pounds/day)))	0.59	0.64	0.41	0.60
P-F (gc/L)	0.63	0.60	0.67	0.60
P-F (gc/day)	0.46	0.51	0.45	0.50
P-F (gc/day/person)	0.46	0.51	0.45	0.50
P-F (gc/mg TSS)	0.67	0.63	0.68	0.60
P-F (gc/(L(pounds/day)))	0.73	0.66	0.76	0.64

V represents VIRADEL, P represents PEG, F represents filtration.

TABLE 3 Dynamic time warping (DTW) minimum distances among gene concentrations by VIRADEL, PEG, and filtration methods.

Methods (Unit)	Gene	
	N1	N2
V-P (gc/L)	4.37E+07	4.07E+07
V-P (gc/day)	3.23E+16	3.06E+16
V-P (gc/day/person)	1.04E+04	9.83E+03
V-P (gc/mg TSS)	3.93E+05	3.68E+05
V-P (gc/(L(pounds/day)))	2.42E+02	2.23E+02
V-F (gc/L)	7.51E+06	3.14E+06
V-F (gc/day)	5.87E+15	2.35E+15
V-F (gc/day/person)	1.89E+03	7.56E+02
V-F (gc/mg TSS)	6.74E+04	2.84E+04
V-F (gc/(L(pounds/day)))	4.33E+01	1.92E+01
P-F (gc/L)	2.60E+07	2.85E+07
P-F (gc/day)	1.83E+16	2.27E+16
P-F (gc/day/person)	5.89E+03	7.30E+03
P-F (gc/mg TSS)	2.45E+05	2.94E+05
P-F (gc/(L(pounds/day)))	1.46E+02	1.66E+02

V represents VIRADEL, P represents PEG, F represents filtration.

improvement of similarity among methods after normalization (Table 3).

3.3. Similarity and TLCC analysis between three concentration methods and COVID-19 cases

3.3.1. Dynamic time warping between three concentration methods and COVID-19 cases

Wastewater surveillance data for COVID-19 primarily contain temporal data of viral gene concentrations and clinical cases. DTW analysis were performed between gene concentrations derived from the three concentration methods (VIRADEL, PEG, and filtration) and the 7-day moving average of total COVID-19 cases for both normalized and non-normalized data. For non-normalized data (gc/L), the smallest DTW distance was found between VIRADEL and total COVID-19 cases (Table 4). This indicates that VIRADEL (gc/L) has the highest similarity to total COVID-19 cases among the three concentration methods tested. The largest DTW distance was found between PEG (gc/L) and total COVID-19 cases, indicating the PEG method for concentration yields the least similarity to clinical cases. Normalizing gene concentration data using flow (gc/day) demonstrated similar findings. Conversely, normalization using TSS and flow×TSS can significantly increase the similarity between PEG and total COVID-19 cases but concurrently decrease the similarity between VIRADEL and total COVID-19 cases. Specifically, for normalized data (gc/mg TSS, gc/L(pounds/day)), the smallest DTW distance was identified between PEG and total COVID-19 cases, indicating the PEG has the highest similarity to total COVID-19 cases. The largest DTW distance was identified between VIRADEL and COVID-19 cases, indicating that VIRADEL has the lowest similarity to total COVID-19 cases.

TABLE 4 Dynamic time warping (DTW) minimum distances between gene concentrations by VIRADEL, PEG, as well as filtration methods and total COVID-19 cases.

Method-cases (Unit)	Gene	
	N1	N2
V-cases (gc/L)	1.04E+05	1.28E+05
V-cases (gc/day)	4.72E+14	4.86E+14
V-cases (gc/day/person)	4.61E+05	4.61E+05
V-cases (gc/mg TSS)	4.55E+05	4.54E+05
V-cases (gc/(L(pounds/day)))	4.61E+05	4.61E+05
P-cases (gc/L)	4.39E+07	4.08E+07
P-cases (gc/day)	3.30E+16	3.14E+16
P-cases (gc/day/person)	4.43E+05	4.42E+05
P-cases (gc/mg TSS)	9.87E+04	1.14E+05
P-cases (gc/(L(pounds/day)))	4.61E+05	4.61E+05
F-cases (gc/L)	7.35E+06	2.95E+06
F-cases (gc/day)	6.20E+15	2.82E+15
F-cases (gc/day/person)	4.57E+05	4.59E+05
F-cases (gc/mg TSS)	2.87E+05	3.92E+05
F-cases (gc/(L(pounds/day)))	4.61E+05	4.61E+05

V represents VIRADEL, P represents PEG, F represents filtration, cases represents total 7-day-moving-average clinical cases.

3.3.2. Time lagged cross correlation and peak synchrony between three concentration methods and COVID-19 cases

The relative timing of the wastewater gene concentrations {gc/L, gc/day, gc/day/person, gc/mg TSS, and gc/[L(pounds/day)]} of VIRADEL, PEG and filtration were compared to the total COVID-19 cases using TLCC and peak synchrony. To evaluate if wastewater viral concentrations of the three methods lead or lag COVID-19 cases, the total COVID-19 case data were shifted by a period of −20 (lagging) to +20 days (leading) and the Pearson's correlation coefficients were calculated between cases and wastewater viral gene concentration for each shift. The leading or lagging metric varied for each method, which was determined by comparing the strongest Pearson's correlation coefficient.

For the VIRADEL method, both N1 and N2 gene concentrations (gc/L) were strongly correlated with COVID-19 cases, covering shifting windows between −20 and + 20 days (Figure 7A). The highest correlation coefficient was observed when offset is +12 days (Figure 7A), indicating that SARS-CoV-2 gene concentrations (gc/L) in wastewater by the VIRADEL method lead COVID-19 cases by 12 days, which concurred with previous findings of a 35-day lead time of gene concentrations preceding total COVID-19 cases prior to the Omicron surge (3). For both non-normalized and normalized data, VIRADEL always led COVID-19 cases with a variety of lead times (Table 5).

For the PEG method (gc/L), the strongest correlation coefficients were observed with an offset of -12 days, indicating that SARS-CoV-2 gene concentrations by the PEG method lagged reported COVID-19 cases by 12 days during the study period (Figure 7B).

For the filtration method (gc/L), the highest correlation coefficient was observed with an offset of -7 days for the N1 gene

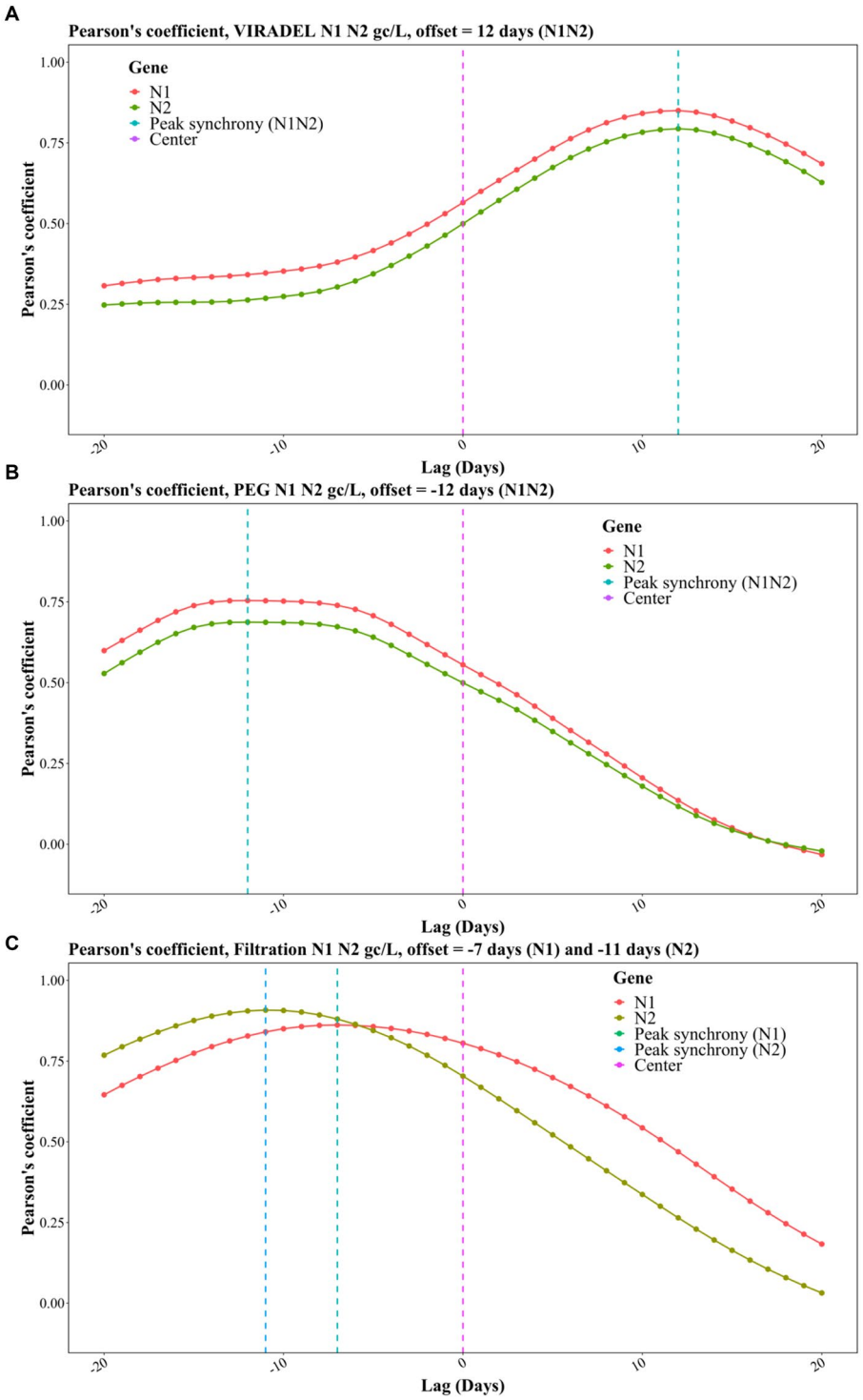

FIGURE 7
Pearson correlation coefficients for TLCC and peak synchrony between wastewater viral concentrations and COVID-19 cases with offsets between −20 (lagging) and + 20 (leading) days for the three methods, including **(A)** VIRADEL, **(B)** PEG, and **(C)** Filtration.

and -11 days for the N2 gene, indicating that SARS-CoV-2 gene concentrations in wastewater lagged reported COVID-19 cases for 7 days (N1) and 11 days (N2), respectively (Figure 7C). Likewise, similar observations were found for normalized data where the filtration method yielded data that lagged clinical cases (Table 5). Table 5 summarized the lead/lag time between VIRADEL, PEG, and filtration methods and total COVID-19 cases. The length of the leading or lagging time differed with dissimilar normalizations. However, the leading or lagging pattern of each method did not change, where VIRADEL measurements were always leading

TABLE 5 Lead/lag time between wastewater viral concentrations by VIRADEL, PEG, as well as filtration methods and total COVID-19 cases.

Units	Method (Gene)					
	V (N1)	V (N2)	P (N1)	P (N2)	F (N1)	F (N2)
gc/L*	+12	+12	-12	-12	-7	-11
gc/day	+13	+13	-6	-6	-2	-10
gc/day/person	+13	+13	-6	-6	-2	-10
gc/mg TSS	+11	+11	-9	-9	-7	-12
gc/(L(pounds/day))	+9	+9	-14	-14	-11	-13

V represents VIRADEL, P represents PEG, F represents filtration, * was demonstrated in Figure 7., + indicates lead time, – indicates lag time.

COVID-19 cases, whereas PEG and filtration measurements routinely lagged COVID-19 cases.

4. Discussion

There is an ongoing effort to optimize methods to recover and concentrate SARS-CoV-2 from wastewater in support of actionable public health outcomes (33, 61). In this study, three concentration methods were evaluated for concentrating SARS-CoV-2 from wastewater, spanning the transition between Delta and Omicron variants circulating in the Detroit, MI metropolitan area. The three methods share common characteristics, especially downstream where they follow similar procedures of nucleic acid extraction and quantification such as RT-ddPCR or RT-qPCR. Likewise, their recovery efficiencies are reported as comparable (2, 3, 22, 34, 62).

4.1. VIRADEL: opportunities and obstacles

Several studies have previously adopted VIRADEL as the concentration method for SARS-CoV-2 in wastewater (1–4, 13). An attribute of the VIRADEL method is the ability to process large volumes (10 – 50 L) of wastewater, thus facilitating capture of free and suspended viral particles that are arguably most representative of viruses shed by recently infected individuals (3, 35). This establishes VIRADEL as a concentration method capable to provide early warning that leads case reporting (1, 3), which was also verified by TLCC analysis in this study (Table 5). Limiting widescale adoption of VIRADEL is labor-intensive preparation of sampling units which require extensive washing and disinfection prior to use. VIRADEL (63) also requires access to large volumes of wastewater which may not be available to all researchers. Further, the required large volumes may necessitate use of grab samples which typically yield higher variability than composite samples which is the sampling method of choice for many wastewater surveillance efforts (64). VIRADEL requires trained personnel for comparatively laborious work with limited samples ($n = 15$) processed over a relatively long time (4-6 h). VIRADEL also requires multiple large centrifuges as well as expensive and at times, supply chain-limited consumables. Therefore, VIRADEL may not be an ideal choice for routine wastewater surveillance projects in common microbiology laboratories. However, it was clear from the comparative analysis conducted that VIRADEL has clear potential to be implemented as a tool to provide early warning to inform public health actions (1, 3, 13).

4.2. PEG: opportunities and obstacles

Apart from requiring access to a centrifuge, the consumables required are widely available and relatively inexpensive, lending itself as one of the most broadly applied concentration methods for routine wastewater surveillance (3, 22, 31, 33, 62, 63). On the other hand, PEG is restricted to processing smaller volumes of wastewater (usually 0.05 to 2 L) and only a portion of the sample pellet is used to recover and extract RNA, which can be affected by the variation of samples and representation of all viruses in wastewater (3, 22, 33, 35).

Unlike VIRADEL, PEG targets particle-associated viruses consistent with reports that identify solids as the phase yielding highest SARS-CoV-2 concentrations in wastewater (63). While a fraction of these particles will represent recently deposited SARS-CoV-2, the majority may represent previously shed and accumulated viruses in the sewer stream and later resuspended during flow fluctuations, thus providing a mechanism for the method to yield data lagging clinical COVID-19 cases. Though the exact mechanism of PEG is not well understood, several studies proposed that it captures viruses that are sorbed to larger precipitates and solids, consistent with a high quantity of TSS in wastewater (3, 22). In this study, through the DTW analysis, PEG yielded data were normalized using TSS and flow × TSS, which increased the degree of similarity between PEG and total COVID-19 cases (Table 4). This demonstrated that PEG yielded data were largely affected by the presence of TSS. VIRADEL, instead, captured free and suspended viruses in the supernatant wastewater. Thus, normalizing the VIRADEL data using TSS and flow × TSS decreased the similarity between VIRADEL and cases (Table 4).

Through the TLCC analysis, this study also demonstrated that PEG gene concentrations lagged COVID-19 cases (Table 5), which embraced the aforementioned sampling mechanism of PEG (22). PEG method did not provide an early warning (leading window) for COVID-19 cases which concurred with our previous findings, whereas VIRADEL provided early warnings ahead of clinical cases while PEG lagged clinical cases for the Detroit area (3).

However, several studies using PEG provided early warnings of impending COVID-19 cases (65). Notably, in these studies, PEG was applied to different types of samples such as primary sewage sludge, which is a different sample matrix from untreated wastewater samples, thus needing more investigation on the impact of sample types on early warnings (65). Kumar et al. (66) identified early warnings using

PEG in the early stage of the pandemic in August 2020 in India (66). PEG and other concentration methods [such as ultrafiltration (17, 67) and adsorption-precipitation (68)] identified early warnings in the early stage of the pandemic when testing capacities were largely limited, and societal responses to the pandemic and clinical data reporting were significantly delayed (3, 69). In addition, earlier prevalent COVID-19 variants including Alpha, Beta and Gamma were reported with longer incubation times than Delta and Omicron variants, leading to prolonged early warning potentials of wastewater surveillance in the early stages of the pandemic (70).

Though PEG was reported to provide early warnings, it may have a shorter early warning window than VIRADEL due to the fundamental disparity of their targets, that being newly contributed free and suspended viral particles versus particle-attached virus, some of which may be considered previously shed and accumulated and subsequently resuspended from sediment (3). In the current study, PEG was shown to lag clinical cases while VIRADEL was leading clinical cases for both normalized and non-normalized data (Table 5). Overall, the early warning potential of PEG needs further investigations in terms of sample types, sampling mechanisms and locations, stage of the epidemic, among other factors.

4.3. Filtration: opportunities and obstacles

Filtration is commonly applied to recover and concentrate viral RNA in water samples. It achieves generally good recovery efficiencies, is relatively inexpensive using commonly available lab equipment and simple protocols and provides consistent performance and inclusive measurement since it captures viruses from both solids and liquid fractions by nature of forcing free viral particles across trapped solids (33, 37). However, filtration has several drawbacks. First, the number of available filtration units restricts the number of samples that can be processed concurrently (33). Meanwhile, clogging of filters can occur due to high variations of turbidity in wastewater. While this can be offset in part by use of a caulking gun to exert more pressure on the sample being filtered, in reality, volumes are limited to ~0.1 L. Additionally, filtration measurements lagged the COVID-19 clinical cases in the current study, thus, its ability to provide early warnings for impending cases is called into question. The recovery efficiencies also differ with different filters (33).

4.4. Future directions

The mechanism and implications of primarily collecting viruses attached to solids that may have settled and resuspended before sampling, such as by the PEG, needs further investigations. Notably, multiple studies have reported that the integrity of SARS-CoV-2 RNA was higher when sorbed to suspended solids, organic matter, and large bio-solids which provide protection from predation and inactivation. This can be explained by the hydrophobicity of SARS-CoV-2 viral particles, leading to their adherence to wastewater solids and longer persistence compared to free viruses in the supernatant wastewater (71–73).

The implications of seasonal variations in SARS-CoV-2 persistence in wastewater needs further investigations. Seasonal variations of wastewater temperature and pH are reported to affect the persistence of viral RNA in wastewater (74). However, SARS-CoV-2 RNA was shown to be highly stable at 4°C aqueous environment or in a wide pH range at room temperature (75, 76). Multiple studies reported the detectability and persistence of SARS-CoV-2 RNA in untreated wastewater solids samples. For instance, researchers found that SARS-CoV-2 RNA was consistently detected for 29 days and 64 days at 4°C and -20°C, respectively in wastewater solids pelleted by centrifugation (77). Another study indicated that only minimal reduction of SARS-CoV-2 RNA was observed for wastewater solids samples after 100 days (78). Additionally, researchers established models to indicate that viral RNA can be detected in wastewater even with long sewer travel time (100 h), especially with lower average wastewater temperature in northern cities such as Detroit (74). A recent study also indicated that biofilms could mediate the fate of SARS-CoV-2 in wastewater, especially leading the viral RNA to prolonged presence (79).

The effect of varying sampling volumes needs further investigation. Some studies indicated that a larger sampling volume can increase the sensitivity of the sampling method, suggesting that it will detect lower levels of viral RNA in wastewater samples (80). Similarly, researchers suggested that processing of larger sample volumes may help to lower the method detection limits (74). But at the same time, keeping the required samples sizes low can reduce shipping costs between sampling location and the analytical laboratory as well as reduce space for storage (74). Other researchers indicated that detection sensitivity can be improved by increasing the sample volume from 100 mL to 500 mL wastewater for testing SARS-CoV-2 (6).

However, other researchers presented that large-volume sampling did not significantly enhance the sensitivity of methods (81). For instance, Zheng et al. (81) found that wastewater concentration methods (they used ultracentrifugation) using less volume of wastewater was preferable than larger volume of wastewater in terms of sensitivity for testing SARS-CoV-2. The study revealed that when using the same concentration methods, no significant difference was observed in the viral RNA concentrations between experiments conducted with a larger volume of wastewater and those conducted with a smaller volume (81). Some studies indicated that a larger sampling volume may also dilute the wastewater sample, which can lead to a lower viral RNA concentration (82).

Overall, the sampling volume for wastewater surveillance of SARS-CoV-2 using different concentration methods will depend on several factors, including the sensitivity of the method, the concentration of viral RNA in the wastewater, and the size of the population being monitored. It is critical to consider and address these factors when analyzing wastewater surveillance data and more in-depth research on how the sampling volume affect statistical results are needed.

The time of sampling may potentially affect results in sewershed sampling. The effect of sampling time in large interceptors, like the ones sampled in this study, is less significant, since the interceptor wastewater is mixed at the pumping stations. A few studies have reported gene concentration varying on an hourly basis (83, 84) although the temporal variability of SARS-CoV-2 concentrations in wastewater remains ambiguous (83, 85). It has been suggested that composite samples may circumvent the within-day variation of viral concentrations (83). Whereas both the PEG and filtration methods used composite samples, the large volume required for VIRADEL necessitated separate sampling which was conducted over a period of several hours to help reduce temporal variability. Further, considering

the vast sewersheds and population of nearly 4 million people that GLWA's three interceptors serve, the concentrations of SARS-CoV-2 in wastewater may be highly diluted and within-day variations can be negligible. Future studies are called to examine within-day variation of SARS-CoV-2.

Admittedly, there are caveats to the current study that should be considered and discussed. The study period was limited to the transition between Delta and Omicron VOCs that occurred between fall 2021 and winter 2022. With each successive resurgence of COVID-19, differences are reported related to disease trajectory including incubation time, shedding dynamics and disease severity (18, 86). For instance, the incubation time was shorter during the Omicron surge compared to the previous variants, inevitably reducing the early warning potentials of wastewater surveillance in the later stage of the pandemic (3, 86). Further, the changing viral shedding dynamics, viral decay kinetics, and shedding duration of the Omicron variant are not well understood and many uncertainties remain (18, 87). As such, the lead and lag times reported here cannot be extrapolated to past or future SARS-CoV-2 variants. In addition, sampling frequency was limited to weekly samples and thus less informative for establishing time series or less likely to depict accurately the actual fluctuations of wastewater viral concentrations (cdc.gov). Feng et al. (88) proposed a minimum of two samples collected weekly to establish the time series data of wastewater viral concentrations for continuous trend analysis. Some researchers have even suggested daily or very frequent sampling, if the laboratory is capable of handling increased numbers of samples, considering rapid resurgence of COVID-19 cases (89). Indeed, the filtration method has been used to analyze samples 5 days weekly since the emergence of the Omicron VOC as part of Ontario's Wastewater Surveillance Initiative in the Windsor-Essex region located across the international border with Detroit (Q. Geng, R. Corchis-Scott, R.M. McKay, unpublished). While SARS-CoV-2 signal intensity derived from this approach does not provide a clear early warning of clinical cases, preliminary analysis supports its use as a leading indicator of COVID-19-related hospitalizations in the region (Q. Geng, R. Corchis-Scott, R.M. McKay, unpublished). This is important considering that clinical testing capacity across North America was overwhelmed by infections attributed to Omicron and is thus no longer a reliable indicator of disease prevalence (90).

5. Conclusion

This study is among the first to implement, evaluate, and compare commonly applied wastewater virus concentration methodologies to recover and concentrate SARS-CoV-2 from wastewater amid the transition between Delta and Omicron VOCs. Analytical approaches, including Pearson and Spearman correlations, Dynamic Time Warping (DTW), and Time Lagged Cross Correlation (TLCC) and peak synchrony, were performed to analyze the relations among three methods as well as the relations between methods and COVID-19 cases. To our knowledge, this is the only study to implement Dynamic Time Warping to compare wastewater surveillance time series data and successfully identify the similarities/dissimilarities among the methods and between methods and clinical data. The analytical approach used can be applied to different sample processing and concentration methods under various pandemic scenarios to evaluate method efficacy for different public health practices.

Data availability statement

The original contributions presented in the study are included in the article/supplementary material, further inquiries can be directed to the corresponding author.

Author contributions

LZ: methodology, investigation, data acquisition, data curation, formal analysis, visualization, writing–original draft, and writing–review and editing. QG and RC-S: methodology, investigation, data acquisition, and writing–review and editing. RM: methodology, investigation, data acquisition, resources, supervision, funding acquisition, and writing–review and editing. JN: funding acquisition and writing–review and editing. IX: conceptualization, funding acquisition, methodology, investigation, project administration, resources, supervision, and writing–review and editing.

Funding

This study was funded by the Michigan Department of Health and Human Services (MDHHS) and the Great Lakes Water Authority (GLWA). RMM acknowledges support from Ontario Genomics (COVID-19 Regional Genomics Initiative) with additional support provided by the Canada Foundation for Innovation–Exceptional Opportunities Fund (COVID-19 program) and National Institutes of Health [1P01ES028939-01], and National Science Foundation [OCE-1840715] awards to the Bowling Green State University Great Lakes Center for Fresh Waters and Human Health.

Acknowledgments

The authors acknowledge the support from operators, the laboratory team and managers of the Wastewater Resource Recovery Facility at the Great Lakes Water Authority. They also thank CDM Smith for supporting this work.

Conflict of interest

The authors declare that the research was conducted in the absence of any commercial or financial relationships that could be construed as a potential conflict of interest.

Publisher's note

References

1. Miyani B, Zhao L, Spooner M, Buch S, Gentry Z, Mehrotra A, et al. Early warnings of COVID-19 second wave in Detroit. *J Environ Eng (New York)*. (2021) 147:6021004. doi: 10.1061/(ASCE)EE.1943-7870.0001907

2. Li Y, Miyani B, Zhao L, Spooner M, Gentry Z, Zou Y, et al. Surveillance of SARS-CoV-2 in nine neighborhood sewersheds in Detroit Tri-County area, United States: assessing per capita SARS-CoV-2 estimations and COVID-19 incidence. *Sci Total Environ*. (2022) 851:158350. doi: 10.1016/j.scitotenv.2022.158350

3. Zhao L, Zou Y, Li Y, Miyani B, Spooner M, Gentry Z, et al. Five-week warning of COVID-19 peaks prior to the omicron surge in Detroit, Michigan using wastewater surveillance. *Sci Total Environ*. (2022) 844:157040:157040. doi: 10.1016/j.scitotenv.2022.157040

4. Miyani B, Fonoll X, Norton J, Mehrotra A, Xagoraraki I. SARS-CoV-2 in Detroit Wastewater. *J Environ Eng (New York)*. (2020) 146:06020004. doi: 10.1061/(ASCE)EE.1943-7870.0001830

5. Sherchan SP, Shahin S, Ward LM, Tandukar S, Aw TG, Schmitz B, et al. First detection of SARS-CoV-2 RNA in wastewater in North America: a study in Louisiana, USA. *Sci Total Environ*. (2020) 743:140621. doi: 10.1016/j.scitotenv.2020.140621

6. Ahmed W, Bertsch PM, Angel N, Bibby K, Bivins A, Dierens L, et al. Detection of SARS-CoV-2 RNA in commercial passenger aircraft and cruise ship wastewater: a surveillance tool for assessing the presence of COVID-19 infected travellers. *J Travel Med*. (2020) 27:116. doi: 10.1093/jtm/taaa116

7. Ahmed W, Bivins A, Simpson SL, Bertsch PM, Ehret J, Hosegood I, et al. Wastewater surveillance demonstrates high predictive value for COVID-19 infection on board repatriation flights to Australia. *Environ Int*. (2022) 158:106938. doi: 10.1016/j.envint.2021.106938

8. Kaya D, Niemeier D, Ahmed W, Kjellerup BV. Evaluation of multiple analytical methods for SARS-CoV-2 surveillance in wastewater samples. *Sci Total Environ*. (2022) 808:152033. doi: 10.1016/j.scitotenv.2021.152033

9. Ai Y, Davis A, Jones D, Lemeshow S, Tu H, He F, et al. Wastewater SARS-CoV-2 monitoring as a community-level COVID-19 trend tracker and variants in Ohio, United States. *Sci Total Environ*. (2021) 801:149757. doi: 10.1016/j.scitotenv.2021.149757

10. Xiao A, Wu F, Bushman M, Zhang J, Imakaev M, Chai PR, et al. Metrics to relate COVID-19 wastewater data to clinical testing dynamics. *Water Res*. (2022) 212:118070. doi: 10.1016/j.watres.2022.118070

11. Bivins A, Bibby K. Wastewater surveillance during mass COVID-19 vaccination on a college campus. *Environ Sci Technol Lett*. (2021) 8:792–8. doi: 10.1021/acs.estlett.1c00519

12. Chik AHS, Glier MB, Servos M, Mangat CS, Pang XL, Qiu Y, et al. Comparison of approaches to quantify SARS-CoV-2 in wastewater using RT-qPCR: results and implications from a collaborative inter-laboratory study in Canada. *J Environ Sci*. (2021) 107:218–29. doi: 10.1016/j.jes.2021.01.029

13. Zhao L, Zou Y, David RE, Withington S, McFarlane S, Faust RA, et al. Simple methods for early warnings of COVID-19 surges: lessons learned from 21 months of wastewater and clinical data collection in Detroit, Michigan, United States. *Sci Total Environ*. (2022):161152. doi: 10.1016/j.scitotenv.2022.161152

14. Jones DL, Baluja MQ, Graham DW, Corbishley A, McDonald JE, Malham SK, et al. Shedding of SARS-CoV-2 in feces and urine and its potential role in person-to-person transmission and the environment-based spread of COVID-19. *Sci Total Environ*. (2020) 749:141364. doi: 10.1016/j.scitotenv.2020.141364

15. He X, Lau EHY, Wu P, Deng X, Wang J, Hao X, et al. Temporal dynamics in viral shedding and transmissibility of COVID-19. *Nat Med*. (2020) 26:672–5. doi: 10.1038/s41591-020-0869-5

16. Haramoto E, Malla B, Thakali O, Kitajima M. First environmental surveillance for the presence of SARS-CoV-2 RNA in wastewater and river water in Japan. *Sci Total Environ*. (2020) 737:140405. doi: 10.1016/j.scitotenv.2020.140405

17. Medema G, Heijnen L, Elsinga G, Italiaander R, Brouwer A. Presence of SARS-Coronavirus-2 RNA in sewage and correlation with reported COVID-19 prevalence in the early stage of the epidemic in the Netherlands. *Environ Sci Technol Lett*. (2020) 7:511–6. doi: 10.1021/acs.estlett.0c00357

18. Boucau J, Marino C, Regan J, Uddin R, Choudhary MC, Flynn JP, et al. Duration of shedding of Culturable virus in SARS-CoV-2 omicron (BA.1) infection. *N Engl J Med*. (2022) 387:275–7. doi: 10.1056/NEJMc2202092

19. Farkas K, Hillary LS, Malham SK, McDonald JE, Jones DL. Wastewater and public health: the potential of wastewater surveillance for monitoring COVID-19. *Curr Opin Environ Sci Health*. (2020) 17:14–20. doi: 10.1016/j.coesh.2020.06.001

20. Xagoraraki I, Yin Z, Svambayev Z. Fate of viruses in water systems. *J Environ Eng*. (2014) 140:04014020. doi: 10.1061/(ASCE)EE.1943-7870.0000827

21. Xagoraraki I. Can we predict viral outbreaks using wastewater surveillance? *J Environ Eng*. (2020) 146:01820003. doi: 10.1061/(ASCE)EE.1943-7870.0001831

22. Flood MT, D'Souza N, Rose JB, Aw TG. Methods evaluation for rapid concentration and quantification of SARS-CoV-2 in raw wastewater using droplet digital and quantitative RT-PCR. *Food Environ Virol*. (2021) 13:303–15. doi: 10.1007/s12560-021-09488-8

23. Wallis C, Henderson M, Melnick JL. Enterovirus Concentration on Cellulose Membranes. *Appl Microbiol*. (1972) 23:476–80. doi: 10.1128/am.23.3.476-480.1972

24. Jakubowski W, Hill WF, Clarke NA. Comparative study of four microporous filters for concentrating viruses from drinking water. *Appl Microbiol*. (1975) 30:58–65. doi: 10.1128/am.30.1.58-65.1975

25. Lee H, Kim M, Paik SY, Lee CH, Jheong WH, Kim J, et al. Evaluation of electropositive filtration for recovering norovirus in water. *J Water Health*. (2011) 9:27–36. doi: 10.2166/wh.2010.190

26. Hill VR, Polaczyk AL, Kahler AM, Cromeans TL, Hahn D, Amburgey JE. Comparison of hollow-Fiber ultrafiltration to the USEPA VIRADEL technique and USEPA method 1623. *JEQ*. (2009) 38:822–5. doi: 10.2134/jeq2008.0152

27. Black LE, Brion GM, Freitas SJ. Multivariate logistic regression for predicting Total Culturable virus presence at the intake of a potable-water treatment plant: novel application of the atypical coliform/Total coliform ratio. *Appl Environ Microbiol*. (2007) 73:3965–74. doi: 10.1128/AEM.02780-06

28. Francy DS, Stelzer EA, Brady AMG, Huitger C, Bushon RN, Ip HS, et al. Comparison of filters for concentrating microbial indicators and pathogens in Lake water samples. *Appl Environ Microbiol*. (2013) 79:1342–52. doi: 10.1128/AEM.03117-12

29. Ye Y, Ellenberg RM, Graham KE, Wigginton KR. Survivability, partitioning, and recovery of enveloped viruses in untreated municipal wastewater. *Environ Sci Technol*. (2016) 50:5077–85. doi: 10.1021/acs.est.6b00876

30. Michael-Kordatou I, Karaolia P, Fatta-Kassinos D. Sewage analysis as a tool for the COVID-19 pandemic response and management: the urgent need for optimised protocols for SARS-CoV-2 detection and quantification. *J Environ Chem Eng*. (2020) 8:104306. doi: 10.1016/j.jece.2020.104306

31. Sapula SA, Whittall JJ, Pandopulos AJ, Gerber C, Venter H. An optimized and robust PEG precipitation method for detection of SARS-CoV-2 in wastewater. *Sci Total Environ*. (2021) 785:147270. doi: 10.1016/j.scitotenv.2021.147270

32. Barril PA, Pianciola LA, Mazzeo M, Ousset MJ, Jaureguiberry MV, Alessandrello M, et al. Evaluation of viral concentration methods for SARS-CoV-2 recovery from wastewaters. *Sci Total Environ*. (2021) 756:144105. doi: 10.1016/j.scitotenv.2020.144105

33. Ahmed W, Bertsch PM, Bivins A, Bibby K, Farkas K, Gathercole A, et al. Comparison of virus concentration methods for the RT-qPCR-based recovery of murine hepatitis virus, a surrogate for SARS-CoV-2 from untreated wastewater. *Sci Total Environ*. (2020) 739:139960. doi: 10.1016/j.scitotenv.2020.139960

34. Pecson BM, Darby E, Haas CN, Amha YM, Bartolo M, Danielson R, et al. Reproducibility and sensitivity of 36 methods to quantify the SARS-CoV-2 genetic signal in raw wastewater: findings from an interlaboratory methods evaluation in the U.S. *Environ Sci (Camb)*. (2021) 7:504–20. doi: 10.1039/d0ew00946f

35. Lu D, Huang Z, Luo J, Zhang X, Sha S. Primary concentration–the critical step in implementing the wastewater based epidemiology for the COVID-19 pandemic: a mini-review. *Sci Total Environ*. (2020) 747:141245. doi: 10.1016/j.scitotenv.2020.141245

36. McKindles KM, Manes MA, DeMarco JR, McClure A, McKay RM, Davis TW, et al. Dissolved microcystin release coincident with lysis of a bloom dominated by Microcystis spp. in Western Lake Erie attributed to a novel Cyanophage. *Appl Environ Microbiol*. (2020) 86:20. doi: 10.1128/AEM.01397-20

37. Gonçalves J, Koritnik T, Mioč V, Trkov M, Bolješič M, Berginc N, et al. Detection of SARS-CoV-2 RNA in hospital wastewater from a low COVID-19 disease prevalence area. *Sci Total Environ*. (2021) 755:143226. doi: 10.1016/j.scitotenv.2020.143226

38. Corchis-Scott R, Geng Q, Seth R, Ray R, Beg M, Biswas N, et al. Averting an outbreak of SARS-CoV-2 in a university residence hall through wastewater surveillance. *Microbiol Spectr*. (2021) 9:21. doi: 10.1128/Spectrum.00792-21

39. Kantor RS, Nelson KL, Greenwald HD, Kennedy LC. Challenges in measuring the recovery of SARS-CoV-2 from wastewater. *Environ Sci Technol*. (2021) 55:3514–9. Available from:. doi: 10.1021/acs.est.0c08210

40. Lu X, Wang L, Sakthivel SK, Whitaker B, Murray J, Kamili S, et al. US CDC real-time reverse transcription PCR panel for detection of severe acute respiratory syndrome coronavirus 2. *Emerg Infect Dis*. (2020) 26:1654–65. doi: 10.3201/eid2608.201246

41. Menkir TF, Chin T, Hay JA, Surface ED, de Salazar PM, Buckee CO, et al. Estimating internationally imported cases during the early COVID-19 pandemic. *Nat Commun*. (2021) 12:311. doi: 10.1038/s41467-020-20219-8

42. Barua VB, Juel MAI, Blackwood AD, Clerkin T, Ciesielski M, Sorinolu AJ, et al. Tracking the temporal variation of COVID-19 surges through wastewater-based epidemiology during the peak of the pandemic: a six-month long study in Charlotte, North Carolina. *Sci Total Environ*. (2022) 814:152503:152503. doi: 10.1016/j.scitotenv.2021.152503

43. Lepot M, Aubin JB, Clemens F. Interpolation in time series: an introductive overview of existing methods, their performance criteria and uncertainty assessment. *Water (Basel)*. (2017) 9:796. doi: 10.3390/w9100796

44. Hopkins L, Persse D, Caton K, Ensor K, Schneider R, McCall C, et al. Citywide wastewater SARS-CoV-2 levels strongly correlated with multiple disease surveillance indicators and outcomes over three COVID-19 waves. *Sci Total Environ*. (2023) 855:158967. doi: 10.1016/j.scitotenv.2022.158967

45. Terry IB, Meschke JS. *Variability in normalization methods of COVID-19 wastewater surveillance*. ProQuest dissertations and theses, Ann Arbor. (2022). Available at: http://ezproxy.msu.edu/login?url=https://www.proquest.com/dissertations-theses/variability-normalization-methods-covid-19/docview/2695037740/se-2?accountid=12598.

46. D'Aoust PM, Mercier E, Montpetit D, Jia JJ, Alexandrov I, Neault N, et al. Quantitative analysis of SARS-CoV-2 RNA from wastewater solids in communities with low COVID-19 incidence and prevalence. *Water Res X*. (2021) 188:116560. doi: 10.1016/j.watres.2020.116560

47. Vadde KK, Al-Duroobi H, Phan DC, Jafarzadeh A, Moghadam SV, Matta A, et al. Assessment of concentration, recovery, and normalization of SARS-CoV-2 RNA from two wastewater treatment plants in Texas and correlation with COVID-19 cases in the community. *ACS ES&T Water*. (2022) 2022:54. doi: 10.1021/acsestwater.2c00054

48. Ye J, Xiao C, Esteves RM, Rong C. *Time series similarity evaluation based on Spearman's correlation coefficients and distance measures*, pp. 319–331. (2015).

49. Keogh E, Ratanamahatana CA. Exact indexing of dynamic time warping. *Knowl Inf Syst*. (2005) 7:358–86. doi: 10.1007/s10115-004-0154-9

50. Izakian H, Pedrycz W, Jamal I. Fuzzy clustering of time series data using dynamic time warping distance. *Eng Appl Artif Intell*. (2015) 39:235–44. doi: 10.1016/j.engappai.2014.12.015

51. Giorgino T. Computing and visualizing dynamic time warping alignments in R: the dtw package. *J Stat Softw*. (2009) 31:1–24.

52. Rakthanmanon T, Campana B, Mueen A, Batista G, Westover B, Zhu Q, et al. *Searching and mining trillions of time series subsequences under dynamic time warping*. In: Proceedings of the 18th ACM SIGKDD international conference on knowledge discovery and data mining - KDD'12. New York, USA: ACM Press, p. 262. (2012).

53. Jeong YS, Jeong MK, Omitaomu OA. Weighted dynamic time warping for time series classification. *Pattern Recogn*. (2011) 44:2231–40. doi: 10.1016/j.patcog.2010.09.022

54. Shen C. Analysis of detrended time-lagged cross-correlation between two nonstationary time series. *Phys Lett A*. (2015) 379:680–7. doi: 10.1016/j.physleta.2014.12.036

55. Mei DC, Du LC, Wang CJ. The effects of time delay on stochastic resonance in a Bistable system with correlated noises. *J Stat Phys*. (2009) 137:625–38. doi: 10.1007/s10955-009-9864-4

56. Li H, Futch SH, Syvertsen JP. Cross-correlation patterns of air and soil temperatures, rainfall and *Diaprepes abbreviatus* root weevil in citrus. *Pest Manag Sci*. (2007) 63:1116–23. doi: 10.1002/ps.1431

57. Lancaster E, Byrd K, Ai Y, Lee J. Socioeconomic status correlations with confirmed COVID-19 cases and SARS-CoV-2 wastewater concentrations in small-medium sized communities. *Environ Res*. (2022) 215:114290. doi: 10.1016/j.envres.2022.114290

58. Berndt DJ, Clifford J. *Using dynamic time warping to find patterns in time series*. KDD workshop. Seattle, WA, pp. 359–370. (1994).

59. Liu L, Li W, Jia H. Method of time series similarity measurement based on dynamic time warping. *Comput Mater Contin*. (2018) 57:97–106. doi: 10.32604/cmc.2018.03511

60. Guan X, Huang C, Liu G, Meng X, Liu Q. Mapping Rice cropping Systems in Vietnam Using an NDVI-based time-series similarity measurement based on DTW distance. *Remote Sens*. (2016) 8:19. doi: 10.3390/rs8010019

61. Kitajima M, Ahmed W, Bibby K, Carducci A, Gerba CP, Hamilton KA, et al. SARS-CoV-2 in wastewater: state of the knowledge and research needs. *Sci Total Environ*. (2020) 2020:139076. doi: 10.1016/j.scitotenv.2020.139076

62. Hata A, Hara-Yamamura H, Meuchi Y, Imai S, Honda R. Detection of SARS-CoV-2 in wastewater in Japan during a COVID-19 outbreak. *Sci Total Environ*. (2021) 758:143578. doi: 10.1016/j.scitotenv.2020.143578

63. Torii S, Furumai H, Katayama H. Applicability of polyethylene glycol precipitation followed by acid guanidinium thiocyanate-phenol-chloroform extraction for the detection of SARS-CoV-2 RNA from municipal wastewater. *Sci Total Environ*. (2021) 756:143067. doi: 10.1016/j.scitotenv.2020.143067

64. Bivins A, Kaya D, Ahmed W, Brown J, Butler C, Greaves J, et al. Passive sampling to scale wastewater surveillance of infectious disease: lessons learned from COVID-19. *Sci Total Environ*. (2022) 835:155347. doi: 10.1016/j.scitotenv.2022.155347

65. D'Aoust PM, Graber TE, Mercier E, Montpetit D, Alexandrov I, Neault N, et al. Catching a resurgence: increase in SARS-CoV-2 viral RNA identified in wastewater 48 h before COVID-19 clinical tests and 96 h before hospitalizations. *Sci Total Environ*. (2021) 770:145319. doi: 10.1016/j.scitotenv.2021.145319

66. Kumar M, Joshi M, Patel AK, Joshi CG. Unravelling the early warning capability of wastewater surveillance for COVID-19: a temporal study on SARS-CoV-2 RNA detection and need for the escalation. *Environ Res*. (2021) 196:110946. doi: 10.1016/j.envres.2021.110946

67. Hasan SW, Ibrahim Y, Daou M, Kannout H, Jan N, Lopes A, et al. Detection and quantification of SARS-CoV-2 RNA in wastewater and treated effluents: surveillance of COVID-19 epidemic in the United Arab Emirates. *Sci Total Environ*. (2021) 764:142929. doi: 10.1016/j.scitotenv.2020.142929

68. Randazzo W, Truchado P, Cuevas-Ferrando E, Simón P, Allende A, Sánchez G. SARS-CoV-2 RNA in wastewater anticipated COVID-19 occurrence in a low prevalence area. *Water Res*. (2020) 181:115942. doi: 10.1016/j.watres.2020.115942

69. Bibby K, Bivins A, Wu Z, North D. Making waves: plausible lead time for wastewater based epidemiology as an early warning system for COVID-19. *Water Res*. (2021) 202:117438. doi: 10.1016/j.watres.2021.117438

70. Wu Y, Kang L, Guo Z, Liu J, Liu M, Liang W. Incubation period of COVID-19 caused by unique SARS-CoV-2 strains. *JAMA Netw Open*. (2022) 5:e2228008. doi: 10.1001/jamanetworkopen.2022.28008

71. Abu Ali H, Yaniv K, Bar-Zeev E, Chaudhury S, Shagan M, Lakkakula S, et al. Tracking SARS-CoV-2 RNA through the wastewater treatment process. *ACS ES&T Water*. (2021) 1:1161–7. doi: 10.1021/acsestwater.0c00216

72. Gundy PM, Gerba CP, Pepper IL. Survival of coronaviruses in water and wastewater. *Food Environ Virol*. (2009) 1:10. doi: 10.1007/s12560-008-9001-6

73. Panchal D, Prakash O, Bobde P, Pal S. SARS-CoV-2: sewage surveillance as an early warning system and challenges in developing countries. *Environ Sci Pollut Res*. (2021) 28:22221–40. doi: 10.1007/s11356-021-13170-8

74. Hart OE, Halden RU. Computational analysis of SARS-CoV-2/COVID-19 surveillance by wastewater-based epidemiology locally and globally: feasibility, economy, opportunities and challenges. *Sci Total Environ*. (2020) 730:138875. doi: 10.1016/j.scitotenv.2020.138875

75. Ahmed W, Bertsch PM, Bibby K, Haramoto E, Hewitt J, Huygens F, et al. Decay of SARS-CoV-2 and surrogate murine hepatitis virus RNA in untreated wastewater to inform application in wastewater-based epidemiology. *Environ Res*. (2020) 191:110092. doi: 10.1016/j.envres.2020.110092

76. Chin AWH, Chu JTS, Perera MRA, Hui KPY, Yen HL, Chan MCW, et al. Stability of SARS-CoV-2 in different environmental conditions. *Lancet Microb*. (2020) 1:e10. doi: 10.1016/S2666-5247(20)30003-3

77. Hokajärvi AM, Rytkönen A, Tiwari A, Kauppinen A, Oikarinen S, Lehto KM, et al. The detection and stability of the SARS-CoV-2 RNA biomarkers in wastewater influent in Helsinki, Finland. *Sci Total Environ*. (2021) 770:145274. doi: 10.1016/j.scitotenv.2021.145274

78. Simpson A, Topol A, White BJ, Wolfe MK, Wigginton KR, Boehm AB. Effect of storage conditions on SARS-CoV-2 RNA quantification in wastewater solids. *PeerJ*. (2021) 9:e11933. doi: 10.7717/peerj.11933

79. Li J, Ahmed W, Metcalfe S, Smith WJM, Choi PM, Jackson G, et al. Impact of sewer biofilms on fate of SARS-CoV-2 RNA and wastewater surveillance. *Nat Water*. (2023) 1:272–80. doi: 10.1038/s44221-023-00033-4

80. McMinn BR, Korajkic A, Kelleher J, Herrmann MP, Pemberton AC, Ahmed W, et al. Development of a large volume concentration method for recovery of coronavirus from wastewater. *Sci Total Environ*. (2021) 774:145727. doi: 10.1016/j.scitotenv.2021.145727

81. Zheng X, Deng Y, Xu X, Li S, Zhang Y, Ding J, et al. Comparison of virus concentration methods and RNA extraction methods for SARS-CoV-2 wastewater surveillance. *Sci Total Environ*. (2022) 824:153687. doi: 10.1016/j.scitotenv.2022.153687

82. Bertels X, Demeyer P, van den Bogaert S, Boogaerts T, van Nuijs ALN, Delputte P, et al. Factors influencing SARS-CoV-2 RNA concentrations in wastewater up to the sampling stage: a systematic review. *Sci Total Environ*. (2022) 820:153290. doi: 10.1016/j.scitotenv.2022.153290

83. Bivins A, North D, Wu Z, Shaffer M, Ahmed W, Bibby K. Within-and between-day variability of SARS-CoV-2 RNA in municipal wastewater during periods of varying COVID-19 prevalence and positivity. *Acs Es&T Water*. (2021) 1:2097–108. doi: 10.1021/acsestwater.1c00178

84. Li B, Di DYW, Saingam P, Jeon MK, Yan T. Fine-scale temporal dynamics of SARS-CoV-2 RNA abundance in wastewater during a COVID-19 lockdown. *Water Res*. (2021) 197:117093. doi: 10.1016/j.watres.2021.117093

85. Ahmed W, Bivins A, Bertsch PM, Bibby K, Gyawali P, Sherchan SP, et al. Intraday variability of indicator and pathogenic viruses in 1-h and 24-h composite wastewater samples: implications for wastewater-based epidemiology. *Environ Res*. (2021) 193:110531. doi: 10.1016/j.envres.2020.110531

86. Baker MA, Rhee C, Tucker R, Badwaik A, Coughlin C, Holtzman MA, et al. Rapid control of hospital-based severe acute respiratory syndrome coronavirus 2 omicron clusters through daily testing and universal use of N95 respirators. *Rev Infect Dis*. (2022) 75:e296–9. doi: 10.1093/cid/ciac113

87. Kandel C, Lee Y, Taylor M, Llanes A, McCready J, Crowl G, et al. Viral dynamics of the SARS-CoV-2 omicron variant among household contacts with 2 or 3 COVID-19 vaccine doses. *J Infect*. (2022) 85:666–70. doi: 10.1016/j.jinf.2022.10.027

88. Feng S, Roguet A, McClary-Gutierrez JS, Newton RJ, Kloczko N, Meiman JG, et al. Evaluation of sampling, analysis, and normalization methods for SARS-CoV-2 concentrations in wastewater to assess COVID-19 burdens in Wisconsin communities. *ACS ES&T Water*. (2021) 1:1955–65. doi: 10.1021/acsestwater.1c00160

89. Zhu Y, Oishi W, Maruo C, Saito M, Chen R, Kitajima M, et al. Early warning of COVID-19 via wastewater-based epidemiology: potential and bottlenecks. *Sci Total Environ*. (2021) 767:145124. doi: 10.1016/j.scitotenv.2021.145124

90. Lawal OU, Zhang L, Parreira VR, Brown RS, Chettleburgh C, Dannah N, et al. Metagenomics of wastewater influent from wastewater treatment facilities across Ontario in the era of emerging SARS-CoV-2 variants of concern. *Microbiol Resour Announc*. (2022) 11:e0036222. doi: 10.1128/mra.00362-22

frontiers | Frontiers in Public Health

TYPE Brief Research Report
PUBLISHED 27 July 2023
DOI 10.3389/fpubh.2023.1141136

OPEN ACCESS

EDITED BY
David Champredon,
Public Health Agency of Canada (PHAC), Canada

REVIEWED BY
Robert Michael McKay,
University of Windsor, Canada
Ingrid Friesema,
National Institute for Public Health and the Environment, Netherlands

*CORRESPONDENCE
Golam Islam
golam.islam@ontariotechu.ca

RECEIVED 10 January 2023
ACCEPTED 10 July 2023
PUBLISHED 27 July 2023

CITATION
de Melo T, Islam G, Simmons DBD, Desaulniers J-P and Kirkwood AE (2023) An alternative method for monitoring and interpreting influenza A in communities using wastewater surveillance.
Front. Public Health 11:1141136.
doi: 10.3389/fpubh.2023.1141136

An alternative method for monitoring and interpreting influenza A in communities using wastewater surveillance

Tomas de Melo, Golam Islam*, Denina B. D. Simmons, Jean-Paul Desaulniers and Andrea E. Kirkwood

Faculty of Science, Ontario Tech University, Oshawa, ON, Canada

Seasonal influenza is an annual public health challenge that strains healthcare systems, yet population-level prevalence remains under-reported using standard clinical surveillance methods. Wastewater surveillance (WWS) of influenza A can allow for reliable flu surveillance within a community by leveraging existing severe acute respiratory syndrome coronavirus 2 (SARS-CoV-2) WWS networks regardless of the sample type (primary sludge vs. primary influent) using an RT-qPCR-based viral RNA detection method for both targets. Additionally, current influenza A outbreaks disproportionately affect the pediatric population. In this study, we show the utility of interpreting influenza A WWS data with elementary student absenteeism due to illness to selectively interpret disease spread in the pediatric population. Our results show that the highest statistically significant correlation ($R_S = 0.96$, $p = 0.011$) occurred between influenza A WWS data and elementary school absences due to illness. This correlation coefficient is notably higher than the correlations observed between influenza A WWS data and influenza A clinical case data ($R_S = 0.79$, $p = 0.036$). This method can be combined with a suite of pathogen data from wastewater to provide a robust system for determining the causative agents of diseases that are strongly symptomatic in children to infer pediatric outbreaks within communities.

KEYWORDS

influenza A, SARS-CoV-2, student absenteeism, wastewater, RT-qPCR

1. Introduction

As the world continues to deal with ongoing challenges associated with the COVID-19 pandemic, the re-emergence of seasonal respiratory pathogens such as influenza poses an additive threat to public health. Influenza and pneumonia are ranked among the top 10 leading causes of death in Canada. It is estimated that influenza causes approximately 12,200 hospitalizations and 3,500 deaths per year (1). With numerous non-pharmaceutical interventions placed during the COVID-19 pandemic, the dynamics of influenza exposure and transmission, incidence rates, and symptom severity may have changed. This is evident by the current increase in influenza infections and influenza-associated hospitalization rates in Canada, which are above-expected levels that are typical for the flu season, spanning from August 2022 to February 2023 (1, 2). Thus, there is now an immediate demand for improved surveillance of this contagious disease.

Influenza viruses arise from the family Orthomyxoviridae. This family is unique in that they are enveloped viruses with genomes that consist of negative-sense single-stranded RNA segments (3). There are four types of influenza viruses, A, B, C, and D. Within these,

influenza A is the only flu virus known to cause flu pandemics (4). The influenza A type virus is further classified into subtypes, clades, and subclades based on the presence of surface viral proteins hemagglutinin (H) and neuraminidase (N). Currently, the most commonly detected subtypes found circulating in human infections are A(H1N1) and A(H3N2) (4). The most commonly reported symptoms of the virus are fever, cough, runny nose, body aches, and sore throat (4).

One of the important lessons learned from the COVID-19 pandemic is that monitoring respiratory pathogens through conventional clinical testing (nasal swabs, sample collection, and RT-qPCR) presents many challenges and may not be sufficient for pathogen surveillance where timely information is required. Thus, the surveillance of pathogens in wastewater has been successfully implemented as a credible technique to complement monitoring SARS-CoV-2 infections within communities (4, 5). When clinical SARS-CoV-2 tests were widely available in Canada, they provided a reliable and robust metric that correlates with SARS-CoV-2 RNA concentrations in domestic wastewater (5, 6). However, interpreting SARS-CoV-2 wastewater data has been challenging (variable correlation strength, lack of reported cases, and inconsistent lead vs. lag association to clinical data). Additionally, public accessibility to clinical COVID-19 PCR tests has been greatly limited in Canada and is currently only available to high-risk groups.

Similar to current COVID-19 testing, influenza A testing is limited to people in hospitals or associated with an institutional outbreak (7). As such, there are incomplete incidence data available to compare with WWS viral signals, thus making the interpretation of wastewater epidemiology data very complex.

Wastewater monitoring is quickly emerging as a powerful epidemiological tool in public health surveillance and the early detection of contagious diseases. It is unbiased, inexpensive, and can be implemented easily, as one wastewater sample can be used to test small communities as well as large populations (8). In addition to SARS-CoV-2, wastewater surveillance can also be applied to target influenza and other pathogens using similar a DNA/RNA-based RT-qPCR detection methodology (9). For example, Mercier et al. (10) recently reported the feasibility of monitoring influenza A viral RNA gene copies in wastewater primary sludge within three distinct communities in Ottawa, Canada, with lead times between 14 and 21 days over clinical testing data.

In this study, we aimed to contribute to the growing WWS knowledge base by exploring other methodological approaches that aid in the interpretation of WWS data, particularly where the clinical case data are limited. Using a detection method focusing on primary influent, we explored the efficacy of school absences due to illness as a proxy measure of community influenza A prevalence and compared these inferred cases with influenza A viral loads in local domestic wastewater samples from Ajax, Ontario, Canada. This analysis will also allow the monitoring of influenza infections in the pediatric population, which likely serves as a major driver of total population influenza A prevalence in sewershed communities that flow into municipal wastewater treatment plants.

Using time-step Spearman's rank correlation analysis and pepper mild mottle virus (PMMoV) normalization to rescale influenza A and SARS-CoV-2 RNA gene copies in wastewater, we compared the relationships between levels of influenza A and SARS-CoV-2 gene copies and (1) student absences due to illness and (2) clinical cases of influenza A to determine the lead and lag time of influenza A WWS data using 1-, 3-, and 5-day averaging times.

2. Materials and methods

2.1. Wastewater sample collection and PEG-NaCl viral concentration

Raw wastewater samples were collected 3 days/week for almost 13 weeks from 15 September to 13 December 2022, from a sanitary sewershed pumping station in Ajax, Ontario, Canada that captures domestic wastewater from approximately 150,000 people. The sewershed primarily reflects a suburban residential area (>80%), with some commercial and light industries. Each sample represented hourly sub-samples of equal volume collected over a 24-h period, for a final composite sample volume of 500 mL that was stored at 4°C. Wastewater samples were transported in sterile, sealed 500 mL plastic containers at 4°C to Ontario Tech University, Oshawa, Ontario, Canada. Upon arrival, the samples were stored at 4°C for up to 24 h until processing and analysis.

To precipitate the influenza viral particles and PMMoV particles from wastewater, all samples were mixed thoroughly before 30 mL of wastewater was transferred to the Nalgene™ Oak Ridge High-Speed PPCO Centrifuge Tubes (Thermo Fisher Scientific, MA, USA) containing 10 mL of 4X PEG–NaCl buffer (40% w/v PEG 8,000 and 1.5 M NaCl), vortexed briefly and centrifuged using a SORVALL RC 6+ Ultracentrifuge (Thermo Fisher Scientific, MA, USA) at 12,000 x *g* for 2 h at 4°C (11, 12). After discarding the supernatant, a second centrifugation step at 12,000 x *g* for 10 min was performed to help solidify the pellet. The PEG–NaCl method was utilized for all experimental samples to concentrate the viral particles. Before RNA extraction, the pellet mass for all samples was measured using a top-loading balance (Sartorius, Goettingen, Germany).

2.2. Nucleic acid extraction

Total RNA was extracted from the concentrated wastewater pellets using the RNeasy® PowerMicrobiome® Kit (Qiagen, Germantown, MD) with the following alterations from the recommended protocol: 100 μL of phenol–chloroform–isoamyl alcohol (25:24:1, pH 6.5–8) was added to each sample prior to the lysis step (Thermo Fisher Scientific, MA, USA). The pellet was resuspended with 650 μL of the lysis buffer and transferred to the PowerBead (glass, 0.1 mm) tubes (QIAGEN, Germantown, MD). The subsequent steps were performed following the recommended protocol from the manufacturer's kit. The total RNA was eluted from the kit spin column using 100 μL of RNase-free water.

2.3. Quantitative reverse transcription PCR

Quantification of the influenza A matrix (M) gene, SARS-CoV-2 viral nucleocapsid (N) gene, and the PMMoV coat protein gene in the composite wastewater samples was performed using the Reliance One-Step Multiplex RT-qPCR Supermix (Bio-Rad, Hercules, CA) utilizing a TaqMan-MGB (Applied Biosystems, Massachusetts, USA) probe-based approach. Gene copy numbers of influenza A in wastewater were determined using the WHO influenza A M gene primer/probe to target a region of the M gene that encodes for the M1 protein. The gene copy numbers of SARS-CoV-2 in wastewater were determined using the US CDC 2019-nCoV N2 Assay RUO primer/probe mix to target a region of the N gene and have been discussed previously (13). PMMoV gene copy numbers were determined using PCR primers developed by Zhang et al. (14) to target a region of the PMMoV strain S genomic sequence. All probes/primers used in this study and their sequences are shown in Table 1.

For each wastewater sample, technical replicates were run in triplicate, and serial dilutions of the Twist Synthetic H3N2 RNA Control (Twist Bioscience, CA, USA) were run on every plate to quantify the gene copies of influenza A (M gene) using the standard curve method. Each reaction comprised a mixture of 5 μL of RNA template, 600 nM (M1) of each forward and reverse primer, 100 nM (M1) probe, and 5 μL of 4X Reliance master mix for a final reaction volume of 20 μL. Reactions were performed in a CFX Connect Real-Time PCR Detection System (Bio-Rad, Hercules, CA) beginning with a reverse transcription (RT) step at 50°C for 10 min, followed by a polymerase activation at 95°C for 10 min, and then 45 cycles of denaturation and annealing/extension at 95°C for 10 s and then at 60°C for 45 s. The RT-qPCR analysis was validated with no-template controls (NTCs) using PCR grade water instead of RNA, no-reverse transcriptase controls (NRTs), and the presence of PCR inhibitors was determined using a serial dilution. All samples analyzed were quantified according to the MIQE recommendations (15) using the standard curve method with a synthetic RNA standard (Twist Synthetic H3N2 RNA Control, Catalog #: 103002) that contains the complete genome of influenza A/H3N2. A minimum 7-point standard curve with technical triplicates for each point was performed for every RT-qPCR experiment. The primer efficiency of influenza A (M1) was approximately 91%. The R^2 value was ≥0.99, and the slope of the standard curve was ∼3.55. The limit of detection for the influenza A M1 gene with a 95% coefficient of variation was 13.71 copies/mL of wastewater. Any crossing threshold values above 40 cycles were identified as negative reactions, assuming no amplification/detection occurred. The dynamic range of our linear standard curve was between 1×10^3 copies/μL and 1.37×10^0 copies/μL.

2.4. Influenza A case data

Influenza A case data for the city of Ajax were provided by the Durham Region Works and Health Department (DRHD) and represented cases identified within the sewershed when they were reported to DRHD.

2.5. School absences

DRHD also collected student absence data due to illness for all elementary and secondary schools within the region, as all schools are required to report absences due to illness. Within the region of Durham, the city of Ajax, ON, contains a total of 24 elementary schools (J.K.–grade 8) with approximately 13,500 students and a total of 3 secondary schools (grades 9–12) with approximately 6,000 students. The absenteeism data provided for this study did not include specific absenteeism for each school in Ajax, but rather a separate daily total percent (%) of absence due to illness (# of students absent due to illness/total student population * 100) for elementary and secondary schools. Absences due to illness were also collected for some Child Care Centers (CCC); however, these data were limited because CCC absence reporting was voluntary, and thus the sample size was too small for analysis.

The percentage of student absences due to illness obtained from DRHD is a measure of the cumulative prevalence of illness across schools (similar to the total number of cases). However,

TABLE 1 Listed are the primers and probes used to obtain WWS data.

Viral target	Primer/Probe	Sequence (5′ -> 3′)	References
Influenza A	MP-39-67For	CCMAGGTCGAAACGTAYGTTCTCTCTATC	(33)
	MP-183-153Rev	TGACAGRATYGGTCTTGTCTTTAGCCAYTCCA	(33)
	MP-96-75ProbeAs	VIC-ATYTCGGCTTTGAGGGGGCCTG-MGBNFQ	(33)
SARS-CoV-2	2019-nCoV_N2 For	TTACAAACATTGGCCGCAAA	(34)
	2019-nCoV_N2 Rev	GCGCGACATTCCGAAGAA	(34)
	2019-nCoV_N2 Probe	FAM-ACAATTTGCCCCCAGCGCTTCAG-MGBNFQ	(34)
Pepper mild mottle virus (PMMoV)	PMMoV For	GAGTGGTTTGACCTTAACGTTGA	(14)
	PMMoV Rev	TTGTCGGTTGCAATGCAAGT	(14)
	PMMoV Probe	VIC-CCTACCGAAGCAAATG-MGBNFQ	(14)

Materials were obtained from Applied Biosystems (MA, USA). M = A/C, Y = C/T, R = G/A.

given that WWS captures the daily abundance of viral genes within the catchment area, for comparison purposes, we transformed the % school absence due to illness data to represent the changes in the daily incidence rate of illnesses in schools by calculating the overall percent change (daily % absence due to illness reported– % absence due to illness from the previous school day) for primary and secondary schools in Ajax. Positive percent change values represented the increase in daily incidence of illness within schools, while negative values represented a decrease in illness (students re-attending after recovery). Since we are not evaluating the effectiveness of non-pharmaceutical interventions, only positive percent changes in absences due to illness were used to infer the incidence of new cases.

2.6. PMMoV normalization for comparisons with influenza A case data and school absenteeism

Viral WWS data are normalized with PMMoV to account for the human fecal content in wastewater as PMMoV is generally found at consistent levels in wastewater (WW) and reflects population-level variability in waste production (14). PMMoV can also be used to account for variability caused by slight changes in extraction efficiency due to the complexity of the WW matrix and variability in pellet weight. This normalization approach is commonly used (10, 16–18) and helps not only reduce noise due to variability but also helps to scale the data for comparison with clinical surveillance data. Since PMMoV acts as a min–max normalization factor to scale the data, the maximum and minimum values are mostly within a 0 to 1 scale. This allows for comparison with other data from different time periods or even different sampling sites.

2.7. Statistical analysis

All data were assessed for normality. Wastewater viral concentrations and % change in absenteeism due to illness were not in compliance with parametric assumptions. Thus, a non-parametric Spearman's rank correlation coefficient (R_s) analysis was performed using the daily PMMoV-normalized viral signals for influenza A: (1) the associated influenza A cases clinically reported and (2) the percentage (%) of change in school absenteeism for primary and secondary schools. To examine if the strength of associations between WWS data and clinical and absenteeism data can be improved with smoothed data, the correlation was also analyzed for 3-day and 5-day averages for both WWS data and the absence/case data.

In addition, to examine the maximum Spearman's correlation values, a time-step correlation analysis was conducted between WWS data and % change in school absenteeism and clinically reported cases with a data offset of a range of +/− 7 days applied to the % change in school absenteeism due to illness and reported cases time series data. This data shift in clinical and absenteeism metrics was applied to observe whether the correlation would be stronger with a lead (− shifted) or lag (+ shifted) time for up to 7 days. Zero-day offset refers to the correlation between wastewater signals and the case counts on the day of the wastewater sampling. Lead times refer to wastewater data being correlated with later case counts (e.g., a lead time of 3 days refers to the correlation between wastewater data and clinical cases 3 days later). Lag times refer to the wastewater data being correlated with earlier case counts (e.g., a lag time of 3 days refers to the correlation between wastewater data and clinical cases 3 days later). Corresponding *p*-values (obtained using the Mann–Whitney test) were also calculated to determine the statistical significance of each correlation ($\alpha = 0.05$). Only *p*-values for strong correlation values ($R_s > 0.50$) are discussed below. For each averaging time, WWS data were only compared to absences/case data for the same averaging time. As per other studies (17) performing similar tests, the averages did not overlap, meaning it was not a moving average.

3. Results and discussion

3.1. Time-step correlation analysis between PMMoV-normalized WWS data and clinical surveillance metrics

Time-step correlation analyses were performed using PMMoV-normalized influenza A WWS data and cases of influenza A reported in the catchment area, which showed a strong correlation between influenza A WWS data and clinical surveillance data (Figure 1A). Comparisons of the daily PMMoV-normalized influenza A signal to the daily number of clinically reported cases showed a maximum Spearman's rank correlation coefficient value $R_s = 0.80$ ($p = 0.579$) when the data were adjusted with a 4-day lead time. Comparing the 3-day average for PMMoV-normalized influenza A WWS data to the 3-day average influenza A cases by reported date, the highest correlation ($R_s = 0.75$, $p = 0.168$) was observed with a 6-day lead time. However, these correlation values were not statistically significant. Only the 5-day average for PMMoV-normalized influenza A WWS data compared with the 5-day average influenza A cases demonstrated a strong significant correlation with clinically reported cases of influenza A ($R_s = 0.79$, $p = 0.036$) with a 5-day lead time (Figure 1A).

Time-step correlation analyses between PMMoV-normalized WWS data and clinical surveillance metrics have been previously explored and shown to effectively determine a lead time for COVID-19 WWS surveillance data (8, 17–23). Although, many have stated that the differences in gastrointestinal replication and fecal shedding of SARS-CoV-2 and influenza A were a cause for concern with respect to the effective detection[/interpretation] of influenza A in wastewater (12, 24–28). Our study has demonstrated that a 5-day lead time between smoothed datasets (5-day averaged influenza A WWS data and 5-day averaged influenza A cases) provided a strong significant correlation ($R_s = 0.79$, $p = 0.036$), indicating the presence of influenza genes in wastewater was found 5 days before the increase in clinically reported influenza cases.

This successful detection of influenza in raw influent wastewater and its correlation to clinical cases complements other recent studies (10, 25) that have also documented successful influenza A detection in both influent and sludge samples. Researchers examining primary sludge from communities in

10.3389/fpubh.2023.1141136

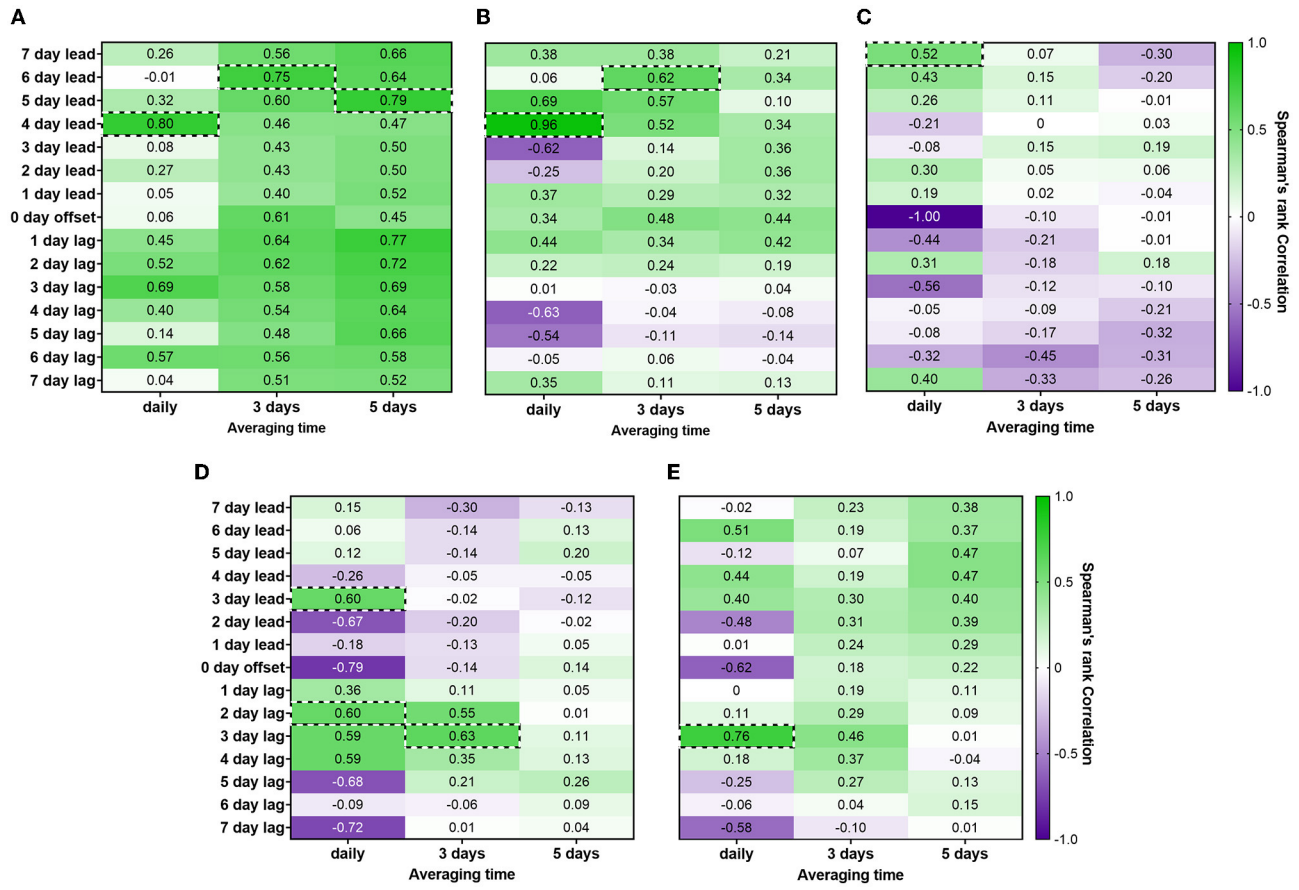

FIGURE 1
Results of time-step Spearman's rank (R_s) correlation analysis with a 7-day lag to a 7-day lead. Maximum Spearman's rank correlation for each averaging time highlighted if $R_s > 0.50$ (strong correlation) or $R_s > 0.30$ but < 0.50 (moderate correlation) **(A)** PMMoV-normalized influenza A (M1 gene) viral signal vs. influenza A cases by reported date, **(B)** PMMoV-normalized influenza A (M1 gene) viral signal vs. % change in elementary school absences due to illness, **(C)** PMMoV-normalized influenza A (M1 gene) viral signal vs. % change in secondary school absences due to illness, **(D)** PMMoV-normalized SARS-CoV-2 (N2 gene) viral signal vs. % change in elementary school absences due to illness, and **(E)** PMMoV-normalized SARS-CoV-2 (N2 gene) viral signal vs. % change in secondary school absences due to illness.

Ottawa were able to detect influenza A with a 14–21-day lead time against reported clinical case data (10). We were unable to detect influenza A in wastewater prior to the first identified case of influenza A within the catchment. However, this is unsurprising given the differences in the viral abundance of enveloped viruses that have been identified between primary sludge and primary influent (17, 21, 29, 30).

3.2. Correlation between PMMoV-normalized viral WWS data and % change in absences due to illness in elementary and secondary schools

Examining the correlation between the daily PMMoV-normalized influenza A WWS signal and the daily percentage of change in elementary school absences (see Figure 1B), the time-step correlation analysis showed that the maximum significant correlation value was obtained with a 4-day lead time (R_s = 0.96, $p = 0.011$). Comparisons of the smoothed 3-day averages of influenza A WWS data and % change in elementary school absences due to illness produced only a weaker correlation with a 6-day lead time ($R_s = 0.62$, $p = 0.035$), while no correlation ($R_s < 0.5$) was observed with the 5-day averaged dataset. The correlation of daily WWS data to primary school absenteeism ($R_s = 0.96$) with a 4-day lead time was much higher than associations with clinically reported cases ($R_s = 0.79$, $p = 0.036$) with a 5-day lead time.

In terms of the correlation between influenza A WWS data and the daily % change in absences due to illness in secondary schools (see Figure 1C), the time-step correlation analysis demonstrated a weak significant correlation with a 7-day lead time ($R_s = 0.52$, $p = 0.011$). Moreover, weak correlations ($R_s < 0.50$) were observed when averaging the data across 3 and 5 days.

We also concurrently monitored for the presence of SARS-CoV-2 RNA viral signal in wastewater from the same samples. This demonstrated that our experimental method can be utilized to detect both SARS-CoV-2 and influenza in wastewater influent. For elementary schools, only the correlations between the daily PMMoV-normalized SARS-CoV-2 WWS data and the daily %

10.3389/fpubh.2023.1141136

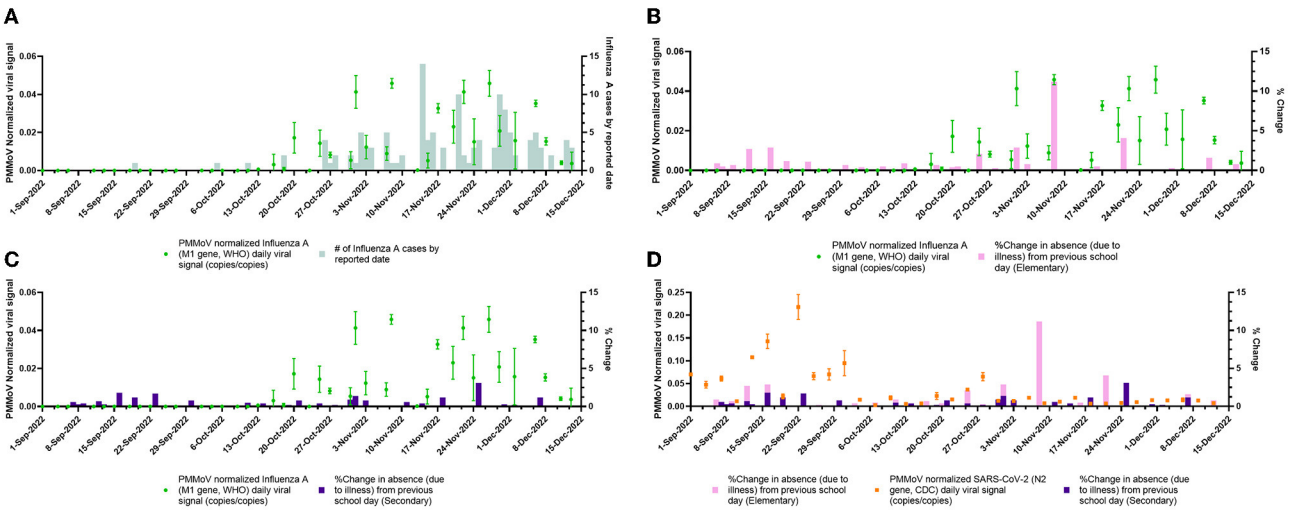

FIGURE 2
PMMoV-normalized viral wastewater signals vs. clinical surveillance metrics over the study period (1 September 2022 to 13 December 2022). **(A)** daily PMMoV-normalized influenza A (M1 gene, WHO) viral signal plotted with the number of new influenza A cases by reported date. **(B)** Daily PMMoV-normalized influenza A (M1 gene, WHO) viral signal plotted with daily % change in elementary school absences due to unspecified illness. **(C)** Daily averaged PMMoV-normalized influenza A (M1 gene, WHO) viral signal plotted with daily % change in secondary school absences due to unspecified illness. **(D)** Daily PMMoV-normalized SARS-CoV-2 (N2 gene, CDC) viral signal plotted with daily % change in elementary and secondary school absences due to unspecified illness.

change in elementary absences due to illness showed a moderate significant correlation ($R_s = 0.60$, $p = 0.017$) with a 3-day lead and 2-day lag time of WWS data. However, in contrast to influenza A, the daily PMMoV-normalized SARS-CoV-2 WWS data showed a stronger statistically significant correlation (Rs = 0.76, $p = 0.005$) with the % change in secondary school absences due to illness, with a 3-day lag time (see Figure 1D).

When comparing the correlations between influenza A WWS data and % change in absences due to illness for elementary and secondary schools, the maximum Spearman's rank correlation coefficients were observed when looking at elementary absences (% change) due to illness. For each data set, regardless of the daily, 3-, or 5-day averages, elementary school absenteeism was observed to correlate significantly higher with influenza A WWS data than secondary school absences. This suggested that influenza A was potentially a causative agent in the absences of the elementary school students in the studied sewershed. Conversely, a strong and significant correlation was found between SARS-CoV-2 WWS data and secondary school absences (% change) due to illness. This may be due to the notable differences in disease presentation between influenza A and COVID-19 in children, where the former is commonly symptomatic compared to the latter (31, 32). However, due to the limited data, we could not confirm the number of SARS-CoV-2 cases in secondary school students (14–18 years old) to corroborate our findings.

3.3. PMMoV-normalized viral WWS data trends over time

The monitoring of PMMoV-normalized influenza and SARS-CoV-2 viral signals over time is shown in Figure 2. An increase in influenza WW signal can be observed from 13 October 2022 to 13 December 2022 along with increasing numbers of new influenza cases reported within that time period which demonstrated that WWS data may have an equivalent predictive power as clinical testing. The PMMoV-normalized influenza wastewater signal to % change due to absenteeism in elementary and secondary school is also shown in Figures 2B, C. Thus, wastewater surveillance was successfully employed using primary influent samples and identified the influenza A outbreak within the community.

4. Conclusion

This study confirms that a primary influent-based wastewater surveillance method is effective at monitoring influenza viral loads in wastewater and that it can be monitored concurrently with other infectious viruses such as SARS-CoV-2 using the same viral RNA concentration and RT-qPCR method for both targets. Additionally, this study demonstrated that school absenteeism may be a useful tool for interpreting influenza A disease prevalence within a pediatric population, and by extension, the total population within a given sewershed.

Our results show that the highest statistically significant correlation ($R_s = 0.96$, $p = 0.011$) occurred between daily influenza A WWS data and elementary school absences due to illness. This correlation coefficient is notably higher than the highest statistically significant correlations observed between influenza A WWS data and influenza A clinical case data ($R_s = 0.79$, $p = 0.036$). Correlations between influenza A WWS data and absences in secondary school were the lowest overall (see Figure 1C). Interestingly, SARS-CoV-2 showed contrasting results compared to influenza A WWS data, and the highest statistically significant correlation observed was between SARS-CoV-2 WWS

data and secondary school absences ($R_s = 0.76$, $p = 0.005$). While SARS-CoV-2 WWS data and elementary absences showed inconclusive results.

While absenteeism is a more coarse metric and relatively ambiguous compared to clinical data, absences are less influenced by sampling bias than clinical tests. This sampling bias is due to clinical tests being reserved for a relatively small subset of the population (typically the elderly or young children) that elect to seek a healthcare intervention, whereas school absences are legally required to be reported to the school by caregivers.

Overall, our results show great promise for inferring influenza A prevalence in sewage-surveilled communities by adding student absenteeism to the wastewater epidemiologist's toolbox. However, the application of this tool comes with some advantages and disadvantages. With respect to advantages, we have confirmed that there is a strong correlative relationship between specific clinical indicators (influenza A cases) and WWS data. In addition, we found an even stronger correlative relationship between a non-specific clinical indicator (% change in elementary absences due to illness) and WWS data. However, this method of comparing non-specific clinical indicators of the pediatric population with WWS data could be further improved by supplementing with more WWS data representing other clinically significant pathogens circulating within the pediatric population such as respiratory syncytial virus (RSV). For example, RSV also has a notable symptomatic presentation in pediatric populations compared with older age children. Another potential limitation with this approach may be that the WWS data are impacted by "legacy viruses" that remain pseudo-persistent in wastewater and are later resuspended under high flow or other turbulence events and detected at higher concentrations using qPCR. However, the fate and stability of viruses in wastewater have not yet been determined. Introducing an effective sampling strategy where sampling sites are carefully selected and composite sampling is utilized with a higher sampling frequency can increase the chances of monitoring for "legacy viruses" due to resuspension or sloughing events. The success of SARS-CoV-2 surveillance programs worldwide has demonstrated that WWTP from different countries, populations, catchment sizes, and designs, can all be sampled and provide a very strong estimation of COVID-19 prevalence without being affected by legacy virus concentrations (6, 26, 35). This WWS method for the detection of influenza is not capable of predicting or forecasting the number of students absent due to a specific pathogen. However, this method, combined with a suite of pathogen data from WWS, is reasonable enough to provide a robust system for determining the causative agents of diseases that are strongly symptomatic in children to infer pediatric outbreaks. This kind of information could then be used to inform public health interventions aimed at pediatric populations as well as the larger community.

Data availability statement

The raw data supporting the conclusions of this article will be made available by the authors, without undue reservation.

Author contributions

TM conceived the study, performed the lab work, generated data, performed data analysis/interpretation, and wrote and reviewed the finished paper. GI contributed to the study concept and design, data interpretation, and writing and review. DS contributed to the study concept and design, data interpretation, and funding. J-PD contributed to the study concept and design, data interpretation, writing and review, and funding. AK contributed to the study concept and design, statistical analyses, data interpretation, writing and review, and funding. All authors contributed to the article and approved the submitted version.

Funding

Funding support for this research was provided by the Ontario Ministry of Environment, Conservation, and Parks as part of their Wastewater Surveillance Initiative.

Acknowledgments

We wish to thank Mary-Anne Pietrusiak, Alexandra Swirski, and Tavis Nimmo from the Regional Municipality of Durham for their assistance in providing data and wastewater sample collection. We also wish to thank Matthew Cranney and Ashley Gedge for their support during the course of this research.

Conflict of interest

The authors declare that the research was conducted in the absence of any commercial or financial relationships that could be construed as a potential conflict of interest.

Publisher's note

References

1. *Infection Prevention and Control Canada. Influenza Resources* | IPAC Canada. (2020). Available online at: https://ipac-canada.org/influenza-resources (accessed January 3, 2023).

2. *Flu (influenza): FluWatch surveillance - Canada.ca*. Available online at: https://www.canada.ca/en/public-health/services/diseases/flu-influenza/influenza-surveillance.html (accessed January 3, 2023).

3. Blümel J, Burger R, Drosten C, Gröner A, Gürtler L, Heiden M, et al. Influenza virus. *Transfus Med Hemotherapy*. (2009) 36:32. doi: 10.1159/000197314

4. *Types of influenza Viruses* | *CDC*. Available online at: https://www.cdc.gov/flu/about/viruses/types.htm (accessed January 3, 2023).

5. *COVID-19 wastewater surveillance dashboard - Canada.ca*. Available online at: https://health-infobase.canada.ca/covid-19/wastewater/ (accessed January 3, 2023).

6. Hopkins L, Persse D, Caton K, Ensor K, Schneider R, McCall C, et al. Citywide wastewater SARS-CoV-2 levels strongly correlated with multiple disease surveillance indicators and outcomes over three COVID-19 waves. *Sci Total Environ.* (2023) 855:158967. doi: 10.1016/j.scitotenv.2022.158967

7. Public Health Ontario. *Respiratory Viruses (including influenza)* | *Public Health Ontario*. Available online at: https://www.publichealthontario.ca/en/Laboratory-Services/Test-Information-Index/Virus-Respiratory (accessed January 5, 2023).

8. Ahmed W, Angel N, Edson J, Bibby K, Bivins A, O'Brien JW, et al. First confirmed detection of SARS-CoV-2 in untreated wastewater in Australia: A proof of concept for the wastewater surveillance of COVID-19 in the community. *Sci Total Environ.* (2020) 728:138764. doi: 10.1016/j.scitotenv.2020.138764

9. Link-Gelles R, Lutterloh E, Schnabel Ruppert P, Backenson PB, St. George K, Rosenberg ES, et al. Public health response to a case of paralytic poliomyelitis in an unvaccinated person and detection of poliovirus in wastewater—New York, June–August 2022. *MMWR Morb Mortal Wkly Rep.* (2022) 71:1065–1068. doi: 10.15585/mmwr.mm7144e2

10. Mercier E, D'Aoust PM, Thakali O, Hegazy N, Jia JJ, Zhang Z, et al. Municipal and neighbourhood level wastewater surveillance and subtyping of an influenza virus outbreak. *Sci Rep.* (2022) 12:15777. doi: 10.1038/s41598-022-20076-z

11. Lewis GD, Metcalf TG. Polyethylene glycol precipitation for recovery of pathogenic viruses, including hepatitis A virus and human rotavirus, from oyster, water, and sediment samples. *Appl Environ Microbiol.* (1988) 54:1983–8. doi: 10.1128/aem.54.8.1983-1988.1988

12. Wu Y, Guo C, Tang L, Hong Z, Zhou J, Dong X, et al. Prolonged presence of SARS-CoV-2 viral RNA in faecal samples. *Lancet Gastroenterol Hepatol.* (2020) 5:434. doi: 10.1016/S2468-1253(20)30083-2

13. Islam G, Gedge A, Lara-Jacobo L, Kirkwood A, Simmons D, Desaulniers JP. Pasteurization, storage conditions and viral concentration methods influence RT-qPCR detection of SARS-CoV-2 RNA in wastewater. *Sci Total Environ.* (2022) 821:153228. doi: 10.1016/j.scitotenv.2022.153228

14. Zhang T, Breitbart M, Lee WH, Run JQ, Wei CL, Soh SWL, et al. Viral community in human feces: Prevalence of plant pathogenic viruses. *PLoS Biol.* (2006) 4:0108–18. doi: 10.1371/journal.pbio.0040003

15. Bustin SA, Benes V, Garson JA, Hellemans J, Huggett J, Kubista M, et al. The MIQE Guidelines: Minimum Information for Publication of Quantitative Real-Time PCR Experiments. *Clin Chem.* (2009) 55:611–22. doi: 10.1373/clinchem.2008.112797

16. Galani A, Aalizadeh R, Kostakis M, Markou A, Alygizakis N, Lytras T, et al. SARS-CoV-2 wastewater surveillance data can predict hospitalizations and ICU admissions. *Sci Total Environ*. (2021) 804:150151. doi: 10.1016/j.scitotenv.2021.150151

17. D'Aoust PM, Graber TE, Mercier E, Montpetit D, Alexandrov I, Neault N, et al. Catching a resurgence: Increase in SARS-CoV-2 viral RNA identified in wastewater 48 h before COVID-19 clinical tests and 96 h before hospitalizations. *Sci Total Environ.* (2021) 770:145319. doi: 10.1016/j.scitotenv.2021.145319

18. Feng S, Roguet A, McClary-Gutierrez JS, Newton RJ, Kloczko N, Meiman JG, et al. Evaluation of sampling, analysis, and normalization methods for SARS-CoV-2 concentrations in wastewater to assess COVID-19 burdens in Wisconsin communities. *ACS ES&T Water.* (2021) 1:1955–65. doi: 10.1021/acsestwater.1c00160

19. Larsen DA, Wigginton KR. Tracking COVID-19 with wastewater. *Nat Biotechnol.* (2020) 38:1151–1153. doi: 10.1038/s41587-020-0690-1

20. Nemudryi A, Nemudraia A, Wiegand T, Vanderwood KK, Wilkinson R, Correspondence BW, et al. Temporal detection and phylogenetic assessment of SARS-CoV-2 in municipal wastewater. *Cell Reports Med.* (2020) 1:100098. doi: 10.1016/j.xcrm.2020.100098

21. Peccia J, Zulli A, Brackney DE, Grubaugh ND, Kaplan EH, Casanovas-Massana A, et al. Measurement of SARS-CoV-2 RNA in wastewater tracks community infection dynamics. *Nat Biotechnol.* (2020) 38:1164–1167. doi: 10.1038/s41587-020-0684-z

22. Zhang T, Cui X, Zhao X, Wang J, Zheng J, Zheng G, et al. Detectable SARS-CoV-2 viral RNA in feces of three children during recovery period of COVID-19 pneumonia. *J Med Virol.* (2020) 92:909–14. doi: 10.1002/jmv.25795

23. Wu F, Xiao A, Zhang J, Moniz K, Endo N, Armas F, et al. SARS-CoV-2 RNA concentrations in wastewater foreshadow dynamics and clinical presentation of new COVID-19 cases. *Sci Total Environ.* (2022) 805:150121. doi: 10.1016/j.scitotenv.2021.150121

24. Chan MCW, Lee N, Chan PKS, To KF, Wong RYK, Ho WS, et al. Seasonal influenza A virus in feces of hospitalized adults. *Emerg Infect Dis.* (2011) 17:2038. doi: 10.3201/eid1711.110205

25. Heijnen L, Medema G. Surveillance of influenza A and the pandemic influenza A (H1N1) 2009 in sewage and surface water in the Netherlands. *J Water Health.* (2011) 9:434–442. doi: 10.2166/wh.2011.019

26. Kumar M, Joshi M, Patel AK, Joshi CG. Unravelling the early warning capability of wastewater surveillance for COVID-19: A temporal study on SARS-CoV-2 RNA detection and need for the escalation. *Environ Res.* (2021) 196:110946. doi: 10.1016/j.envres.2021.110946

27. Santos VS, Gurgel RQ, Cuevas LE, Martins-Filho PR. Prolonged fecal shedding of SARS-CoV-2 in pediatric patients. A quantitative evidence synthesis. *J Pediatr Gastroenterol Nutr.* (2020) 71:150–2. doi: 10.1097/MPG.0000000000002798

28. Xing YH Ni W, Wu Q, Li WJ Li GJ, Wang W Di, Tong JN, Song XF, et al. Prolonged viral shedding in feces of pediatric patients with coronavirus disease 2019. *J Microbiol Immunol Infect.* (2020) 53:473. doi: 10.1016/j.jmii.2020.03.021

29. Ye Y, Ellenberg RM, Graham KE, Wigginton KR. Survivability, partitioning, and recovery of enveloped viruses in untreated municipal wastewater. *Environ Sci Technol.* (2016) 50:5077–85. doi: 10.1021/acs.est.6b00876

30. Graham KE, Loeb SK, Wolfe MK, Catoe D, Sinnott-Armstrong N, Kim S, et al. SARS-CoV-2 RNA in wastewater settled solids is associated with COVID-19 cases in a large urban Sewershed. *Environ Sci Technol.* (2021) 55:488–98. doi: 10.1021/acs.est.0c06191

31. Pierce CA, Herold KC, Herold BC, Chou J, Randolph A, Kane B, et al. COVID-19 and children. *Science.* (2022) 377:1144. doi: 10.1126/science.ade1675

32. Kondrich J, Rosenthal M. Influenza in children. *Curr Opin Pediatr.* (2017) 29:297–302. doi: 10.1097/MOP.0000000000000495

33. Collaborating Centers WHO. *WHO information for the molecular detection of influenza viruses*. (2021) 1–68.

34. Victoriano CM, Pask ME, Malofsky NA, Seegmiller A, Simmons S, Schmitz JE, et al. Direct PCR with the CDC 2019 SARS-CoV-2 assay : optimization for limited—resource settings. *Sci Rep.* (2022) 12:11756. doi: 10.1038/s41598-022-15356-7

35. Plaza-Garrido A, Ampuero M, Gaggero A, Villamar-Ayala CA. Norovirus, Hepatitis A and SARS-CoV-2 surveillance within Chilean rural wastewater treatment plants based on different biological treatment typologies. *Sci Total Environ.* (2023) 863:160685. doi: 10.1016/j.scitotenv.2022.160685

frontiers | Frontiers in Public Health

TYPE Original Research
PUBLISHED 02 August 2023
DOI 10.3389/fpubh.2023.1141837

OPEN ACCESS

EDITED BY
Simon Ching Lam,
Tung Wah College, Hong Kong SAR, China

REVIEWED BY
Annalaura Carducci,
University of Pisa, Italy
Sanjeeb Mohapatra,
National University of Singapore, Singapore
Ananda Tiwari,
University of Helsinki, Finland
Tahir Ahmad,
National University of Sciences and Technology, Pakistan
Deejay Suen-yui Mak,
Tung Wah College, Hong Kong SAR, China

*CORRESPONDENCE
Marc-Denis Rioux
✉ marc-denis_rioux@uqar.ca

RECEIVED 10 January 2023
ACCEPTED 30 June 2023
PUBLISHED 02 August 2023

CITATION
Rioux M-D, Guillemette F, Lemarchand K, Doiron K, Lemay J-F, Maere T, Dolcé P, Quessy P, Abonnenc N, Vanrolleghem PA and Frigon D (2023) Wastewater-based epidemiology: the crucial role of viral shedding dynamics in small communities. *Front. Public Health* 11:1141837. doi: 10.3389/fpubh.2023.1141837

Wastewater-based epidemiology: the crucial role of viral shedding dynamics in small communities

Marc-Denis Rioux[1]*, François Guillemette[2], Karine Lemarchand[3], Kim Doiron[4], Jean-François Lemay[5], Thomas Maere[6], Patrick Dolcé[7], Patrik Quessy[5], Nanouk Abonnenc[5], Peter A. Vanrolleghem[6] and Dominic Frigon[8]

[1]Department of Mathematics and Engineering, Université du Québec à Rimouski, Quebec, QC, Canada, [2]Department of Environmental Science, Université du Québec à Trois-Rivière, Quebec, QC, Canada, [3]Institut des Sciences de la Mer, Université du Québec à Rimouski, Quebec, QC, Canada, [4]Northern Institute for Research in Environment and Occupational Health and Safety, Quebec, QC, Canada, [5]Centre National en Électrochimie et Technologies Environnementales, Cegep of Shawinigan, Quebec, QC, Canada, [6]modelEAU, Département de génie civil et de génie des eaux, Université Laval, Quebec, QC, Canada, [7]Centre Intégré de Santé et de services sociaux du Bas-Saint-Laurent, Quebec, QC, Canada, [8]Department of Civil Engineering, McGill University, Quebec, QC, Canada

Background: Wastewater surveillance (WWS) of pathogens is a rapidly evolving field owing to the 2019 coronavirus disease pandemic, which brought about a paradigm shift in public health authorities for the management of pathogen outbreaks. However, the interpretation of WWS in terms of clinical cases remains a challenge, particularly in small communities where large variations in pathogen concentrations are routinely observed without a clear relation to clinical incident cases.

Methods: Results are presented for WWS from six municipalities in the eastern part of Canada during the spring of 2021. We developed a numerical model based on viral kinetics reduction functions to consider both prevalent and incident cases to interpret the WWS data in light of the reported clinical cases in the six surveyed communities.

Results: The use of the proposed numerical model with a viral kinetics reduction function drastically increased the interpretability of the WWS data in terms of the clinical cases reported for the surveyed community. In line with our working hypothesis, the effects of viral kinetics reduction modeling were more important in small communities than in larger communities. In all but one of the community cases (where it had no effect), the use of the proposed numerical model led to a change from a +1.5% (for the larger urban center, Quebec City) to a +48.8% increase in the case of a smaller community (Drummondville).

Conclusion: Consideration of prevalent and incident cases through the proposed numerical model increases the correlation between clinical cases and WWS data. This is particularly the case in small communities. Because the proposed model is based on a biological mechanism, we believe it is an inherent part of any wastewater system and, hence, that it should be used in any WWS analysis where the aim is to relate WWS measurement to clinical cases.

KEYWORDS

wastewater-based epidemiology, viral shedding dynamics, small communities, wastewater surveillance, pathogens

1. Introduction

The main objective of the epidemiology of infectious diseases is to assess the distribution and effects of the etiologic agents on the health and wellbeing of human populations. In the context of the 2019 coronavirus disease (COVID-19) pandemic, this has led to large-scale testing of suspected infected individuals who underwent nasal and/or throat swab sampling followed by polymerase chain reaction (PCR) assay detection of severe acute respiratory syndrome coronavirus 2 (SARS-CoV-2). The objectives of these campaigns were 2-fold: (i) to identify positive virion carriers and (ii) to evaluate the acute progression of the pandemic in the population. These data are fundamental for predicting short-term demands on the healthcare system and assisting in the pandemic management decision-making process. However, the 2 years of the pandemic have shown that obtaining population data through individual tests is expensive both in terms of human and monetary resources.

An alternative approach based on wastewater surveillance (WWS) (1, 2) was proposed in the early phase of the COVID-19 pandemic (3). WWS provides two types of information. The first is the absence–presence in the community, which makes WWS a tool corollary to a canary in coal mines. The second type of information is the trend in the number of infections in the population, which has the potential to detect trends earlier than by monitoring clinical manifestations.

When coupled with a Geo-Data software (e.g., ArcGiS), WWS allows us for the first time to obtain on a daily basis *real population health data*. It is likely the first epidemiological data that are truly populational in nature. This reality needs to be emphasized as this new approach to generating population health data is an open field of research that did not previously exist. Classical epidemiological data are obtained from individuals presenting with clinical manifestations of infection with or without confirmatory molecular testing. Hence, classical data provide two specific types of information: positivity and identity of the carrier. In the case of WWS, information is populational. This means that one obtains information on the presence and abundance of an etiologic agent in a population of interest but not on the identity of the carriers. Thus, the data provide an indication of the health of the community as a whole. This is especially important to consider in an outbreak, such as the COVID-19 pandemic, because the optimal exploitation of WWS population data in relation to public health intervention is not straightforward and requires a new paradigm.

Correct interpretation of WWS data remains challenging as viral concentrations can vary substantially from 1 day to the next (4). In addition to the inherent daily variability in the concentration of SARS-CoV-2 in wastewater, the midterm temporal dynamics differs between large (collecting wastewater from hundreds of 1,000's of individuals) and small (collecting wastewater from a few tens of 1,000's of individuals) sewer systems. Although the temporal trends of SARS-CoV-2 concentrations in large systems (urban centers) typically follow a wave-like pattern over several weeks consequent to local outbreaks (4), these trends exhibit rapid increases and decreases in small systems (towns and rural communities) (5). Similar observations are reported here for samples obtained from sewer systems of different sizes. These strong signal oscillations make it challenging to adequately interpret wastewater data in small communities. Is the increasing trend observed today a strong indication of an increased number of incident[1] cases in screened populations? To be a useful early indicator of population viral infection, WWS data need to be interpreted in terms of an overall viral attack in the population, hence presenting as little unexplainable variability as possible. It is hypothesized that the variability in temporal trends originates from the different aspects of the system being analyzed. Two important contributing factors are (i) interhuman variability in viral excretion kinetics coupled with the size of the outbreaks and (ii) the structure of the sewer system under study (including the water residence time and accumulation of solids). Following this hypothesis, large systems cover large populations with a high number of incident and prevalent[2] cases at any time and with long water and solid residence times. Together, these elements tend to smooth out the variation in SARS-CoV-2 concentrations. Conversely, small systems receive fecal discharges from only a small number of prevalent cases at any time and are characterized by short water residence times.

From a biological perspective, we would expect prevalent cases to excrete a dwindling quantity of virions down to a null value within a certain number of days following infection. Concentrations measured from WWS reflect the combination of several individuals at different stages of infection. From this work hypothesis, we assumed that considering prevalent cases using a reduction function to consider the evolution of virions in time would better correlate with WWS data than simply considering incident cases. Because this effect is more impactful in small sewer systems, we hypothesized that considering viral excretion kinetics would improve the interpretability of WWS data in small sewer systems.

To test our hypothesis, we aimed to differentiate the effects of incident and prevalent COVID-19 cases on temporal trends in SARS-CoV-2 concentrations observed in wastewater samples from wastewater treatment plant influents in large urban settings and small towns and rural communities. To this end, we built a numerical model that explicitly considers the evolution of viral excretion over time. The main novelty of this work is that it identifies key differences in the interpretation of WWS data from large (densely populated) and small (with low population density) sewer systems (where data are sparser than in large communities) (6) and quantifies the effects of viral excretion kinetics in different contexts.

2. Materials and methods

2.1. Sampling

Our study was conducted in six municipalities of different sizes between January and June 2021 (Table 1). The size of the communities included in our study ranged from 2,000 to > 540,000 citizens. Table 1 shows the type of raw wastewater samples and the frequency of sampling used in each municipality. Grab samples

1 Individuals changing in status from non-disease to disease carrier (new cases).

2 Individuals with positive disease over a specified period of time (existing cases).

refer to samples where all volumes are collected at instant t. Composite samples refer to either samples where constant volumes are collected over the course of a certain time (Composite 24 h) or samples where the volume collected during a time interval varies depending on the instantaneous flow rate (Composite-Flow 24 h). The concentrations of SRAS-CoV-2 in grab samples typically show a good correlation with the ones in composite samples (7–10). However, grab sampling taken in mid to late mornings leads to higher day-to-day variability and often to higher concentrations than composite sampling (7–10). In most communities, direct measurement of the flow rate was not possible, and the value was estimated based on the pump power and time of usage.

Generally, samples were either analyzed the day they were sampled or refrigerated (4°C) for no more than 2 days before analysis. Some specimens (4 January to 15 January) sampled at the beginning of the project before the laboratory equipment for analysis was ready were frozen. Two different temperatures were used for frozen specimen: −20 and −80°C. Although reported work shows no loss of signal within 58 days at either −20 or −75°C (11), Centers for Disease Control and Prevention standards suggested the use of < −70°C for the preservation of samples (12).

2.2. Molecular analyses

The laboratory analysis of the samples was performed in three steps. Filtration was performed to concentrate the organic materials on the filters. SARS-CoV-2 virions tend to agglomerate with organic material rather than to float in free water. Thus, the collection of such organic materials and their concentrations on a filter during the filtration phase is crucial. Each sample underwent the first treatment in duplicate with a volume of 100 mL (50 mL for Quebec City) and was stirred at 200 rpm for 30 min at room temperature. After stirring, the pH was adjusted to 4.0 ± 0.5, and magnesium chloride (final concentration, 25 mM) was added. Each sample was filtered on 0.2 µm mixed cellulose ester filters with 47 mm diameter and stored at −80°C until further analysis.

RNA was extracted using the Qiagen RNeasy PowerMicrobiome Extraction Kit (QIAGEN). Briefly, all sample filters were cut into eight pieces and placed in 1.5 mL centrifuge tubes. In each tube, 100 µL of bovine respiratory syncytial virus (BRSV) was added as external control marker, and a reference sample of BSRV was extracted simultaneously to obtain the recovery rate to validate the extraction process. The remaining samples were extracted according to the manufacturer's instructions.

A one-step reverse transcription quantitative PCR (RT-qPCR) approach was used to quantify SARS-CoV-2, pepper mild mottle virus (PMMoV), and BRSV gene markers in wastewater samples. All primers and probes used in this study are listed in Table 2. For all samples, amplification reaction mixtures (final volume, 20 µL) contained 5 µL template RNA, 10 µL of 2 × Luna® Universal Probe One-Step RT-qPCR (BioLabs Inc., New England), 0.25 µM for each forward and reverse primer, 0.125 µM of probe, and 1 µL of RT enzyme mix. The thermal cycling protocol was as follows: 10 min at 55°C for RT denaturation and 5 min at 95°C for initial denaturation followed by 40 cycles of two steps consisting of 10 s at 95°C and 30 s at 60°C. All RT-qPCR analyses were performed in triplicate (duplicate in Quebec) and in multiplex mode using a real-time PCR apparatus. Calibration curves were generated using the 2019-nCoV_N_Positive Control provided by Integrated DNA Technologies. The internal marker was PMMoV (14) and the external marker was BRSV. SARS-CoV-2 concentrations (gc/mL) were calculated from the cycle threshold (Ct) values using a calibration curve. Ct values < 38 were considered positive for SARS-CoV-2.

2.3. Mathematic modeling and statistical analyses

For each sample, external and internal markers were assessed for aberrant data. Mean Ct values were converted into concentrations (gene copies per volume) using SARS-CoV-2 standard curves.

Viral load excretion from affected individuals varies with time from a maximal value to a null value at time *t*. Hence, incident cases obtained from health authorities from populational screening were used along a kinematic reduction-viral load function to consider this evolution in time. The modeled data comprise our first dataset and are referred to in the rest of the work as the *modeled equivalent shedding cases*. These modeled equivalent shedding cases were subsequently compared with the second dataset composed of SARS-CoV-2 concentrations obtained from the wastewater sample analyses. The main objective is to establish whether it is possible to define a function between SARS-CoV-2 concentration data and modeled data using regression analysis, assuming that modeled cases represent the *real* prevalence of viral infection in the population (or a close approximation). If applicable, this function would theoretically allow the calculation of an approximate number of prevalent cases based on WWS data.

To define the relationship between the two datasets, we hypothesized that the evolution of viral load shedding over time was an important factor. We call this evolution of the time of the viral load the kinetics reduction-viral load function.

To define the kinetics reduction-viral load function, we sought clinical data from anal swab and/or fecal analyses, where viral concentrations were measured at different time intervals. Positive carriers carry higher viral loads from throat swabs at or just before the onset of symptoms and that viral loads recede monotonically, leading to a significant decline in infectiousness 8–9 days after symptoms (15). For anal swabs, data (16) indicate that the mean duration of SARS-CoV-2 shedding is 17.2 days in feces, although live viruses have not been reported beyond 9 days of illness. Cevik et al. (16) also reported studies that show that the viral shedding duration is positively associated with age and severity of illness and that asymptomatic SARS-CoV-2 infection is associated with significantly lower viral loads after the initial stages compared with symptomatic individuals (faster clearance), although the initial viral load might be similar in both asymptomatic and symptomatic individuals. Because little is known about the C_t threshold used and because virus isolation was not conducted in studies on feces, it is difficult to establish a clear comparison. Considering these facts, the following hypotheses were used in this study to construct

10.3389/fpubh.2023.1141837

TABLE 1 Municipalities and their specifics.

Municipality	Population		Start month in 2021	Sampling frequency	Type[I]	Area classification**	Average flow (m^3/d)
	In sewershed	Density (citizen/km^2)					
Québec City	542,300	1,210	February	Daily	1	Large urban	359,000
Rimouski	48,650	146	January	3/week	1	Rural area	30,600 (est.*)
Rivière-du-Loup	19,450	237	Mars	1/week 3/week	1–2	Rural area	15,250 (est.)
Drummondville	68,600	310	April	3/week	1	Rural area	61,700 (est.)
Saint-Alexandre-de-Kamouraska	2,050	18	April	3/week	1	Rural area	1,185
La Tuque	11,125	0.39	Mars	2/week	1	Rural area	6,010 (est.)

*Flow rate estimated based on pump power and usage.
[I]Type: 1 is composite sample (24 h), and 2 is grab (instantaneous) sample.
**Classification based on POPCTRs (21).

TABLE 2 Sequences of primers and probes for the detection of SARS-CoV-2, PMMoV, and BRSV.

Target	Primer/probe name	Primer/probe sequence	References
SARS-CoV-2	Forward primer	GAC CCC AAA ATC AGC GAA AT	(12)
	Reverse primer	TCT GGT TAC TGC CAG TTG AAT CTG	
	Probe (FAM)	FAM ACC CCG CAT/ZEN/TAC GTT TGG TGG ACC IABkFQ	
BRSV	Forward primer	GCA ATG CTG CAG GAC TAG GTA TAA T	(13)
	Reverse primer	ACA CTG TAA TTG ATG ACC CCA TTC T	
	Probe (Cy5)	Cy5 ACC AAG ACT/ZEN/TGT ATG ATG CTG CCA AAG CA IABkFQ	
PMMoV	Forward primer	TAC TTC GGC GTT AGG CAA TCA G	(14)
	Reverse primer	TGA AAC CAG TAG CAG GAA ATC TAA C	
	Probe (HEX)	5HEXCA GCA GTT CZENT CTG ATG TGT GG3IABkFQ	

a recursive curve for viral loads: (i) the maximum viral load is assumed to be on the day of symptom onset (assumed to be on the day of a positive screening test), and (ii) the viral load monotonically decreases from the maximum value to zero at a certain time t (Equation 1):

$$\Gamma(t)_v = \Gamma_0(1 - \beta(t)) \quad (1)$$

where Γ_0 is the maximal viral load and $\beta(t)$ is the function that correlates the viral concentration at time t with the value of Γ_0. The shape and value of $\Phi_t = (1-\beta(t))$ is dependent on assumption (ii), which translates to a specific shape for the kinetics reduction shape function ($\Phi(t)$). Several candidate Φ_t functions were tested, and their relative efficiencies in relating the SARS-CoV-2 concentration to the modeled cases were evaluated using the squared residual approach (Equation 2):

$$r^2 = 1 - \frac{SSR}{TSS} \quad (2)$$

where r^2 is the coefficient of determination, SSR is the sum of squares of the residuals, and TSS is the total sum of squares. Specifically, we tested different hypotheses on the decay intensity for Γ_0 to recede to a null value. All shape functions assumed an exponential form with varying degrees of decay between days 4 and 9. The regressions are based on linear and polynomial functions (third order). The r^2 value for each regression in each city, as presented in Table 1, was calculated to establish the efficiency of the proposed procedure. We have included Supplementary material describing the other curves. However, because it was statistically impossible to distinguish between each curve and because the aim of this study was to demonstrate the usefulness of viral kinetics modeling, we presented only the curve that best fitted our data, based on Equation 2, and applied it to all municipalities:

$$\Phi_t = 1 - \beta(t) \quad (3)$$

$$\beta(t) = 1 - 0,455 \ln(t) \ : t \in \mathbb{N} \mid [0, 9] \quad (4)$$

The data obtained from Φ_t (Equation 3) are compared with incident cases, that is, for $\beta(1) = 0$, $\beta(1 + \Delta t) = 1$.

With an in-house built code using *TcL*, a matrix of incident (d_0) and prevalent (d_t) cases [**C**] by the day of sampling (d) was compiled. The 1-$\beta(t)$ coefficient is then provided in the form of a column vector quantity {1-β} so that the modeled equivalent

10.3389/fpubh.2023.1141837

TABLE 3 Candidate shape function parameter values.

Days from symptoms onset	β	
	Viral kinetic function	Incident
1	0	0
2	0.315	1
3	0.5	1
4	0.631	1
5	0.732	1
6	0.815	1
7	0.885	1
8	0.946	1
9	1	1

shedding cases for each day of the study are obtained in a vector form $\{\varsigma(\mathrm{d})\}$ using Equation 1:

$$\varsigma(d) = \mathbf{C}(d,t)\ \Phi(t) \tag{5}$$

This is a simple vector-matrix product. To illustrate this process, we considered five incident cases at d = 0. The following day (d = 1), four incident cases occurred, and the next day (d = 2), seven. In this example, the [C] matrix is a 3×3 matrix, with three rows for d = 1, 2, and 3, and with three columns representing the day t that is appropriate for the 1-$\beta(t)$ coefficient, where $\beta(t)$ is given in Table 3 and $\varsigma(d)$ obtained by matrix × vector multiplication resulting in the following values:

$$C = \begin{bmatrix} 5 & 0 & 0 \\ 4 & 5 & 0 \\ 7 & 4 & 5 \end{bmatrix} \Phi(t) = \begin{Bmatrix} 1 \\ 0.68 \\ 0.5 \end{Bmatrix} \varsigma(d) = \begin{bmatrix} 5 & 0 & 0 \\ 4 & 5 & 0 \\ 7 & 4 & 5 \end{bmatrix} * \begin{Bmatrix} 1 \\ 0.68 \\ 0.5 \end{Bmatrix} = \begin{Bmatrix} 5 \\ 7.4 \\ 12.2 \end{Bmatrix} \tag{6}$$

This simple matrix × vector product provides a time-dependent cumulative contribution of all incident and prevalent cases to the evolution of the viral load excreted, which better relates to the actual WWS measurements. This allowed us to consider the effects of viral kinetics by multiplying each incident and prevalent case by an appropriate factor. These factors are dependent on the assumptions considered in defining the viral kinetics reduction function.

Figure 1 illustrates this mathematical approach. The horizontal axis in Figure 1 displays the day, whereas the vertical axis represents the number of clinical cases (or modeled equivalent shedding cases). In the example used, there were four incident cases on day 1. On day 2, there were 15 incident cases. Continuing with this logic would lead to the incident case curves (red dotted line) displayed in Figure 1. However, as previously stated, there is no logic behind the idea that incident cases from the previous day would stop contributing to the virion concentration measured in the WWS samples. Consider an example of the period between days 1 and 5. If we consider only incident cases, we would expect to observe a decrease in the trend of cases. However, from a wastewater concentration perspective, this would not be the case because prevalent cases still excrete virions in the sewers. Our proposed model, using shedding curves that decrease over time (dotted black lines, Figure 1), allows the effects of prevalent cases to be included in the modeled equivalent shedding cases (solid black curves, Figure 1).

For example, on day 4, the total number of modeled equivalent shedding cases is the sum of the contributions of all previously determined incident cases (days 1, 2, 3) and the incident cases on that day. This provides a significantly different portrait of what is happening, as can be observed by comparing the incident cases (dashed red line, Figure 1) with the modeled equivalent shedding cases (solid black line, Figure 1). This approach is underlined by a simple biological mechanism, that is, sick individuals keep excreting a receding number of virions during the course of the disease, from a peak at symptom onset to a null value after a certain amount of time. The work hypothesis was that the modeled equivalent shedding cases would be better related to the WWS concentration.

3. Results

Figure 2 shows the curves of SARS-CoV-2 (Gc) in Rimouski City during the screening period (Table 1). The graph also displays the curves for incident cases. The incident case curve was highly jagged compared with the SARS-CoV-2 signal. Consequently, the relationship between the two datasets was not good, with an r^2 of 0.61 using conventional linear regression. Figure 2 shows the modeled COVID-19 cases obtained using Equation 1. Using Equation 1 led to the smoothing of the curves by considering the prevalent cases and their evolution over time. The r^2 between the modeled COVID-19 cases and the SARS-signal datasets significantly increased and reached a value of 0.69 for a standard linear regression. Using a third-order polynomial regression, r^2 reached a value of 0.82, which was remarkably good given the uncertainty in the physical process being modeled.

There was a clear effect, for Rimouski city's dataset, when adding the effects of prevalent cases through viral kinetics reduction curves in the relationship between measured SARS-CoV-2 concentration in wastewater samples and populational COVID-19 cases. This is logical and follows a significantly simple biological mechanism; during the course of COVID-19 infection, the excretion of virions into the sewer network varies in time, with a maximum value at the beginning and dwindling down to a null value after a certain amount of time.

In the case of larger communities, such as Quebec City, the picture is less clear. Figure 3 shows the evolution of SARS-CoV-2 signal in the wastewater samples from Quebec City. The graph also shows the values of the incident cases and the modeled COVID-19 cases (incident and prevalent) using the same viral kinetics reduction function as used by Rimouski.

The results in Figure 2 showed that using viral kinetics reduction led to the smoothing of the COVID-19 cases compared with the incident case curve. When considering the r^2 value, using viral kinetics reduction led to a marginal decrease of r^2,

10.3389/fpubh.2023.1141837

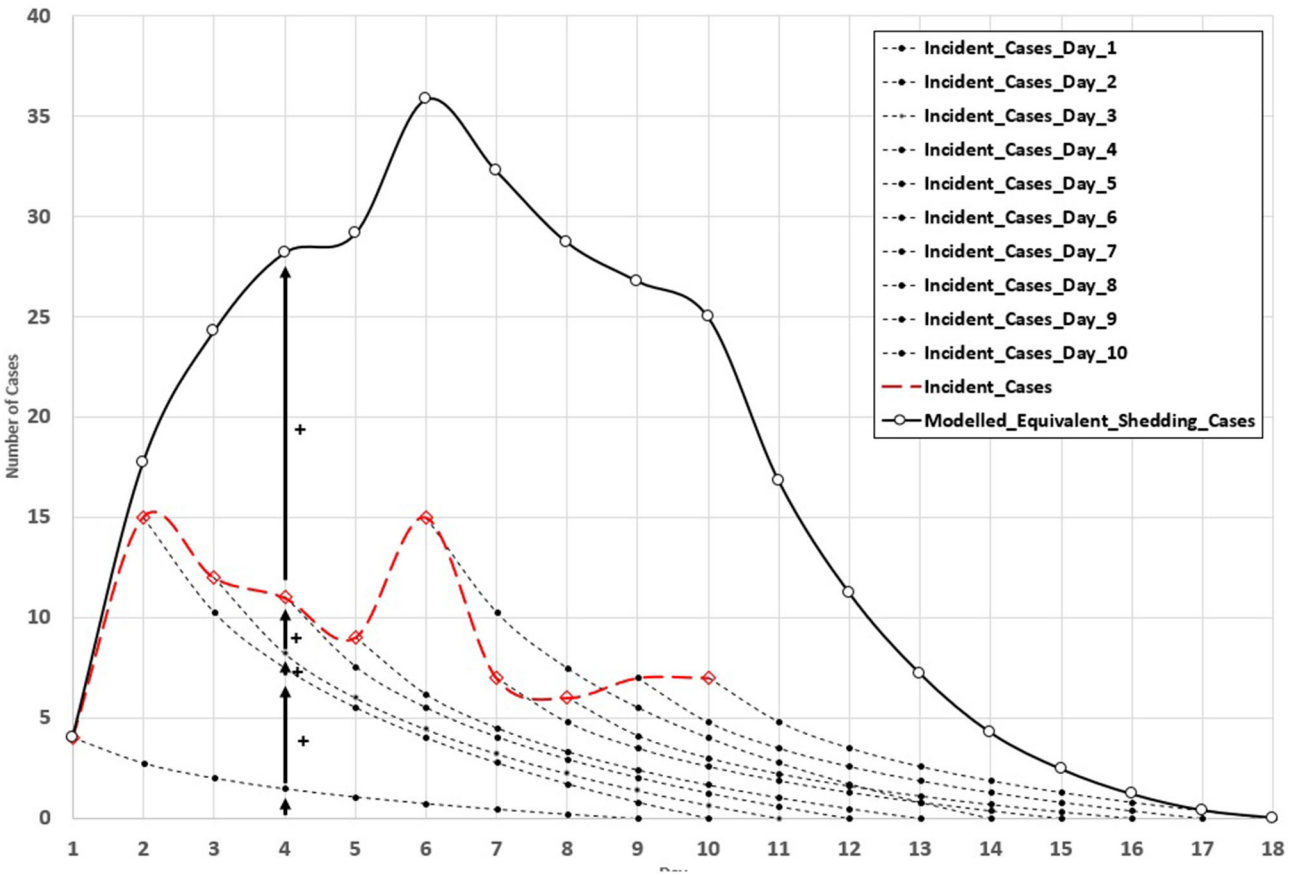

FIGURE 1
Effects of viral kinetics reduction on correlation with COVID 19 cases—Rimouski (more explanation, see text).

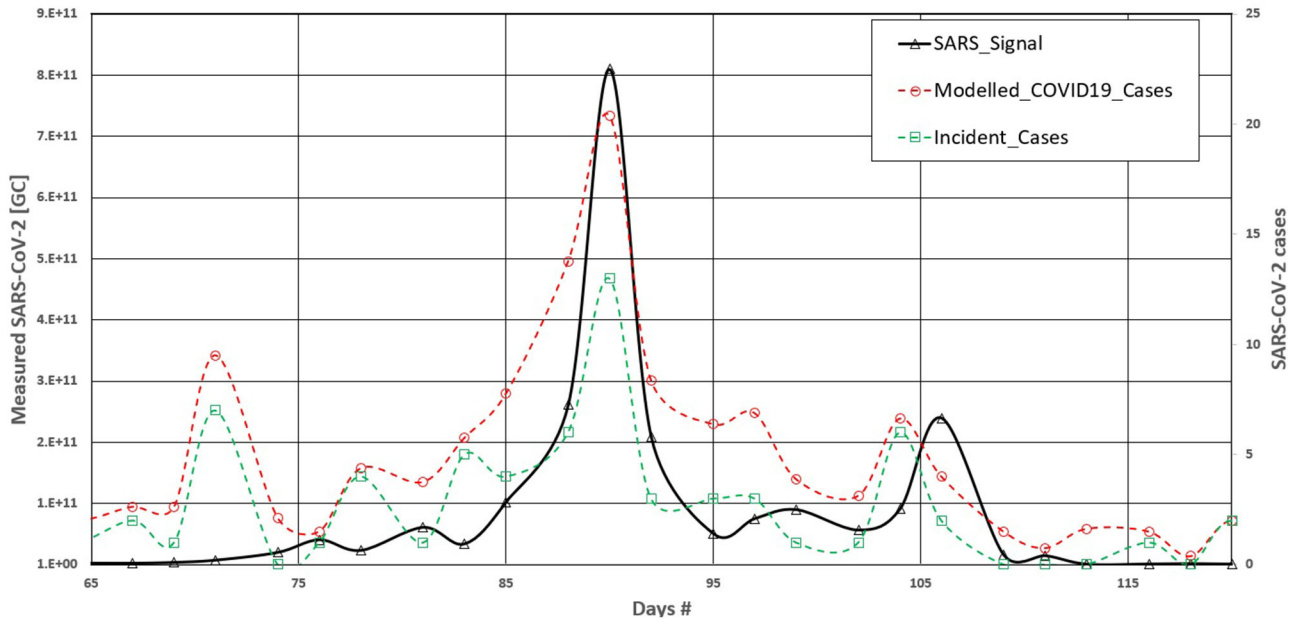

FIGURE 2
Effects of viral kinetics reduction on correlation with COVID 19 cases—Rimouski.

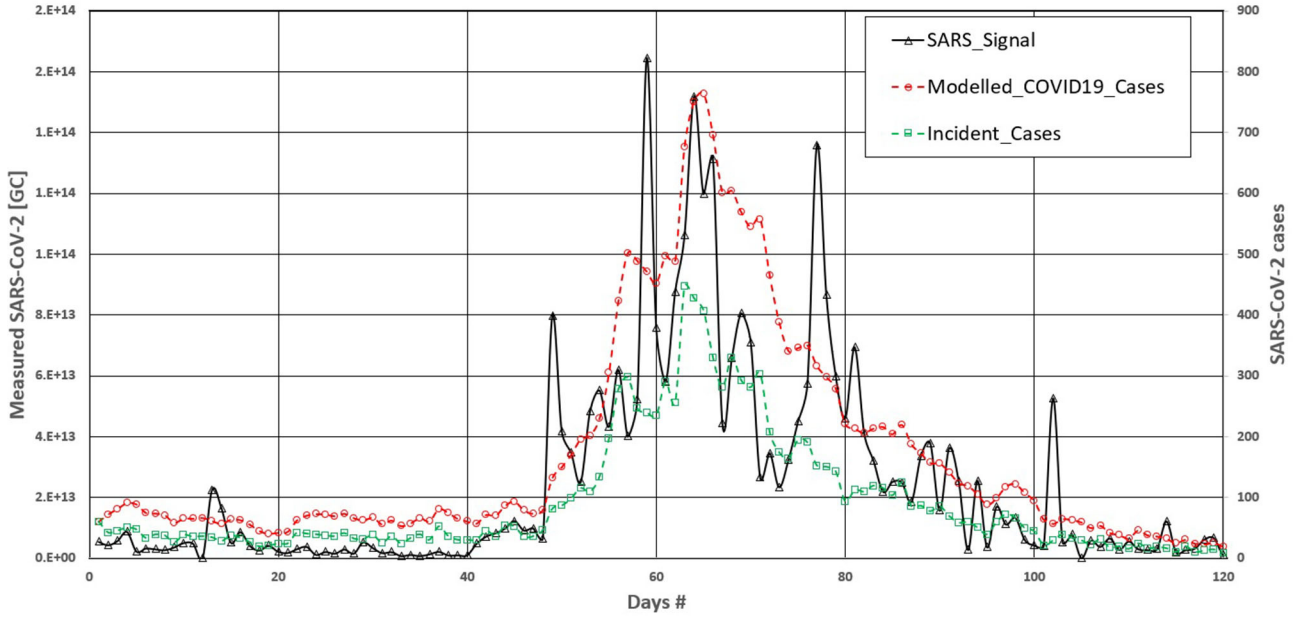

FIGURE 3
Effects of viral kinetics reduction on correlation with COVID 19 cases—Quebec.

passing from 0.63 for the incident case dataset to 0.62 with the modeled datasets in standard linear regression and from 0.66 to 0.67 using the third order polynomial regression. We explain this by considering that the large number of incident cases reduces the effects of the prevalent cases in this population.

3.1. Population biomarkers

Before presenting the complete results (see Section 3.2), it is important to detail how SARS-CoV-2 concentrations were normalized before being used in the regression. Based on previously published documentation available early during the pandemic (17, 18), PMMoV was initially considered to normalize the SARS-CoV-2 concentration. This biomarker is thought to be abundant in bell pepper-based foods, is unaffected by seasonal changes, and persists in wastewater (with a half-life of 6–10 days) from populated areas (19). Population biomarkers are important for two reasons. First, these biomarkers validate the presence of a sufficient quantity of organic materials in samples. Second, they can be used to normalize the concentration of detected virions to account for changes in wastewater dilution and differences in relative human waste input over time due to tourism, weekday commuters, and temporary workers (19). However, based on these data, PMMoV was a poor biomarker (Figure 4).

In fact, normalization of the SARS-CoV-2 concentration with PMMoV reduced the quality of the correlation obtained from the linear regression compared with the raw data. This result is in accordance with the recently published literature (19). The data indicate that flow rate is the most important factor related to virion concentration in the reported cases, and this conclusion is in line with that of a prior study (20).

3.2. Linear regression analysis results

As shown in Section 3, the data collected in spring 2021 showed a rapid increase and decrease when plotting COVID-19 incident cases vs. SARS-CoV-2 concentrations measured in wastewater samples obtained from small communities. Hence, in this study, we consider the effects of prevalent cases using a viral kinetics reduction function, as described previously. In this section, the results of the linear and polynomial regression analyses for all municipalities involved in the project are presented (Table 1).

Linear and third-order polynomial regression analyses were performed for each municipality. Graphs of SARS-CoV-2 concentration versus modeled equivalent shedding cases for all regression analysis are shown in Supplementary material.

Table 4 compares the r^2 coefficients of all regressions for all communities considered between the datasets with incident cases only and those considering the modeled data.

4. Discussion

Values of r^2 considering both incident and prevalent cases using third-order polynomial regression along with a viral kinetics reduction function led to an increase in the correlation between the WWS data and clinical data (Table 4). This is particularly true in small communities. For urban centers with low population densities (Rimouski, Drummondville, and La Tuque), the modeled cases of COVID-19 were better correlated with SARS-CoV-2 concentrations measured in wastewater when prevalent cases were included according to the model. In the case of the city of Drummondville (+48.8%) WWS data were simply unusable without considering the viral kinetics evolution. In the case of a large community (Quebec, +1.5%), inclusion of viral kinetics

10.3389/fpubh.2023.1141837

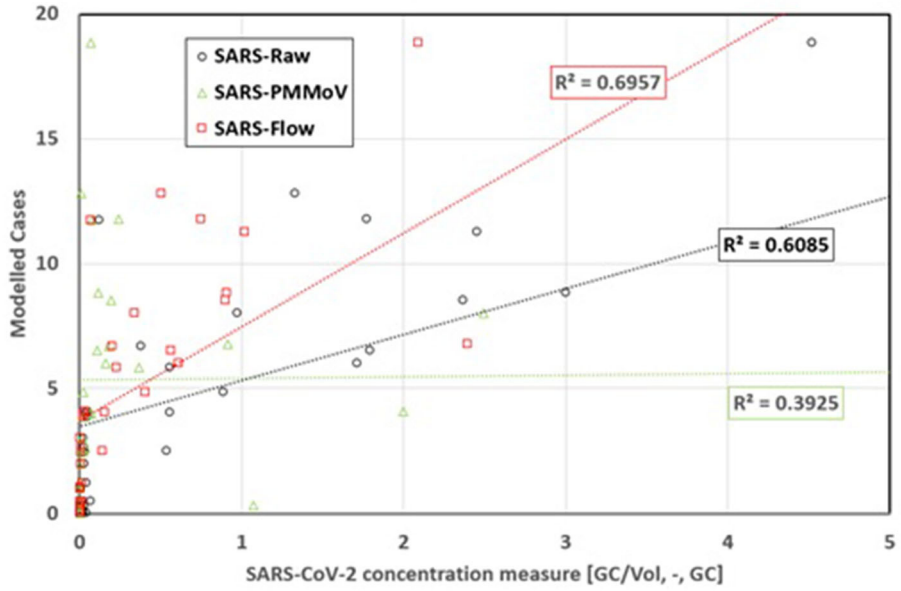

FIGURE 4
Comparison of the effect of pepper mild mottle virus and flow for normalization of data to modeled equivalent shedding cases—Rimouski.

TABLE 4 Summary of the regression analyses for all of the studied cities.

Municipality	r^2			r^2		
	Linear incident	Linear kinetics reduction	Variation (%)	Poly (3rd) incident	Poly (3rd) kinetics reduction	Variation (%)
Québec City	0.63	0.62	−1.6	0.66	0.67	+1.5
Rimouski	0.61	0.69	+13.1	0.6	0.82	+36.7
Rivière-du-Loup	0.7	0.69	−1.4	0.87	0.87	0.0
Drummondville	0.02	0.0054	−73.0	0.41	0.61	+48.8
Saint-Alexandre-de-Kamouraska	0.62	0.6	−3.2	0.88	0.91	+3.4
La Tuque	0.7	0.77	+10.0	0.63	0.83	+31.7

had a less profound effect. This can be explained by the following mechanism.

4.1. Biological mechanism underlying the importance of viral kinetics

An individual's quantity of virions excreted in the feces varies during the course of SARS-CoV-2 infection. The maximum excretion of virions closely matches the initiation of disease symptoms and gradually decreases to a null value. When plotted in the time domain, variations in virion excretion can be described by a viral kinetics reduction function. During a viral outbreak, several individuals become ill at different times. Hence, the virion concentration in wastewater is a superposition of several individual viral kinetics reduction functions (Figure 1). It appears logical that as the number of infected individuals increases, this effect becomes less evident because of the cumulative effects of incident cases. However, when a limited number of individuals are affected, as is the case in small communities, failing to consider this effect may lead to a large discrepancy between the measured concentration in wastewater and clinical cases, making the interpretation of WWS data cumbersome.

To highlight this biological mechanism, we built a mathematical model that explicitly considers viral excretion kinetics. The main novelty of this work is that it identifies key differences in the interpretation of WWS data from large (densely populated) and small (with low population density) sewer systems and quantifies the effects of viral excretion kinetics in different contexts. Through regression analysis of SARS-CoV-2 measurements in wastewater samples from six municipalities located in Quebec (Canada), we showed that the inclusion of a viral kinetics reduction function to consider prevalent COVID-19 cases in the screened population led to an increase in correlation. The effect of this increase was especially visible in low-affected communities, where viral transmission remained low during SARS-CoV-2 screening. The impact was less evident in

communities where a large number of incident cases concealed the effect of viral reduction.

4.2. Effects

Our results show that it is possible to accurately estimate prevalent cases at time t in a population using WWS data. However, making a good estimate requires the definition of a well-defined (data-supported) viral kinetics reduction function. Currently, the authors of this paper are unaware of any data that can provide specific viral kinetics reduction functions for the expression of SARS-CoV-2 virions in the feces of infected individuals in the general population. As stated previously, most supporting data originated from hospitalized individuals whose virion excretion might differ significantly from that of the general population. Furthermore, vaccination and varying viral lineages may produce different viral kinetics reduction functions. However, defining the maximum and minimum virion excretion evolutions in time based on a statistical analysis of data collected from voluntarily sick individuals representative of the general population would allow for a good estimation of population cases at any time based on WWS data. This would be revolutionary for WWS usage in epidemiology because WWS falls short when interpreting data. The ability to estimate population cases from WWS data using a sound biological mechanism would maximize the efficiency of WWS in future pandemic surveillance.

5. Conclusion

The data collected in this study support the hypothesis that the viral kinetics reduction function is a fundamental aspect of describing the biological evolution of SARS-CoV-2 virion shedding, which should be considered in the analysis. In all six municipalities studied, except for Rivière-du-Loup, the inclusion of such a reduction function led to an increase in the correlation for the third-order polynomial regression. For the specific cases of Rivière-du-Loup, we explained the negative effect of the nature of the COVID-19 infection in this particular community during our screening time. During our screening, the Rivière-du-Loup community observed two large outbreaks related to workers in a large company, but there was little contamination in the community. This means that, in both situations, we observed a large increase in incident cases on a daily basis over a relatively long period of time ($\approx$ *days*). In this context, the effect of the reduction in virions from the prevalent individual's excretion is lost in the increase in newly affected individuals.

This study aimed to differentiate the effects of incident and prevalent COVID-19 cases on the temporal trends in SARS-CoV-2 concentrations observed in wastewater samples from large urban settings and small towns and rural communities. Therefore, it was essential to consider the smoothing effect. There were more incidents in large cities than in small communities. In absolute terms, SARS-CoV-2 concentrations measured in wastewater were also higher in larger cities than in small communities. Because the incident cases are larger in number, the variation in SARS concentration is less significant from 1 day to the next because the kinetics of viral excretion is overwhelmed by the large number of incident cases, which contributes to the smoothing effect. Thus, the consideration of prevalent cases is important in small communities where fewer incident cases occur. When there are few incident cases in a population, the contribution of the prevalent cases to the SARS-CoV-2 signal is more significant.

However, our data suggest that the normalization of SARS-CoV-2 concentrations in wastewater samples should consider the flow rate and that there is a lack of consensus on a good biomarker for population normalization and a need for studies on this particular question.

The specific contributions of this work include (1) compelling evidence from several rural and urban municipalities to robustly demonstrate that viral kinetics-induced variability needs to be considered, especially in lower-density communities, and (2) a simple model to account for this viral kinetics effect and its application to regression analysis for estimating SARS-CoV-2 prevalence in screened populations.

6. Limitations and recommendations

Because the biological model proposed in this study was established based on the basic assumption of disease progression, it is thought to be general and applicable to various types of biological etiologic agents worldwide. However, the specific shape function used in the model varies, depending on several factors. For example, in the case of SARS-CoV-2, the vaccination status, age, and viral lineage are all susceptible to influence the function used in the model. It is expected that virus different from that of SARS-CoV-2 has different shape functions. Hence, our results should be understood in this context as a general demonstration of the importance of considering disease evolution in affected individuals in the interpretation of wastewater data while keeping in mind that the specific function developed in this study should not be directly used in another context.

These findings highlight the need for further studies on the temporal evolution of virion excretion in different pathogens, including different SARS-CoV-2 lineages. If wastewater data are used to estimate infection in a population, which should be the main objective of this technique, studies on the evolution of virion excretion in body fluids are fundamental to refining the reduction function used in our model and allowing such estimates to be made on a sound basis.

Data availability statement

The datasets used for the regression analysis in this article can be found at https://zenodo.org/record/8010506.

Author contributions

FG, J-FL, PQ, and NA substantially contributed to the article by providing data for Drummondville, Sainte-Alexandre-de-Kamouraska, and La Tuque and suggested ideas for the writing of the article. KL, KD, PV, and TM substantially contributed to

the article by providing data for Rimouski, Quebec, and Rivière-du-Loup and suggested several important modifications to the article. M-DR contributed to the article by producing the numerical model, making the calculations, producing the image, writing the article, and maturing key ideas with the other authors of the paper. DF contributed to the article by reviewing key ideas, suggesting several critically important intellectual elements of the model, and rewriting several parts of the document. PD contributed to the work by providing key intellectual ideas and important data. All authors contributed to the article and approved the submitted version.

Funding

This work was made possible by funding from the Fond de Recherche du Québec—Nature et Technologie (1,000,000$), the Molson Foundation (300,000$), the Trottier Foundation (357,000$), the Centre Intégré de Santé et Services Sociaux du Bas-Saint-Laurent and Santé Publique du Bas-Saint-Laurent (20,000$), CentrEau (20,000$), CNETE (50,000$), and the McGill Interdisciplinary Initiative in Infection Immunity (300,000$).

Acknowledgments

The authors wish to thank the Fond de Recherche du Québec—Nature et Technologie, Molson Foundation, Trottier Foundation, McGill Interdisciplinary Initiative in Infection and Immunity, and CentrEau, Québec's Water Research Center for financially supporting this project. The authors also wish to thank the Centre Intégré de Santé et Services Sociaux du Bas-Saint-Laurent and Santé Publique du Bas-Saint-Laurent for their financial and logistical support.

Conflict of interest

The authors declare that the research was conducted in the absence of any commercial or financial relationships that could be construed as a potential conflict of interest.

Publisher's note

Supplementary material

The Supplementary Material for this article can be found online at: https://www.frontiersin.org/articles/10.3389/fpubh.2023.1141837/full#supplementary-material

References

1. Ahmed W, Tscharke B, Bertsch PM, Bibby K, Bivins A, Choi P, et al. SARS-CoV-2 RNA monitoring in wastewater as a potential early warning system for COVID-19 transmission in the community: a temporal case study. *Sci Total Environ.* (2021) 761:144216. doi: 10.1016/j.scitotenv.2020.144216

2. Pöyry T, Stenvik M, Hovi T. Viruses in sewage waters during and after a poliomyelitis outbreak and subsequent nationwide oral poliovirus vaccination campaign in Finland. *Appl Environ Microbiol.* (1988) 54:371–4. doi: 10.1128/aem.54.2.371-374.1988

3. Lodder W, de Roda Husman AM. SARS-CoV-2 in wastewater: potential health risk, but also data source. *Lancet Gastroenterol Hepatol.* (2020) 5:533–4. doi: 10.1016/S2468-1253(20)30087-X

4. Nourbakhsh S, Fazil A, Li M, Mangat CS, Peterson SW, Daigle J, et al. A wastewater-based epidemic model for SARS-CoV-2 with application to three Canadian cities. *medRxiv.* (2021) 2021:21260773. doi: 10.1101/2021.07.19.21260773

5. Daigle J, Racher K, Hazenberg J, Yeoman A, Hannah H, Duong D, et al. A sensitive and rapid wastewater test for SARS-CoV-2 and its use for the early detection of a cluster of cases in a remote community. *Appl Environ Microbiol.* (2022) 88:e0174021. doi: 10.1128/aem.01740-21

6. Hubert CRJ, Acosta N, Waddell BJM, Hasing ME, Qiu Y, Fuzzen M, et al. Tracking emergence and spread of SARS-CoV-2 Omicron variant in large and small communities by wastewater monitoring in Alberta, Canada. *Emerg Infect Dis.* (2022) 28:1770–6. doi: 10.3201/eid2809.220476

7. Kmush BL, Monk D, Green H, Sachs DA, Zeng T, Larsen DA. Comparability of 24-hour composite and grab samples for detection of SARS-2-CoV RNA in wastewater. *FEMS Microbes.* (2022) 3:17. doi: 10.1093/femsmc/xtac017

8. George AD, Kaya D, Layton BA, Bailey K, Mansell S, Kelly C, et al. Impact of sampling type, frequency, and scale of the collection system on SARS-CoV-2 quantification fidelity. *Environ Sci Technol Lett.* (2022) 9:160–5. doi: 10.1021/acs.estlett.1c00882

9. Augusto MR, Claro ICM, Siqueira AK, Sousa GS, Caldereiro CR, Duran AFA, et al. Sampling strategies for wastewater surveillance: evaluating the variability of SARS-CoV-2 RNA concentration in composite and grab samples. *J Environ Chem Eng.* (2022) 10:107478. doi: 10.1016/j.jece.2022.107478

10. Bivins A, North D, Wu Z, Shaffer M, Ahmed W, Bibby K. Within- and between-day variability of SARS-CoV-2 RNA in municipal wastewater during periods of varying COVID-19 prevalence and positivity. *ACS ES&T Water.* (2021) 1:2097–108. doi: 10.1021/acsestwater.1c00178

11. Hokajärvi A-M, Rytkönen A, Tiwari A, Kauppinen A, Oikarinen S, Lehto K-M, et al. The detection and stability of the SARS-CoV-2 RNA biomarkers in wastewater influent in Helsinki, Finland. *medRxiv.* (2020) 2020:20234039. doi: 10.1101/2020.11.18.20234039

12. Centers for Disease Control and Prevention (CDC), National Wastewater Surveillance System (NWSS). *Developing a Wastewater Surveillance Sampling Strategy.* (2020).

13. Boxus M, Letellier C, Kerkhofs P. Real Time RT-PCR for the detection and quantitation of bovine respirtory syncytial virus. *J Virol Methods.* (2005) 125:125–30. doi: 10.1016/j.jviromet.2005.01.008

14. Kitajima M, Sassi HP, Torrey JR. Pepper mild mottle virus as a water quality indicator. *NPJ Clean Water.* (2018) 1:19. doi: 10.1038/s41545-018-0019-5

15. He X, Lau EHY, Wu P, Deng X, Wang J, Hao X, et al. Temporal dynamics in viral shedding and transmissibility of COVID-19. *Nat Med.* (2020) 26:672–5. doi: 10.1038/s41591-020-0869-5

16. Cevik M, Tate M, Lloyd O, Maraolo AE, Schafers J, Ho A. SARS-CoV-2, SARS-CoV, and MERS-CoV viral load dynamics, duration

of viral shedding, and infectiousness: a systematic review and meta-analysis. *Lancet Microbe*. (2021) 2:e13–22. doi: 10.1016/S2666-5247(20)30172-5

17. Rosario K, Symonds EM, Sinigalliano C, Stewart J, Breitbart M. Pepper mild mottle virus as an indicator of fecal pollution. *Appl Environ Microbiol*. (2009) 75:7261–7. doi: 10.1128/AEM.00410-09

18. Kitajima M, Iker BC, Pepper IL, Gerba CP. Relative abundance and treatment reduction of viruses during wastewater treatment processes–identification of potential viral indicators. *Sci Total Environ*. (2014) 488–9:290–6. doi: 10.1016/j.scitotenv.2014.04.087

19. Hsu SY, Bayati MB, Li C, Hsieh HY, Belenchia A, Klutts J, et al. Biomarkers selection for population normalization in SARS-CoV-2 wastewater-based epidemiology. *medRxiv*. (2022) 2022:22272359. doi: 10.1101/2022.03.14.22272359

20. Isaksson F, Lundy L, Hedström A, Székely AJ, Mohamed N. Evaluating the use of alternative normalization approaches on SARS-CoV-2 concentrations in wastewater: experiences from two catchments in northern sweden. *Environments*. (2022) 9:39. doi: 10.3390/environments9030039

21. Canada Go. *Population Centre and Rural Area Classification. Stats Can: 2016 06-09-2022*. (2017).

frontiers | Frontiers in Public Health

TYPE Original Research
PUBLISHED 30 August 2023
DOI 10.3389/fpubh.2023.1186525

OPEN ACCESS

EDITED BY
Charlene Ranadheera,
Public Health Agency of Canada (PHAC), Canada

REVIEWED BY
Linda R. Lara-Jacobo,
San Diego State University, United States
Vasiliki Syngouna,
University of Patras, Greece

*CORRESPONDENCE
Hadi A. Dhiyebi
✉ hdhiyebi@uwaterloo.ca
Mark R. Servos
✉ mservos@uwaterloo.ca

RECEIVED 14 March 2023
ACCEPTED 04 August 2023
PUBLISHED 30 August 2023

CITATION
Dhiyebi HA, Abu Farah J, Ikert H, Srikanthan N, Hayat S, Bragg LM, Qasim A, Payne M, Kaleis L, Paget C, Celmer-Repin D, Folkema A, Drew S, Delatolla R, Giesy JP and Servos MR (2023) Assessment of seasonality and normalization techniques for wastewater-based surveillance in Ontario, Canada.
Front. Public Health 11:1186525.
doi: 10.3389/fpubh.2023.1186525

Assessment of seasonality and normalization techniques for wastewater-based surveillance in Ontario, Canada

Hadi A. Dhiyebi[1]*, Joud Abu Farah[1], Heather Ikert[1], Nivetha Srikanthan[1], Samina Hayat[1], Leslie M. Bragg[1], Asim Qasim[2], Mark Payne[2], Linda Kaleis[2], Caitlyn Paget[2], Dominika Celmer-Repin[3], Arianne Folkema[3], Stephen Drew[3], Robert Delatolla[4], John P. Giesy[5,6] and Mark R. Servos[1]*

[1]Department of Biology, University of Waterloo, Waterloo, ON, Canada, [2]Regional Municipality of York, Newmarket, ON, Canada, [3]Regional Municipality of Waterloo, Waterloo, ON, Canada, [4]Department of Civil Engineering, University of Ottawa, Ottawa, ON, Canada, [5]Department of Biomedical Sciences and Toxicology Centre, University of Saskatchewan, Saskatoon, SK, Canada, [6]Department of Environmental Science, Baylor University, Waco, TX, United States

Introduction: Wastewater-based surveillance is at the forefront of monitoring for community prevalence of COVID-19, however, continued uncertainty exists regarding the use of fecal indicators for normalization of the SARS-CoV-2 virus in wastewater. Using three communities in Ontario, sampled from 2021–2023, the seasonality of a viral fecal indicator (pepper mild mottle virus, PMMoV) and the utility of normalization of data to improve correlations with clinical cases was examined.

Methods: Wastewater samples from Warden, the Humber Air Management Facility (AMF), and Kitchener were analyzed for SARS-CoV-2, PMMoV, and crAssphage. The seasonality of PMMoV and flow rates were examined and compared by Season-Trend-Loess decomposition analysis. The effects of normalization using PMMoV, crAssphage, and flow rates were analyzed by comparing the correlations to clinical cases by episode date (CBED) during 2021.

Results: Seasonal analysis demonstrated that PMMoV had similar trends at Humber AMF and Kitchener with peaks in January and April 2022 and low concentrations (troughs) in the summer months. Warden had similar trends but was more sporadic between the peaks and troughs for PMMoV concentrations. Flow demonstrated similar trends but was not correlated to PMMoV concentrations at Humber AMF and was very weak at Kitchener ($r = 0.12$). Despite the differences among the sewersheds, unnormalized SARS-CoV-2 (raw N1–N2) concentration in wastewater ($n = 99–191$) was strongly correlated to the CBED in the communities ($r = 0.620–0.854$) during 2021. Additionally, normalization with PMMoV did not improve the correlations at Warden and significantly reduced the correlations at Humber AMF and Kitchener. Flow normalization ($n = 99–191$) at Humber AMF and Kitchener and crAssphage normalization ($n = 29–57$) correlations at all three sites were not significantly different from raw N1–N2 correlations with CBED.

Discussion: Differences in seasonal trends in viral biomarkers caused by differences in sewershed characteristics (flow, input, etc.) may play a role in determining how effective normalization may be for improving correlations (or not). This study highlights the importance of assessing the influence of viral fecal indicators on normalized SARS-CoV-2 or other viruses of concern. Fecal indicators used to normalize the target of interest may help or hinder establishing trends with

clinical outcomes of interest in wastewater-based surveillance and needs to be considered carefully across seasons and sites.

KEYWORDS

fecal indicators, normalization, seasonality, SARS-CoV-2, PMMoV, crAssphage

Introduction

Due to the COVID-19 pandemic, there has been increased interest in wastewater-based surveillance (WBS) to monitor community prevalence of SARS-CoV-2, with the majority of studies taking place in high-income countries (1). A number of these studies have compared the raw SARS-CoV-2 concentration to clinical metrics (e.g., active cases, new cases, or hospitalizations) [see Li et al. (2) for a review]. However, wastewater systems are very diverse with contrasting infrastructure (3) even within regional settings. The characteristics of the sewer (e.g., sanitary or combined with stormwater, network dynamics, residence time) can influence the fate of fecal matter and viral pathogens, such as SARS-CoV-2, and pose challenges for the interpretation of WBS data. Industrial or commercial inputs and inflow and infiltration (I/I) events can also cause challenges to WBS due to inhibition, dilution, or scouring of settled material (4). Normalization of the viral signal to fecal indicators or flow is frequently done to partially address these concerns. However, normalization of the viral signal is often done without consideration of the complexity of the wastewater or the sewershed and may lead to additional variability. A better understanding of the variability of parameters used to normalize the viral signal and the relationship to key clinical indicators is needed to ensure WBS is optimized for each community.

Several wastewater parameters have been used as fecal indicators for normalization of SARS-CoV-2 in many studies including the pepper mild mottle virus (PMMoV) and cross-assemblage phage (crAssphage). PMMoV is a highly abundant RNA virus found on plants that are commonly found in human diets. It is consistently found in human feces and therefore has been recommended and applied widely as a fecal contamination indicator (5–7). crAssphage is a DNA-based bacteriophage that has been proposed as another human fecal contamination indicator as it is highly associated with human feces, is abundant and ubiquitous in wastewater (8, 9), and has been used in previous studies to normalize viral signals (10). Commonly measured wastewater parameters such as flow, NH_3, total Kjeldahl nitrogen (TKN), total suspended solids (TSS), carbonaceous biological oxygen demand (CBOD), pH, and biological oxygen demand (BOD) have also been proposed and used for normalization of viral signals (11, 12). Other normalization techniques using chemical tracers such as artificial sweetener (acesulfame), caffeine, and its metabolite paraxanthine as well as human metabolites (creatine, 5-hydroxyindoleacetic acid) have also been used with various success (13, 14).

In some sewersheds, normalization of SARS-CoV-2 using fecal indicators has been shown to improve correlations with clinical metrics (15, 16). However, others have shown normalization by fecal indicators has minimal improvement or negatively impacts correlations between the SARS-CoV-2 wastewater measurements and clinical metrics (13, 17, 18). Many factors may influence the patterns of each fecal indicator, including seasonal patterns in sewer flow (e.g., I/I), and sources. For example, PMMoV may be influenced by the seasonal availability of produce or consumption patterns in diets (6). There is therefore a need to investigate why normalizations with fecal indicators seem to be useful in some sewersheds and not others, including the influence of seasonal differences. As WBS will undoubtedly continue to be a widely applied tool, understanding and reducing the uncertainty regarding the value of normalizing will be important for future surveillance programs. This study examines the value of viral signal normalization by assessing wastewater measurements from three communities in Ontario over an extended period during the COVID-19 pandemic (January 2021–February 2023). The seasonal variability in the fecal biomarker PMMoV is examined and the utility of using biomarkers (i.e., PMMoV, crAssphage) and flow to improve the correlations between SARS-CoV-2 wastewater estimates and clinical cases by episode date (CBED) is assessed across seasons and sites.

Methods

Wastewater sampling and locations

Twenty-four-hour time-weighted composite influent wastewater samples were collected at the Kitchener municipal wastewater treatment plant (Kitchener, Ontario, Canada) and at a well at the Humber Air Management Facility (AMF) pumping station that collects wastewater from the west side of Vaughan, Regional Municipality of York (York Region). A third site (Warden main sewer line in York Region) was grab sampled due to the depth of the sewer. Three grab samples were collected at the same time each sampling day and were combined, mixed, and then sub-sampled. The 2021 populations served in the three wastewater sampling sites were approximately 256,000, 105,000, and 659,000 at the Kitchener, Humber AMF, and Warden sewersheds, respectively. Samples were stored in pre-cleaned HDPE containers, kept at 4°C, and transported to the University of Waterloo (Waterloo, Ontario, Canada) for nucleic acid concentration, extraction, and qPCR analysis. As part of a surveillance program, the data were analyzed and normally reported within 3 days of receiving the samples. Wastewater parameters (i.e., TSS, pH, TKN, CBOD, BOD, and NH_3) and flow rates were provided by the public works department of the respective regions and are summarized in Appendix Table S1.

Nucleic acid concentration, extraction, and quantification via RT-qPCR

A modified PEG-precipitation/centrifugation method was used for each wastewater sample as described in Dhiyebi et al. (19). Briefly, a 40 mL wastewater sample was added to a 50 mL Falcon centrifuge tube with PEG 8000 (4 g) and NaCl (0.9 g). The sample was shaken on

ice for 2 h and left to settle at 4°C overnight. The sample was then centrifuged at 12,000 *g* for 1.5 h at 4°C with no brake to concentrate the virus into the solids with the supernatant discarded. A second centrifugation step at 12,000 *g* for 15 min at 4°C with no brake was used to solidify the pellet and discard any remaining supernatant. Nucleic acids were extracted and purified from the solids using Power Microbiome Kit (QIAGEN, United States) following the manufacturer's protocol with up to 250 mg (wet weight) of the pellet resuspended in a TRIzol/PM1 solution, respectively, using an automated QIAcube (QIAGEN, United States). The DNase step was excluded from extraction to allow for the measurement of crAssphage, a DNA virus. The nucleic acids were eluted in 100 µL nuclease-free water. Extracted nucleic acids then underwent one-step RT-qPCR for SARS-CoV-2 N1, N2 gene targets (20) and PMMoV (21). A subset of samples was later analyzed by qPCR to measure crAssphage [CPQ056; (9)]. The PCR assays, cycling conditions, and performances are described in Appendix Tables S2–S4, respectively. Each sample was also assessed for inhibition (reverse transcription and PCR) and each plate had standard curves, positive control, and non-template controls (NTCs) as recommended by the MIQE guidelines (22). Samples that were inhibited were removed from the dataset prior to analysis and accounted for less than 10% (46/477) of the total samples analyzed. As there was a strong correlation between N1 and N2 concentrations (Pearson's $r = 0.858$) and it is essentially measuring the same virus, the SARS-CoV-2 concentrations were presented as the mean of N1 and N2 (N1–N2) to reduce variability and improve the estimate. PCR data is presented as log2 concentration (gene copies/mL).

Assessing seasonal trends

Seasonality was assessed with a Seasonal-Trend-Loess (STL) decomposition (23) with the "timetk" R package (version 2.8.2). STL decomposition is a robust method to filter a time series into 3 components: Seasonal, Trend, and Remainder using LOESS (23). This method allows for determining any temporal patterns (seasonal or trend) within a timeseries dataset and minimizes the effects of outliers. The frequency was defined as 1 week intervals and the trend was defined as 3 months intervals. PMMoV seasonality was analyzed from all sites for the entire study period for each site. For Humber AMF and Kitchener, the sample dates ranged from January 2021 to February 2023, while for Warden the sampling began in April 2021. Flow rates from Humber AMF and Kitchener (minimum of three measurements a week) were available, but Warden flow rates were not available from the main sewer line (a modelled estimate of 150 ML/d was provided by York Region). Flow rates were used to determine the possible impact of rain events and snowmelt (e.g., storm water/infiltration) on wastewater endpoints. Data are presented as monthly boxplots and STL decomposition plots (i.e., observed, trend).

Clinical cases correlation comparison

SARS-CoV-2 copies/mL was determined as the mean of N1 and N2 (N1–N2) in each sample. All viral concentrations were log2(x) transformed and CBED was transformed as log($x+1$) prior to analysis for normality. The Pearson's correlation (pairwise) was performed the transformed SARS-CoV-2 concentrations (raw or PMMoV normalized) and CBED between January and 1 December 2021. During this period, the number of daily clinical tests (mean ± standard deviation) conducted in the province was 34,585 ± 15,040 (24). This timeframe was chosen as clinical testing was conducted at a high level in Ontario until the emergence of the Omicron variant overwhelmed the testing capacity and testing eligibility was changed, resulting in a bias that underestimated clinical cases after late December 2021 (19). The relationships between clinical metrics (i.e., clinical cases or hospitalizations) and wastewater may also be confounded by the emergence of variants (e.g., Delta) and changes in the vaccination status of the population and test-seeking behaviors (25–27). The emergence of the Delta variant in the mid-summer of 2021 may have partially changed the wastewater ratio in some Ontario communities but not others (25). In the US, the appearance of Delta may have only weakly altered the relationship to COVID-19 incidence rates at other sites (28). The entire period prior to the appearance of Omicron was therefore used for the comparison between the raw and normalized correlations to CBED. A time-step comparison of the correlations between CBED and wastewater for up to 10 days lag was also conducted. A subset of samples was later analyzed for crAssphage to compare the crAssphage normalization technique directly to the PMMoV normalized or raw signal ($n = 32$, 31, and 57 for Warden, Humber AMF and Kitchener respectively).

The "cocor" R package (version 1.1.4) was then used to compare whether these correlations between clinical cases by episode date (CBED) and the raw or normalized (PMMoV or crAssphage) SARS-CoV-2 concentrations were significantly different from one another (29). This package offers a wide range of statistical tests to compare correlations (29). The comparisons were between two overlapping correlations based on dependent groups. The correlations were overlapping since CBED was used in all correlation comparisons and dependent as the same N1–N2 concentration was used for both the raw and normalized values (i.e., the same wastewater sample). The correlations were deemed significantly different ($\alpha = 0.05$) if the confidence interval did not include zero (30).

Results

Trend/seasonality analysis

At all sites, PMMoV concentrations were consistently high between January and May 2021 (Figures 1, 2). PMMoV concentrations were the lowest between the summer months and early fall (June–October). There were two main peaks at Humber AMF and Kitchener for PMMoV concentrations in January and April 2022 with monthly median values of 15.8 log2 copies/mL for both months in Kitchener and 16.9 and 16.5 log2 copies/mL, respectively, for Humber AMF. At Warden, PMMoV concentrations appeared to follow the general trend of the other two sites with peaks in the late fall and early winter months (November to February) and lower concentrations in the summer months. However, PMMoV concentrations were more sporadic between the peaks and troughs at Warden due to the lower interquartile range (IQR; 0.75 log2 cp/mL) compared to the other two sites (IQR = 0.98–1.11 log2 cp/mL; Appendix Table S5). This variability in PMMoV concentrations over the entire period in Warden compared to the other two sites is further demonstrated in the violin distribution plots (Figure 3), where there are more concentrations that have higher probability densities compared to Humber AMF and Kitchener.

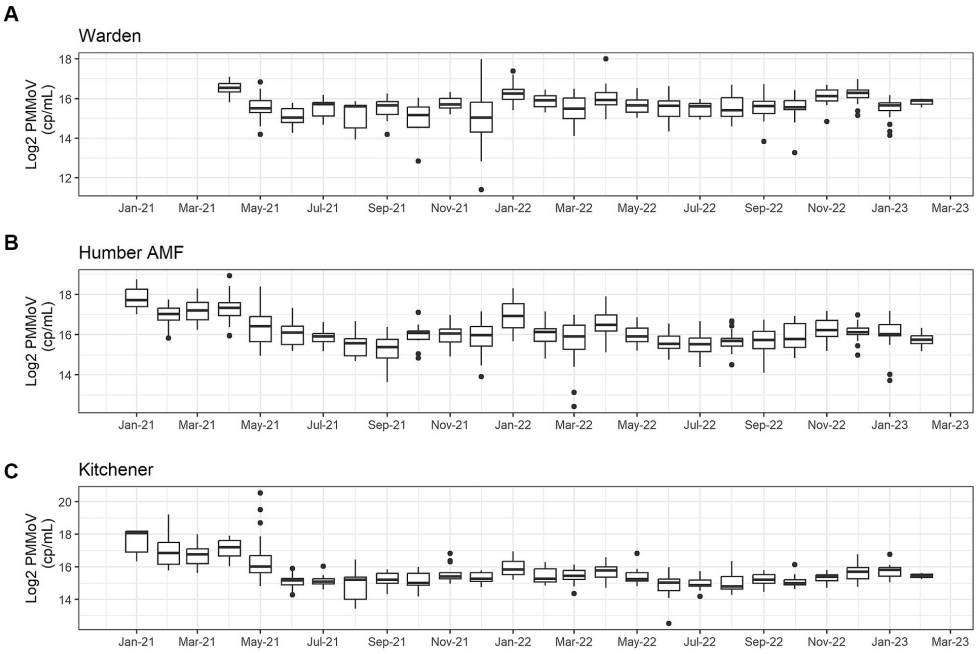

FIGURE 1
Monthly log2 PMMoV concentrations (copies/mL) from January 2021-Februrary 2023 at the Warden **(A)**, Humber AMF **(B)**, and Kitchener **(C)** wastewater sampling sites.

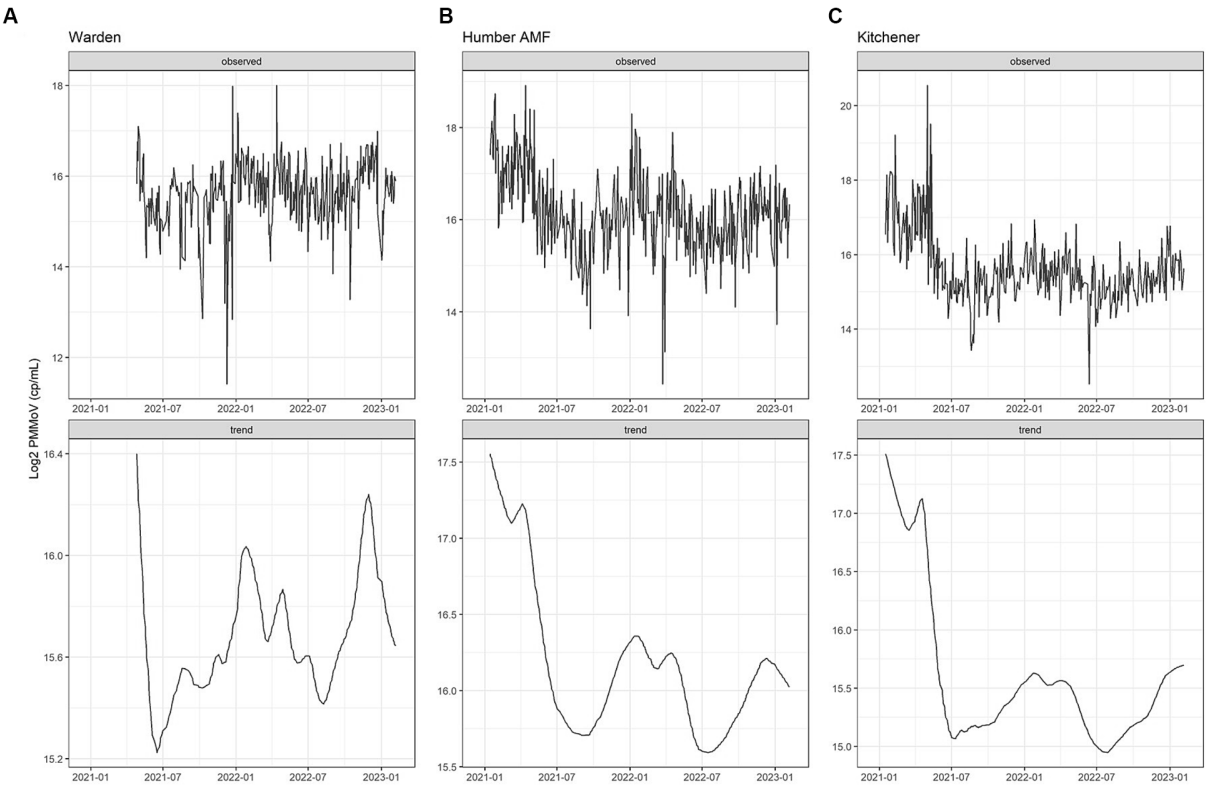

FIGURE 2
PMMoV Seasonal Trend Loess (STL) decomposition plots for the Warden **(A)**, Humber AMF **(B)**, and Kitchener **(C)** wastewater sampling sites. The frequency was set as 1 week and the trend length was 3 months.

FIGURE 3
Violin distribution plots for the Warden, Humber AMF, and Kitchener wastewater sampling sites. Warden collections were from April 2021 to February 2023, and Humber AMF and Kitchener collections were from January 2021 to February 2023.

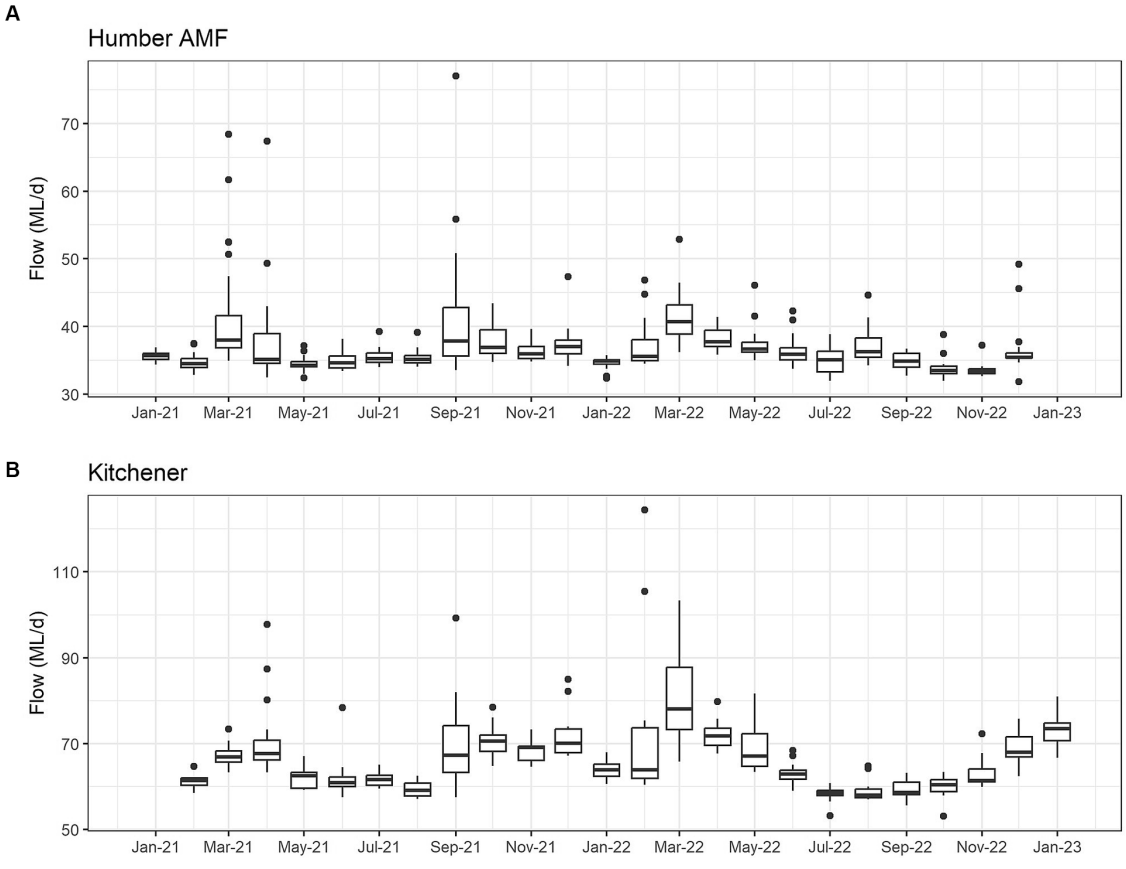

FIGURE 4
Monthly wastewater flow (ML/d) from January 2021 to February 2023 at the Humber AMF **(A)** and Kitchener **(B)** wastewater sampling sites.

The seasonal flow trends in Humber AMF and Kitchener were higher in the spring and fall seasons with the late summer months having the lowest flow. Specifically, in March 2022, both sites had the highest median flow at the sampling location with Humber AMF having a median of 40.7 ML/d and Kitchener having a median of 78.1 ML/d. In general, the peak flow seasons in Humber AMF were March–April and August–September, whereas in Kitchener the changes in flow rates seemed to be more gradual with a few exceptions (Figures 4, 5). There was no correlation and a weak correlation ($r = 0.12$) between flow rates and PMMoV concentrations at Humber AMF and Kitchener, respectively. conveys the intended meaning.

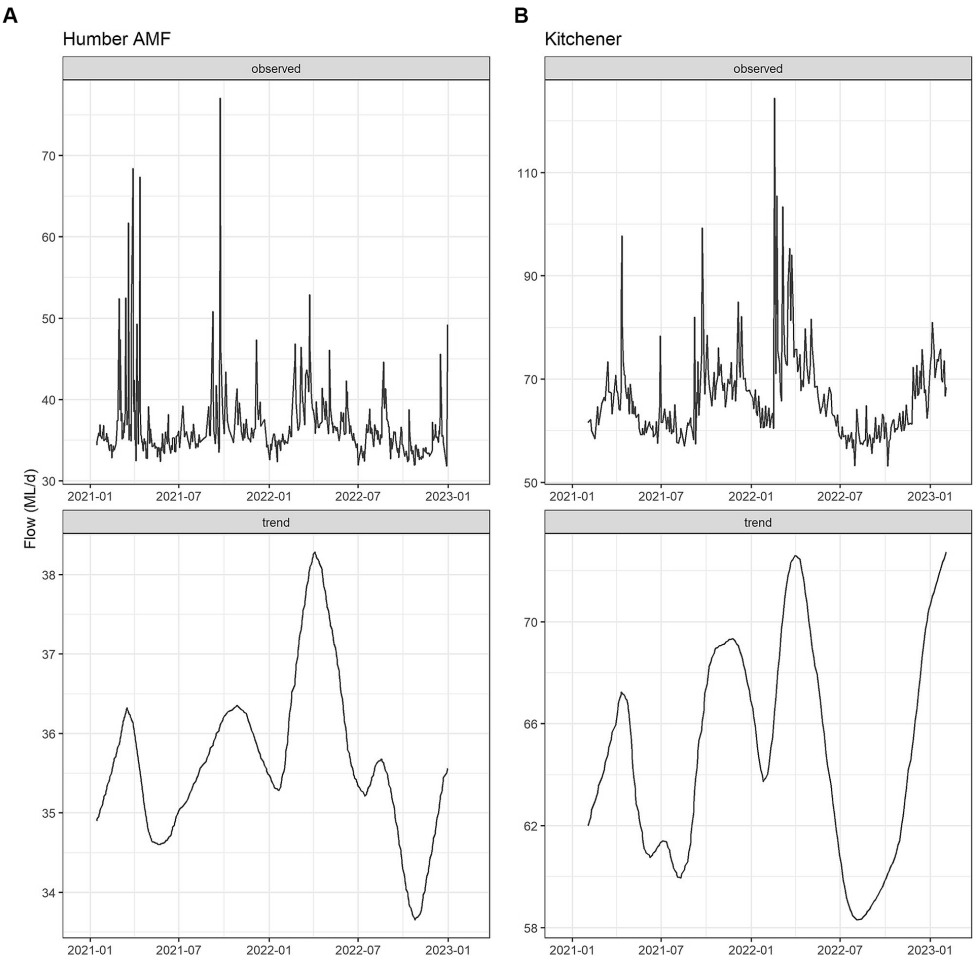

FIGURE 5
Flow Seasonal Trend Loess (STL) decomposition plots for the Humber AMF **(A)** and Kitchener **(B)** wastewater sampling sites. The frequency was set as 1 week and the trend length was 3 months.

Clinical cases correlation comparisons

Raw N1–N2 and PMMoV normalization compared to clinical cases in 2021

A comparison of correlations using a time lag between the CBED and wastewater signals determined that it did not impact the relative differences between the raw and normalized relationships (Appendix Table S6). Additionally, there were no significant differences ($\alpha = 0.05$) in the correlation estimates between the highest correlation with lag and correlations with no lag (Appendix Table S7), so only the data without consideration of a lag is presented further for clarity. At Humber AMF and Kitchener, the raw mean N1 and N2 copies/mL (N1–N2) correlations with CBED were significantly better than the normalized (N1–N2/PMMoV) correlations with CBED (Figure 6; Table 1). At Kitchener, the normalized correlation (Pearson's r) was substantially lower than the raw N1–N2 (non-normalized) correlation (0.167 compared to 0.620, Table 1). However, at Warden, there were no significant differences between the PMMoV normalized correlation and the raw N1–N2 correlation for the entire study period. The flow normalization correlations were not significantly different from the raw correlations with $r = 0.856$ for Humber AMF and $r = 0.613$ for Kitchener.

Subset of data with crAssphage normalization

For Kitchener, the correlation between the raw concentration of SARS-CoV-2 and cases by episode date was significantly better than the PMMoV normalization and the crAssphage normalization (Figure 7; Table 2). However, in the subset data, the correlation of clinical cases with the PMMoV normalized concentration was significantly higher than using the raw concentration or the crAssphage normalized concentrations at Warden. Interestingly, at Humber AMF, there were no significant differences between the raw concentration correlation and both the PMMoV and the crAssphage normalization correlations (Table 2).

Discussion

PMMoV normalization did not improve the correlations between wastewater SARS-CoV-2 concentrations and clinical cases at three Ontario sites sampled in 2021. The raw N1–N2 concentrations had significantly better correlations with clinical cases at both Kitchener and Humber AMF compared to the PMMoV-normalized correlations with clinical cases. At Warden, the raw and PMMoV-normalized correlations were similar. This may be due to the different

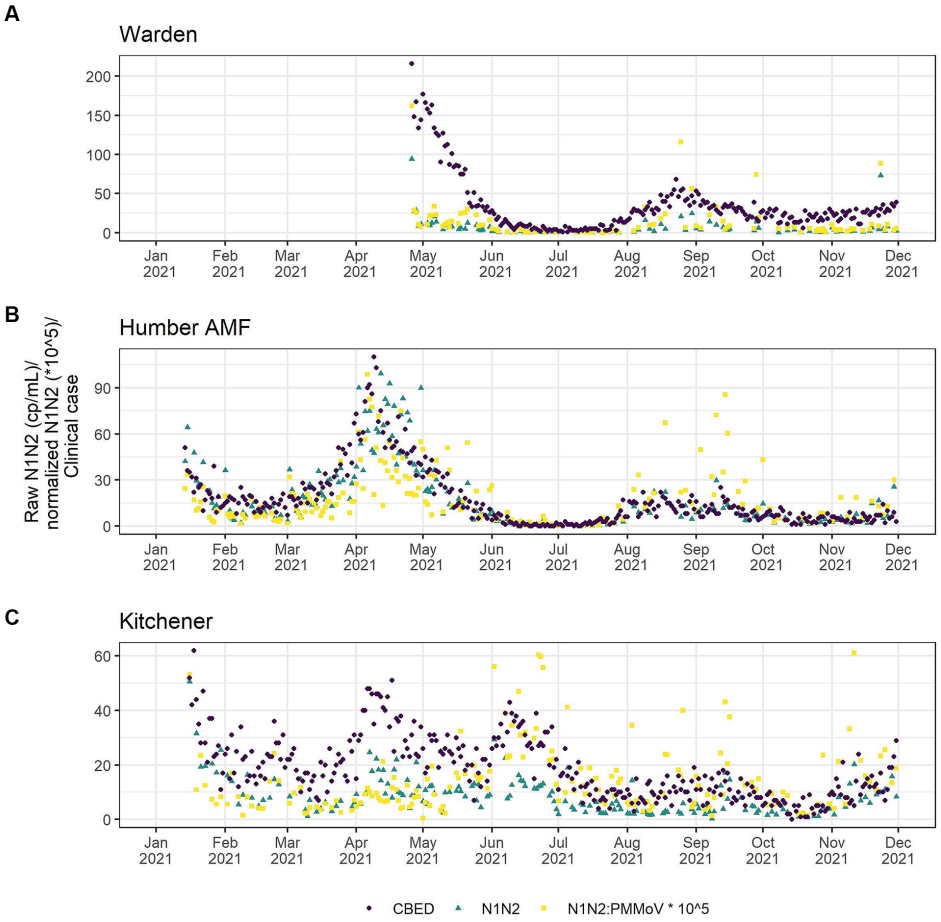

FIGURE 6
Clinical cases by episode date (purple circle) and wastewater SARS-CoV-2 in raw (green triangle) and PMMoV normalized (yellow square) N1–N2 concentrations from the Warden **(A)**, Humber AMF **(B)** and Kitchener **(C)** Wastewater sampling sites. Warden sample dates were from April to December 2021. Humber AMF and Kitchener sample dates were from January to December 2021.

characteristics of this sewershed, such as higher flow (nearly double the other two sites), potentially longer travel time (up to 24 h), and a larger population covered. The lack of improved correlations with clinical cases using PMMoV normalization is in agreement with other studies that also did not report a consistent advantage in normalizing the SARS-CoV-2 concentration (16–18, 31). Maal-Bared et al. (17) found that PMMoV normalization only improved correlation to clinical cases in 2 of 12 sites in Alberta, Canada, and Duvallet et al. (32) found that normalization of 55 sites in the United States was inconsistent in improving correlations. At all sites, crAssphage normalization did not improve correlations to clinical cases compared to the raw N1–N2 correlations using a subset of the data (i.e., Figure 7). However, using this subset of data from Warden, the PMMoV normalization correlation to clinical cases was slightly better than the raw N1–N2 correlation (95% confidence interval of the difference, 0.268 to 0.006), which is in contrast to the larger dataset where there was no difference. This demonstrates the complexity of wastewater-based surveillance and how difficult it is to establish these relationships, especially with small datasets. Normalization of the SARS-CoV-2 signal with PMMoV may be an advantage in some sites or times possibly by accounting for variation in flow, fecal content, or sampling technique, but great care needs to be taken with the interpretation of normalized data. It may be dependent on the source of the sample (pipe, influent, sludge), and characterizing over multiple seasons would greatly improve our insights into how these biomarkers might be used effectively.

Numerous studies have shown that fecal biomarker normalization (PMMoV or crAssphage) is very site-specific in terms of improving correlations with clinical cases (16, 33, 34). Normalization might help in comparisons among sites, however, within sewersheds normalization might not assist in enhancing the relationships with clinical cases (35). The differences observed across sites indicate that in some cases normalization with fecal indicators could play an important role in improving WBS trends, but this needs to be assessed on a site-specific basis using statistical approaches such as STL analysis and the correlation comparisons described in this study.

The usefulness and appropriateness of normalization remains a topic of considerable debate. The limitations of using fecal viral biomarkers, such as PMMoV and crAssphage, include the uncertainty associated with relative fecal shedding rates of viruses and their fate in the sewershed. However, recent studies on individual shedding rates of SARS-CoV-2 (36) and fecal biomarkers (37) are addressing this knowledge gap although there remains considerable uncertainty. Additional studies on the

TABLE 1 Pearson correlation coefficients (*r*) between cases by episode date and wastewater measure between January 15th and December 1st, 2021 at the Warden, Humber AMF, and Kitchener wastewater sampling sites.

Site (*n*)	Raw N1–N2	PMMoV normalized N1–N2
Warden (99, 98)	0.781	0.696
Humber AMF (191)	0.854*	0.702
Kitchener (175)	0.620*	0.167

Comparisons were done on two overlapping correlations based on dependent groups with the cocor package using 95% confidence intervals (30). An * indicates significantly different correlations ($p = 0.05$).

TABLE 2 Pearson correlation coefficients (*r*) between cases by episode date and wastewater measure on the subset of data from the Warden, Humber AMF, and Kitchener wastewater sampling sites.

Site (*n*)	Raw N1–N2	PMMoV normalized N1–N2	CrAssphage normalized N1–N2
Warden (32)	0.608[a]	0.712[b]	0.553[a]
Humber AMF (29–31)	0.726	0.696	0.767
Kitchener (57)	0.833[a]	0.766[b]	0.751[b]

Comparisons were done on two overlapping correlations based on dependent groups with the cocor package using 95% confidence intervals (30). Letters indicate significant differences between correlations ($p = 0.05$).

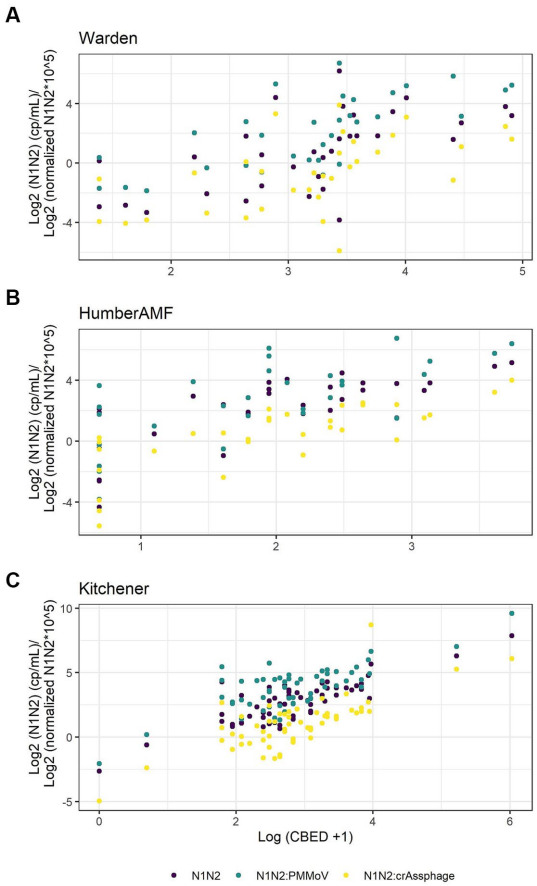

FIGURE 7
Scatterplots of new cases by episode date (CBED) and the raw (N1–N2), crAssphage normalized (N1–N2/crAssphage), and pepper mild mottle virus normalized (N1–N2/PMMoV) wastewater concentrations at Warden ($n = 32$, **A**), Humber AMF ($n = 29–31$, **B**) and Kitchener ($n = 57$, **C**).

fate of viruses once in the sewershed are needed as this is important for the interpretation of the surveillance results. In addition, it has been shown that viruses partition differently under various conditions (38, 39). Flow has been used to normalize SARS-CoV-2 as well (10, 19), however, in this study flow normalization correlations were not significantly different from unnormalized correlations. A limitation of flow normalization is that flow measurements may be unobtainable at some locations due to site characteristics (such as the Warden site in this study). In addition, rapid access to flow data, if available, may also be a limitation. Despite all these limitations, normalization and specifically measuring fecal biomarkers can be effective as a quality check of wastewater samples and lab processes and therefore has additional value (40).

Despite the weak or lack of correlation between PMMoV and flow rates at Humber AMF and Kitchener, the PMMoV concentrations were generally higher during the higher flow seasons. This suggests that environmental factors, such as rain events, were not diluting fecal material but in fact, the high flow events were scouring settled materials in the sewer and increasing the concentration of PMMoV at the collection site. PMMoV tends to partition primarily to the supernatant fraction, likely associated with very fine particles or colloids of the wastewater samples even after centrifugation at 12,000 *g*, however, a substantial proportion (~15%) of PMMoV is still associated with solids (39). The fate of PMMoV in the sewer may therefore differ from SARS-CoV-2 which is more evenly partitioned between the solids and supernatant (39). If wastewater volume increases because of environmental effects (i.e., rain events, snow melt) it would be anticipated that the viral concentration of the biomarker would decrease as wastewater gets diluted. However, this pattern was not observed in the three Ontario sites in the current study. Additionally, even though the temperature in the sewershed does not fluctuate as much as air temperature (e.g., Warden wastewater ranged from 10.4°C to 20.2°C), it may still play a significant role in the prevalence of PMMoV. This adds additional uncertainty when assessing the suitability of PMMoV as a fecal indicator and might be one of the contributions to the variability in the normalized SARS-CoV-2 signal at some sites.

The higher variability of PMMoV in Warden might be due in part to the collection approach applied at this site. Grab samples, even when well mixed from large flows, may not be as representative as 24 h composite sampling. In the case of SAR-CoV-2 wastewater sampling, Bivins et al. (41) demonstrated temporal variability in concentration during the day. This variability may lead to lower detection rates of grab samples, especially in small sewersheds (42, 43). However, others have seen good concurrence for the detection of SARS-CoV-2 in wastewater when directly comparing grabs and composite samples (44–46). Grab samples from the Warden site represent a major wastewater flow and large population which results in batch samples having some variability, but still relatively consistent PMMoV over time. Additional studies comparing the two sampling approaches from a single site over an extended period of time would be helpful to understand the impact of the sampling approach. In situations where

there is considerable sample or temporal variability, normalization may still provide an advantage.

The goal of early studies using fecal indicators, such as PMMoV and crAssphage, was for the detection of fecal contamination of surface/source water, therefore a good indicator would be highly abundant in wastewater to increase the sensitivity of detection (6). However, for the normalization of respiratory or enteric viruses, the goal is to have an indicator that reflects the inputs and fate of fecal material in the sewershed so that variations in the sewershed, environmental conditions, and flow can be accounted for. This poses a challenge for the selection of a robust endpoint that can be used for normalization to improve the correlation of the viral signal to clinical endpoints of interest. As PMMoV and crAssphage are present at much higher levels (10^5 to 10^9 copies/mL) in wastewater compared to SARS-CoV-2 concentrations (usually less than 10^3 copies/mL) considerable variation can be added when normalizing. Ideally, the viral signal would be normalized with a marker that has similar properties and fate in the sewershed, can be reliably detected, and is strongly correlated with the source of the viral signal of interest. Currently, there are no ideal indicators available to universally normalize viral signals, such as SARS-CoV-2, in wastewater. Identification of reliable and validated indicators (e.g., viruses, bacteria, human genes, or chemicals) or groupings of indicators, that can be used to normalize viral signals in wastewater will greatly enhance the application of WBS and our ability to correlate wastewater signals to clinical endpoints of concern.

Data availability statement

The data has been deposited in the Federated Research Data repository (FRDR) with DOI: 10.20383/102.0702.

Author contributions

HD and MS contributed to the conception and original writing of the manuscript. HD, MS, NS, SH, and HI contributed to the methodology, investigation, data curation, and project administration. LK and JA contributed to the methodology and investigation of the manuscript. LB contributed to the project administration. JG and MS provided the funding acquisitions for this project. AQ, MP, CP, DC-R, AF, SD, and RD contributed to the conception of this manuscript. All authors contributed to the article and approved the submitted version.

Funding

This research was funded from the Ontario Ministry of the Environment, Conservation and Parks: Wastewater Surveillance Initiative (Grant No. TPA 2021-02-1-1564736554). In addition, this research was in part funded by the Canada First Research Excellence Fund under the Global Water Futures Program (Grant # 410295/419205). This research was also supported by an NSERC Discovery Grant (MS RP-2017-03816); the Canada Research Chairs program (MS and JG); and Distinguished Visiting Professorship in the Department of Environmental Sciences, Baylor University in Waco, TX (JG).

Acknowledgments

We would like to acknowledge the support from the public health units and public works departments of York Region and Region of Waterloo. Specifically, we would like to acknowledge Jennifer Khemai, Graham Beach, Gavin Walker and Beth Weir for the support from Operations Maintenance and Monitoring in York Region. We would like to thank Kyle Atanas from Peel Region for the sample collection and wastewater parameter data from the Humber AMF site. We would like to acknowledge the support from the Ontario Wastewater Surveillance Initiative for collating clinical cases metrics from the Ministry of Health used in this study. We would also like to thank the members of the Servos Group especially Carly Sing-Judge, Patrick Breadner and Kirsten Nikel and acknowledge the support from the members of the Ontario Wastewater Consortium.

Conflict of interest

The authors declare that the research was conducted in the absence of any commercial or financial relationships that could be construed as a potential conflict of interest.

Publisher's note

Supplementary material

The Supplementary material for this article can be found online at: https://www.frontiersin.org/articles/10.3389/fpubh.2023.1186525/full#supplementary-material

References

1. Naughton CC, Roman FA Jr, Alvarado AGF, Tariqi AQ, Deeming MA, Kadonsky KF, et al. Show us the data: global COVID-19 wastewater monitoring efforts, equity, and gaps. *FEMS Microbes*. (2023) 4:xtad003. doi: 10.1093/femsmc/xtad003

2. Li X, Zhang S, Sherchan S, Orive G, Lertxundi U, Haramoto E, et al. Correlation between SARS-CoV-2 RNA concentration in wastewater and COVID-19 cases in community: a systematic review and meta-analysis. *J Hazard Mater*. (2023) 441:129848. doi: 10.1016/j.jhazmat.2022.129848

3. von Sperling M. *Wastewater characteristics, treatment and disposal* (2015). 9781780402086 p Available at: http://iwaponline.com/ebooks/book-pdf/1075/wio9781780402086.pdf.

4. Bertels X, Demeyer P, van den Bogaert S, Boogaerts T, van Nuijs ALN, Delputte P, et al. Factors influencing SARS-CoV-2 RNA concentrations in wastewater up to the sampling stage: a systematic review. *Sci Total Environ*. (2022) 820:153290. doi: 10.1016/j.scitotenv.2022.153290

5. Rosario K, Symonds EM, Sinigalliano C, Stewart J, Breitbart M. Pepper mild mottle virus as an indicator of fecal pollution. *Appl Environ Microbiol*. (2009) 75:7261–7. doi: 10.1128/AEM.00410-09

6. Symonds EM, Rosario K, Breitbart M. Pepper mild mottle virus: agricultural menace turned effective tool for microbial water quality monitoring and assessing (waste) water treatment technologies. *PLoS Pathog*. (2019) 15:1–7. doi: 10.1371/journal.ppat.1007639

7. Kitajima M, Sassi HP, Torrey JR. Pepper mild mottle virus as a water quality indicator. *npj Clean Water*. (2018) 1:19. doi: 10.1038/s41545-018-0019-5

8. Stachler E, Bibby K. Metagenomic evaluation of the highly abundant human gut bacteriophage CrAssphage for source tracking of human fecal pollution. *Environ Sci Technol Lett*. (2014) 1:405–9. doi: 10.1021/ez500266s

9. Stachler E, Kelty C, Sivaganesan M, Li X, Bibby K, Shanks OC. Quantitative CrAssphage PCR assays for human fecal pollution measurement. *Environ Sci Technol*. (2017) 51:9146–54. doi: 10.1021/acs.est.7b02703

10. Langeveld J, Schilperoort R, Heijnen L, Elsinga G, Schapendonk CEM, Fanoy E, et al. Normalisation of SARS-CoV-2 concentrations in wastewater: the use of flow, electrical conductivity and crAssphage. *Sci Total Environ*. (2023) 865:161196. doi: 10.1016/j.scitotenv.2022.161196

11. Hoar C, Li Y, Silverman AI. Assessment of commonly measured wastewater parameters to estimate sewershed populations for use in wastewater-based epidemiology: insights into population dynamics in New York city during the COVID-19 pandemic. *ACS ES T Water*. (2022) 20:2014–24. doi: 10.1021/acsestwater.2c00052

12. Hutchison JM, Li Z, Chang C-N, Hiripitiyage Y, Wittman M, Sturm BSM. Improving correlation of wastewater SARS-CoV-2 gene copy numbers with COVID-19 public health cases using readily available biomarkers. *FEMS Microbes*. (2022) 3:xtac010. doi: 10.1093/femsmc/xtac010

13. Xie Y, Challis JK, Oloye FF, Asadi M, Cantin J, Brinkmann M, et al. RNA in municipal wastewater reveals magnitudes of COVID-19 outbreaks across four waves driven by SARS-CoV-2 variants of concern. *ACS ES T Water*. (2022) 2:1852–62. doi: 10.1021/acsestwater.1c00349

14. Hsu S-Y, Bayati M, Li C, Hsieh H-Y, Belenchia A, Klutts J, et al. Biomarkers selection for population normalization in SARS-CoV-2 wastewater-based epidemiology. *Water Res*. (2022) 223:118985. doi: 10.1101/2022.03.14.22272359

15. D'Aoust PM, Mercier E, Montpetit D, Jia JJ, Alexandrov I, Neault N, et al. Quantitative analysis of SARS-CoV-2 RNA from wastewater solids in communities with low COVID-19 incidence and prevalence. *Water Res*. (2021) 188:116560. doi: 10.1016/j.watres.2020.116560

16. Nagarkar M, Keely SP, Jahne M, Wheaton E, Hart C, Smith B, et al. SARS-CoV-2 monitoring at three sewersheds of different scales and complexity demonstrates distinctive relationships between wastewater measurements and COVID-19 case data. *Sci Total Environ*. (2022) 816:151534. doi: 10.1016/j.scitotenv.2021.151534

17. Maal-Bared R, Qiu Y, Li Q, Gao T, Hrudey SE, Bhavanam S, et al. Does normalization of SARS-CoV-2 concentrations by pepper mild mottle virus improve correlations and lead time between wastewater surveillance and clinical data in Alberta (Canada): comparing twelve SARS-CoV-2 normalization approaches. *Sci Total Environ*. (2023) 856:158964. doi: 10.1016/j.scitotenv.2022.158964

18. Feng S, Roguet A, McClary-Gutierrez JS, Newton RJ, Kloczko N, Meiman JG, et al. Evaluation of sampling, analysis, and normalization methods for SARS-CoV-2 concentrations in wastewater to assess COVID-19 burdens in Wisconsin communities. *ACS ES T Water*. (2021) 1:1955–65. doi: 10.1021/acsestwater.1c00160

19. Dhiyebi HA, Cheng L, Varia M, Atanas K, Srikanthan N, Hayat S, et al. Estimation of COVID-19 case incidence during the omicron outbreaks based on SARS-CoV-2 wastewater load in previous waves, Peel region, Canada. *Emerg Infect Dis*. (2023) 29:1580–8. doi: 10.3201/eid2908.221580

20. Center for Disease Control. Research use only 2019-novel coronavirus (2019-nCoV) real-time RT-PCR primers and probes. *CDC's diagnostic test for COVID-19 only and supplies* (2020) 2019–2020. Available at: https://www.cdc.gov/coronavirus/2019-ncov/lab/virus-requests.html

21. Zhang T, Breitbart M, Lee WH, Run J-Q, Wei CL, Soh SWL, et al. RNA viral community in human feces: prevalence of plant pathogenic viruses. *PLoS Biol*. (2006) 4:e3. doi: 10.1371/journal.pbio.0040003

22. Bustin SA, Benes V, Garson JA, Hellemans J, Huggett J, Kubista M, et al. The MIQE guidelines: minimum information for publication of quantitative real-time PCR experiments. *Clin Chem*. (2009) 55:611–22. doi: 10.1373/clinchem.2008.112797

23. Cleveland RB, Cleveland WS, McRae JE, Terpenning I. STL: a seasonal-trend decomposition procedure based on loess (with discussion). *J Off Stat*. (1990) 6:3–73. Available at: http://cs.wellesley.edu/~cs315/Papers/stl statistical model.pdf

24. Government of Ontario. *Status of COVID-19 cases in Ontario*. (2020). Available at: https://data.ontario.ca/en/dataset/status-of-covid-19-cases-in-ontario/resource/ed270bb8-340b-41f9-a7c6-e8ef587e6d11 (Accessed June 1, 2023).

25. D'Aoust PM, Tian X, Towhid ST, Xiao A, Mercier E, Hegazy N, et al. Wastewater to clinical case (WC) ratio of COVID-19 identifies insufficient clinical testing, onset of new variants of concern and population immunity in urban communities. *Sci Total Environ*. (2022) 853:158547. doi: 10.1016/j.scitotenv.2022.158547

26. Hegazy N, Cowan A, Aoust PMD, Mercier É, Towhid ST, Jia J. Understanding the dynamic relation between wastewater SARS-CoV-2 signal and clinical metrics throughout the pandemic. *Sci Total Environ*. (2022) 853:158458. doi: 10.1016/j.scitotenv.2022.158458

27. Boehm AB, Wolfe MK, White BJ, Hughes B, Duong D. Divergence of wastewater SARS-CoV-2 and reported laboratory-confirmed COVID-19 incident case data coincident with wide-spread availability of at-home COVID-19 antigen tests. *medRxiv* (2023). Available at: https://www.medrxiv.org/content/10.1101/2023.02.09.23285716v1. [Epub ahead of preprint]

28. Schoen ME, Wolfe MK, Li L, Duong D, White BJ, Hughes B, et al. SARS-CoV-2 RNA wastewater settled solids surveillance frequency and impact on predicted COVID-19 incidence using a distributed lag model. *ACS ES T Water*. (2022) 2:2167–74. doi: 10.1021/acsestwater.2c00074

29. Diedenhofen B, Musch J. Cocor: a comprehensive solution for the statistical comparison of correlations. *PLoS One*. (2015) 10:1–12. doi: 10.1371/journal.pone.0121945

30. Zou GY. Toward using confidence intervals to compare correlations. *Psychol Methods*. (2008) 12:399–413. doi: 10.1037/1082-989X.12.4.399

31. Greenwald HD, Kennedy LC, Hinkle A, Whitney ON, Fan VB, Crits-Christoph A, et al. Tools for interpretation of wastewater SARS-CoV-2 temporal and spatial trends demonstrated with data collected in the San Francisco Bay Area. *Water Res X*. (2021) 12:100111. doi: 10.1016/j.wroa.2021.100111

32. Duvallet C, Wu F, Mcelroy KA, Imakaev M, Endo N, Xiao A, et al. Nationwide trends in COVID-19 cases and SARS-CoV-2 RNA wastewater concentrations in the United States. *ACS ES T Water*. (2022) 2:1899–909. doi: 10.1021/acsestwater.1c00434

33. Mitranescu A, Uchaikina A, Kau AS, Stange C, Ho J, Tiehm A, et al. Wastewater-based epidemiology for SARS-CoV-2 biomarkers: evaluation of normalization methods in small and large communities in southern Germany. *ACS ES T Water*. (2022) 2:2460–70. doi: 10.1021/acsestwater.2c00306

34. Kim S, Kennedy LC, Wolfe MK, Criddle CS, Duong DH, Topol A, et al. SARS-CoV-2 RNA is enriched by orders of magnitude in primary settled solids relative to liquid wastewater at publicly owned treatment works. *Environ Sci Water Res Technol*. (2022) 8:757–70. doi: 10.1039/D1EW00826A

35. Wolfe MK, Archana A, Catoe D, Coffman MM, Dorevich S, Graham KE, et al. Scaling of SARS-CoV-2 RNA in settled solids from multiple wastewater treatment plants to compare incidence rates of laboratory-confirmed COVID-19 in their sewersheds. *Environ Sci Technol Lett*. (2021) 8:398–404. doi: 10.1039/D1EW00826A

36. Natarajan A, Zlitni S, Brooks EF, Vance SE, Dahlen A, Hedlin H, et al. Gastrointestinal symptoms and fecal shedding of SARS-CoV-2 RNA suggest prolonged gastrointestinal infection. *Med*. (2022) 3:371–387.e9. doi: 10.1016/j.medj.2022.04.001

37. Arts PJ, Daniel Kelly J, Midgley CM, Anglin K, Lu S, Andino R, et al. Longitudinal and quantitative fecal shedding dynamics of SARS-CoV-2, 1 pepper mild mottle virus and CrAssphage. *mSphere*. (2023) e00132–23. doi: 10.1128/msphere.00132-23

38. Roldan-Hernandez L, Boehm AB. Adsorption of respiratory syncytial virus (RSV), rhinovirus, SARS-CoV-2, and F^+ bacteriophage MS2 RNA onto wastewater solids from raw wastewater. *bioRxiv* (2023) Available at: https://www.biorxiv.org/content/10.1101/2023.05.04.539429v1. [Epub ahead of preprint]

39. Breadner PR, Dhiyebi HA, Fattahi A, Srikanthan N, Hayat S, Aucoin MG, et al. A comparative analysis of the partitioning behaviour of SARS-CoV-2 RNA in liquid and solid fractions of wastewater. *Sci Total Environ*. (2023) 895:165095. doi: 10.1016/j.scitotenv.2023.165095

40. Torii S, Oishi W, Zhu Y, Thakali O, Malla B, Yu Z, et al. Comparison of five polyethylene glycol precipitation procedures for the RT-qPCR based recovery of murine hepatitis virus, bacteriophage phi6, and pepper mild mottle virus as a surrogate for SARS-CoV-2 from wastewater. *Sci Total Environ*. (2022) 807:150722. doi: 10.1016/j.scitotenv.2021.150722

41. Bivins A, North D, Wu Z, Shaffer M, Ahmed W, Bibby K. Within- and between-day variability of SARS-CoV-2 RNA in municipal wastewater during periods of varying COVID-19 prevalence and positivity. *ACS ES T Water*. (2021) 1:2097–108. doi: 10.1021/acsestwater.1c00178

42. George AD, Kaya D, Layton BA, Bailey K, Mansell S, Kelly C, et al. Impact of sampling type, frequency, and scale of the collection system on SARS-CoV-2 quantification fidelity. *Environ Sci Technol Lett*. (2022) 9:160–5. doi: 10.1021/acs.estlett.1c00882

43. Nguyen Quoc B, Saingam P, RedCorn R, Carter JA, Jain T, Candry P, et al. Case study: impact of diurnal variations and stormwater dilution on SARS-CoV-2 RNA signal intensity at neighborhood scale wastewater pumping stations. *ACS ES T Water*. (2022) 2:1964–75. doi: 10.1021/acsestwater.2c00016

44. Kmush BL, Monk D, Green H, Sachs DA, Zeng T, Larsen DA. Comparability of 24-hour composite and grab samples for detection of SARS-2-CoV RNA in wastewater. *FEMS Microbes*. (2022) 3:xtac017. doi: 10.1093/femsmc/xtac017/6609772

45. Augusto MR, Claro ICM, Siqueira AK, Sousa GS, Caldereiro CR, Duran AFA, et al. Sampling strategies for wastewater surveillance: evaluating the variability of SARS-COV-2 RNA concentration in composite and grab samples. *J Environ Chem Eng*. (2022) 10:107478. doi: 10.1016/j.jece.2022.107478

46. Curtis K, Keeling D, Yetka K, Larson A, Gonzalez R. Wastewater SARS-CoV-2 concentration and loading variability from grab and 24-hour composite samples. *medRxiv* (2020). Available at: https://www.medrxiv.org/content/10.1101/2020.07.10.20150607v2. [Epub ahead of preprint]

frontiers | Frontiers in Public Health

TYPE Original Research
PUBLISHED 02 November 2023
DOI 10.3389/fpubh.2023.1141494

OPEN ACCESS

EDITED BY
Charlene Ranadheera,
Public Health Agency of Canada (PHAC), Canada

REVIEWED BY
Sanjeeb Mohapatra,
National University of Singapore, Singapore
Robert Delatolla,
University of Ottawa, Canada

*CORRESPONDENCE
Erwin Nagelkerke
✉ erwin.nagelkerke@rivm.nl

RECEIVED 10 January 2023
ACCEPTED 22 September 2023
PUBLISHED 02 November 2023

CITATION
Nagelkerke E, Hetebrij WA, Koelewijn JM, Kooij J, van der Drift A-MR, van der Beek RFHJ, de Jonge EF and Lodder WJ (2023) PCR standard curve quantification in an extensive wastewater surveillance program: results from the Dutch SARS-CoV-2 wastewater surveillance.
Front. Public Health 11:1141494.
doi: 10.3389/fpubh.2023.1141494

PCR standard curve quantification in an extensive wastewater surveillance program: results from the Dutch SARS-CoV-2 wastewater surveillance

Erwin Nagelkerke*, Wouter A. Hetebrij, Jaap M. Koelewijn, Jannetje Kooij, Anne-Merel R. van der Drift, Rudolf F. H. J. van der Beek, Eline F. de Jonge and Willemijn J. Lodder on behalf of Consortium NRS

Centre for Infectious Disease Control, National Institute for Public Health and the Environment (RIVM), Bilthoven, Netherlands

Since the start of the COVID-19 pandemic in 2020, wastewater surveillance programs were established, or upscaled, in many countries around the world and have proven to be a cost-effective way of monitoring infectious disease pathogens. Many of these programs use RT-qPCR, and quantify the viral concentrations in samples based on standard curves, by including preparations of a reference material with known nucleic acid or virus concentrations in the RT-qPCR analyses. In high-throughput monitoring programs it is possible to combine data from multiple previous runs, circumventing the need for duplication and resulting in decreased costs and prolonged periods during which the reference material is obtained from the same batch. However, over time, systematic shifts in standard curves are likely to occur. This would affect the reliability and usefulness of wastewater surveillance as a whole. We aim to find an optimal combination of standard curve data to compensate for run-to-run measurement variance while ensuring enough flexibility to capture systematic longitudinal shifts. Based on more than 4000 observations obtained with the CDC N1 and N2 assays, taken as a part of the National Sewage Surveillance program at the Dutch National Institute for Public Health and the Environment, we show that seasonal and long-term shifts in RT-qPCR efficiency and sensitivity occur. We find that in our setting, using five days of standard-curve data to quantify, results in the least error prone curve or best approximation. This results in differences up to 100% in quantified viral loads when averaged out over a nationwide program of >300 treatment plants. Results show that combining standard curves from a limited set of runs can be a valid approach to quantification without obscuring the trends in the viral load of interest.

KEYWORDS

WBE, wastewater, sewer, surveillance, standard, calibration, qPCR assay

1. Introduction

The idea of monitoring pathogens through wastewater has been applied for decades (1, 2), but interest in waste waterbased epidemiology (WBE) has significantly increased with its applications during the COVID-19 pandemic. SARS-CoV-2 detection in wastewater is currently employed as a monitoring tool in over 70 countries, with several programs reaching significant population coverage (3).

Many of these surveillance programs, and WBE studies on SARS-CoV-2 in general, make use of reverse transcription quantitative polymerase chain reaction (RT-qPCR) on one or more regions of the virus genome as the primary method to quantify the number of RNA copies in wastewater samples (4, 5). Absolute quantification of RNA concentrations in this way relies heavily on the use of standard curves with which the initial RT-qPCR results, in the form of cycle threshold values (Ct-values), are converted to a known concentration.

Similar to virtually all measurement instruments, RT-qPCR is known to produce results with test–retest variability. That is, multiple tests of the same sample are known to result in slightly different Ct-values. This not only applies to the results of the Ct-values of samples, but also to the Ct-values of the standard dilutions that result in PCR efficiency estimates and ultimately determine the standard curve that is used for quantification. Although such variation is smaller in (synthetic) preparations with known RNA particle counts, this variation can still affect the quantification process. Therefore, it is recommended to construct a standard curve using multiple replicates and dilutions for each assay (6–8).

The sources of variation in outcomes between duplicate analyses are plentiful and often hard to identify, as it may be any external factor that has the potential to affect the efficiency and sensitivity of the RT-qPCR, as small as changes in mains voltage (9). These may cause stochastic measurement error, where variations occur due to, e.g., randomness in the chemical processes during the RT-qPCR, temperature fluctuations, or external factors such as minor differences in the preparations made by laboratory technicians. Yet, other sources of variation in outcomes, such as the use of different batches of chemicals, seasonal differences in laboratory atmosphere, or general wear and tear of equipment may result in longer-term, systematic changes.

On the one hand, in a more traditional research setting with a predetermined number of experiments conducted in a limited timeframe, such structural external influences are easier to control than in a long-term monitoring setting. When analyses continue over a period of multiple years, it becomes prohibitively difficult to guarantee exactly identical circumstances, chemicals from the same batch run out, and there is personnel turnover. On the other hand, with continuous analyses, the opportunity exists to combine standard curve data from multiple runs, avoiding the need to duplicate the dilutions of the reference material in each run.

This implies that a trade-off exists between on the one hand combining duplicates between runs that reduce random variation caused by stochastic measurement error, and on the other hand updating the standard curve over time to take systematic shifts into account that would bias the quantification process when ignored. This issue of systematic shifts is also identified by Bivins et al. (10), who suggest to monitor shifts in Ct-values over time to determine when to replace the reference material, or use an overall calibration curve based on a mixture model to incorporate run-to-run variability. The trade-off is implicitly recognized throughout the literature where duplication is often recommended, but with consideration for between-run variability (e.g., 8).

Here we investigate this trade-off and present the results from the Dutch National Wastewater Surveillance (NRS) program, based on more than 4000 standard curves obtained using the US CDC SARS-CoV-2 assay targeting two parts of the nucleocapsid protein (N1 and N2 assays) (11), between September 2021 and November 2022. Based on these data we propose and investigate an approach of combining observations of the standard from multiple runs to reduce the effect of random variations in the analyses, while still taking systematic shifts in RT-qPCR efficiency and sensitivity into account. This approach has the potential to be a cost-saving method in high-throughput programs, when it can reduce or eliminate the requirement to duplicate reference material series per run, and may allow quantification of samples from successful PCR runs with an erroneous standard curve. Conversely, in programs with lower analysis frequencies the method may instead lead to a reduction of unwanted variation in standard curve estimation without extra resources, when the results for the reference material can be combined over multiple runs.

2. Materials and methods

2.1. Standard curve methodology

2.1.1. Log-linear standard curves

Absolute quantification by using a standard curve is an intuitive solution to the problem that initial values are only comparable within one PCR run (12). By including a consistent reference material with, in the case of SARS-CoV-2 analysis, a known RNA concentration the relationship between the Ct-value this reference material produces and its concentration can be determined. By including multiple dilutions of reference material, a curve can be constructed that allows interpolation of the relationship between the Ct-value and the RNA concentration. These standard dilutions are generally 10-fold because of practical considerations in laboratory protocols. Due to the expected exponential growth of particles in the RT-qPCR process, the theoretical relationship between the Ct-value and concentration can be described as:

$$\mathrm{Ct} = \mathrm{Intercept} + \mathrm{Slope} * \log_{10}\left(\mathrm{Concentration}\right) \qquad (1)$$

Since not the Ct-value is of interest, but the RNA concentration of the sample, this is rewritten as:

$$\log_{10}\left(\mathrm{Concentration}\right) = \left(\mathrm{Ct} - \mathrm{Intercept}\right) / \mathrm{Slope} \qquad (2)$$

With the increasing popularity of RT-qPCR, advances to the basic approach have been developed, many of them focusing on the implicit assumption that the efficiency is equal for all samples included in a PCR run (13–15). Further improvements focus on better estimates of the efficiency, and a higher precision of the resulting standard curve (16–18). However, despite these efforts, simple ordinary least squares

(OLS) curve estimation is still predominant in current research. This may be explained by the intuitive theory behind it, the need to maintain comparability to earlier studies, and the varying results of alternatives (14, 19). Moreover, it is surprisingly rare that obtaining the true RNA or DNA particle count is needed, and in the vast majority of applications maintaining an acceptable level of unbiased comparability between analyses suffices.

Since RT-qPCR is an approximately exponential process whereby PCR doubles the number of DNA particles per cycle, the ideal circumstance would be that each unit increase in Ct-value leads to exactly doubling the number of particles per amplification cycle. On a base-10 logarithmic scale this results in a slope of −3.32. That is, under ideal circumstances, a 3.32 point increase in Ct-value should occur per 10-fold dilution, regardless of the dilution's absolute particle count.

In that light, the slope of a standard curve is determined by the relative distance between Ct-values of the dilutions of the reference material, assuming that log-linearity holds. As a result, the slope and associated efficiency are primarily indicative of the difference in concentration between high- and low concentration samples or dilutions. Anything that affects the RT-qPCR process in full, is captured in the intercept and could be deemed indicative of the sensitivity.

Of course, directly controllable factors such as the threshold of the analyses linearly affect the resulting Ct-values and can be chosen arbitrarily as long as they are placed in the log-linear phase of the amplification process. However, other factors can impact run-to-run comparability as they may shift the intercept of the standard curve, such as equipment wear and tear, differences between batches of materials and reagents, and laboratory temperatures or humidity. Such factors may affect both the degree of fluorescent luminescence of the sample material, as well as the sensitivity of sensors to the fluorescence (16). When such external factors affect the process equally for all, or a majority, of the dilutions of the reference, the resulting Ct-values change by an approximately equal amount. This would result in a largely unchanged slope, and an increase or decrease of the intercept proportional to the change in Ct-values.

The above has led to suggesting different ways to construct the standard curve when multiple analyses are conducted, based on the circumstances. Generally, when quantifying RNA or DNA from samples, researchers use either the Ct-values of the standard curve per run, or use a master curve where multiple runs are combined. Neither option is very useful or theoretically sensible in long-running surveillance programs, because these would either allow stochastic variance to affect trend estimation, or cause structural changes in quantification parameters to be ignored over time.

Two alternative approaches are based on multilevel random intercept and random slopes mixture models. These approaches combine information from all runs to reduce stochastic error, but allow either the intercept to vary with a fixed slope, or allow both the intercept and slope to vary per run (16). Although elegant solutions, there are some caveats when applying them for long-term, real-time monitoring. Firstly, these methods are introduced with the assumption that the complete data is available before standard curve estimation, and would require extensive computation after each PCR analysis in a continuous monitoring setting. Secondly, and more problematic, is that the approaches do not guarantee that shifts over time are properly captured. The estimation assumes that between-run variation randomly fluctuates around a midpoint. That midpoint, however, suffers the same problem as a master curve and is slow to incorporate systematic shifts due to it being based on all historically available data.

2.1.2. Rolling window master curve

To overcome the latter point, we here suggest an approach that uses historic data on standard curves within a rolling window as a pragmatic way to take advantage of the continuous observations of the standard in a monitoring setting. Such an approach may simultaneously reduce unwanted, stochastic variance by using more of the available data while still being able to incorporate longitudinal shifts in RT-qPCR efficiency and sensitivity. Due to its widespread use we do so using common standard curve methodology, where future steps are to combine these findings with advances such as using mixture models in curve estimation to allow plate-specific variance in efficiency estimation.

The assumption here is that, on average, an ideal amount of historic data of the reference dilutions exists. Using the data from this period reduces stochastic error in standard curves more than error that is introduced by structural shifts in the standard curves. Specifically, the distance between the expected Ct-values based on the current standard curve, and the Ct-values from the standard curve based on earlier observations of the reference material can be minimized. At the point of the smallest error, the standard curve based exclusively on historic data is the best approximation of the current standard curve parameters. That is, we propose an analysis using previously obtained standard curves, or measurements of the reference dilutions, whereby these observations of dilution series are used to obtain a standard curve that is compared to the current curve.

Because systematic changes are a function of time, the curves based on previous observations of the reference material are here obtained per day, but the span could be any theoretical sensible timeframe, or can be a number of previous runs. Based on the observations within this historical span a standard curve can be constructed using the observed Ct-values of the dilution series. Subsequently, the root mean square error (RMSE) between the curve based on a given number of previous days and the per-run curves of today can then obtained by computing the Ct-values associated with the known particle counts on the line per run, and the difference to the Ct-values resulting from the line based on historical data. Note that the error should be obtained per current day run, and only subsequently be aggregated. Not doing so would average out any differences between standard curves before obtaining the residual, which would significantly reduce the potential impact of individual runs. Doing the above for different amounts of historical data, e.g., 1 through 20 days prior to today, the span that on average best approximates all standard curve observations of today can be determined by minimizing the RMSE. The expectation here is that the ideal tradeoff between systematic and random error can be determined. As more data is used, stochastic error variance will be reduced, but error due to systematic shifts in the standard curve parameters will increase. At the point with the lowest RMSE the reduction in stochastic variance is smaller than the error introduced due to systematic shift in standard curves, identifying the ideal size of the window of the smoothed, rolling window curve.

Further note that the curves estimated on data obtained in the preceding days should be based exclusively on data preceding the current day or current run. Including observations from the current

run or day in this analysis would give an arbitrary advantage to curves based on less historic data, since current observations are the best approximation of themselves and would form a larger share of the data when less previous information is used. For this same reason the most current data does need to be incorporated for the final curve that is used for quantification.

As a final remark, in the presented situation, curves based on one or two previous days are systematically missing due to weekends and national holidays. This is resolved by using the last estimate available in the cases where no data is observed on days prior to today. This would be the most pragmatic solution when applying the idea of a rolling window in practice.

2.2. Reference material

A synthetic DNA construct containing complementary sequences of the CDC 2019-nCoV Real-Time RT-PCR Diagnostic Panel, consisting of primers and probes that target the nucleocapsid (N) gene (11, G-block sequence in S1), downstream of a T7 RNA-polymerase promotor (Thermo Fisher Scientific) was used to transcribe RNA using the MEGAshortscript™ T7 Transcription Kit (Thermo Fisher Scientific).

Following transcription, and after a DNase step to remove the synthetic DNA construct, the generated RNA was quantified using a clinical isolate with a known concentration of SARS-CoV-2 genome copy numbers. In RT-qPCR, each assay, consisting of different primers/probes, has a different priming reaction. Therefore the performance of the N1 and N2 assay on the generated standard RNA has to be evaluated separately (11).

Ten-fold serial dilutions of the generated standard RNA were tested to determine which dilutions could be included in the quantification curve, resulting in five dilutions of the RNA standard generating a positive signal.

The generated standard RNA was aliquoted in large batches of 7 µL per tube (for single use) and stored in a −80°C freezer. Before each RT-qPCR run the standard RNA is serially diluted for direct use. Per 96-wells PCR plate the RNA of 20 samples are tested in duplicate using the N1 and N2 assays. The RT-qPCR is performed as prescribed previously (11) with minor modifications; Each reaction contained 1x TaqMan Fast Virus 1-step Master Mix (Thermo Fischer Scientific) and a final concentration of 0.5 µM and 0.25 µM of primers and probes, respectively. In each RT-qPCR run, for each assay, a negative control, a positive control and five dilutions of the standard RNA are included. All analyses were performed in an in-house laboratory at the Dutch National Institute for Public Health and the Environment, using nine different QIAquant 96 5-plex instruments (Qiagen). The threshold with which a Ct-value is determined is fixed across all runs in the log-linear phase of the RT-qPCR process.

2.3. Data

Data collection took place between September 1st 2021 and November 11th 2022 as part of the Dutch NRS program. During this period approximately 125 to 250 wastewater samples were quantified daily, resulting in four to ten PCR runs on average. In each run, five 10-fold dilutions of the RNA standard were included. However, the most diluted reference resulted in inconsistent Ct-values that strongly affect estimated standard curves. Therefore, only the other four standard dilutions are used for the analyses below. To improve readability of figures these are referred to as −04 to −07 in the following. Although general recommendations for dilution series include 5–6 points, we have confidence that the obtained standard curves are adequate, as they very closely match the curves reported in Bivins et al. (10) for the N1 and N2 CDC assay. Furthermore, if additional 10-fold dilutions were added these can occasionally fall outside the log-linear phase of the quantification curves.

The procedures for the quantification are based on the NEN-EN-ISO-15216-1 (20) standard for hepatitis A virus and norovirus quantification in food chain microbiology. The construction of standard curves prescribed follow the widely used criteria for standard curve estimation, requiring a minimum of three 10-fold dilutions. These should log-linearly result in a slope between −3.60 and −3.10, which equates to a PCR efficiency estimate of 90 to 110%, and a minimum correlation between standard dilutions of 0.99, which translates to an R-squared of 0.980 or higher. In the assessment of RT-qPCR data obvious deviations in the results of the reference dilutions are manually removed before standard curve construction. An example would be two wells with reference material resulting in almost identical Ct-values.

The ISO standard further allows the removal of dilutions based on outlying Ct-values, maintaining the minimum requirement of three or more observed dilutions per standard curve. Here the following procedure is applied: a standard curve is estimated on all four directly observed dilutions, or three in the case of aforementioned reasons for removal. When the resulting curve does not adhere to the criteria, but an acceptable curve exists when excluding any one out of the four dilutions, we use the combination excluding the most diluted reference that leads to an acceptable curve.

Standard curves were obtained on 308 out of 437 days. All days without data are weekends or national holidays. A total of 2282 unique runs were performed, the majority of which contain two series of RNA standard for both the N1 and N2 gene, respectively resulting in 4455 and 4442 approved dilution series. Applying curve construction as described, this leads to 3755 (84%) and 3145 (71%) curves that adhere to the criteria.

To approximate the comparison between using historical data and the recommended duplication of dilution series of the standard, one line per RT-qPCR duplication is constructed for the results in section 3.3. As mentioned, samples within the NRS program are analyzed in duplicate for both N1 and N2 genes, where 40 wells are used for N1 and 40 wells for N2 on a 96-wells plate. Both runs contain a dilution series. The between-plate dependence of these analyses is high, plates contain identical reference material, and although two separate instruments are often used, the external circumstances are close to identical. These two sets of dilutions from the duplicate runs are combined to better approach the situation in which reference material is duplicated, and a standard curve is estimated on 3 – in the worst case scenario where one of the standard curves is unusable – to 8 dilutions, after which the same criteria as before are applied.

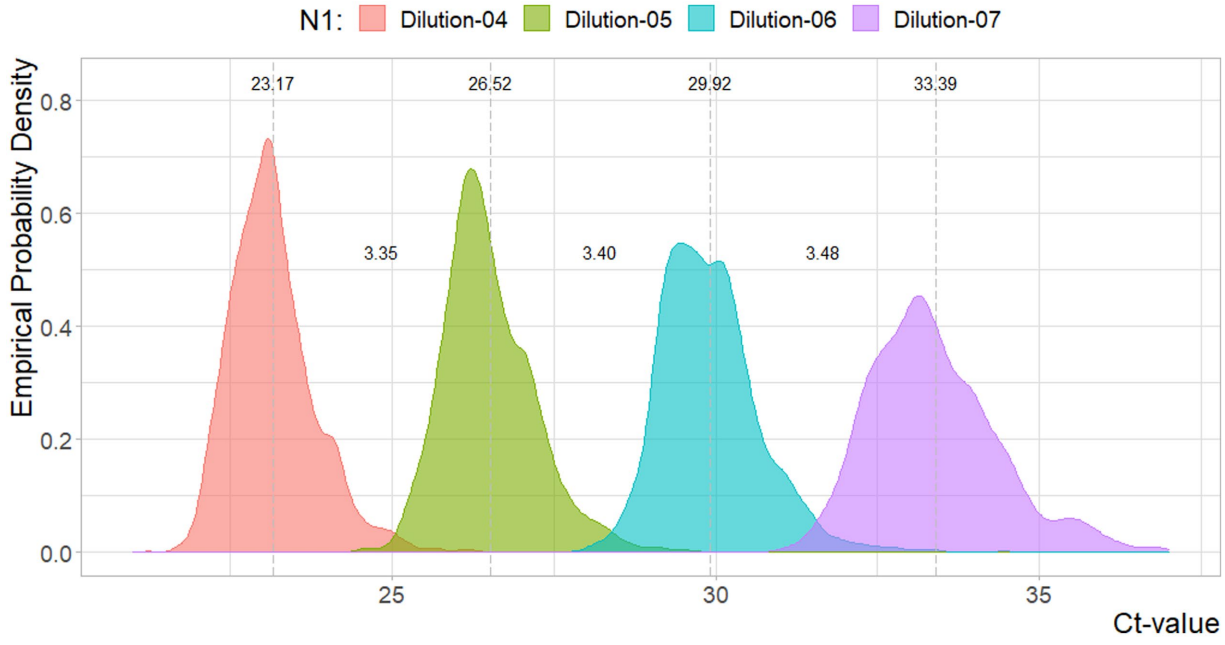

FIGURE 1
Density plot for the Ct-values per N1 reference dilutions. Dotted lines and values indicate the mean value, and distances between the mean values. Sample sizes are 3754, 3753, 3754, 3689, respectively.

3. Results

3.1. Univariate descriptive statistics

To be able to combine the generated data and give a single overview, dependencies in the performance of the different qPCR instruments (QIAquants) are tested by conducting an ANOVA on the slopes and intercepts of constructed standard curves. A description and the results of this analysis can be found in S2. The largest mean difference in standard curve intercepts between two machines equals 0.157 for the N1 assay, and 0.220 on the N2 assay. Explained variance in the estimated intercepts by differences in qPCR instruments does not exceed 0.43% for N1 ($F(8, 3634) = 1.96$, $p = 0.048$), and 1.12% for N2 ($F(8, 2985) = 4.24$, $p < 0.001$). The statistical significance is a result of the large sample sizes, whereas the practical implication of these differences is negligible. With regard to the slopes, the mean differences and explained variance are, respectively, 0.024 and 0.38% for N1, and 0.048 and 0.85% for N2. Although this does not exclude temporary, larger differences between pairs of instruments, the results give confidence that the qPCR results from instruments can be combined.

In Figures 1, 2, the density estimates and mean Ct-values for all observations of the four standard dilutions are shown when any combination leads to a curve within the criteria. Summary statistics are presented in Table 1. For both N1 and N2 the different concentrations show very comparable distributions. Combined with Figures 3, 4, which show a relatively stable long-term slope, the different dilutions seem to be affected in a similar fashion over time. This also explains the slight right-tail skew of the distribution as the intercept is, on average, trending upwards over time. The decreasing kurtosis of the distributions indicates larger variability in lower concentrations, which is expected given the higher levels of uncertainty in PCR analyses in more diluted samples.

3.2. Temporal trends in curve parameters

In Figures 3, 4 the curve parameters estimated on each set of reference material are shown, where the colored scatter indicates standard curves that fall within the selection criteria described in section 2.3. Locally estimated scatterplot smoothing (LOESS) is used for trend estimation.[1] Long-term, structural fluctuation in the standard curves, as well as significant run-to-run variation in both the slope and intercept terms are visible. The former, structural trend, mostly manifests itself in terms of the intercept, which implies that all dilutions of the standard are similarly affected by the external factors that cause the shift, and the standard curve as a whole shifts upwards or downwards over time, in line with Figures 1, 2. Shifts in both the N1 and N2 curves are substantial, with approximately 2 Ct difference between the highest and lowest points. A difference of this magnitude will have a notable impact on the virus concentration obtained for the samples. The slopes of the standard curves, and associated efficiency of the analyses, show less structural fluctuation, indicating that the sensitivity of analyses varies more strongly and systematically than their efficiency.

Moreover, the trends in the N1 and N2 intercepts deviate from one another, and often show shifts in opposite directions, while the RNA is generated using the same G-block. For example, in the period from January to February 2022 the N1 assay shows a decrease in sensitivity (increasing intercept Ct-value) and the N2 assay shows an

1 With a span of 0.25 a quarter of all points is used at each given day, which have a weight based on distance as $(1-(\text{distance}/\text{distance}_{max})^3)^3$. This gives points closest to the day of interest a much higher weight than more distant points.

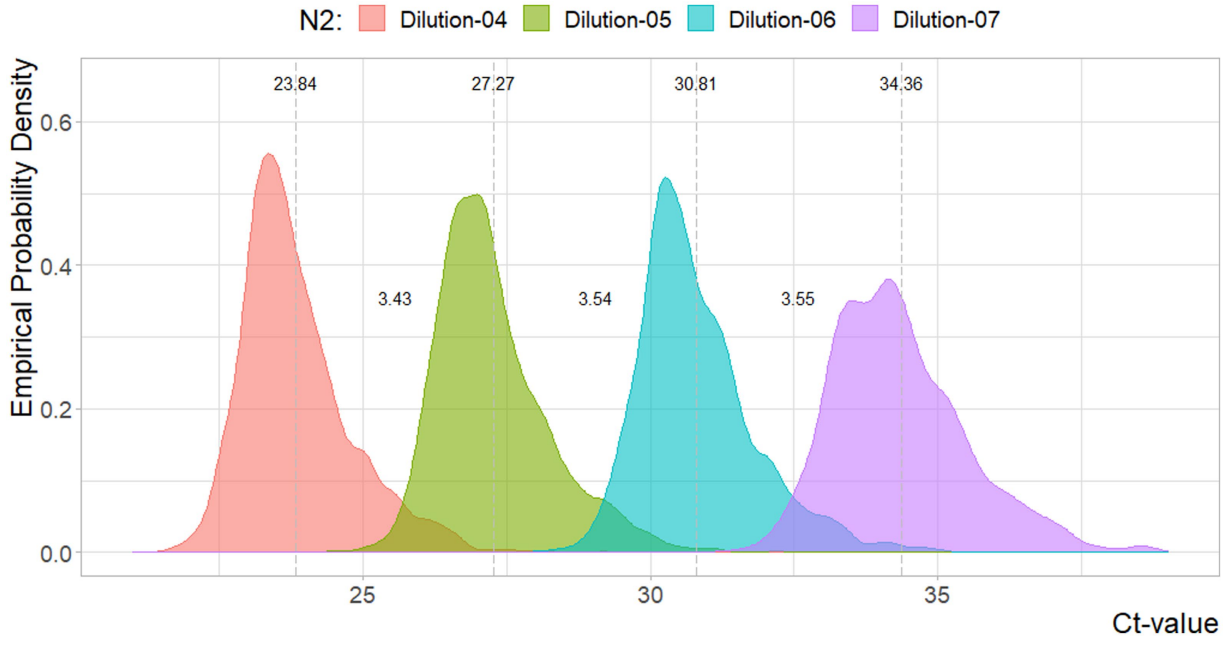

FIGURE 2
Density plot for the Ct-values per N2 reference dilutions. Dotted lines and values indicate the mean value, and distances between the mean values. Sample sizes are 3144, 3140, 3144, 3049, respectively.

TABLE 1 Summary statistics of the reference dilutions.

	N1				N2			
	Mean	Median	Density	Var	Mean	Median	Density	Var
St-04	23.17 (–)	23.08 (–)	23.09 (–)	0.50	23.87 (–)	23.64 (–)	23.37 (–)	0.90
St-05	26.52 (3.35)	26.39 (3.31)	26.21 (3.12)	0.61	27.27 (3.43)	27.08 (3.44)	26.98 (3.61)	1.03
St-06	29.92 (3.40)	29.83 (3.44)	29.46 (3.25)	0.61	30.81 (3.54)	30.60 (3.52)	30.28 (3.31)	1.12
St-07	33.39 (3.48)	33.25 (3.42)	33.13 (3.67)	1.13	34.36 (3.55)	34.18 (3.58)	34.15 (3.87)	1.50

Distances between dilutions between parentheses.

almost equal increase in sensitivity. This is plausible given that the N-gene primers and probes show different concentrations after preparation, but also implies that they react to different external factors, or react differently to similar external factors.

Disregarding the seasonal variation in Figures 3, 4, both assays also show a steady upward trend over the year. This is less apparent for the N2 assay from the figure, due to the trendline being somewhat distorted at the endpoints. The first and last week of data have above and below average intercept estimates, respectively. This upward trend is seemingly small (N1; $B = 0.004$, $t = 39.72$, $p < 0.001$. N2; $B = 0.003$, $t = 24.65$, $p < 0.001$), but results in a theoretical shift of 1.57 Ct for N1 and 1.18 Ct for N2 over the course of one year, which will cause a significant upward trend in terms of the obtained viral concentrations from samples. We assume this to be the result of general wear and tear, as all data is obtained from PCR equipment that was brand new at the start of the measurements when sensitivity is expected to decline faster during a period of breaking in the new instruments. A similar trend is not observed in data before September 2021 obtained in a laboratory with older equipment.

The slopes in the second panel of the figures indicate good efficiency, but structurally result in efficiency estimates just below the 90% limit. The net result of this is hard to determine. A steeper slope causes smaller differences in concentration for equal differences in Ct-values. However, this may cause both over- and underestimation, and is further compounded by the interaction between the slope and the intercept terms. One explanation may be so-called compound errors; the different standard RNA dilutions are obtained through serial dilution of one batch preparation. In practice it is almost always the case that when minor variations occur, too little standard material is pipetted, causing the assumed concentration to be higher than the true concentration. This error is then carried over to any dilutions made afterwards.

To inspect if the mentioned interaction between slope and intercept terms does not result in systematic bias, the $\log_{10}$ viral load of three Ct-values associated with high (29) / medium (33) / low (37) viral concentrations is plotted over time in Figure 5. Here any systematic over- or underestimation of samples with different concentrations would result in diverging trends over time (i.e., increasing or decreasing distances between the respective $\log_{10}$ concentrations), of which there is no evidence. In addition, the N1 and N2 gene show the same overall trend, but have almost diametrically opposed short-term fluctuations, again indicating that external factors

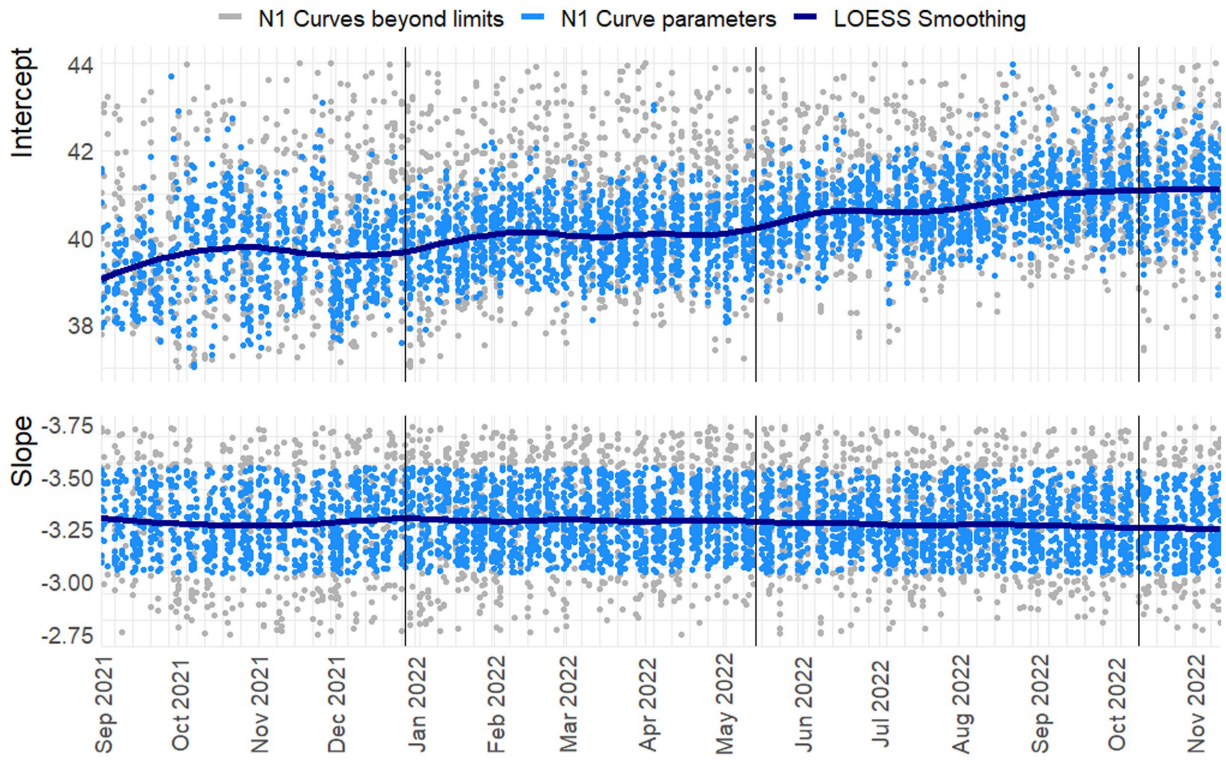

FIGURE 3
Slope and intercept for the N1 Target. LOESS smoothing with span = 0.25, degree = 2. N = 3755/4455. Vertical lines indicate a new preparation from the CDC assay. Blue dots indicate line parameters of accepted standard curves, gray dots show rejected curves. For readability 242 and 650 observations are beyond the y-axis limits for the intercept and slope, respectively.

affect the sensitivity, efficiency, and quantification of the samples differently.

3.3. Rolling window master curve

In Figure 6 the RMSE between the Ct-values associated with the different dilutions of the reference material are shown, per number of previous days included in the curve based on historic data.

In line with the expectation, including more data to reduce random variance works for a brief period of time, signified by the error reduction as a result of using data over one through four days. The shifts in error reduction on day three for the N2, and between days six and fifteen of the N1 assay can both be explained by the remaining effects of days without observations. The average age of the data used to approximate the current curve fluctuates, and is oldest when Monday is predicted using last week's data. That is, due to having no new data in the weekend, a prediction based on three days of data causes a prediction of Monday by only using Friday, which explains the sudden increase of error for the N2 assay. This effect re-occurs every seven days, where there is a transition between having either more data available, and that data being older data on average.

Figure 7 shows the aggregated error between the historic curve and the curves obtained on the current day. The weekend-weekday effect is amplified here, as the error is combined across dilutions. It is nonetheless apparent that using standard curves estimated on the data of four days prior gives the best approximation of today's standard curves, although it should be noted that using between four and seven days would not give significantly different results, both in the statistical and substantive sense.

Figure 8 contains the slopes and intercepts for three methods – duplicate standard combined in two simultaneous runs, a cumulative master curve using all data up to that point, and the suggest rolling curve over five days of data – when used to estimate standard curves using the Ct-values of the N1 standard dilutions (see S3 for N2). To depict the trend in the day-to-day quantification, a line is also estimated using the combined data from each day. As previously mentioned, the rolling curve was re-estimated to include a total of five days: the four previous dates as shown in Figure 6, plus today.

The suggested approach of including five days of data results in standard curves that follow the trend in day-to-day variation, with the exception of October 2021, and the third week of August 2022. In contrast, the master curve clearly shows increasing underestimation of the intercept and steepness of the slope compared to the other methods. Note that the slope is negative, and a shallower, less negative, slope indicates increased efficiency. This result is, of course, specific to the trends in standard curve parameters that are observed in the data from the NRS program, where a steady increase in intercepts, and decrease in slopes occur in the data.

Whether or not over- or underestimation of the concentration occurs depends on the observed Ct-value of a sample, and the over- or

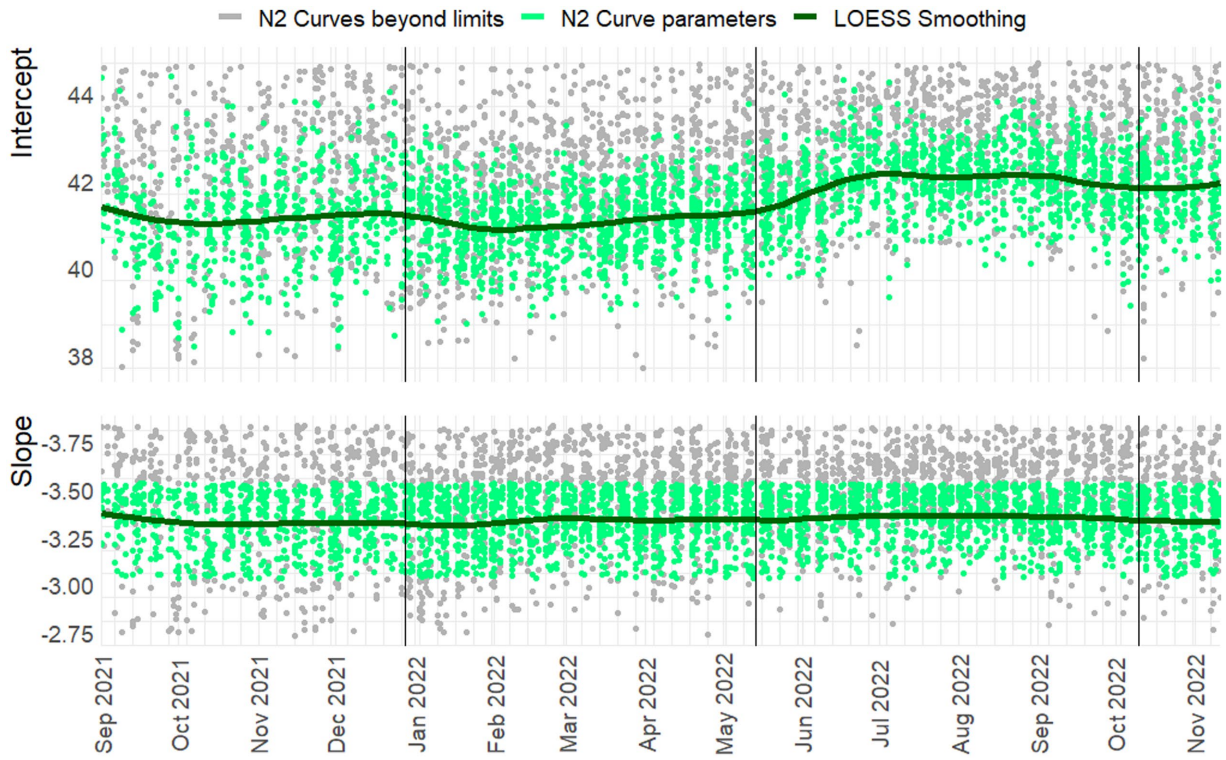

FIGURE 4
Slope and intercept for the N2 Target. LOESS smoothing with span = 0.25, degree = 2. N = 3145/4442. Vertical lines indicate a new preparation from the CDC assay. Green dots indicate line parameters of accepted standard curves, gray dots show rejected curves. *Note:* For readability 548 and 855 observations are beyond the y-axis limits for the intercept and slope, respectively.

underestimation of the intercept and slope. For example, when a high intercept and steep slope are found, it may be the case that the concentration of samples with low Ct-values may be underestimated based on the high number of cycles associated with the intercept. However, due to the steep slope, using the same curve may cause overestimation of the concentration of samples with high Ct-values.

3.4. Trends in quantified viral concentrations

In Figure 9 a fixed Ct-value of 30 is quantified using the different standard curves, of which the parameters are plotted in Figure 8. Note that general trends occur gradually even when new preparations of the standard are made, and these do not seem to cause sudden changes.

Figure 9 makes clear how relatively limited changes in the standard curve parameters can have large effects on the sample concentrations due to the logarithmic relationship between Ct-values and concentration. Even when applying replication of the standard dilutions, run-to-run variation can be high between days and regularly causes extreme values. Standard curves of these runs adhere to the specified criteria and although their intercept terms, for which no criterion is applied, are relatively high, they are not so high as to raise immediate suspicion in light of the daily variation observed. Concentrations of that magnitude would, of course, be subject to further inspection after quantification as clear outliers, but the properties of the standard curve do not indicate problems in isolation.

The proposed approach of including several previous days reduces the run-to-run, and day-to-day variance. Due to the outlying virus concentrations based on per-run standard curves, Figure 9 does not do full justice to the day-to-day variance. For example, in December 2021 there is an almost 100% larger shift in viral concentration based on daily standard curves than based on the other approaches to quantification. Moreover, daily runs already partially use historical data due to the use of the ISO criteria for the curves and using the most recently accepted curve if the current curve is problematic. This paradoxically leads to the situation where the daily standard curves capture less of the variance in standard curve variance, and would occasionally show almost equally extreme concentrations as run-based curves when they are used on face value.

Finally, in Figure 10 a selection of 44500 samples from the NRS program, collected between January 1st and November 11th 2022 are quantified and aggregated to country level using the described methods. For details on sample collection, aggregation, and hospitalization data, see Geubbels et al. (21). Samples are only included if a standard curve is available for the RT-qPCR run on which they were originally analyzed. Note that due to data selection, and not using inflow or inhabitant corrections for the final concentration, the trend presented cannot be interpreted as the viral trend in The Netherlands. It does nonetheless track the virus concentration to an acceptable level for the purpose of this study.

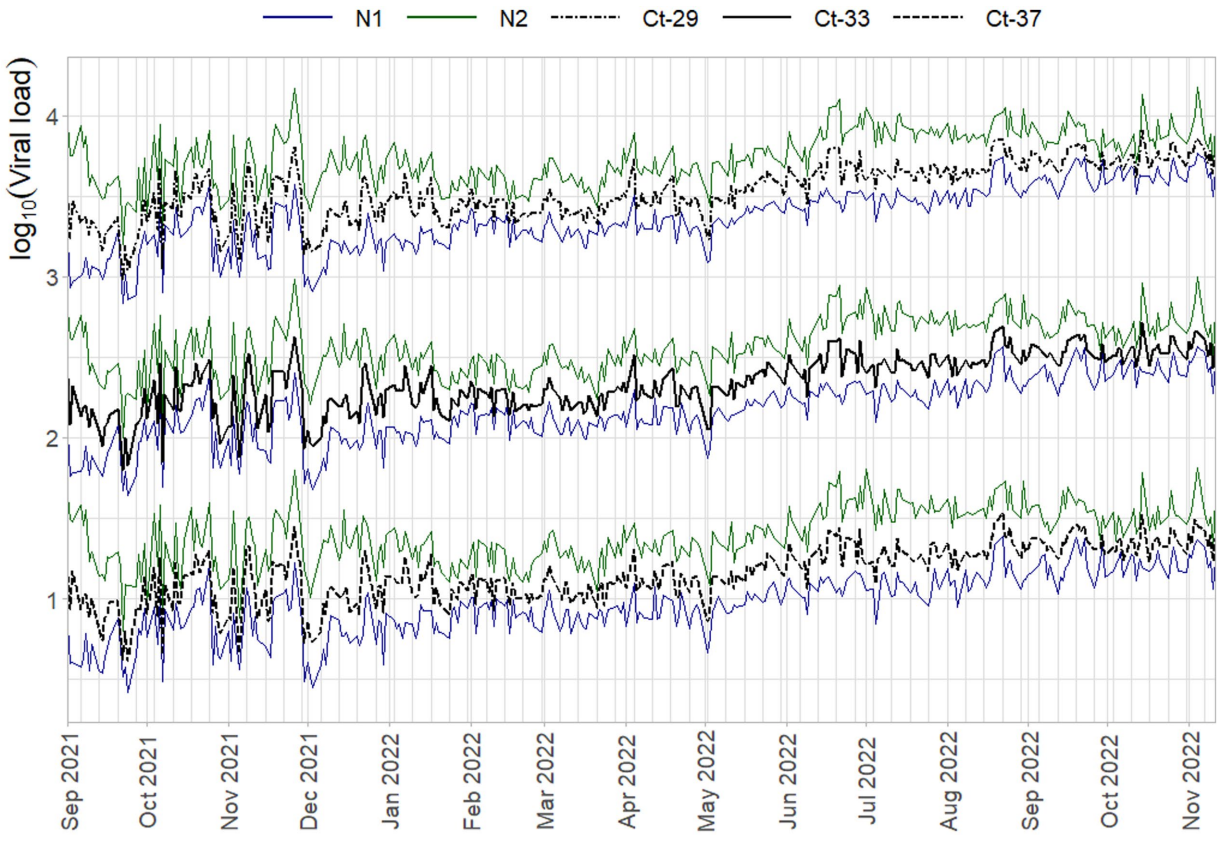

FIGURE 5
Average daily $\log_{10}$ concentration of three Ct-values when quantified with the standard curves per run on that day. N1 (blue) and N2 (green) trends are superimposed on all three Ct-value sets (black lines), which are plotted on a base-10 log-scale to be able to distinguish them from each other.

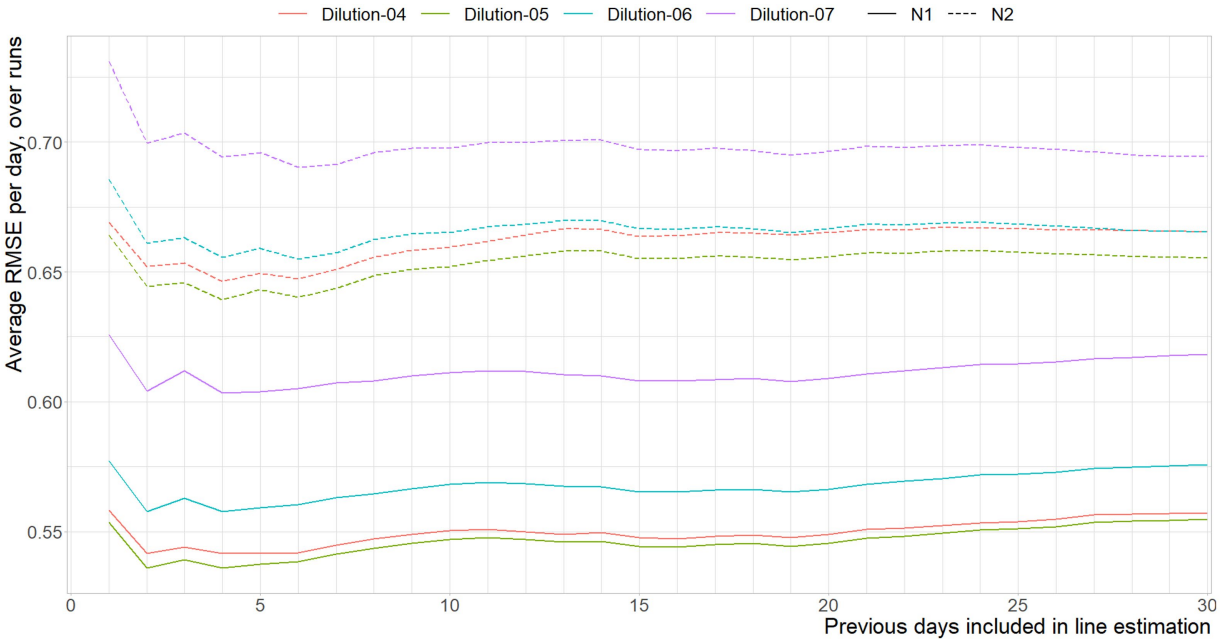

FIGURE 6
Mean RMSE between the Ct-values interpolated from the standard curve per run, and the standard curve based on *x* previous days, per dilution, per gene target.

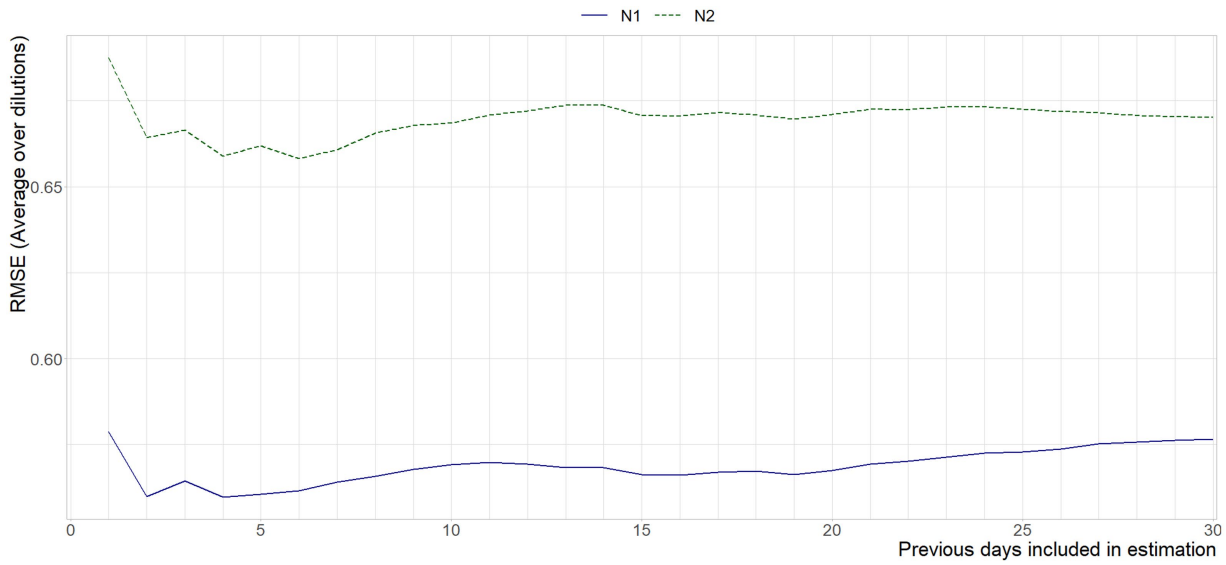

FIGURE 7
Mean RMSE between the Ct-values interpolated from the standard curve per run, and the standard curve based on *x* previous days, per gene target.

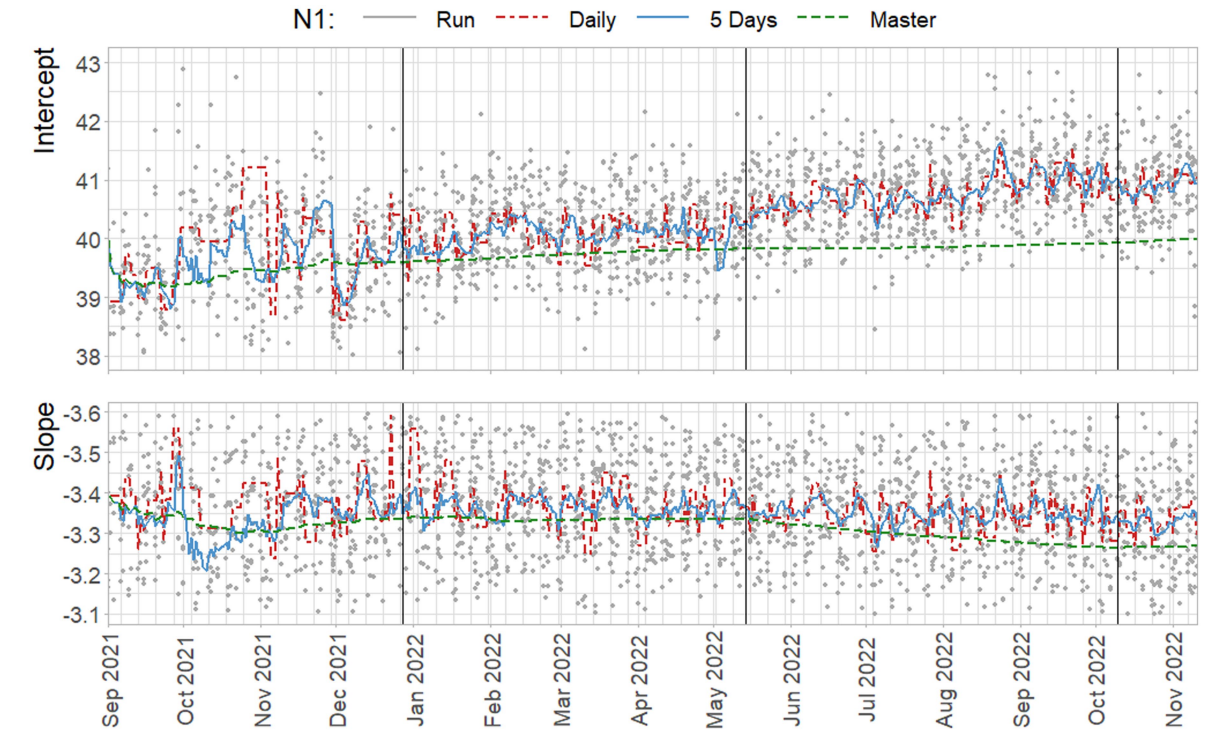

FIGURE 8
Estimated standard parameters for the N1 target, based on estimation per run (gray), on all daily observations of standard dilutions (red), on all observations within a five day rolling window (blue) and on all cumulative data up to that point (green). Vertical lines indicate a new preparation from the CDC assay.

The master curve starts of performing very similar to the 5 day rolling window standard curves. However, as can also be seen from Figures 3, 4, 8, increasingly underestimate the virus concentrations over time compared to the other methods, where the signal is decreased to about 50% of the virus loads compared to the alternative approaches. Per run curves show more, and especially in the beginning of 2022, unrealistic levels of variance, with changes in estimated virus concentrations occasionally in- or decreasing more than 100% between days.

Differences between the rolling and run-to-run quantification approaches can exceed 400%, but these cases are an exception where the standard curve of one run is markedly different from the rolling window curve. The median absolute difference on the daily nationwide average equals 8%, Some noticeable, prolonged periods of larger

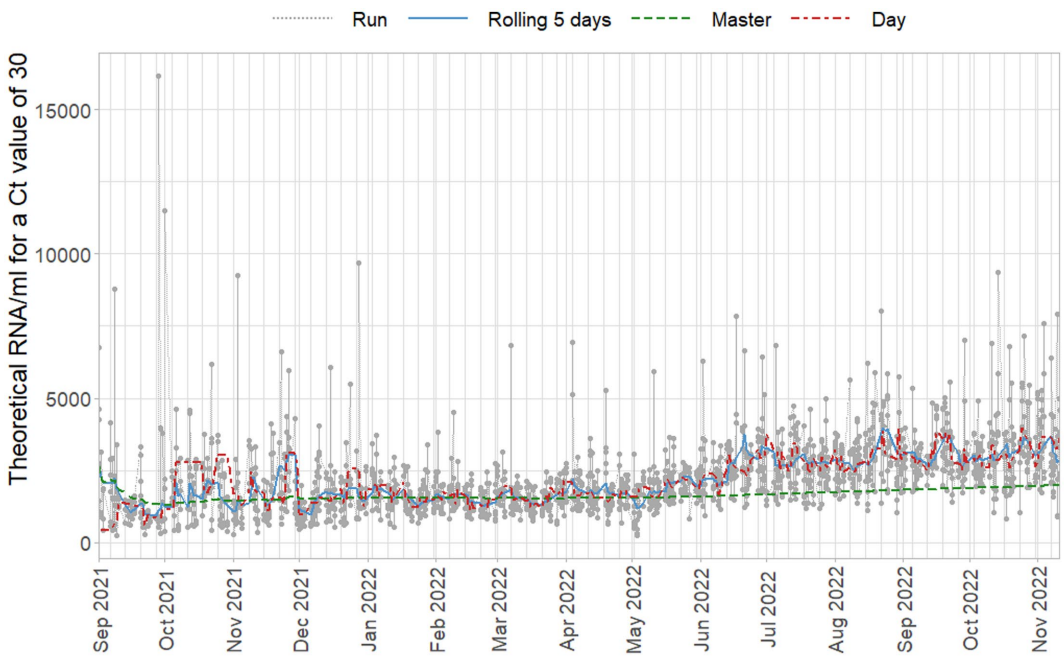

FIGURE 9
Estimated concentrations for a fixed Ct-value of 30, based on standard curves per duplicate run (gray), per day (red), on a five day rolling window (blue), and cumulative master curve (green).

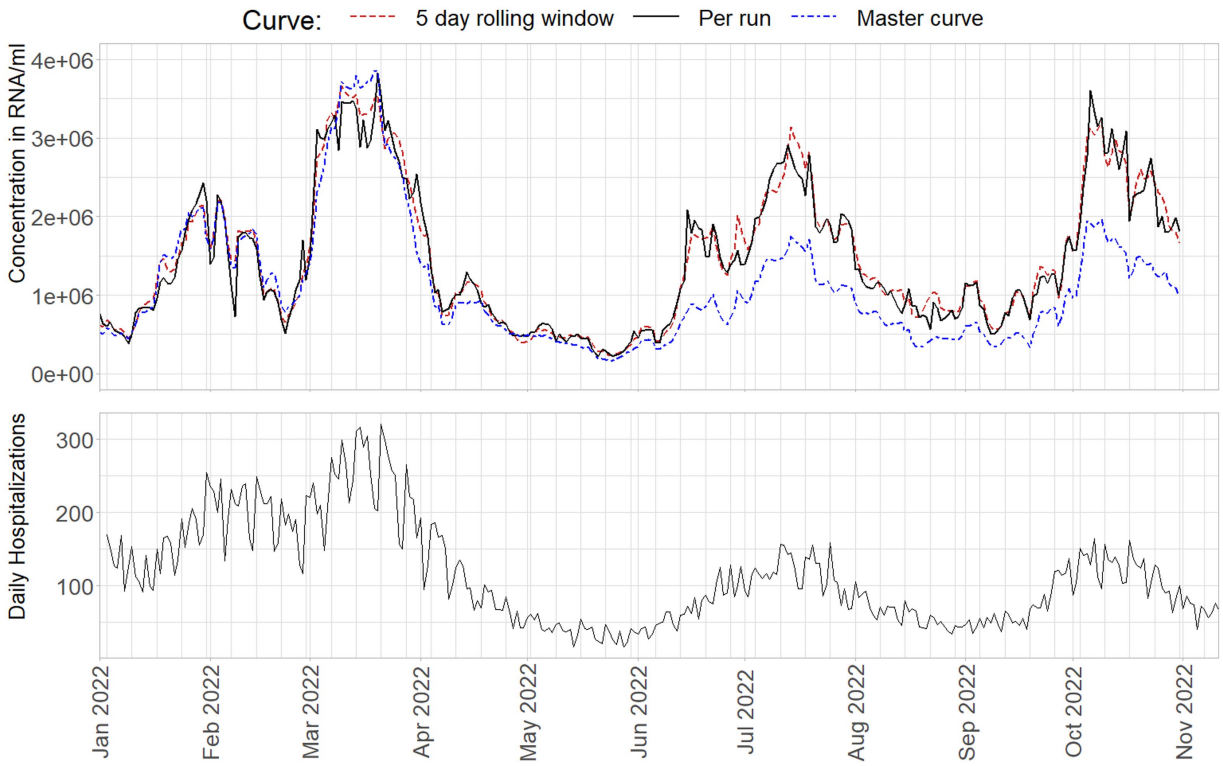

FIGURE 10
National level aggregate virus loads from January 1st 2022 to November 11th 2022 as obtained from a standard curve per run (black), on a 5-day rolling window (red), or a cumulative master curve (blue), compared to daily hospitalizations.

differences, upwards of 25% between the approaches, can be seen in the first and third peak in the data. The median absolute difference on the daily nationwide average equals 8%, with prolonged period in the first and third peak in the data showing differences upwards of 25%. The difference between the reported median percentages also illustrates that on a higher level of aggregation the effect of a different

standard curve will be smaller, as the viral loads averages out over many observations. On more regional, or on WWTP level, trend estimates will show more marked differences.

This is far from being definitive proof, but when comparing the virus concentrations to the number of daily hospitalizations as a proxy variable, the standard curves using several previous days of data seem to outperform the other methods in capturing the correct levels of virus concentration on the aggregate level. Note that the lower peaks in hospitalizations do not indicate better performance of the master curve, as immunity through vaccination changed the ratio between viral load and hospitalizations over time (22, 23). This is especially important toward the end of 2022, as the standard curve affects estimated trends more severely in high virus concentrations: Small shifts in the curve intercept and slope have the potential to cause large trend variations by the nature of Ct-values being logarithmically related to virus concentration.

4. Conclusion

We present the resulting standard curves from more than 4000 analyses of standard dilutions constructed from the CDC 2019-nCoV Real-Time RT-PCR Diagnostic Panel over the period of sixteen months. Further we propose a method of combining observations of standard dilutions over multiple runs in a high-throughput wastewater monitoring setting.

Results indicate that both the slope and intercept parameters of standard curves show high levels of run-to-run variance, and are subject to systematic shifts over a year that can exceed 2 Ct-values. Especially the sensitivity of the RT-qPCR process varies, as indicated by changes in the intercept of the standard curves. This is an important finding with regards to commonly applied criteria for standard curve construction, as the intercept is often, and surprisingly, absent from the quality indicators. As a result it may be a parameter that receives less attention when efficiency estimates are within their bounds, despite the potentially large impact on the concentrations obtained from samples.

The systematic fluctuations in the estimated standard curves make the application of a general master curve problematic. As time progresses the amount of data required to shift a master curve toward its current true value becomes exceedingly large, until the curve is virtually constant. In contrast, concentrations obtained from standard curves obtained from individual dilution series, even when duplicated on simultaneous runs, can result in large variation, with obtained sample concentrations that can exceed surrounding measurements by an order of magnitude.

Using the proposed approach of combining standard curve data from multiple runs, may not only have the practical benefits of extending the period for which the reference batch is identical, and cost-saving through less wells per run being occupied by reference dilutions. Results indicate that it also has the potential to solve problems associated with standard curve estimation, as a more plausible degree of variation in curve parameters is obtained than from run based standard curves, while systematic changes are properly captured. Both of these can be beneficial in high throughput surveillance programs, such as wastewater surveillance.

The newest data is often of major importance to fulfill the real-time monitoring objective that many surveillance programs are tasked with. Problematic or outlying concentrations can compromise this task, given potential delays through re-testing or partial rejection of output. Depending on the degree to which true variance is captured by partially smoothed standard curves, the proposed approach can reduce such problematic data where they are caused by standard curves that contain significant measurement error. Furthermore, trends in the data roughly coincide with meteorological seasons. Although multiple years of data would be required and controlled for laboratory atmosphere to ascertain this with certainty, if these trends do indeed have a yearly recurrence they may cause the viral load signal of interest to be dampened or amplified. Specifically during autumn and winter seasons there is a potential for these trends to coincide with seasonal variations of certain infectious disease prevalence, most notably respiratory viruses such as influenza and SARS-CoV-2.

Despite promising results, this work should be seen primarily as a proof of concept, since the major caveat is that the true standard curve is unknown. Given the observed changes in qPCR efficiency and sensitivity, and the theoretical basis for standard curve estimation, usage of a master curve for a longer period of time can be advised against. However, whether short term variance is captured to a sufficient degree when using standard curve estimation on a rolling window requires further work through a simulation study in which the properties of the true standard curves are known, and recovery of those curves can be investigated.

Such a study would further allow investigation of the required density of standard curve data. Preliminary results obtained over the year prior, where the weekly analysis frequency was one fourth of the data presented, show similar results. However, whether or not good approximation of standard curves per run is possible by using a rolling window, is dependent on the specific properties of the RNA or DNA target, the reference material used, and the laboratory setup and equipment, combined with data availability over a given period of time.

Data availability statement

The datasets presented in this article are not readily available because contractual obligations with third parties providing data to the program prohibit sharing the data contained in this manuscript without reservation. Full analysis results, programming code, and underlying data are available upon request. Requests to access the datasets should be directed to afvalwatersurveillance@rivm.nl.

Members of consortium

National Wastewater Surveillance Program (NRS), National Institute for Public Health and the Environment (RIVM), Bilthoven, Netherlands.

Author contributions

EN: conceived and wrote the manuscript, conceived and implemented the method described therein. WL: designed and set up

the infrastructure and laboratory methods of the Dutch National Sewage Surveillance program, wrote parts of the manuscript related to laboratory methods, and contributed to manuscript revisions. JMK: constructed reference materials, assisted in data collection, and reviewed the final manuscript. WH: contributed to the methodological description, contributed to manuscript revisions, and reviewed the programming code and description thereof. JK: coordinated laboratory analyses, and including reference materials. AD, RB, and EJ: contributed to manuscript revisions. All authors contributed to the article and approved the submitted version.

Funding

This research was funded by the Dutch Ministry of Health, Welfare and Sport as part of the Dutch National Sewer Surveillance program. This work was partly conducted under the European Union, DG Environment Emergency Support Instrument (no 060701/2021/864486/SUB/ ENV.C).

Acknowledgments

We thank the DARA Team and Centre for Infectious Diseases, Epidemiology and Surveillance for the national hospitalization data. We thank the Dutch Water Authorities, the Unie van Waterschappen, and the Ministry of Health, Welfare and Sport for their invaluable cooperation on sample and data collection, data management and reporting, and funding of the NRS.

Conflict of interest

The authors declare that the research was conducted in the absence of any commercial or financial relationships that could be construed as a potential conflict of interest.

Publisher's note

Supplementary material

The Supplementary material for this article can be found online at: https://www.frontiersin.org/articles/10.3389/fpubh.2023.1141494/full#supplementary-material

References

1. Bates J, Goddard MR, Butler M. The detection of rotaviruses in products of wastewater treatment. *J Hyg (Lond)*. (1984) 93:639–43. doi: 10.1017/S0022172400065219

2. Tambini G, Andrus JK, Marques E, Boshell J, Pallansch M, de Quadros CA, et al. Direct detection of wild poliovirus circulation by stool surveys of healthy children and analysis of community wastewater. *J Infect Dis*. (1993) 168:1510–4. doi: 10.1093/infdis/168.6.1510

3. Naughton CC, Roman FA, Alvarado AGF, Tariqi AQ, Deeming MA, Kadonsky K, et al. Show us the data: global COVID-19 wastewater monitoring efforts, equity, and gaps. *FEMS Microbes*. (2023) 4:xtad003. doi: 10.1093/femsmc/xtad003

4. Ahmed W, Bivins A, Bertsch PM, Bibby K, Choi PM, Farkas K, et al. Surveillance of SARS-CoV-2 RNA in wastewater: methods optimisation and quality control are crucial for generating reliable public health information. Curr Opin environ Sci. *Health*. (2020) 17:82–93. doi: 10.1016/j.coesh.2020.09.003

5. Michael-Kordatou I, Karaolia P, Fatta-Kassinos D. Sewage analysis as a tool for the COVID-19 pandemic response and management: the urgent need for optimised protocols for SARS-CoV-2 detection and quantification. *J Environ Chem Eng*. (2020) 8:104306. doi: 10.1016/j.jece.2020.104306

6. Svec D, Tichopad A, Novosadova V, Pfaffl MW, Kubista M. How good is a PCR efficiency estimate: recommendations for precise and robust qPCR efficiency assessments. *Biomol Detect Quantif*. (2015) 3:9–16. doi: 10.1016/j.bdq.2015.01.005

7. Ruijter JM, Pfaffl MW, Zhao S, Spiess AN, Boggy G, Blom J, et al. Evaluation of qPCR curve analysis methods for reliable biomarker discovery: bias, resolution, precision, and implications. *Methods*. (2013) 59:32–46. doi: 10.1016/j.ymeth.2012.08.011

8. Lai KK, Cook L, Krantz EM, Corey L, Jerome KR. Calibration curves for real-time PCR. *Clin Chem*. (2005) 51:1132–6. doi: 10.1373/clinchem.2004.039909

9. Hastings WJ, Eisenberg DTA, Shalev I. Uninterruptible power supply improves precision and external validity of telomere length measurement via qPCR. *Exp Results*. (2020) 1:1. doi: 10.1017/exp.2020.58

10. Bivins A, Kaya D, Bibby K, Simpson SL, Bustin SA, Shanks OC, et al. Variability in RT-qPCR assay parameters indicates unreliable SARS-CoV-2 RNA quantification for wastewater surveillance. *Water Res*. (2021) 203:117516. doi: 10.1016/j.watres.2021.117516

11. Lu X, Wang L, Sakthivel SK, Whitaker B, Murray J, Kamili S, et al. US CDC real-time reverse transcription PCR panel for detection of severe acute respiratory syndrome coronavirus 2. *Emerg Infect Dis*. (2020) 26:1654–65. doi: 10.3201/eid2608.201246

12. Bustin SA, Nolan T. Pitfalls of quantitative real-time reverse-transcription polymerase chain reaction. *J Biomol Tech*. (2004) 15:155–66.

13. Rutledge RG. Sigmoidal curve-fitting redefines quantitative real-time PCR with the prospective of developing automated high-throughput applications. *Nucleic Acids Res*. (2004) 32:e178. doi: 10.1093/nar/gnh177

14. Goll R, Olsen T, Cui G, Florholmen J. Evaluation of absolute quantitation by nonlinear regression in probe-based real-time PCR. *BMC Bioinformatics*. (2006) 7:107. doi: 10.1186/1471-2105-7-107

15. Guescini M, Sisti D, Rocchi MB, Stocchi L, Stocchi V. A new real-time PCR method to overcome significant quantitative inaccuracy due to slight amplification inhibition. *BMC Bioinformatics*. (2008) 9:326. doi: 10.1186/1471-2105-9-326

16. Sivaganesan M, Haugland RA, Chern EC, Shanks OC. Improved strategies and optimization of calibration models for real-time PCR absolute quantification. *Water Res*. (2010) 44:4726–35. doi: 10.1016/j.watres.2010.07.066

17. Panina Y, Germond A, David BG, Watanabe TM. Pairwise efficiency: a new mathematical approach to qPCR data analysis increases the precision of the calibration curve assay. *BMC Bioinformatics*. (2019) 20:295. doi: 10.1186/s12859-019-2911-5

18. Moniri A, Rodriguez-Manzano J, Malpartida-Cardenas K, Yu LS, Didelot X, Holmes A, et al. Framework for DNA quantification and outlier detection using multidimensional standard curves. *Anal Chem*. (2019) 91:7426–34. doi: 10.1021/acs.analchem.9b01466

19. Peirson SN, Butler JN, Foster RG. Experimental validation of novel and conventional approaches to quantitative real-time PCR data analysis. *Nucleic Acids Res*. (2003) 31:e73:73e–773e. doi: 10.1093/nar/gng073

20. ISO. *Microbiology of the food chain - horizontal method for determination of hepatitis a virus and norovirus using real-time RT-PCR - part 2: Method for detection*. Delft: Royal Netherlands Standardization Institute (NEN) (2019).

21. Geubbels ELPE, Backer JA, Bakhshi-Raiez F, van der Beek RFHJ, van Benthem BHB, van den Boogaard J, et al. The daily updated Dutch national database on COVID-19 epidemiology, vaccination and sewage surveillance. *Scientific Data*. (2023) 10:469. doi: 10.1038/s41597-023-02232-w

22. Wu N, Joyal-Desmarais K, Ribeiro PAB, Vieira AM, Stojanovic J, Sanuade C, et al. Long-term effectiveness of COVID-19 vaccines against infections, hospitalisations, and mortality in adults: findings from a rapid living systematic evidence synthesis and meta-analysis up to December, 2022. *Lancet Respir Med*. (2023) 11:439–52. doi: 10.1016/S2213-2600(23)00015-2

23. de Gier B, Huiberts AJ, Hoeve CE, den Hartog G, van Werkhoven H, van Binnendijk R, et al. Effects of COVID-19 vaccination and previous infection on omicron SARS-CoV-2 infection and relation with serology. *Nat Commun*. (2023) 14:4793. doi: 10.1038/s41467-023-40195-z

Frontiers in Public Health

Explores and addresses today's fast-moving healthcare challenges

One of the most cited journals in its field, which promotes discussion around inter-sectoral public health challenges spanning health promotion to climate change, transportation, environmental change and even species diversity.

Discover the latest Research Topics

See more →

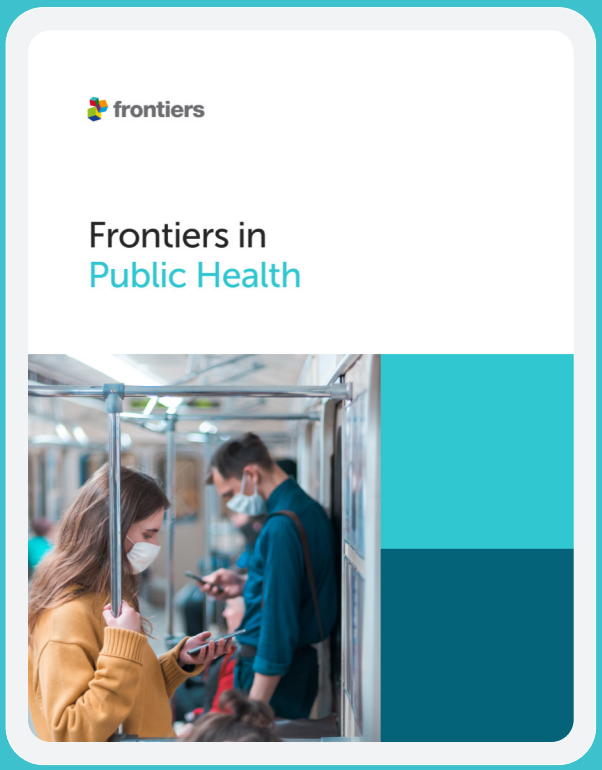

Frontiers

Avenue du Tribunal-Fédéral 34
1005 Lausanne, Switzerland
frontiersin.org

Contact us

+41 (0)21 510 17 00
frontiersin.org/about/contact